Click-mediated Enrichment of Specific Genomic Loci

Dissertation

Submitted for the degree of Doctor of Natural Science

(Dr. rer. nat.)

Presented by

Anna Witte

at the

fakultät für chemie
und chemische biologie

of the

technische universität
dortmund

Dortmund 2020

The study presented in this thesis comes from the work done between January 2016 and April 2020 in the group of Prof. Dr. Daniel Summerer, at TU Dortmund. The work was funded by TU Dortmund.

Acknowledgments

First and foremost, I would like to thank Prof. Dr. Daniel Summerer, who gave me the opportunity to work as a scientist in his group to complete my doctorate. I would like to thank him for his open-mindedness, trust and the creative freedom that I was given as a doctoral student, as well as for the constructive discussions during my doctoral thesis. Furthermore, I would like to thank Prof. Dr. Rauh for his kind willingness to act as second reviewer of this work.

I would also like to thank the proteomics team at the MPI Dortmund, namely Petra Janning, Malte Metz and Andreas Brockmeyer, for the processing and time-consuming analysis of my large sample volume and for their constant willingness to discuss the matter, which has significantly advanced my know-how and that of the entire research group in the field of proteomics. I would also like to thank our cooperation partner Michal Schweiger, whose group had significantly enriched my work with their research at the SatIII locus.

Not to forget I want to thank all current and former members of the Summerer group, namely Álvaro Muñoz-López, Anne Jung, Benjamin Buchmuller, Brinja Kosel, Christoph Hoppe, Damian Schiller, Dr. Gerzegorz Kubik, Jan Wolffgramm, Katharina Kuhr, Dr. Mario Gieß, Nadine Schmidt, Dr. Preeti Rathi, Dr. Sara Mauerer, Dr. Shubhendu Palei, Simone Eppmann, Sudakshina Banerjee and Tzu-Chen Lin for their contributions to my work and/or the great time we spent inside and outside the laboratory.

I would also like to thank the student assistants for their help with the daily lab tasks and my bachelor student Leijla Maksumic for supporting me with her bachelor thesis.

I would like to thank the staff of the Department of Chemical Biology, Maria Sergani, Martina Reibner, Petra Alhorn and Ulrich Schoppe, for their work and their help with bureaucratic matters and all things related to general laboratory management. Furthermore, I would like to thank the Rauh and Dehmelt laboratory for allowing me to use some of their equipment. Special thanks also go to Suchet Nanda for improving my English writing skills.

Very special thanks go to my late mother, to my father and to my partner Dominic Kamps, who always supported and encouraged me even in the hardest hours. I can also express my deepest gratitude to my aunt, uncle, grandmother, mother-in-law and my closest friends, as they were always there for me and showed their interest in my work.

Table of Contents

1 List of Figures

2 List of Tables

3 Abbreviations

2-OG	2-Oxoglutarate
5caC	5-carboxylcytosine
5fC	5-formylcytosine
5hmC	5-hydroxymethylcytosine
5mC	5-methylcytosine
A	adenine, adenosine
aa	amino acid
aaRS	aminoacyl-RNA Synthetase
AD	activation domain
Ala, A	alanine
Arg	arginine
Asn, N	asparagine
Asp, D	aspartic acid
ATIC	bifunctional purine biosynthesis protein PURH
ATRX	alpha-thalassemia mental retardation X-linked
BAH	bromo-adjacent homology domain
BCN	endo-Bicyclo [6.1.0] nonyne - lysine
BER	base excision repair
BirA	E. coli biotin ligase
Boc	t-butyloxycarbonyl-lysine
bp	base pair
BRD4	bromodomain-containing protein 4
BSA	bovine serum albumin
C	cytosine, cytidine
CD	catalytic domain
Cdc6p	cell division cycle 6 protein
Cdt1p	chromatin licensing and DNA replication factor 1 protein
CGIs	CpG islands
ChIP	chromatin immunoprecipitation
CpG	cytosine-phosphate-guanine

CRD	central repeat domain
CREBBP	CREB-Binding-Protein
CRISPR	clustered regulatory interdispersed short palindromic repeat
CTR	C-terminal domain
CuAAC	Cu^{I}-catalysed alkyne−azide cycloaddition
CXXC	cysteine-rich domain
Cys, C	cysteine
dATP	desoxyadenosintriphosphat
dCTP	desoxycytosintriphosphat
dfCTP	desoxy-5-formyl-cytosintriphosphat
dGTP	desoxyguanintriphosphat
dhmCTP	desoxy-5-hydroxymethyl-cytosintriphosphat
dmCTP	desoxy-5-methyl-cytosintriphosphat
DNA	deoxyribonucleic acid
DNMT	DNA methyl transferases
DNMT3L	DNMT3-like
dNTP	deoxyribonucleoside triphosphates
DSBH	double-stranded β-helix
dTTP	desoxythymintriphosphat
e.g.	exempli gratia (lat.) – for example
ELISA	enzyme-linked immunosorbent assay
EPL	expressed protein ligation
EPR	electron paramagnetic resonance
ES	embryonic stem cells
ESI	electrospray ionization
FAM	fluorescein
Fig.	Figure
G	guanine, guanosine
gDNA	genomic DNA
GFP	green fluorescent protein
Gln, Q	glutamine
Glu, E	glutamate, Glutamic acid
Gly, G	glycine
GR	G-Rich repeats

H	histone
His, H	histidine
hrp	hypersensitive response and pathogenicity
HS	heat shock
HSF1	heat shock factor 1
IgG	immunglobulin G
Ile, I	isoleucine
k_2	second order rate constant
kb	kilobases
Leu, L	leucine
LGALS3	galectin-3
LINE	long-interspersed element
LNA	locked nucleic acids
LR	last repeat
LTR	long terminal repeat
Lys, K	lysine
MBD	methyl-binding domain
Mcm2–7p	mini-chromosome maintenance proteins 2–7
MeCP2	methyl-CpG-binding protein 2
mESC	mouse embryonic stem cell
minCMV	minimal CMV promoter
mRNA	messenger RNA
MS	mass spectrometry
MS/MS	tandem mass spectrometry
MV	module vector
MW	molecular weight
ncAA	non-canonical amino acid
NCP	nucleosome core particle
NES	nuclear export signal
NLS	nuclear localization signal
NPC	neural precursor cells
nSB	nuclear stress bodie
nt	nucleotide
NTR	N-terminal domain

NuRD	nucleosome remodeling and deacetylase complex
OGT	O-linked β-N-acetylglucosamine (O-GlcNAc) transferase
ORC	origin recognition complex
ORF	open reading frame
p	false discovery rate
PCNA	proliferating cell nuclear antigen
PCR	polymerase chain reaction
pdb	protein database
PHD	plant homeodomain
Phe, F	phenylalanine
Pol II	RNA polymerase II
pre-RC	pre-replicative complex
Pro, P	proline
PTM	post-translational modification
PWWP	“proline-tryptophan-tryptophan-proline” motif
Pyl	pyrrolysine
qPCR	quantitative PCR
R	residues
RFP	red fluorescent protein
RFT	replication foci targeting domain
RLU	relative luminescence unit
RNA	ribonucleic acid
rpm	rounds per minute
rRNA	ribosomal RNA
RVD	repeat divariable residue
SAH	S-adenosyl-l-homocysteine
SAM	S-adenosyl-l-methionine
SatII	satellite-II
SatIII	satellite-III
sc	scrambled
SCO	cyclooctyne-lysine
SeC	selenocysteine
Ser, S	serine
SINE	short-interspersed element

SPAAC	strain-promoted alkyne−azide cycloaddition
SPANC	strain promoted alkyne−nitrone cycloaddition
SPIEDAC	strain-promoted inverse electron demand Diels-Alder cycloaddition
SRSF1	serine/arginine-rich splicing factor 1
STR	short tandem repeat
T	thymine, Thymidine
T3SS	type III secretion system
TAD	topologically associating domain
TALE	transcription activator-like effector
TCO	trans-cyclooct-2-en – L – lysine
TDG	thymine DNA glycosylase
TE	transposable element
TET	ten-eleven translocation
Tet-biotin	tetrazine-biotin
TF	transcription factor
Thr, T	threonine
Tm	melting temperature
TRD	transcriptional repressor domain
tRNA	transfer RNA
Trp, W	tryptophan
TSS	transcription start site
Tyr, Y	tyrosine
U	uracil, uridine
UBA1	ubiquitin E1 activating enzyme
UHRF1	ring finger domain protein
Val, V	valine
α-KG	α-ketoglutarate
αSat	α-satellite

4 List of Publications

[1] A. Witte, A. Muñoz-López, M. Schweiger, P. Janning, D. Summerer, “Encoded, Click-reactive Receptors for Programmable Capture of Specific Chromatin Segments.” *Chem Sci.* **2020**, manuscript in preparation.

[2] H. Neumann, P. Neumann-Staubitz, A.Witte and D. Summerer, “Epigenetic chromatin modification by amber suppression technology.” *Curr Opin Chem Biol.* **2018**, 45, 1.

[3] M. Gieß, A. Witte, J. Jasper, O. Koch and D. Summerer, “Complete, Programmable Decoding of Oxidized 5-Methylcytosine Nucleobases in DNA by Chemoselective Blockage of Universal Transcription-Activator-Like Effector Repeats.” *JACS* **2018**, 140, 5904.

[4] P. Rathi, A. Witte and D. Summerer, “Engineering DNA Backbone Interactions Results in TALE Scaffolds with Enhanced 5-Methylcytosine Selectivity.” *Sci Rep.* **2017**, 7, 15067.

5 Abstract

In all organisms, the genetic information of cells is stored in the nucleotide sequence of deoxyribonucleic acid (DNA) [1,2]. The human organism consists of more than 200 different somatic cell types with the same genetic information (genotype). Even though, they drastically differ in their morphology and function (phenotype), which is related to different gene expression levels. Gene expression is controlled by macromolecular interactions and epigenetic modifications on chromatin[1] that are highly locus-specific and drive functional aspects of each locus[2]. Even though, the compositions of macromolecules and modifications on many chromosome loci remain poorly understood[3], in part due to the lack of locus-specific chromatin purification methods that would allow for targeted, discovery-oriented analyses[4]. Therefore, there is a particular interest in methods that allows the purification of user-defined genomic loci while maintaining molecular compositions and modifications which are suitable for proteomic analyses. The methods will enable correlations of local chromatin states with phenotypes as the key to a deeper understanding of the regulation landscape of the eukaryotic genome.

In this work, the first enrichment method based on bio-orthogonal conjugation ("click-chemistry) with encoded programmable DNA binding domains for purification of user-defined genomic loci (Fig. 1) was established. In particular, transcription activator-like effector (TALE) proteins were designed for sequence-specific binding of user-defined genomic repeat elements. For the purification of the targeted genomic loci, a non-canonical amino acid (ncAA) bearing a trans-cyclooctene functional group was introduced in the N-terminal region of the TALE protein using genetic code expansion[5]. After expression of the TALE protein with simultaneous incorporation of ncAA in mammalian cells, the ncAA enables click-mediated biotinylation via strain-promoted inverse electron demand Diels-Alder cycloaddition (SPIEDAC). After validation of the incorporation site for the ncAA, the SPIEDAC-mediated biotinylation was established with tetrazine-biotin conjugates[6–9]. The biotin-functionalized TALE protein, cross-linked together with other chromatin proteins to the DNA, could selectively be enriched on streptavidin-conjugated beads.

This click-mediated enrichment provides complementary potential compared to the existing enzymatic biotinylation strategies used in chromatin enrichment methods in the view of site-specificity and proteome-wide background. As a first outlook experiment, we extended our approach to fusion constructs of specific TALE proteins and ten-eleven translocation (TET) dioxygenases for epigenetic editing *in vivo*. TETs catalyze the oxidation of 5-methylcytosine (5mC) to the oxidized derivates 5-hydroxymethylcytosine (5hmC)[10,11], 5-formylcytosine (5fC), and 5-carboxylcytosine (5caC)[12–14]. In combination with the click-mediated enrichment and proteomics analysis, this will enable studying how local epigenetic changes modulate the local chromatin landscape *in vivo* as basis for alterations in gene expression.

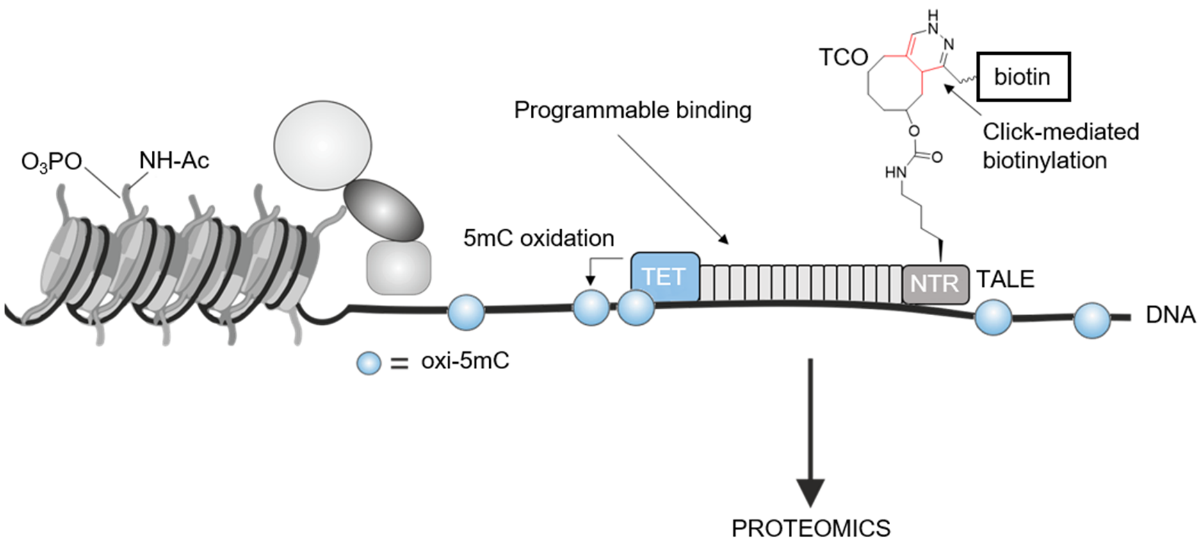

Figure 1 Concept of click-mediated enrichment of genomic loci for targeted programmable 5mC oxidation, enrichment, and proteomic analyses.

6 Zusammenfassung

Bei allen Organismen ist die genetische Information der Zellen in der Nukleotidsequenz der Desoxyribonukleinsäure (DNA) gespeichert [15,16]. Der menschliche Organismus besteht aus mehr als 200 verschiedenen somatischen Zelltypen, die alle die gleiche genetische Information (Genotyp) enthalten. Sie unterscheiden sich jedoch drastisch in ihrer Morphologie und Funktion (Phänotyp), was mit unterschiedlichen Genexpressionsniveaus zusammenhängt. Die Genexpression wird durch makromolekulare Interaktionen und epigenetische Modifikationen am Chromatin gesteuert[1], die hochgradig lokusspezifisch sind und einzelne funktionelle Aspekte jedes Locus steuern[2]. Die Zusammensetzung der Makromoleküle und die Modifikationen an vielen Chromosomenloci sind jedoch nach wie vor nur unzureichend verstanden[3] was zum Teil auf einen Mangel an locusspezifischen Chromatinreinigungsmethoden zurückzuführen ist, welche gezielte, entdeckungsorientierte Analysen ermöglichen würden[4]. Daher besteht ein besonderes Interesse an Methoden, die die Reinigung von benutzerdefinierten genomischen Bereichen unter Beibehaltung der molekularen Zusammensetzung und Modifikationen erlauben und die für Proteomanalysen geeignet sind. Diese werden Korrelationen von lokalen Chromatinzuständen mit Phänotypen als Schlüssel zu einem tieferen Verständnis der Regulationslandschaft des eukaryotischen Genoms ermöglichen.

In dieser Arbeit wurde die erste Anreicherungsmethode basierend auf bio-orthogonaler Konjugation ("Klick-Chemie") mit kodierten, programmierbaren DNA-Bindungsdomänen zur Aufreinigung von benutzerdefinierten genomischen Loci (Fig. 2) etabliert. Insbesondere wurden *transcription-activator-like-effector* (TALE)-Proteine für die sequenzspezifische Bindung von benutzerdefinierten genomischen Repeat-Elementen entwickelt. Für die Reinigung der angestrebten genomischen Loci wurde eine nicht-kanonische Aminosäure (ncAA), die eine trans-cycloocten-funktionelle Gruppe trägt, in die N-terminale Region des TALE-Proteins mittels genetischer Code-Expansion eingeführt[5]. Nach der Expression des TALE-Proteins bei gleichzeitigem Einbau der ncAA in Säugetierzellen ermöglicht die ncAA eine Click-vermittelte Biotinylierung über die *strain-promoted inverse electron demand*

Diels-Alder cycloaddition (SPIEDAC). Nach der Validierung der Inkorporationsstelle für die ncAA wurde die SPIEDAC-vermittelte Biotinylierung mit Tetrazin-Biotin-Konjugaten etabliert[6–9]. Das mit Biotin funktionalisierte TALE-Protein, das zusammen mit anderen Chromatinproteinen an die DNA vernetzt wurde, konnte selektiv an Streptavidin-konjugierten Beads angereichert werden.
Das Biotin-funktionalisierte TALE-Protein, das zusammen mit anderen Chromatin-Proteinen mit der DNA vernetzt ist, konnte selektiv an Streptavidin-konjugierten Beads angereichert werden. Diese Click-vermittelte Anreicherung bietet ein komplementäres Potenzial im Vergleich zu den bestehenden enzymatischen Biotinylierungsstrategien[4,17–22], die in Chromatin-Anreicherungsmethoden verwendet werden, im Hinblick auf die Spezifität des Ortes und den proteomweiten Hintergrund.

Als erstes Ausblicksexperiment erweiterten wir unseren Ansatz auf Fusionskonstrukte aus spezifischen TALE-Proteinen und *ten-eleven-translocation* Dioxygenasen (TET) für die epigenetische Editierung *in vivo*. TETs katalysieren die Oxidation von 5-Methylcytosin (5mC) zu den oxidierten Derivaten 5-Hydroxymethylcytosin (5hmC)[10,11], 5-Formylcytosin (5fC) und 5-Carboxylcytosin (5caC)[12–14]. In Kombination mit der Click-vermittelten Anreicherung und der Proteomanalyse ermöglicht dies die Untersuchung, wie lokale epigenetische Veränderungen die lokale Chromatinlandschaft *in vivo* als Grundlage für Veränderungen in der Genexpression modulieren.

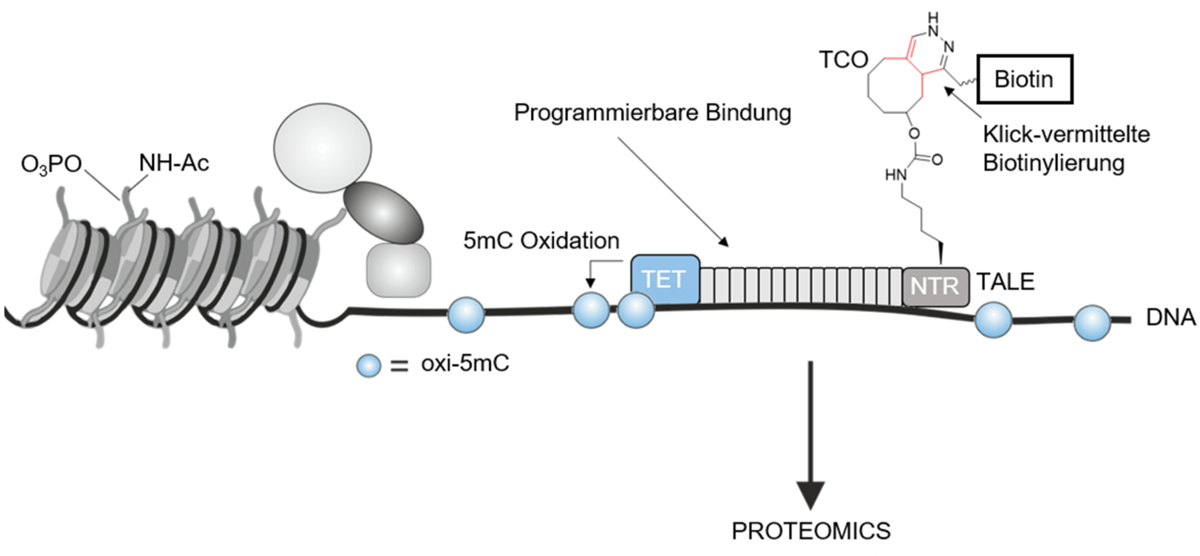

Figure 2 Konzept der Click-vermittelten Anreicherung von genomischen Loci für gezielte, programmierbare 5mC-Oxidation, Anreicherung und Proteomanalysen.

7 Introduction

7.1 Molecular Structure and Function of Deoxyribonucleic acid (DNA) in the Genome

7.1.1 The DNA

Between 1940 and 1944 Oswald Avery discovered that the DNA is the chemical basis for specific and apparently heritable transformations in bacteria[15], showing the central role of DNA for storing a cell's genetic information. Avery's discovery was not widely accepted due to Schrödinger's book "What is life" where he argued the essence of life, as information present in our chromosome, had to be present on a non-repetitive molecule[23]. It took the work of Erwin Chargaff, inspired by Avery, to show that DNA composition is species specific, suggesting the potential of this molecule. Inspired by Schrödinger, in 1953 Watson and Crick created the first DNA model based on X-ray diffraction analysis, today known as the Watson-Crick DNA structure[24–26].

The DNA is a linear polymer formed of four different nucleotides. The nucleobases adenine (A), guanine (G), cytosine (C) and thymine (T) are connected by phosphate-diester groups joining two deoxyribose through their 3' and 5' hydroxyl groups. Two polynucleotide strands form a double helix by coiling around a common axis (Fig. 3a, b) and interact via hydrogen bonds between the purine (A and G) and pyrimidine (T and C) bases, according to the Watson-Crick base-pairing[24] (Fig. 3c). This double helical structure is stabilized by π-π stacking interactions of the aromatic nucleobases (Fig. 3c), leading to an energetically favorable packing of the nucleobases inside the DNA double helix[27]. The nucleobases are located on the inside of the double helix whereas the deoxyribose-phosphate backbone faces towards the outside (Fig. 3b). Two distinct grooves, the major and the minor groove, present in the DNA double helix, are formed by the virtue of the position of the glyosidic bonds of one base pair, which are not positioned exactly opposite of each other (Fig. 3a). The grooves provides potential donor and acceptor atoms for hydrogen bonds that allow for specific protein interactions[28,29].

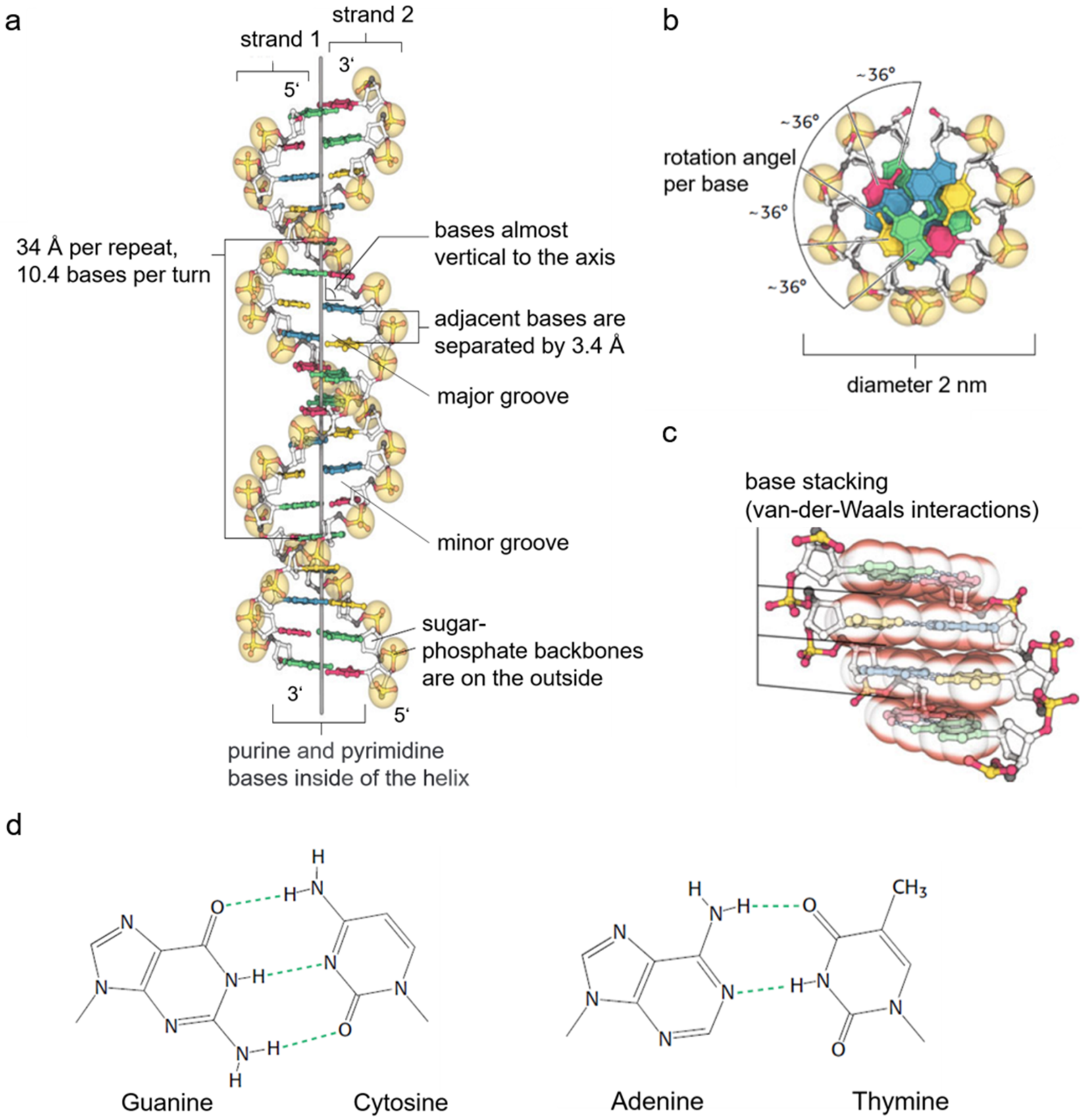

Figure 3 Watson - Crick model of a DNA double helix: **a** Axial view along the vertical helix axis; the structure repeats every 34 Å, which corresponds to ten base residues on each chain. **b** Radial view of the helix axis from above. A rotation of 36° per base residue as well as the stacking of the bases can be seen. **c** Side view of the DNA. The base pairs within the double helix are stacked almost exactly on top of each other. Van-der-Waals interactions of the stacked bases stabilize the double helix. **d** base pair interaction based on the DNA model of Watson and Crick. (adapted from[28])

7.1.2 The DNA double helix conformation

One of the first X-ray diffraction analyses of DNA, done by Rosalind Franklin in 1953, showed two different conformations of DNA, known as A-DNA and B-DNA[26,30]. Under physiological conditions the most common conformation of DNA is the B-DNA conformation, initially proposed by Watson and Crick in 1953[24]. The A-DNA conformation was revealed by X-Ray diffraction analyses of dehydrated states of DNA at a relative humidity of less than 75 %[31]. The molecular structures of these two forms are essentially similar in their handedness, chain orientation and hydrogen-bonding scheme. Both DNA double helices are right-handed with two antiparallel nucleotide strands, which are connected *via* Watson-Crick base pairing[28,32]. The A-DNA double helix is wider and shorter compared to the B-DNA helix with 11 instead of 10 residues per turn and a translation of 2.56 Å along the helical axis[28,33], whereas the B-DNA is translated by ~3.4 Å. Furthermore, in the A-DNA the C-3' atom of the sugar residues lies outside the plane, which is formed by the other four carbon atoms (C-3'endo conformation) whereas in the B-DNA the C-2´ is outside the plane (C-2´ endo conformation). This leads to a stronger tilting of the bases in the A-DNA[28]. In 1979 a left-handed DNA double helix was revealed as a third conformation of DNA. This conformation was called Z-DNA due the zig-zag course of the ribose-phosphate backbone resulting from the alternating residue conformation[34,35]. Certain proteins, associated with viral diseases, have been discovered as a product of a DNA molecule with a left-handed (Z-DNA) conformation[35] (Fig. 4). Even though the biological relevance of the Z-DNA is still unclear.

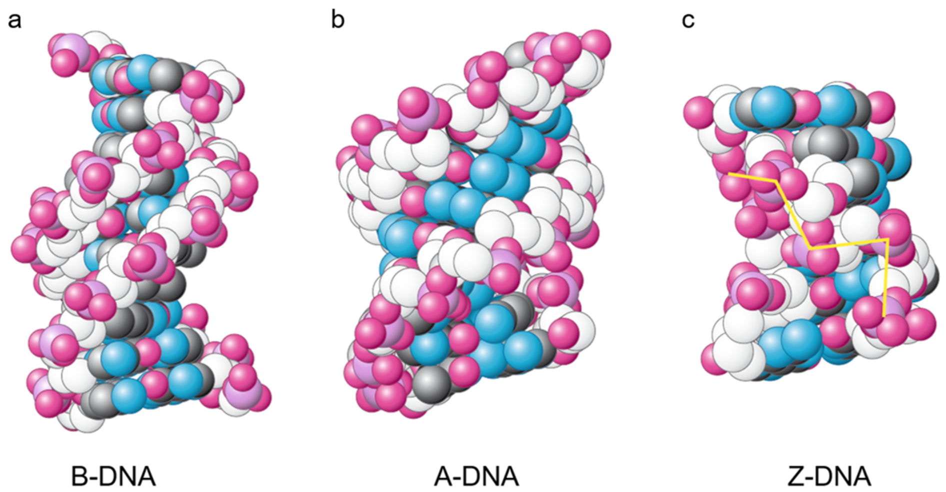

Figure 4 Helical structures of DNA: Space-filling models of ten base pairs of the B-, A- and Z-DNA form. The carbon atoms of the backbone are shown in white and the phosphate groups are shown in pink. **a** Right handed B-DNA double helix with a large major groove (1BNA pdb[32]). **b** A-form of DNA, also right handed, but structurally more condensed helix (1DNZ pdb[36]). **c** Left handed Z-DNA containing a dinucleotide repeat and the backbone follows a zig-zag path (131D pdb[37]).(adapted from[28])

7.1.3 Transcription of DNA

In 1958, Crick published the term central dogma of molecular biology, describing all possible directions of information flow between DNA, RNA, and protein and stated that the information flow stops at the protein level[38,39] (Fig. 5a, b). In 1965 Watson published a second version of the central dogma in a more simple two step pathway (DNA → RNA and RNA → protein) (Fig. 5c)[40].

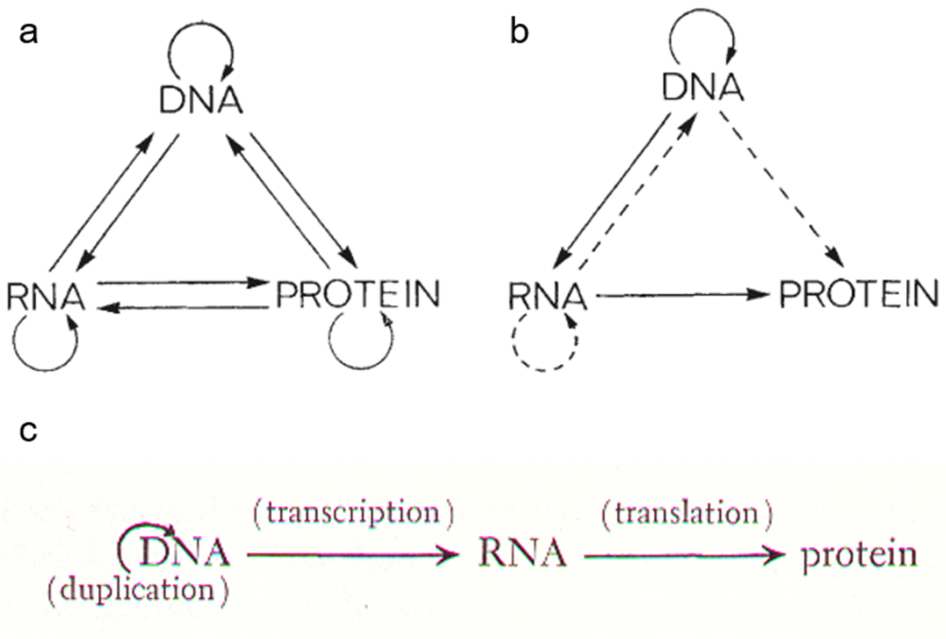

Figure 5 Central Dogma by Crick vs. Central Dogma by Watson: **a** Diagram of potential information flow by Crick (1958), illustrating all possible transfers of information. **b** Diagram of potential information flow by Crick (1958), illustrating all permitted transfers of information[39]. **c** Watson's version of the Central Dogma[40].

Both pathways show the flow of genetic information, based on the expression of specific DNA sequence fractions called genes. Even if the genome of each eukaryotic cell is identical, the cells differ in their function by expressing only a subset of their entire genetic information. In every organism the gene expression starts with the transcription of DNA into RNA catalyzed by RNA polymerases. Like DNA, the RNA polymer consists of four nucleotides. In RNA the sugar moiety is ribose instead of deoxyribose and the nucleobase T is replaced by uracil (U). RNA molecules can be subclassified into (protein)-coding and non-coding RNAs, as not all RNAs are templates for protein syntheses. In eukaryotes there are three different RNA polymerases namely RNA polymerase I, II and III, and each processes a distinct type of RNA. RNA polymerases I and III transcribe genes to the noncoding RNAs, like transfer RNA (tRNA) and ribosomal RNA (rRNA), whereby RNA polymerase II produces the protein-coding messenger RNA (mRNA). The transcription starts with the formation of the pre-initiation complex, consisting of a set of transcription factors, and the binding of the RNA polymerase at the gene promoter. The RNA polymerase transcribes the respective gene from the transcription start site (TSS) of the corresponding gene. After RNA processing, steps like 5'-capping and 3'-polyadenylation complete the transcription. The mRNA is exported from the nucleus to the cytosol and recruited to ribosomes, cytosolic RNA/protein complexes containing rRNA, which catalyze the protein biosynthesis.

7.1.4 Genome organization

In eukaryotes the DNA is nonlinear, hierarchically packed inside the nucleus, forming chromatin fibers in which the DNA is organized in arrays of nucleosomes[41]. The nucleosome core particle (NCP) is formed by a DNA segment of 145–147 base pairs wrapping around the octameric histone protein complex consisting of two copies of the histone proteins, H2A, H2B, H3 and H4.[42,43] (Fig. 6a). In the first organization layer the nucleosomes are linked together through additional 10–80 base pairs, leading to the characteristic “beads-on-a-string” resemblance of a 10 nm chromatin fiber[44,45]. The organization of nucleosomal units, showing the “hand shake motif”[46], was investigated by X-ray crystallographic studies, showing that the dimer sets of H2A and H2B are associated with H3-H4 (half tetramer). The organization of the DNA around the octamers surface leads to a symmetric particle with a defined dyad axis[47].
Even though, outside of the repeating and particulate nature of chromatin, details of nucleosomal organization is not completely clear. In the higher ordered structure the nucleosomes can be stabilized by the fifth histone H1[42,48,49] and / or by chromatin associated factors, like HP1[50] or polycomb (Pc)[51], leading to a more condensed 30 nm chromatin fiber (Fig. 6b). The formation of the 30 nm chromatin fiber can be described either by the “solenoid” (one-start helix) model[52,53], wherein the nucleosomes are gradually coiled around a central axis or by the ”zigzag” model[54], which adopts higher-order self-assemblies (two-start helix). A fiber arrangement more

consistent with the zigzag model, wherein linker DNA connects two stacks of nucleosomes, is suggested by X-ray structures of *in vitro* assemblies[55–57]. More condensed chromatin, like looped chromatin domains (300–700 nm) occurs, perhaps, by linking the chromatin fiber to the nuclear periphery through chromatin-associated proteins[58]. In the most condensed chromatin structure, there is a 10000-fold compaction of the DNA from an ~2-m molecule into a discrete chromosome measuring 1.5 µm in diameter[47]. This can be achieved by H1 hyperphosphorylation and selective phosphorylation in the H3 amino terminus[47,59]. In addition, the ATP-dependent action of topoisomerase II, the condensin[60] and cohesion complexes[61], are important for chromatin condensation as there is only little chromatin condensation in their absence. This complex genome organization modulates biological processes such as transcription, DNA replication, cell division and meiosis[41].

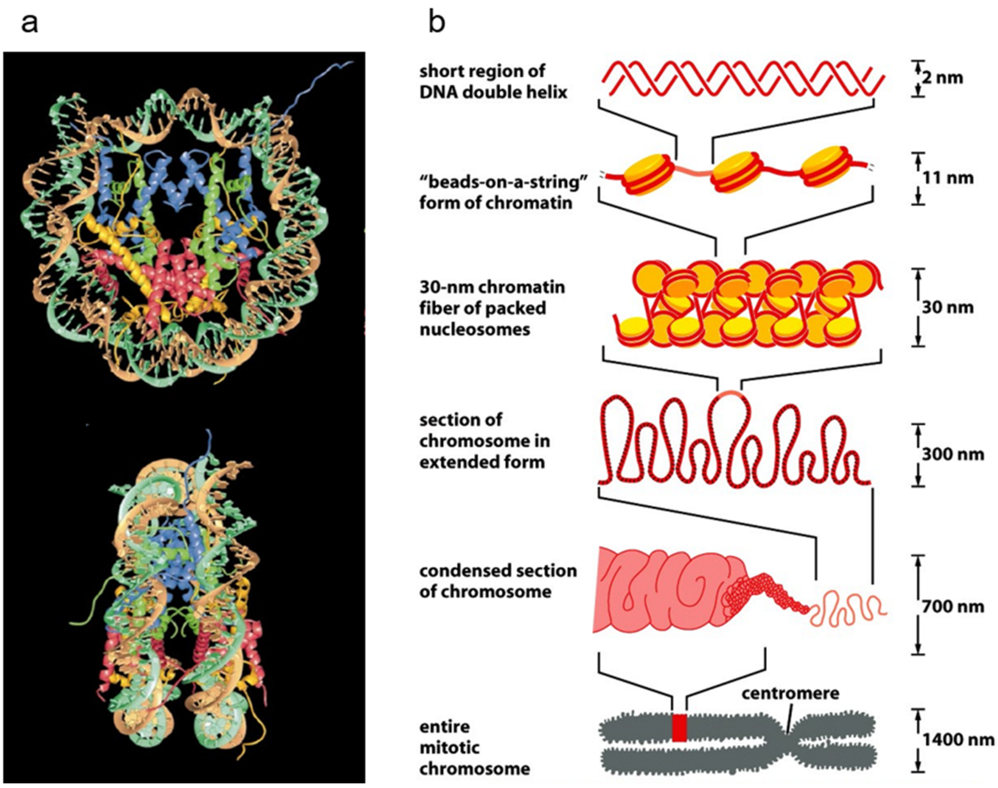

Figure 6 Organization layers of the human genome: **a** Crystal structure of the nucleosome core particle: Ribbon traces for the 146-bp DNA-phosphodiester backbone (brown and light green), eight histone protein main chains (blue: H3, green: H4, yellow: H2A, red: H2B).(adapted from[42]) **b** Levels of chromatin packing: DNA shown in red and Histones shown in yellow. (adapted from[29])

7.2 Epigenetics

Although the chromatin structure has a large impact on the regulation of gene expression, there is still a lack of information about how individual epigenetic marks are transduced and maintained though DNA replication and cell division[62]. In 1958 Waddington introduced the term epigenetic as “the branch of biology which studies the causal interactions between genes and their products which bring the phenotype into being”[63]. Since then the term epigenetics has been essentially redefined by many to refer to chemical modifications of histones and DNA. Today epigenetics is defined as “the study of mitotically and/or meiotically heritable changes in gene functions that cannot be explained by changes in the DNA sequence”[64]. Epigenetic modifications lead to different gene expression levels by shaping the chromatin structure, thereby inducing cell type specific phenotypes[62]; hence, epigenetic modification provide an additional layer of information stored on the DNA. This is for example achieved by switching between transcriptionally inactive heterochromatin or transcriptionally active euchromatin, which differ in their DNA accessibility. This mechanism is regulated by histone modifications, like methylation, acetylation or ubiquitinoylation, and DNA methylation[47].

7.2.1 Epigenetic Histone Modifications

The small and highly basic core histone proteins are composed of a globular domain and flexible “histone tails”, which protrude from the surface of the nucleosome[47]. Beside the initial covalent modifications, acetylation and methylation of core histones[65,66], many types of covalent histone modifications, including phosphorylation, ubiquitination, sumoylation, ADP-ribosylation, biotinylation, crotonylation and proline isomerization, have been identified and characterized[67,68]. The site and residue specific histone modifications are established by histone-modifying enzymes (“writers”), catalyzing their reactions with remarkable specificity to target residue and cellular context. A steady-state balance of each modification is achieved together with antagonizing activities (“erasers”), removing these modifications[47] (Fig. 7). Histone modifications are catalyzed by four major enzymatic systems. Histone lysine residues are acetylated by histone acetyltransferases (HATs)[69], whereas opposing histone deacetylases (HDACs) remove these acetyl-groups[70]. The histone kinase family achieves the phosphorylation of serine, threonine and tyrosine residues, whereas the phosphatases remove the phosphorylation marks[47]. Beside these two major enzymatic systems, two general classes of histone methylating enzymes have been described. Histone lysine methyltransferases (KMTs) catalyze the more chemically stable methylated lysine residues, which are present in mono-, di- or trimethylated states[71]. These methyl groups can be removed by histone lysine demethylases (KDMs). The mono- and dimethylation of H3K4 and H3K9 is removed by the lysine-specific amino oxidases histone demethylase 1 (LSD1) and histone demethylase 2 (LSD2)[72]. Other methylated residues on the H3 tail are demethylated by hydroxylases[72] containing a JMJC domain[73]. Histone arginine residues are methylated by protein arginine methyltransferases (PRMTs)[71]. This methyl groups can be indirectly removed by the action of protein arginine deiminases, converting methylarginine or arginine itself to a citrulline residues[74].

Covalent histone modifications can change the physical properties of histone tails, such as a modulation in the electrostatic charge or tail structure, altering inter-nucleosomal contacts and spacing[47]. For example phosphorylation can generate “charge patches” by the addition of negative charge[75], leading to altered nucleosome packaging or an altered higher-order folded state of the chromatin polymer, exposing histone amino termini[76,77]. Also the addition of bulky modifications, like ubiquitin[78], ADP-ribose[79] or *O*-GlcNAcylation[80] changes the arrangement of histone tails and might decondense nucleosome arrays. Modification-binding partners (“readers”) can further affect the chromatin (Fig. 7). Such readers, like bromodomain, chromodomain or Tudor domain have affinities specific for particular histone modifications. Bromodomains together with HAT enzymes are often part of larger chromatin remodelling complexes[81,82] and recognize acetylated histone residues[69]. Methylated histone tail residues can be read by chromodomains or Tudor domains, which are part of complexes that facilitate chromatin-modulating events[83].

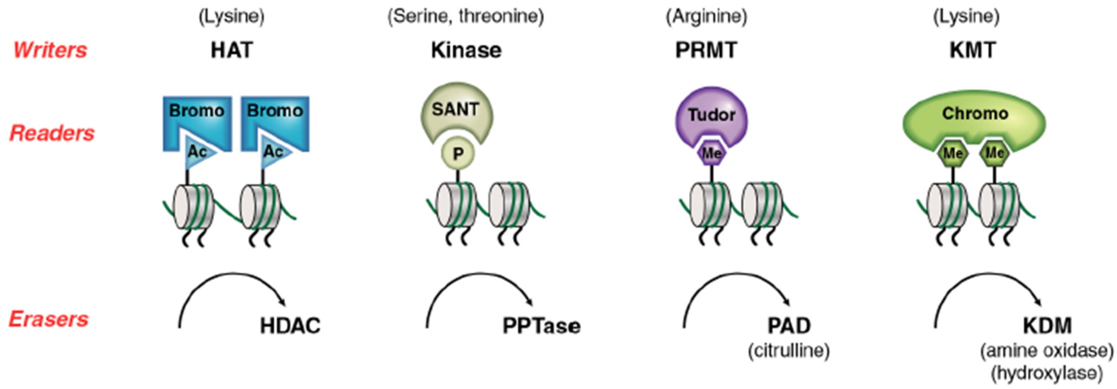

Figure 7 Writer, readers and erasers of histone modifications. Histone-modifying enzyme ("writers") introduce covalent histone modification that are detected by modification-binding partners ("readers"). These histone modifications can be removed by antagonizing activities ("erasers"). HAT: Histone acetyltransferase; PRMT: Protein arginine methyltransferase; KMT: Lysine methyltransferases; HDAC: Histone deacetylase; PPTase: Protein phosphatase; PAD: peptidylarginine deiminase; KDM: Lysine demethylase; Ac: Acetylation; P: Phosphorylation; Me: Methylation.

Nucleosomes bound to repressive chromatin-associated factors can lead to an intrinsic inhibition of the transcription machinery, which leads to a hindrance in binding of transcription factors and regulators to their binding site. Hence, only a few transcription factors and regulators can access their binding site[84]. Protein complexes, that mobilize nucleosomes or alter their structure[85], can create higher accessible chromatin. Chromatin-remodeling activitiesoften work in concert with activating chromatin-modifying enzymes that can engage remodelling complexes to cause a transition from a repressive chromatin state to an active one[68]. Such chromatin remodelers can cause significant changes in histone:DNA contacts, resulting in looping, twisting and sliding of nucleosomes[86]. The covalent histone modifications and the noncovalent mechanisms, are important for gene regulation. An interplay of these mechanisms is shown by the transcription initiation and elongation by the RNA polymerase II (Pol II). The primary contact of Pol II to a promoter region for transcription initiation as well as the transcriptional elongation can be obstructed by the presence of nucleosomes. Through an interplay of histone modifications, modification binding partners and chromatin-remodelling complexes[87] Pol II can passage through nucleosomal arrays[88–90].

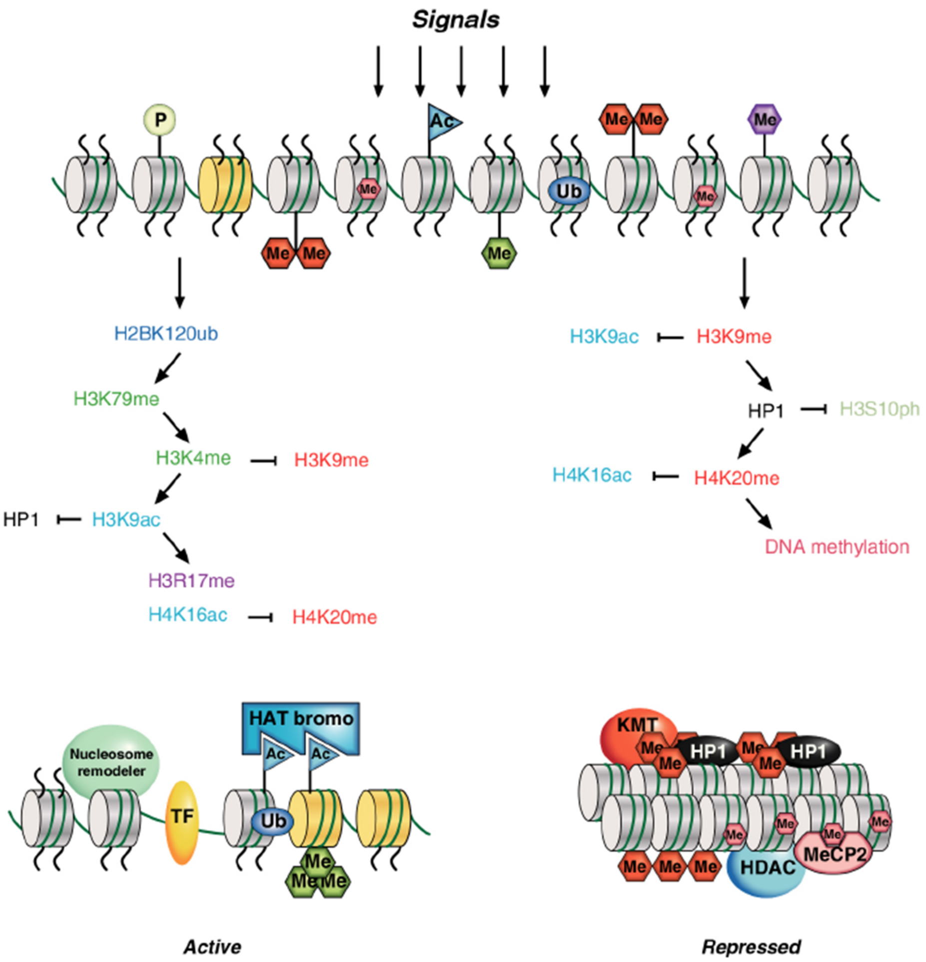

Figure 8 Cascade of histone modifications. Transition of chromatin to active euchromatin (left) or repressive heterochromatin (right) through coordinated chromatin modifications. Transcriptional activation is achieved by nucleosome remodelling complexes that create nucleosome-depleted regions (NDR) at the promoter, accessible for TFs and the replacement of core histones with other histone variants (yellow). An enrichment of histone acetylation recruits readers with bromodomains. In addition, euchromatin contains ubiquitinated histones and H3K4me3. In the repressive state DNA methylation (pink) recruits methyl-CpG-binding domain (MBD) readers, like MeCP2. Heterochromatin marking proteins, such HP1, are recruited through H3K9 methylation, introduced by KMTs.

The establishment of covalent histone modifications requires the presence or absence of other histone modifications and their recognition by other factors. The transition from active euchromatin to repressive heterochromatin is achieved by numerous combinations of histone marks, that function in a concerted fashion (Fig. 8). Histone acetylation is often associated with transcriptionally active chromatin regions, whereas other modifications, like phosphorylation, are associated with condensed and inactive chromatin. Constitutive heterochromatin is found in centromere regions, where clustered repeats and repetitive elements generate stable heterochromatic domains marked by repressive epigenetic marks.[47] Some of these repetitive elements are transposed to other chromosomes, where these “silencing domains” can suppress gene expression[91]. Furthermore, telomeres are also regions of constitutive heterochromatin, serving as chromosomal “caps” to stabilize the genome. Last, heterochromatin formation serves as defense mechanism against invading DNA, particular in higher eukaryotes[47].

7.2.2 Epigenetic Cytosine Modification

Modification of nucleobases in the major groove can affect binding of regulatory DNA-binding proteins without dissociating Watson-Crick base pairing and shape the structure and function of the genome; hence, the major groove contains a nucleobase-specific layer of chemical information. The first and most common epigenetic nucleobase modification is the methylation of the at the fifth position of the pyrimidine ring of cytosine (5-methylcytosine, 5mC), which plays a vital role in tissue-specific gene expression, cell differentiation, and developmental processes such as X-chromosome inactivation and imprinting in mammals[92–96]. The methylation of the fifth position of cytosine occurs most likely in a cytosine-phosphate-guanine (CpG) context, even if the mammalian genome is globally CpG depleted. However, 60–80 % of the existing CpGs are methylated, which are mainly present in repetitive sequences, intergenic regions, and gene bodies. In contrast, only 10 % of CpGs, located in CpG dense regions, named CpG islands (CGIs), are hypomethylated[96,97]. These regions are prevalent at promoters of housekeeping or developmental regulator genes. As their methylation is generally associated with gene silencing, it affects gene expression of individual genes that define the cellular phenotype[98].

DNA methylation patterns are often highly dynamic, which is essential during early development. In the very early development, the epigenetic methylation pattern is erased by DNA demethylation, and pluripotency associated genes are expressed, while developmental genes are repressed[95,96,98]. Later, the pluripotency-associated genes of pluripotent cells, such as embryonic stem (ES) cells, are repressed to induce cell differentiation[96].

In eukaryotes, three different DNMTs, DNMT1, DNMT3a and DNMT3b drives DNA methylation. Although the three DNMTs display the same methylation mechanism, they act in different manners. While DNMT3a and DNMT3b introduce cytosine 5-methyl-group *de novo*, DNMT1 is responsible for the maintenance methylation[99–101]. DNMT1 is specific to CpG context and prefers hemimethylated DNA, i.e. DNA methylated at CpG on one of the two strands[102]. Thus, DNMT1 restores the methylation pattern of a cell after chromosome replication and repair, explaining its high expression in proliferating cells compared to the low expression in non-dividing cells. UHRF1 (ubiquitin-like plant homeodomain (PHD) and ring finger domain protein) binds selectively to hemimethylated CpGs[103]. UHRF1 also interacts with H3K9me3-marked chromatin, connecting DNA methylation and the repressive histone methylation[47]. In contrast, the other two methyltransferases DNMT3a and DNMT3b introduce cytosine methylation *de novo* by interacting with catalytic inactive DNMT3L; hence, they show no preference for methylating hemimethylated DNA[104]. The histone modification H3K4me3 counteracts DNA methylation by inhibiting the binding of DNMT3L to DNMT3a and DNMT3b, thereby protecting CGIs from DNA methylation[71]. The inactivation of both Dnmt3a and Dnmt3b in ES cells leads to the inability of *de novo* methylation, confirming that these genes are the missing *de novo* DNA methyltransferases [105]. This shows the importance of DNMT3a and DNMT3b for the introduction of new methylation patterns during early embryonic development.

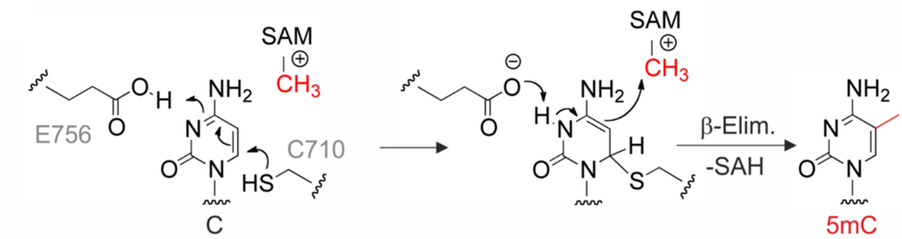

Figure 9 DNMT-mediated methylation of Cytosine with SAM: The conserved cytosine residue C710 of DNA methyltransferases serves in its deprotonated form (thiol anion) as a strong nucleophile, attacking the C(6) cytosine atom. The negative charge on cytosine is stabilized by interacting with a glutamate residue. By transferring the methyl group *via* a Nucleophilic attack, S-adenosyl-l-methionine (SAM) is converted to *S*-adenosyl-l-homocysteine (SAH). The β-elimination releases the enzyme.

DNMT1, DNMT2, and the DNMT3 family members have conserved signature motifs, I, IV, VI, IX, and X in the catalytic domains, whereas among their amino terminal regulatory domains they only show little similarity. The motifs I and X are responsible for the cofactor binding, while the motifs IV and VI are involved in catalytic functions[102]. Furthermore, the catalytic domain contains the amino acid motif SAM-dependent MTase fold, which catalyzes the binding of DNMT to its cofactor S-adenosyl-L-methionine (SAM) and the targeting of the cytosine substrate [106] (Fig. 9).

Cytosine 5-methylation is generally associated with repressed transcription states in mammalian genomes. This can be accomplished by direct inhibition of proteins that recognize DNA *via* the DNA major groove. For example, transcription factors (TFs), binding to non-methylated DNA motifs in open chromatin regions can be repelled by methylation on the CpG sites in these motifs. Alternatively, methyl-CpG binding-domain (MBD) proteins can be recruited to the methylated DNA motifs and compete with TFs by the virtue of their higher affinity to 5mC sites in a sequence independent fashion[107]. These so-called methylation readers are proteins that specifically bind to methylated CpG dinucleotides and mediate the epigenetic crosstalk between DNA methylation, histone modifications and chromatin organization. The main MBD proteins are MBD1, MBD2, MBD3, MBD4 and MeCP2, binding single symmetrically methylated CpGs *via* their MBD domains[47].

However, whereas the process of C methylation by DNMTs is relatively well studied, the process of 5mC demethylation is not. It has long been assumed that DNA demethylation occurs only passively through replication-dependent 5mC dilution due to the inhibition of maintenance methylation by DNMT1. However, in the early development, the paternal methylation levels decrease rapidly, thus an active demethylation pathway was presumed. In 2009 the oxidation of 5mC to 5-hydroxymethylcytosine (5hmC) by ten-eleven translocation (TET) dioxygenases was discovered. Further studies investigated the iterative oxidation from 5hmC to 5-formylcytosine (5fC), and 5-carboxylcytosine (5caC) by TET, indicating an active demethylation cycle[10–14]. Restoration of unmodified cytosine is completed by excision and replacement of 5fC or 5caC with C *via* thymine DNA glycosylase (TDG)-mediated base excision repair (BER)[13] (Fig. 10). These findings have revealed that gene expression regulation by 5mC is not static, but rather a highly dynamic process.

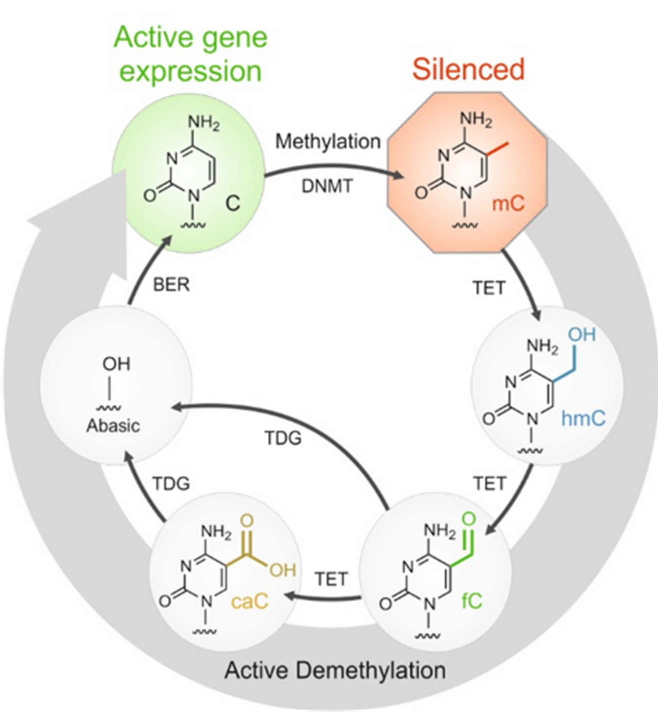

Figure 10 DNA Demethylation Pathway and Dynamics: **a** Cycle of cytosine methylation and active demethylation. Cytosine Methylation occurs at the carbon 5-position, catalyzed by DNA-methyltransferases (DNMT). The stepwise oxidation from 5mC to 5hmC, 5fC and 5caC is catalyzed by ten-eleven translocation (TET) dioxygenase. 5fC and 5caC are being excised and replaced with C *via* thymine DNA glycosylase (TDG)-mediated base excision repair (BER)[108].

The DNA methylation can reverse in two different ways. First *via* the passive demethylation mechanism and second through the active demethylation pathway which is mainly catalyzed by TET enzymes[109,110]. TET enzymes are members of the large superfamily of Iron/2-OG (2-oxoglutarate) dependent dioxygenases. During the oxidation the oxygen atoms of molecular oxygen are transferred to the co-substrate α-KG (α-ketoglutarate) and to the 5-methyl-group, leading to decarboxylation and hydroxylation under the formation of a reactive Fe(IV)-oxo intermediate and the by-products CO_2 and succinate(Fig. 11)[111,112]. After hydrogen abstraction from the cytosine 5-group, a respective oxidized group is generated. TET1 and TET3 possess an N-terminal CXXC zinc finger, which has a high affinity for demethylated CpG dinucleotides. This enables TET1 and TET3 to bind methylated, hydroxymethylated as well as unmethylated CpGs. TET enzymes preferentially oxidize 5mC in a CpG context to 5hmC, instead of 5hmC to 5fC or 5fC to 5caC, which could be explained by the different binding and catalytic activity towards the different cytosine modifications or their variable ability for hydrogen abstraction.[12,113]

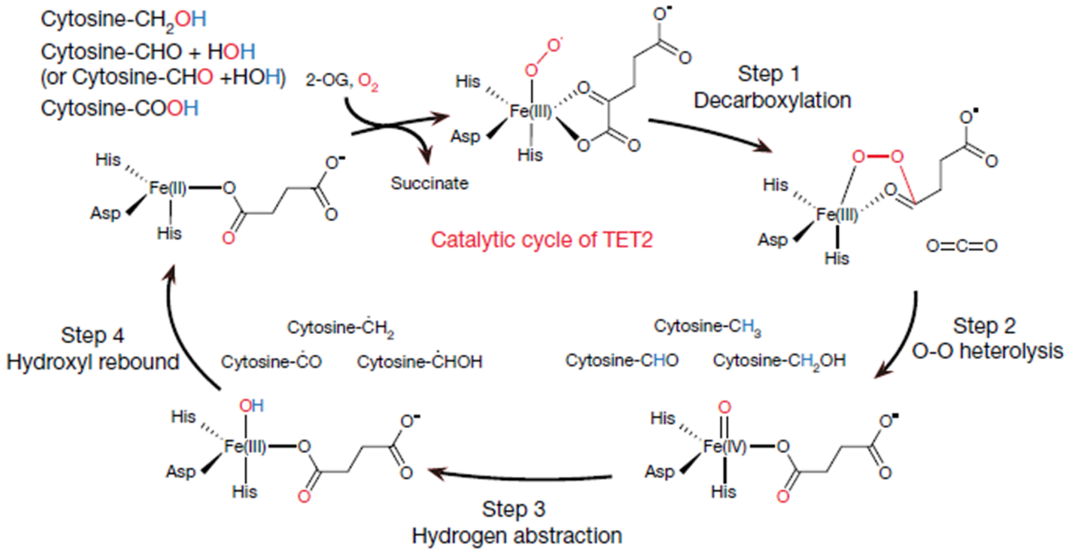

Figure 11 Step-wise Oxidation catalyzed by ten eleven translocation (TET) dioxygenase: Transfer of oxygen to 5-methyl group and 2-oxoglutarate under decarboxylation. Followed by hydrogen-abstraction from cytosine the 5-group and generation of the respective oxidized group. (adapted from[114])

The genomic levels of oxidized 5mC derivates are cell type dependent and are relatively low compared to 5mC levels. 5hmC is the most stable and the most abundant oxidized form (~5 % of all 5mC). The lowest level was found for 5caC, with approximately 0.01 % of 5mC. In between that, the levels of 5fC ranges from 0.06 % to 0.6 % of the entire 5mC fraction[12,13,115]. However, the genomic content of the oxidized derivates is highly variable in different tissues[12]. The levels of 5hmC range from 0.03 % of all cytosines in the spleen to the highest steady-state level of 0.7 % in the brain[116,117]. The variability in 5hmC levels and the detection of 5hmC binding proteins, like methyl-CpG-binding protein 2 (MeCP2), suggests that 5hmC is a stable epigenetic mark for regulation of chromatin structure and gene expression[118,119]. Further studies have shown 5fC as a stable DNA modification[117] and have discovered 5fC binding partners. They concluded that the stable 5fC-modified DNA has functional roles going beyond being a demethylation intermediate, and is therefore rather playing a role in the regulation of gene expression[117,119]. Also for 5caC, even if it is rather low in abundance, several reader proteins were detected and a functional impact of both, 5fC and 5caC, on cellular processes were demonstrated[119,120]. For example, 5fC and 5caC can stall transcription by eukaryotic RNA polymerase II *in vitro*. All of the oxidized

5mC derivates may impact DNA flexibility in nucleosomes, where 5fC can form covalent imine crosslinks with lysine/arginine residues of the NCP and other DNA binding proteins *in vitro*.

While the variability of oxidized 5mC derivate levels is important in pre-implantation development and differentiation, aberrant levels of these forms have been linked to various diseases. For example, an up to eightfold reduction of 5hmC levels in cancer tissue relative to healthy tissue was observed, probably due to a downregulation of TET family enzymes[117,121]. Hypermethylation in CGIs of tumor suppressor gene promoters leads to cancer development by downregulation of a gene[122]. On the other side DNA hypomethylation can lead to the activation of single copy proto-oncogenic genes. Furthermore, hypomethylation of repetitive DNA is associated with decondensing of the chromatin structure, which changes the transcriptional landscape of the cell[123].

Even if connections between aberrant levels of epigenetic cytosine modifications and abnormal cell behavior have been shown, there is still a need of further investigation to understand the epigenetic network, its mechanisms, and the biological relevance of the individual cytosine modifications and their readers.

7.3 Components of the human genome

Euchromatin largely consists of coding and regulatory sequences of the genome, whereas over 50 % of the mammalian genome consists of noncoding sequences that can adopt heterochromatic marks[47]. Studies like the ENCODE project provided new insides into the organization and regulation of our genes and genome by assigning biochemical functions for 80 % of the genome[124]. The overall sequence composition and structure divides the genome sequence into different goups. Less than 1.5 % of the total human genome sequence consists of protein-coding genes. In contrast, non-coding sequences such as introns (~26%) and transposable elements (~45%)[125] build the majority of the human genome. Transposable elements are part of repetitive DNA, which is estimated to represent 50–70 % of the human genome (Fig. 12).

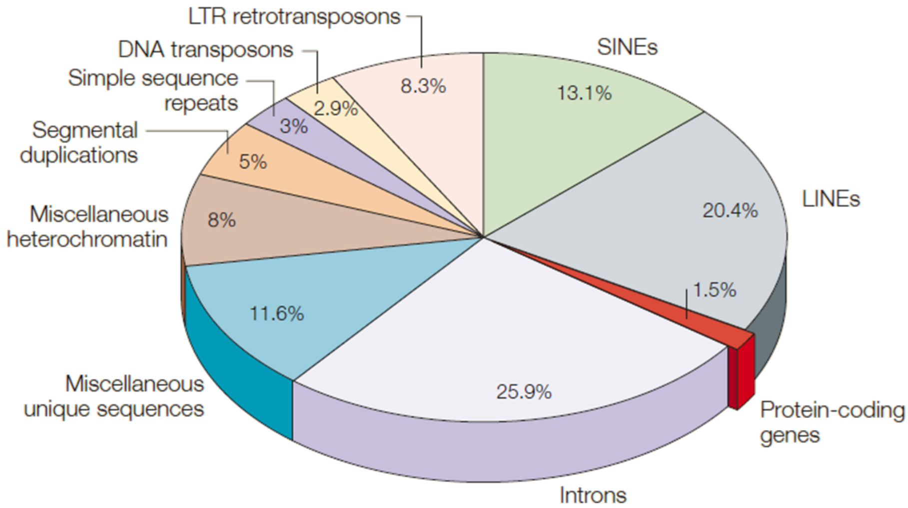

Figure 12 Main components of the human genome: Less than 1.5% of the genome consists of the suspected 20,000–25,000 protein-coding sequences. A large majority is made up of non-coding sequences such as introns (~26%) and transposable elements (~45%). (adapted from[126])

Repetitive DNA is defined as sequences that occur multiple times in the genome. This encompasses a huge variety of DNA elements of diverse structure and origin. They are grouped into two broad distinct classes, the tandem repeats and the interspersed sequences[123]. Tandem repeats are short, non-coding sequence stretches that are repeated in a head to tail fashion, whereas interspersed repetitive sequences are mostly retrotransposons, which have a defined structure. Retrotransposons are flanked by short repeats and often encode for a unique set of proteins, which enable them to change position in the genome[127]. The excision and insertion of non-coding sequences into coding sequences or regulatory elements lead to alterations of gene structure or gene expression. However, epigenetic marks represent a second layer of regulation that do not alter the genetic sequence of chromosomal DNA[128]. The activation and expansion of the CpG-rich retrotransposons[123] can prevented by the formation of heterochromatin by methylation of H3K9 and DNA[127].

Tandem repeats are accumulated in centromeric and pericentromeric heterochromatin and at telomeres[127,129]. Centromere function and chromosome segregation is regulated by the gene-poor pericentric heterochromatin[130–132] by interacting with other subnuclear components of diverse function[130]. For instance, in human, the pericentric SatIII DNA is transcribed upon various stress signals (e.g. heat, heavy metals, UV-C, oxidative and hyperosmotic stress), leading to the formation of nuclear stress bodies (nSBs)[133]. The heat shock response of mammalian cells is a highly conserved and regulated process to overcome cellular stress. Upon heat stress the BRD4 proteins are recruited to nSBs, where the transcription factors HSF1 and CREBBP accumulate in response to the HS. The recruitment of BRD4 by HSF1 may enhance the elongation rate of Pol II and thereby increases the transcription of heat induced SatIII RNA. Subsequently, SatIII transcripts recruit several RNA-binding proteins, such as the splicing factors SRSF1 to nSBs that may induce splicing processes (Fig. 13).[134–136] Furthermore, SatIII DNA shows an aberrant methylation pattern in various cancer types[129,137]. However, so far, the high abundance of these repetitive loci complicates their selective amplification, sequencing and alignment; hence, the epigenetic control of SatIII DNA and of nSB formation is poorly understood [123,127].

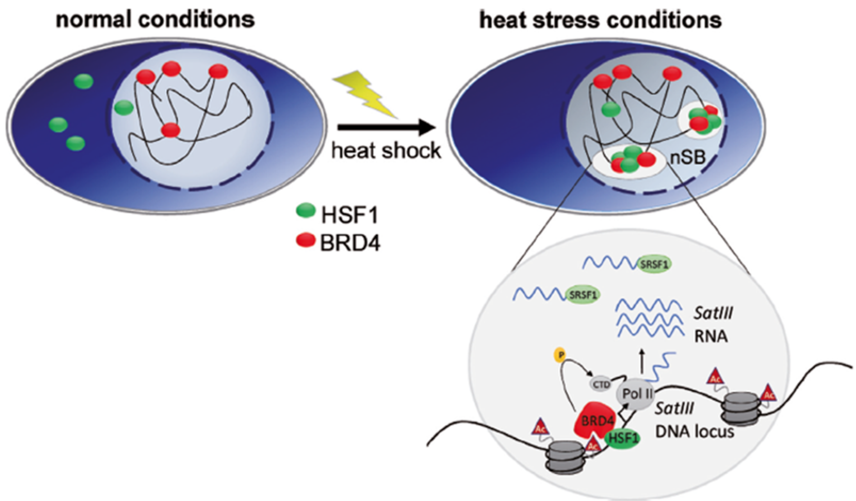

Figure 13 Schematic representation of the heat shock response: Upon heat stress, nuclear stress bodies (nSB) are formed and BRD4 and HSF1 are recruited to the nSB. In the nSB Polymerase II (Pol II) transcribes SatIII DNA. SatIII RNA recruit several RNA-binding proteins, such as the splicing factors SRSF1 to nSB that may induce the splicing process. (adapted from[135])

7.4 Purification of User-defined Genomic-Loci

The heterogeneity in the chromatin composition depends on cell type and the stages in the cell cycle and is mostly locus specific, thus, determining the function of the locus[138]. However, the biochemical nature of chromatin domains is poorly understood compared to other cellular organelles[3], indicating the need for purification methods of user-defined genomic loci, that retain molecular interactions and are suitable for proteomics. This would allow correlations of local chromatin states with phenotypes and thus is the key to a deeper understanding of the regulation of the eukaryotic genome.

Such methods should allow efficient isolation of user-defined genomic loci, while being independent of genetic engineering of the target locus and fully programmable. Furthermore, isolation of soluble chromatin containing user-defined genomic loci, while maintaining molecular interactions with reduced false positive detection is necessary. This is a highly challenging goal, due to the low abundance of proteins in comparison to the overall background. Consequently, locus specific chromatin purification requires a suitable enrichment factor with regard to the relative abundance of locus in the genome.[138]

Several years ago already some approaches for the isolation of repetitive loci were developed[139–142]. With the upcoming development in mass spectrometry, new techniques in combination with proteomic analyses were developed to identify proteins interacting with a locus of interest[4,143–147]. Since chromatin, as a complex heterogeneous mixture of nucleic acids and proteins, requires specific conditions to preserve noncovalent interactions and solubility *in vitro*, chromatin preparation is a challenging goal[148]. Classical native chromatin preparation methods uses solubility-increasing regents, which, however, can perturb important interactions. Covalent chemical crosslinking, using formaldehyde[149], can stabilize the chromatin and conserves many interactions. Furthermore, the abundance of the locus of interest determines the amount of starting material, since the detection limit by standard MS is in the low femtomole range (10^{-15} mol), which correspond to 600 million molecules[138]. 300 million diploid cells are required to identify a single protein interacting with a single-copy locus if a purification yield of 100 % can be achieved[138,150]. In addition, the abundance of components to be identified plays a major role, considering the amount of starting material. For instance, at pericentric regions only one SUV39H histone methyl transferase per 170 nucleosomes can be found[151]. Not only the number but rather the size of the target locus determines its relative abundance. A 3 kb-long target sequence represent 0.0001 % of the human genome, whereas telomeres with a size of 300 kb cover 0.01 %[138,150]. The relative abundance in turn defines the needed enrichment factor and thereby the purifications requirements. For example, a 33-fold enrichment of the pericentromere, representing 3 % of the human genome, would lead to a nearly pure pericentromeric fraction, whereas a single copy 3 kb target sequence would require a 1-million fold enrichment[138]. However, the binding event used for target isolation, which defines the stringency of the procedures used to reduce false positive components, determines sensitivity and selectivity of the purification method of user-defined genomic loci.

The first reported method, proteomics of isolated chromatin segments (PICh), for the purification of user-defined genomic loci in combination with proteomics uses synthetic nucleic acids (locked nucleic acids (LNA) or modified RNA) as hybridization probes[2,4,152–154]. In this case, the locus specific capture results from hybridization of the complementary synthetic nucleic acid probe to the unique DNA sequence. This makes prior knowledge about the proteins, which bind to the user-defined locus, or genetic engineering of target cell unnecessary. Further isolation is given by the harboring biotin analog desthiobiotin interacting with streptavidin-conjugated beads (Fig. 14a). In the current version this methods provides a 10.000-fold enrichment[138]. However, the method is limited by the difficulty of obtaining PICh capture probes from oligonucleotide companies. In addition, these probes are only working at the 3' end of the target locus, complicating the preparation and fragmentation of chromatin[154]. Moreover, the required cell numbers were extremely high[138], indicating a low sensitivity. A similar approach is the hybridization capture of chromatin-associated proteins for proteomics (HyCCAPP)[147,155] (Fig. 14a). With an 80–800-fold enrichment[155,156], it was used to characterize the composition of repetitive and single-copy loci in yeast. Even if the synthesis of HyCCAP DNA probes is easier, which facilitates the targeting of large complex loci, the DNA probes bind with lower stability, explaining maybe the lower enrichment factor compared to PICh. This enrichment factor gives only 8 % of the used single-copy ~1.4 kb locus from the yeast genome (~0.01 % of the genome)[147], which is only sufficient for the identification of interaction partners, only abundant at the target sequence.

Other approaches use hybridization of the target DNA sequence in combination with nuclease-dead Cas9 (dCas9). A programmable 20-nucleotide-long guide RNA (gRNA) is associated with affinity-tag functionalized dCas9 (Fig. 14b). In first settings, theses complexes for targeted binding were combined with immunoprecipitation by bead-bound antibodies[146,157]. The CRISPR-dCas9 (target specificity clustered regulatory interdispersed short palindromic repeat) system can lack in target sensitivity due to 10 to 1000 off-target binding sequences[158], depending on the gRNA. Consequently, the non-covalent antibody binding results in a bottle-neck for the necessary reduction of false positives, which requires stringent washing steps[1,146,157]. Alternative approaches like CAPTURE[17] (Fig. 14b) uses CRISPR-dCas9 together with biotin acceptor sequences *via* BirA for *in vivo* biotinylation of close-by proteins followed by isolation with streptavidin-conjugated beads. This provides stronger interactions, but could also come with high off-target biotinylation levels[17,144]. The purification of telomeres, showing several telomere- specific binding proteins, validated the method. Nevertheless, three abundant shelterin proteins could not be identified, which may indicate that the binding of dCas9 compete with some relevant proteins from telomeres *in vivo*. This issue was recently addressed by performing Cas9-locus-asscoicated proteome (CLASP) affinity capture (Fig. 14b) *in vitro* using soluble crosslinked chromatin on an immobilized dCas9-gRNA complex[159]. However, not all shelterin proteins could be identified, suggesting a bias in the method.

Other epitope-tagged programmable proteins, such as transcription-activator-like effectors (TALEs) can be designed to bind specific DNA sequences[160], which can be enriched by immunoprecipitation[1,143,161] (Fig. 14d). Similar to dCas9 the binding of the TALE proteins can also compete with specific interaction partners *in vivo*, since the purification of telomeric chromatin did not show shelterin proteins[1]. If endogenous proteins uniquely bind the DNA sequence, an immunoprecipitation can be performed against these proteins after crosslinking to the chromatin[162,163] (Fig. 14c). However, this approach requires prior knowledge about the proteins that only bind to the specific locus.

Another strategy introduces a DNA sequence to the locus of interest by genomic engineering, which can be bound by adaptor proteins, like Tet or LexA[143–145,164] (Fig. 14e). The purification of the PHO5 gene promoter by performing two orthogonal enrichment steps provided a 100.000-fold enrichment[18]. However, the native chromatin preparation led to the loss of important interaction partners[18,145].

Proximity-labelling approaches like CasID uses the promiscuous biotin ligase BirA* fused to dCas9[19], thereby overcoming the issues in chromatin preparation to maintain relevant protein interactions (Fig. 14f). After *in vivo* biotinylation of nearby proteins, these proteins are individually enriched on streptavidin-conjugated beads. Similarly, the recent developed approaches C-BREST[20], CAPLOCUS[21] and GLoPro[22] fuse the engineered ascorbate peroxidase APEX2 to dCas9. APEX2, generates phenoxyl radicals from biotin–phenol compounds in the presence of hydrogen peroxide. The radicals react with surface exposed tyrosine residues, thus labelling nearby proteins with biotin derivatives[165]. In comparison to BirA* based methods APEX2 biotinylation is much faster, which shortens the incubation time and thereby may reduce unspecific biotinylation. However, the enrichment of a single-copy promoter showed an enrichment of some canonical promoters factors or RNA polymerase II subunits, also in the negative controls[22], suggesting unspecific biotinylation of biological relevant proteins. Since the overexpression of dCas9 fused to biotinylating factors leads to a vast majority of non-associated or nonspecific bound fusion construct, an undefined background is created by nonspecific biotinylated proteome contributing to noise. Although biotin-streptavidin interaction is preferred over antibody interactions, the high proportion of nonspecific biotinylation in these methods shows the need for alternative biotinylation methods in combination with the purification of user-defined genomic loci.

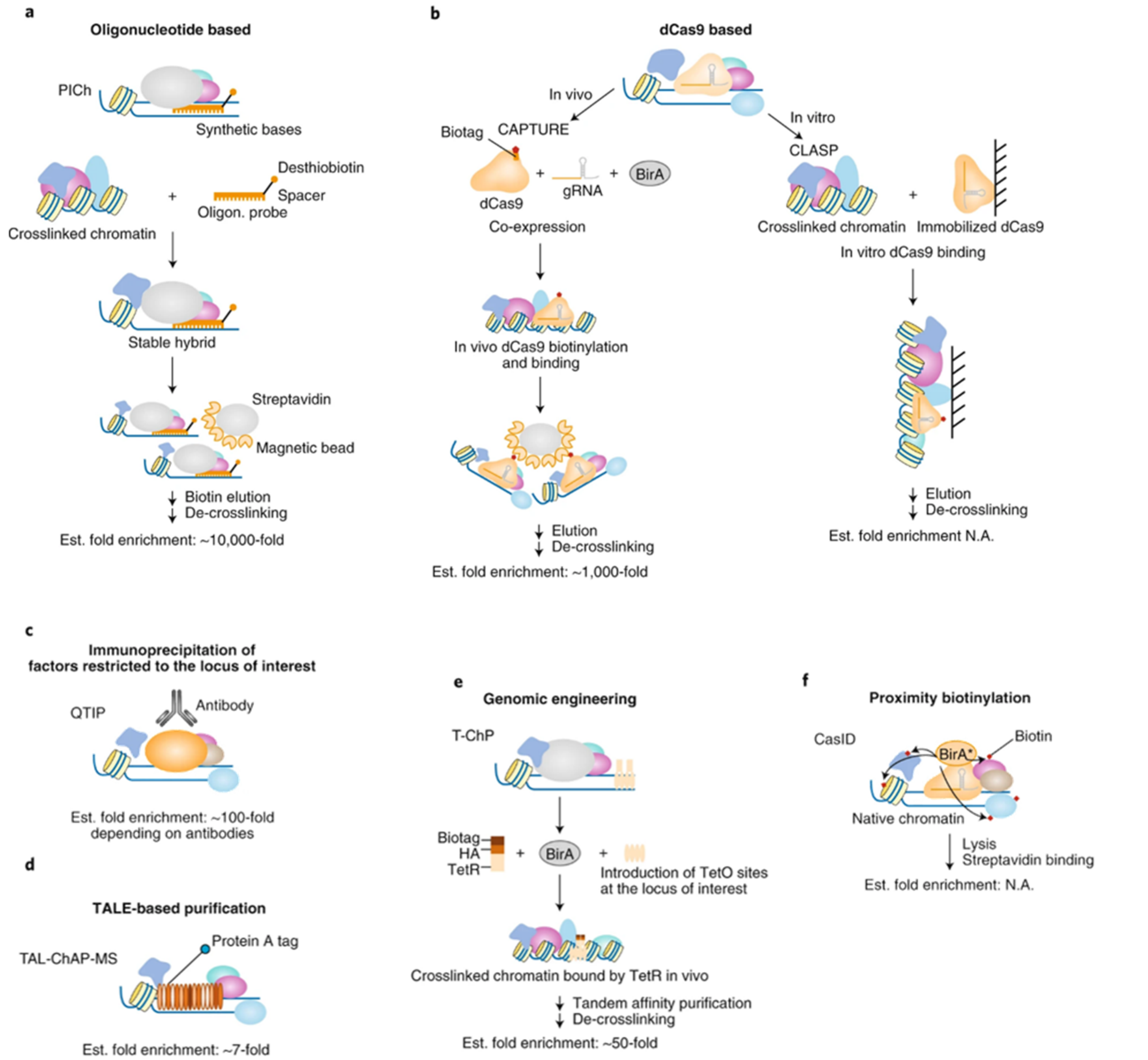

Figure 14 Approaches for specific chromatin loci isolation. **a** Direct hybridization of capture probes to chromatin. **b** Purification based on nuclease-dead Cas9 (dCas9). **c** Immunoprecipitation of proteins, binding uniquely at the target locus. **d** Purification based on the binding of sequence specific adaptor proteins. **e** Tandem affinity purification that requires genomic engineering of the target locus **f** Proximity-labelling approaches. (adapted from[138])

7.5 TALEs

7.5.1 Origin of TALE proteins

In the gram-negative plant pathogenic *Xanthomonas* bacteria found TALE proteins are naturally occurring DNA binding proteins. TALEs function as transcription activators of plant genes which are involved in infection and disease resistance[166–168]. A type III secretion system (T3SS) leads to pathogenicity in susceptible hosts and the induction of the hypersensitive response in resistant plants. A 23-kb hrp (hypersensitive response and pathogenicity) gene cluster encodes this specialized protein transport system, which is required for translocation of TALEs into the host cell. Here, the type III-secreted proteins are in close contact with the Hrp pilus (filamentous structures produced at the cell surface) during their secretion. These structures create a novel surface appendage, allowing the translocation of the TALE proteins into the plants cell cytoplasm[169].

7.5.2 Structure and binding mode of TALE proteins

TALE proteins consist of three different parts[170]. The N-terminal regions of wild type TALE proteins carries the type III secretion signal[171]. This region is followed by the central repeat domain, which is responsible for DNA binding. The third part is the C-terminal region, containing a nuclear localization signal (NLS) and an activation domain (AD)[172,173]. The central repeat domain (CRD) is built up by an array of repeat units and is terminated by a truncated “half repeat”[170]. Each repeat is highly conserved and consists of 33 to 35 amino acids. Only the two amino acids 12 and 13 of every repeat are not conserved and therefore named repeat variable di-residue (RVD). Every repeat of the CRD interacts with one single nucleobase *via* the RVD[174,175]. The RVDs can consist of the amino acids HD (His12, Asp13), NG (Asn12, Gly13), NI (Asn12, Ile13) or NN (Asn12, Asn13), thereby selectively recognizing C, T, A, and G, respectively[176,177] (Fig. 15).

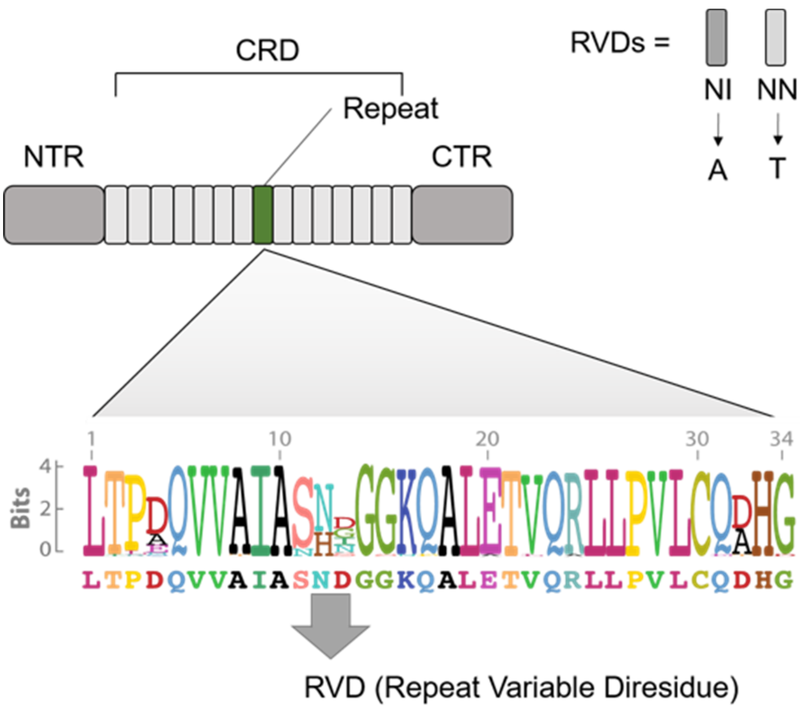

Figure 15 General design a transcription activator-like effector (TALE) and the canonical TALE code: Schematic structure of the TALE including the N-terminal domain (NTR), the central repeat domain (CRD), and the C-terminal domain (CTR). Canonical RVDs NI (Asn12, Ile13), NN (Asn12, Asn13), NG (Asn12, Gly13), and HD (His12, Asp13) recognizing adenine (A), guanine (G), thymine (T) and cytosine (C), respectively. (adapted from[178])

The RVD is located in a loop region, facing the target nucleobase *via* the major groove of the DNA duplex. Besides the RVD, the core of single repeats consists of small aliphatic residues, enabling close stacking *via* van-der-Waals interactions. The loop region is flanked by two α-helices, containing distinct polar residues that interact with each other. Furthermore, positively charged amino acids like Lys16 and Gln17 in the inner surface contribute to nonspecific contact to the negatively charged DNA phosphate backbone. Together, the concatenated repeats build a right-handed superhelical structure, wrapping around the DNA double helix (Fig. 16).[175,179]

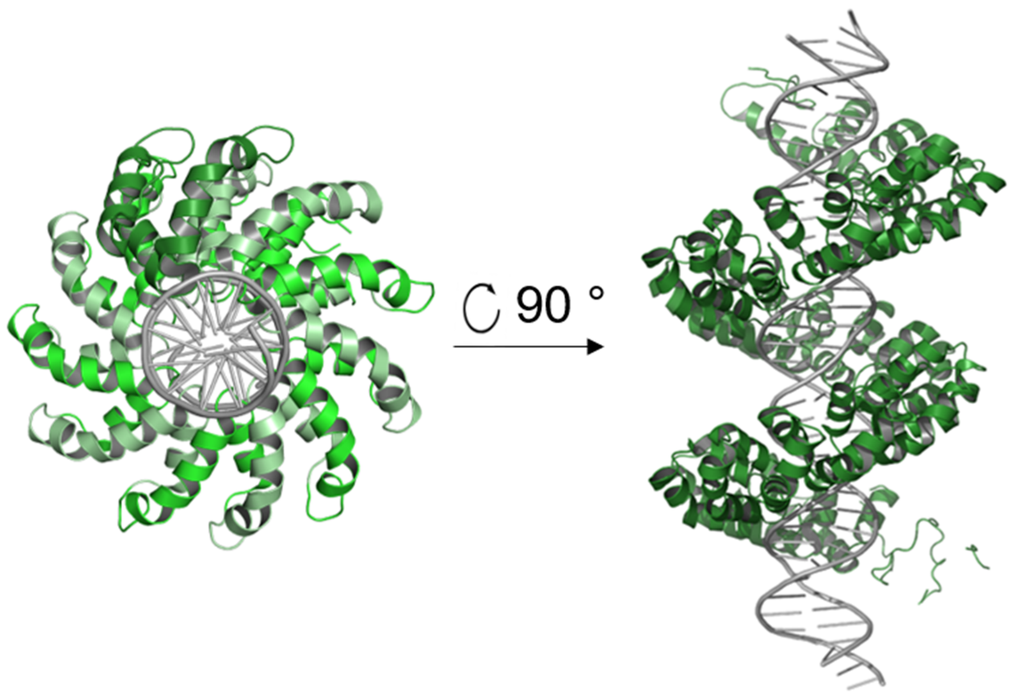

Figure 16 Crystal structures of transcription activator-like effector (TALE) proteins bound to the corresponding DNA sequence: Radial and axial view of the TALE (green) binding to the major groove of the DNA (gray). The individual repeats are separated by different shades of green in the radial view (3UGM pdb[179]). (adapted from[179])

Besides the canonical repeats in the CDR, the N-terminal region contains four similarly structured cryptic repeats, contributing to nonspecific DNA binding. The cryptic repeats (termed repeats –3, –2, –1 and 0) contain two α-helices, which are connected *via* a loop region[180]. The repeat 0 continues the superhelical structure of the canonical repeats, whereas repeat –1 interacts through the indole ring of the conserved tryptophan residue with the methyl group of the 5'thymine *via* van-der-Waals interactions. This leads to the assumption that a 5'thymine in the TALE target sequence is required for an optimal TALE-DNA interaction[180–183]. However, the process of the TALE-DNA complex formation is still not fully understood. It has been observed that the TALEs are loosely wrapped around the DNA duplex while searching their target sequences. In doing so, the TALE slides rapidly along the DNA through reduction in the electrostatic interactions between the positively charged inner surface of the CRD and the negatively charged DNA backbone [175,180]. Upon encountering the DNA target sequences the TALE proteins transits from the search state to the binding state by conformational compaction[175,184].

7.5.3 The DNA recognition code of TALE repeats

The most specific RVDs of the 20 naturally occurring RVD sequences in TAL effectors are HD, NG, NI and NN, that specifically target the nucleobases C, T, A, and G, respectively[170,176,177] (Fig. 17). Therefore, they were used in the design of numerous artificially TALE proteins. Only amino acids 13 of the RVD makes direct contact to the DNA, whereas the amino acid 12 interacts with the carbonyl oxygen of amino acid residue 8 to stabilize the RVD loop structure. Amino acid 13 either interacts with the nucleobase *via* hydrogen bonds or nonpolar van-der-Waals interactions, depending on the RVD[175,179]. The carboxylate oxygen of aspartate 13 (Asp13) in the RVD HD forms a hydrogen bond with the cytosine N4 amino group. The asparagine residue (Asn13) in the RVD NN forms a hydrogen bond to the N7 of the corresponding guanine base. In the other two RVDs, NG and NN, the second amino acid builds van-der-Walls contacts to the corresponding nucleobase. Here, the backbone Cα-atom of glycine 13 (Gly13) of the RVD NG interacts with the methyl group of the thymine base, whereas in the RVD NI the aliphatic side chain of isoleucine 13 (Ile13) builds van-der-Waals contacts to the C8 and N7 of the adenine purine ring[175,179] (Fig. 17).

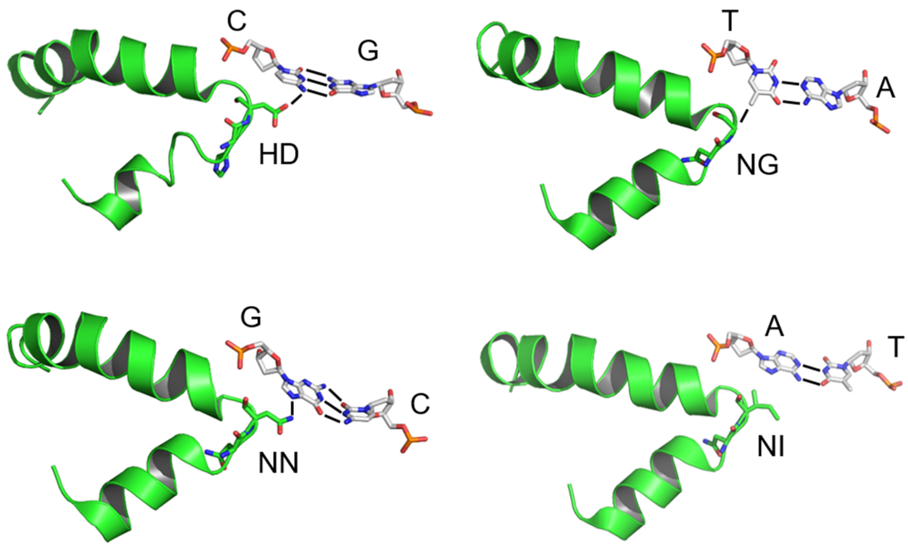

Figure 17 Repeat variable di-residue (RVD)-nucleobase interactions for the canonical RVDs HD, NG, NN, and NI: HD forms a steric and electrostatic contact with cytosine; NG Forms nonpolar interactions between a glycine and the thymine methyl group. NN interacts with the N7 nitrogen of guanine. NI forms a desolvating interface adenine. RVDs shown in green, DNA base pairs shown in grey. (adapted from[179])

7.6 Genetic Code Expansion

7.6.1 Artificial Expansion of the Genetic Code

In mammalian protein translation, the mRNA is translated to the corresponding protein sequence dictated by the genetic code. Three consecutive RNA nucleotides (a codon) code for one of the 20 canonical amino acids. Since there are more than 20 (4^3) codon possibilities, the genetic code is degenerated (Fig. 18b). The translation starts with the loading of an amino acid to a corresponding tRNA molecule catalyzed by the aminoacyl-tRNA-synthetase (aaRS). Through its anticodon loop the tRNA will bind to the complementary mRNA codon which encodes for a specific amino acid. The translation starts with the start codon (AUG) and is terminated at one of the three stop codons, amber (UAG), ochre (UAA) or opal (UGA). After the termination the newly synthesized protein is released from the ribosome and folds into a functional three-dimensional structure (Fig. 18a).[28,29,185]

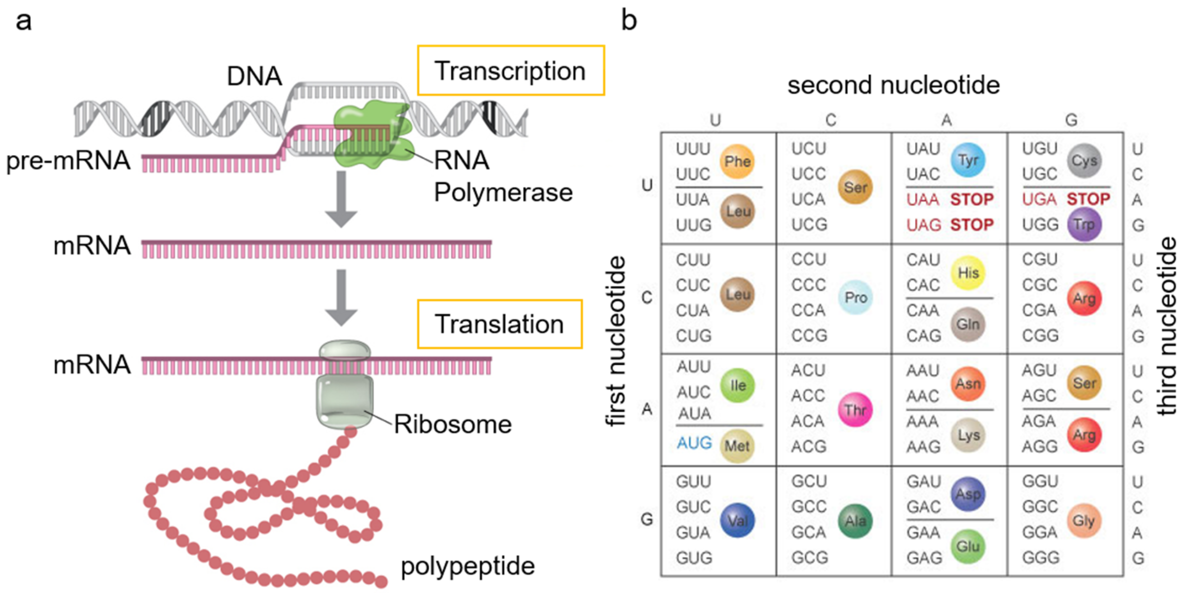

Figure 18 Schematic representation of the protein biosynthesis by transcription and translation with listing of the genetic code: **a** Transcription and translation. During transcription, the enzyme RNA polymerase (green) uses DNA as a template to produce a pre-mRNA transcript (pink). The pre-mRNA is processed to form a mature mRNA molecule that can be translated to a protein molecule (polypeptide) encoded by the original gene. **b** Genetic code. Three consecutive RNA nucleotides (a codon) code for one of the 20 canonical amino acids.(adapted from[186])

The complex processes taking place in organisms require a higher chemical functional diversity of proteins. The protein functions are significantly extend by a variety of cofactors and post-translational modifications (PTM), such methylations, glycosylations and phosphorylations.[187,188]

In organisms there are usually 20 different aminoacyl-tRNA-synthetases (aaRS) that process a larger number of tRNAs. If an amino acid is encoded by several codons, the corresponding aaRS processes several isoacceptor tRNAs. The tRNA recognizes the corresponding mRNA codons either by different, fully complementary anticodon loops or by Wobble base pairing, i.e. one nucleotide in a triplet does not form a Watson-Crick pair[189]. Despite this full occupancy of all sense codons, organisms are sometimes able to extend the function of proteins by co-translational incorporation of non-canonical amino acids (ncAA) using nonsense (stop) codons[190,191]. Two ncAA and associated tRNAs have been found in natural organisms so far[192,193]. Selenocysteine (SeC), also known as the 21st proteinogenic amino acid, can be found in all three domains of life and is incorporated by using a tRNA that recognizes the opal codon (UGA)[194]. In addition, the amino acid pyrrolysine (Pyl) has been found in certain methanogenic archaea and bacteria using a distinct aaRS (PylRS) and tRNA ($tRNA^{Pyl}$) pair, that recognizes the amber stop codon (UAG)[195]. This allows the incorporation of Pyl at the amber codon by an otherwise unchanged ribosomal protein biosynthesis.

Nonsense suppression can be used to artificially expand the genetic code. In this context, the targeted design of tailor-made aaRS can site-specifically introduce new ncAAs into proteins, thus creating novel tools for the analysis of protein structures, functions and interactions[5] (Fig. 19). This approach has some major advantages over other strategies, as modified proteins can be generated directly *in vivo* using the cell's own translation machinery[196]. Previously known systems, such as solid phase synthesis[197], expressed protein ligation (EPL)[198] or chemical modifications of single amino acids[199], come with multiple disadvantages compared to amber suppression, such as size limitation of synthesized proteins, low selectivity in chemical amino acid modifications or the need for microinjections into cells *in vivo* experiments[200].

In 1989 the first *in vitro* experiments were published, showing the expansion of the amino acid repertoire in protein biosynthesis by applying an amber stop codon suppressing tRNA, chemically aminoacylated with noncanonical amino acids[191]. However, the suppression of a stop codon also presents a challenge, since the selective incorporation requires an aaRS/tRNA pair and a corresponding ncAA that are orthogonal to the specific translational components of the organism. Consequently, the tRNA must only serve as a substrate of the associated aaRS and not as a substrate of endogenous aaRSs, otherwise a proteome-wide incorporation of the ncAA potentially leads to mistranslation of proteins[201]. Furthermore, the tRNA must only be loaded with the desired ncAA, which in turn must not be recognized by another aaRS of the host organism. In the first *in vitro* translation experiments, orthogonality was established through natural divergence by applying a mutated variant of phenylalanine-tRNA from yeast, which was used in crude E. coli extracts[202]. First orthogonal aaRS were evolved to direct the site-specific incorporation of natural amino acids in response to the amber stop codon. In 1998 the group of Rolf Furter could demonstrate the first genetic encoding of a ncAA in living *E. coli* cells[201,203]. Later, a heterologously expressed and evolved aaRS/tRNA pair from archaea led to a truly orthogonal expansion of the genetic code in *E. coli*[204]. In addition, the ncAAs must be cell permeable, stable and non-toxic. Despite efforts of genetically encoding ncAAs in response to quadruplet codons[205], the incorporation in response to the amber stop codon UAG is still the most widely applied technique. Since a reassignment of a nonsense codon with an ncAA should have as little effect on the proteome as possible, the amber codon is usually used because it is less frequent and not recognised by endogenous tRNAs[206].

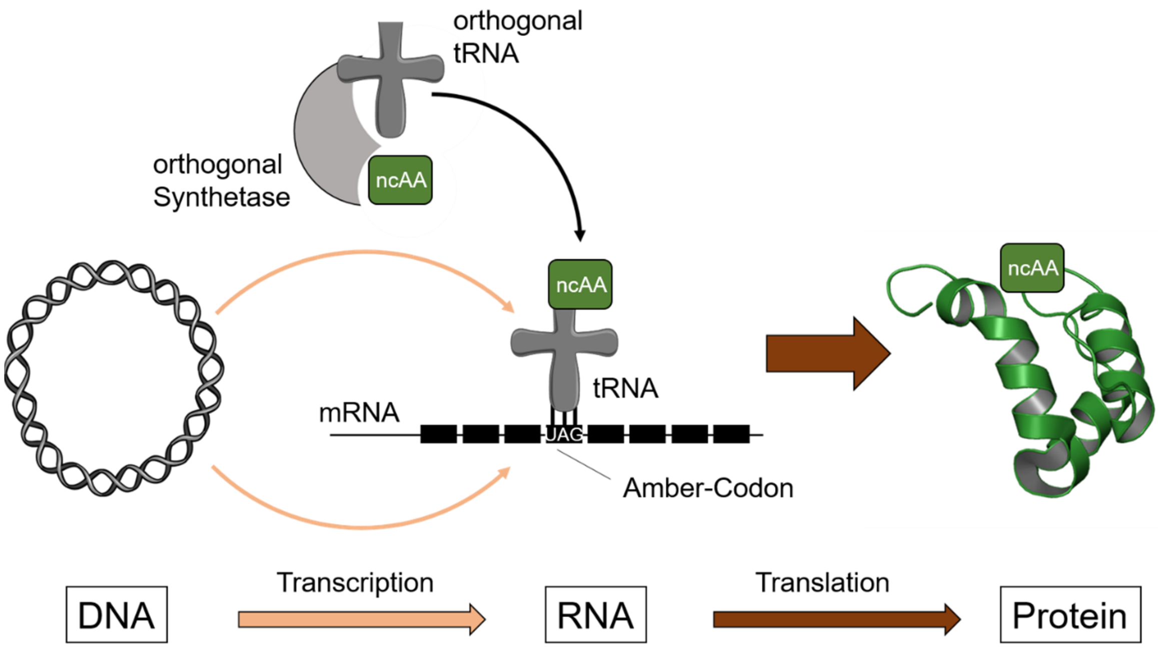

Figure 19 Protein expression using amber suppression: The amino acid is recognized by its cognate aaRS. The cognate tRNA is bound and the activated amino acid is transferred on the tRNA. The additional, orthogonal aaRS/tRNA pair is specific for a noncanonical amino acid, which is incorporated site-specifically in response to a unique codon (e.g. the amber stop codon) during translation.

So far, orthogonal aaRS/tRNA pairs have been developed for a variety of ncAA, usually based on three pairs: the *Methanocaldococcus jannaschii* tyrosyl pair (orthogonal in bacteria like *E. coli*)[207], the *E. coli* leucyl and tyrosyl pairs (orthogonal in eukaryotes)[208] and the pyrrolysyl pairs from *Methanosarcina barkei* and *Methanosarcina mazei* (orthogonal in all domains of life)[209,210].

7.6.2 Pyrrolysyl-tRNA Synthetase

For the development of an orthogonal aaRS for new ncAAs the amino acid binding pocket must be re-engineered by directed evolution to create the desired substrate specificity. The 2002 discovered PylRS/tRNA^{Pyl} pair from *Methanosarcina barkeri* is orthogonal with respect to most pro- and eukaryotic tRNAs and aaRS, making it interesting for artificial expansions of the genetic code with new chemistries[195,210,211]. Furthermore, there is no need for further engineering of the tRNA^{Pyl}, due to their natural amber suppression ability. Since the PylRS has evolved naturally, high efficiency and compatibility with general translational components is given in bacteria and archaea. Moreover, wild type PylRS is surprisingly promiscuous towards Nε-modified lysine derivatives and the genetic encoding of ncAAs.

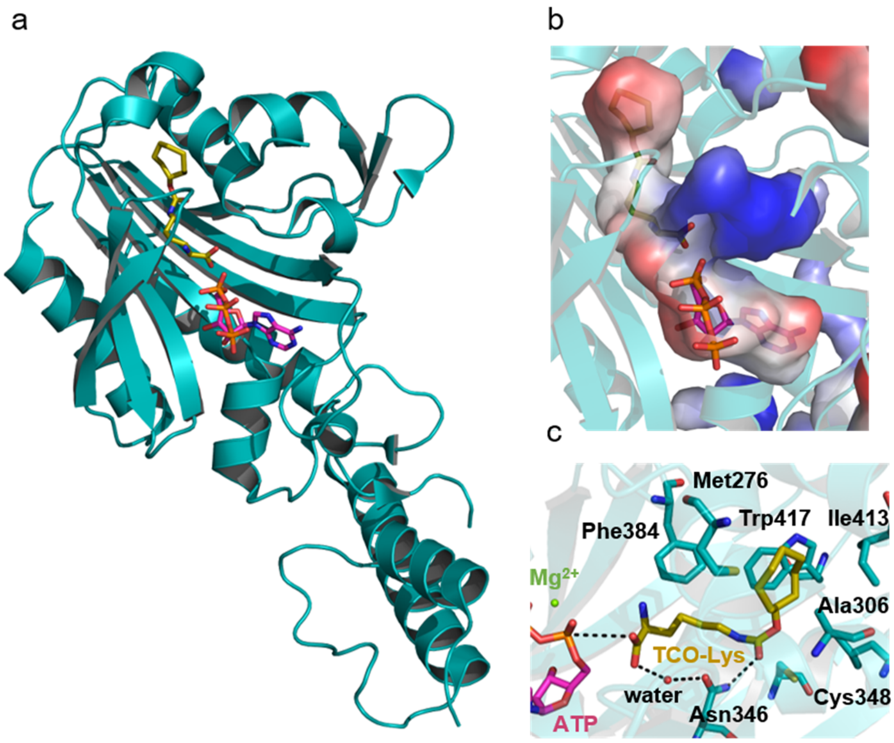

Figure 20 Crystal structure of pyrrolysyl-tRNA synthetase: **a** Overall structure of *M. mazei* PylRSc(Y306A/Y384F) (turquoise cartoon model) bound to TCO-Lys (yellow stick model) and ATP (pink stick model). **b** Surface model indicating hydrophobic binding pocket with approximate protein contact potentials calculated using PyMOL vacuum electrostatics function. The colours represent potentials ranging from −70 mV (red) to +70 mV (blue). Transparent cartoon models of PylRS(Y306A/Y384F) are visible in the background. **c** Water-mediated hydrogen bonds between TCO-Lys (yellow stick model) and the side-chain amide group of Asn346 are represented by dotted lines. Transparent cartoon models of PylRS(Y306A/Y384F) are visible in the background (6AAO pdb[212]).

In 2007 a crystal structure of a catalytically active C-terminal fragment of PylRS was solved, showing the large hydrophobic binding pocket (Fig. 20b) and precise structural organization of the enzyme (Fig. 20). These insights in the protein organization facilitated the directed evolution of new PylRS variants[213]. Today there are manifold PylRS variants, which show substrate specificity to more than 100 lysine and phenylalanine derived ncAAs[214] (Fig. 21).

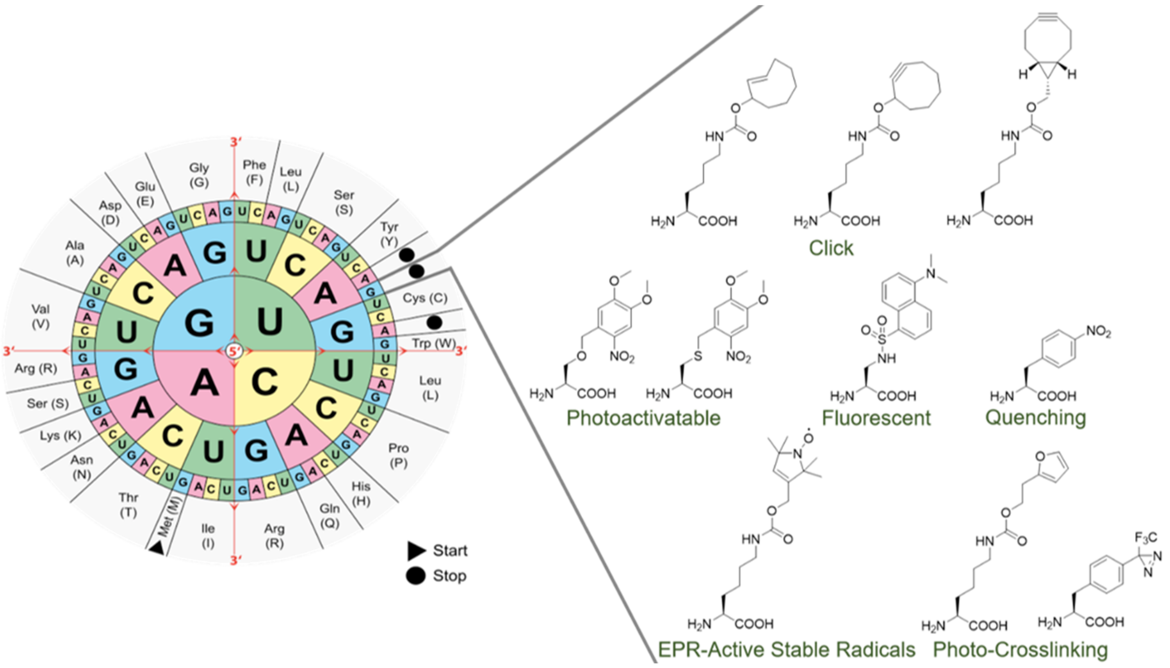

Figure 21 Illustration of a codon sun with ncAAs that were successful genetically encoded by wild type and evolved PylRS enzymes in response to the amber stop codon.

7.6.3 Bioorthogonal Reactions for Protein Labelling

The major advances in the field of cotranslational incorporation of ncAAs in living cells, combined with a significant increase in chemoselective reactions opens a new space of possibilities for labelling proteins with a diverse range of probes *in vitro* and *in vivo*[215]. New bioorthogonal functional groups do not react with biological entities under physiological conditions but selectively react with each other. The genetic code expansion facilitates the site-specific incorporation of new biorthogonal functionalized ncAAs in proteins of bacteria, mammalian cells and animals.[216]

In a bioorthogonal reaction the reactants must be kinetically, thermodynamically, and metabolically stable before the reaction takes place. For protein labelling in a living system the two bioorthogonal moieties must have low toxicity and react selectively with each other under physiological conditions. In the last few years, several reactions have been developed, showing good biocompatibility and selectivity *in vivo*.

Most bioorthogonal reactions follow second-order kinetics, whereby their second-order rate constants span 9 orders of magnitude with the fastest bioorthogonal labelling reactions reaching rates up to 10^5 M^{-1} s^{-1}[216] (Fig. 22a). The rates depend directly on the concentrations of the reaction partners and on the second order rate constant k_2 [M^{-1} s^{-1}]. For labelling during biological processes or low abundant proteins, bioorthogonal reactions with high second order rate constants are preferred. Also, a huge excess of the reactant can increase the reaction rate[217], but this often leads to off target reactions and an increased toxicity.

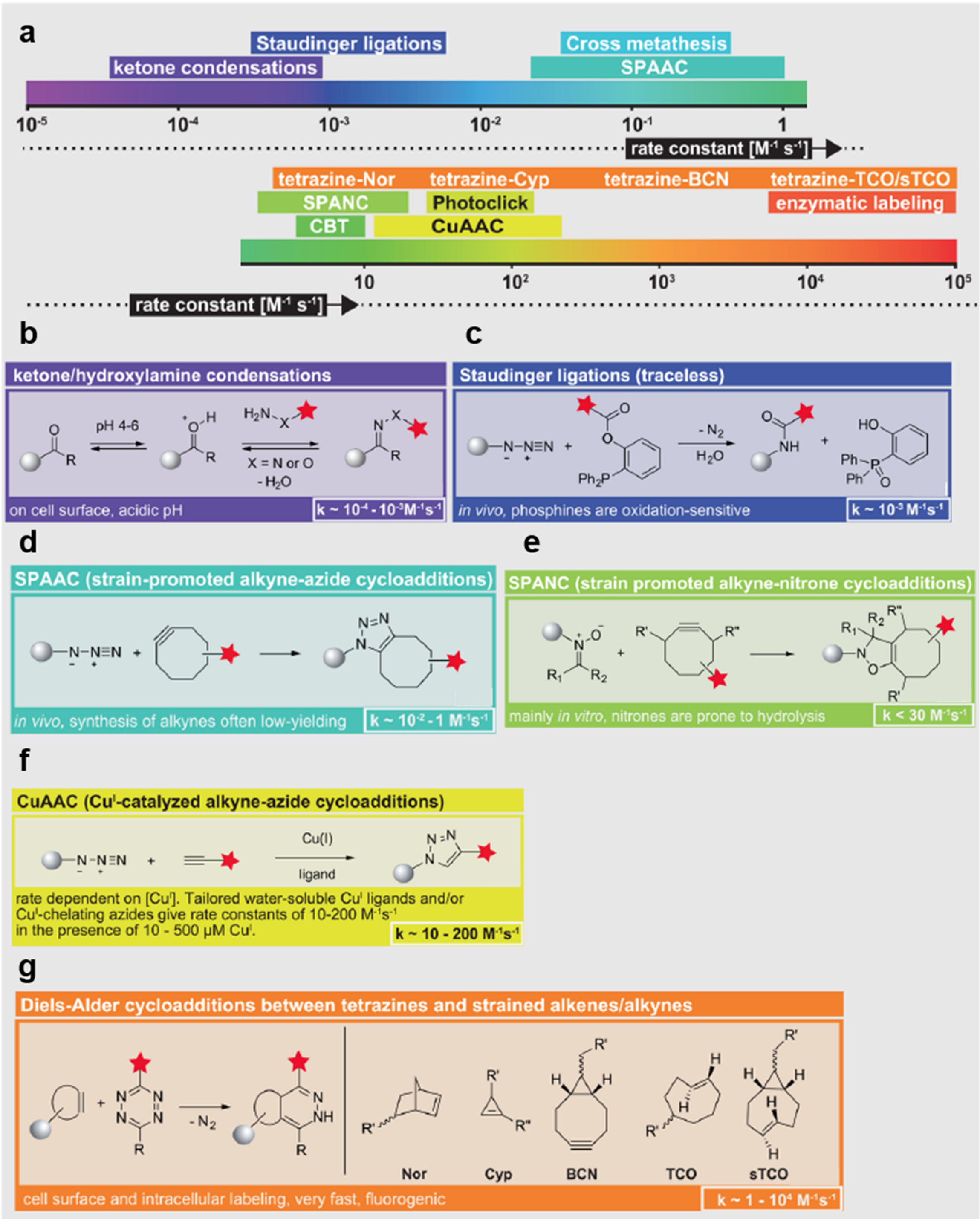

Figure 22 Overview of known conjugation reactions and their kinetic constants: **a** Overview of second order rate constants of different biorthogonal reactions. **b** Ketone/hydroxylamine condensations. **c** Staudinger ligations. **d** Strain-promoted alkyne-azide cycloadditions (SPAAC). **e** Strain-promoted alkyne-nitrone cycloadditions (SPANC). **f** Cu^{I}-catalyzed alkyne-azide cycloadditions (CuAAC). **g** Inverse-strain-promoted Diels-Alder Cycloadditions (SPIEDAC). (adapted from[216])

The first published bioorthogonal reactions, based on ketones and aldehydes, have relatively low second order rate constants[218–220], necessitating high reactant concentrations. Their carbonyl groups react with strong α-effect nucleophiles, like hydrazines and alkoxyamines, under acidic conditions[221,222] (Fig. 22b); hence, ketone/aldehyde condensations are best suited for *in vitro* or cell-surface labelling. In contrast, azide-bearing ncAAs can be used to label biomolecules in living cells and animals, as their chemistry is absent from biological systems and truly orthogonal in its reactivity to most biological functionalities[223–228]. The azide groups react with phosphines in Staudinger ligations[229,230] (Fig. 22c). However, the Staudinger ligations show slow second-order rate constants[231]. Together with terminal alkynes, azides react in a [3 + 2] cycloaddition, catalyzed by copper salts[232,233] (Fig. 22f). The CuAAC (Cu^{I}-catalysed alkyne−azide cycloaddition) reaction shows a higher reaction rate than the Staudinger ligation under physiological conditions[234,235]. However, the toxicity of copper is a limiting factor for *in vivo* settings, since the reaction rate depends on the copper concentration[236,237]. The uncatalyzed alkyne−azide cycloaddition has a relatively low reaction rate, which can be increased by introducing ring strain into the alkyne[216], leading to the “strain-promoted alkyne−azide cycloaddition” (SPAAC)[235,238] (Fig. 22d). This reaction can be used to label abundant biomolecules within complex biological systems like living mammalian cells, since metal catalysts are not required[238–240]. Instead of azides, the use of nitrones together with cyclooctyne derivatives accelerates the [3 + 2] cycloaddition (Fig. 22e) (SPANC = strain promoted alkyne−nitrone cycloaddition) by 30 fold[241,242]. The remarkable fast Inverse-electron demand Diels−Alder reactions between tetrazines and strained alkenes or alkynes (SPIEDAC) (Fig. 22f) can be used to chemoselectively label and manipulate biomolecules in their native settings[6–9]. This approach provides a step-change in methods to site specifically label proteins.

However, despite the reaction rates, there are many additional factors that contribute to the utility of labelling approaches, e.g. the cost efficiency and simplicity of the reagent synthesis as well as the cell permeability.

8 Aim of this work

The aim of this work was to develop an alternative biotinylation strategy, providing a click-mediated enrichment of user-defined genomic loci for proteomics studies. The protein composition of individual chromatin loci defines their local function[138], which, however, is only poorly understood[3]. To get a deeper understanding of the regulation of the eukaryotic genome, purification methods of user-defined genomic loci are needed that can retain molecular interactions and are also suitable for proteomics. Such methods should allow efficient isolation of user-defined genomic loci, while being independent of genetic engineering of the target locus and being fully programmable.

The aim of this study was to develop a click-mediated biotinylation technology that allows the enrichment of user-defined genomic loci based on copper-free click chemistry in combination with proteome analysis.. The click-mediated enrichment should be based on transcription-activator-like effector (TALE) proteins due to their high selectivity and fully programmability for genomic loci[170,176,177]. In specific, TALE proteins should be designed, targeting human repetitive sequences, like the pericentromeric SatIII DNA[133,134] in a natural chromatin context. For the click-mediated enrichment of a user-defined genomic loci, a clickable non-canonical amino acids should be introduced in the constructed TALE proteins[5], allowing artificial biotinylation by using the Diels-Alder cycloaddition between a trans-cyclooctene bearing ncAA and tetrazine-biotin[6–9]. This should allow for a highly sensitive and selective streptavidin-based enrichment in combination with proteomic analysis.

Furthermore, a TALE-TET2CD fusion construct with the ability to deposit oxidized 5mC at user-defined genomic loci in cells should be designed. In combination with the click-mediated enrichment, this would help in studying the influence of 5hmC, 5fC and 5caC on the local chromatin landscape *in vivo* by the discovery of proteins, directly or indirectly recruited or repelled by oxidized 5mC derivates.

9 Results and Discussion

9.1 Target selection, TALE Design and Characterization

The proposed click-mediated enrichment is based on TALE proteins. In the last few years, methodology for the design of TALEs for the *in vitro* isolation of target sequences from the human genome were established in the group[94,178,243–247]. Furthermore, the simple recognition code, with the RVDs NI, NN, HD and NG binding the nucleotides A, G, C and T, respectively (Fig. 15) makes them fully programmable[176,177,248]. These programmability of TALEs by simple concatenation of individual repeats has been extensively proven in various sequence contexts and does not show context dependences or sequence constraints[249].

The important biological functions and the poorly understood epigenetic control mechanism of repetitive DNA, as well as the high genomic abundance, makes it interesting as target sequences[136]. Generally, target sequence selection considers factors like high information complexity, moderate GC content, expected accessibility in chromatin and target uniqueness in the genome. For TALE binding the first nucleotide of the target sequence has to be a thymine[180–183] and the sequence should be absent of CpGs, since 5mC can inhibit the interaction[94].

The chosen TALE target sequence for the repetitive pericentromeric SatIII locus (Tab. 14) were assembled in a TALE entry vector using a golden gate approach with a high success rate[183]. In this approach, up to 11 plasmids encoding canonical repeats were assembled in a first ordered, single reaction assembly by using type IIS restriction enzymes and a ligase under thermal cycling. In a second step, full-length expression plasmids were assembled into type IIS BsmBI sites of an lacZα reporter cassette containing entry vector (EV), designed for the assembly of TALEs with C-terminal fusion of a VP64 transcriptional activator domain. The combination with a reporter plasmid, containing the firefly luciferase gene under control of a minimal CMV promoter (minCMV), shows the expression level and the binding affinity of the TALE protein in mammalian cells based on a luciferase assay[250]. Upstream of the minCMV promoter, a TALE binding site was introduced *via* restriction ligation cloning. The binding of the TALE protein, fused to the transcription activator domain VP64 can induce the expression of the firefly luciferase gene (Fig. 23a). The expression level of the firefly luciferase directly correlates with the amount of luminescence, thereby reporting the expression level and binding affinity of the chosen TALE protein to its cognate target sequence *in vivo*.

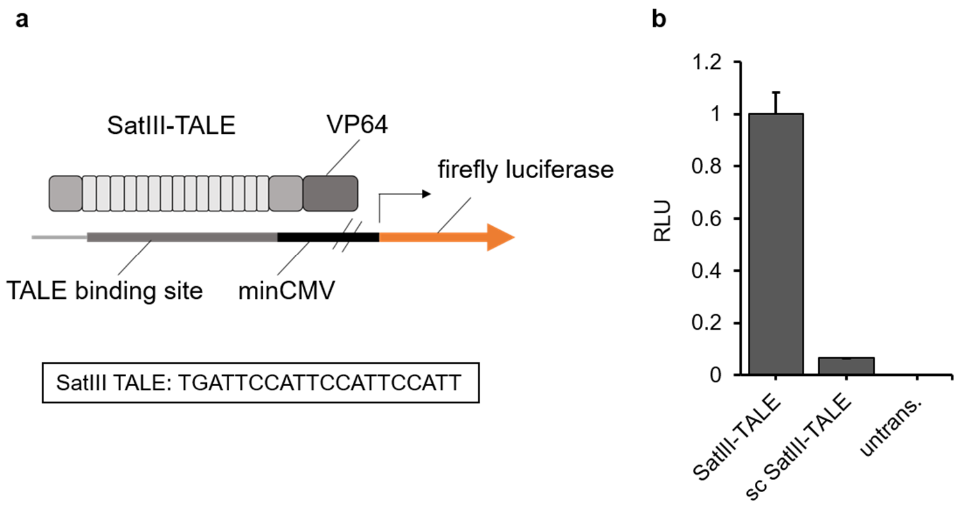

Figure 23 *In vivo* reporter activation assay for studying TALE affinity: **a** Schematic overview of the *in vivo* reporter activation assay. A TALE protein specific for the SatIII-locus (SatIII-TALE) is fused with a VP64 domain driving transcription of a luciferase reporter by binding its minimal CMV promoter (minCMV) enabled by TALE binding to its corresponding recognition site. Assaying luciferase activity allows assessing of binding affinity of the SatIII-TALE. **b** Relative luminescence units (RLU) plotted for different TALE constructs from biological duplicates. SatIII-TALE fused to VP64; sc SatIII-TALE: scrambled SatIII-TALE containing the same RVDs but in a different order; untransfected HEK293T cells representing the overall background generated by the cells itself.

The luciferase activator assay showed, compared to the untransfected control, high relative luminescence unit (RLU) values, indicating a successful SatIII-TALE expression in HEK293T cells. Furthermore, the binding of the SatIII-TALE was compared to the scrambled SatIII-TALE, which contains the same RVDs but in a different order, thereby not allowing it to bind the SatIII-locus. The observed difference in the RLU values between the SatIII-TALE and the scrambled SatIII-TALE showed a specific binding of the SatIII-TALE to its corresponding target site. The extremely low RLU values of the untransfected sample also illustrate a low background signal and reliability of the established luciferase activator assay (Fig. 23b).
However, the luciferase activator assay only displayed the binding of the TALE proteins to their binding site located on a plasmid and not in the native chromatin. Consequently, a chromatin immunoprecipitation (ChIP) assay[157] was performed (Fig. 24a), to

illustrate the accessibility of the DNA target sequence in a natural chromatin context and target uniqueness in the genome. The same SatIII-TALE, fused to a N-terminal FLAG-tag, was expressed in HEK293T cells and the bound amount of SatIII DNA was investigated *via* real time quantitative PCR (RT-qPCR) after nuclear extraction (Fig. 24b).

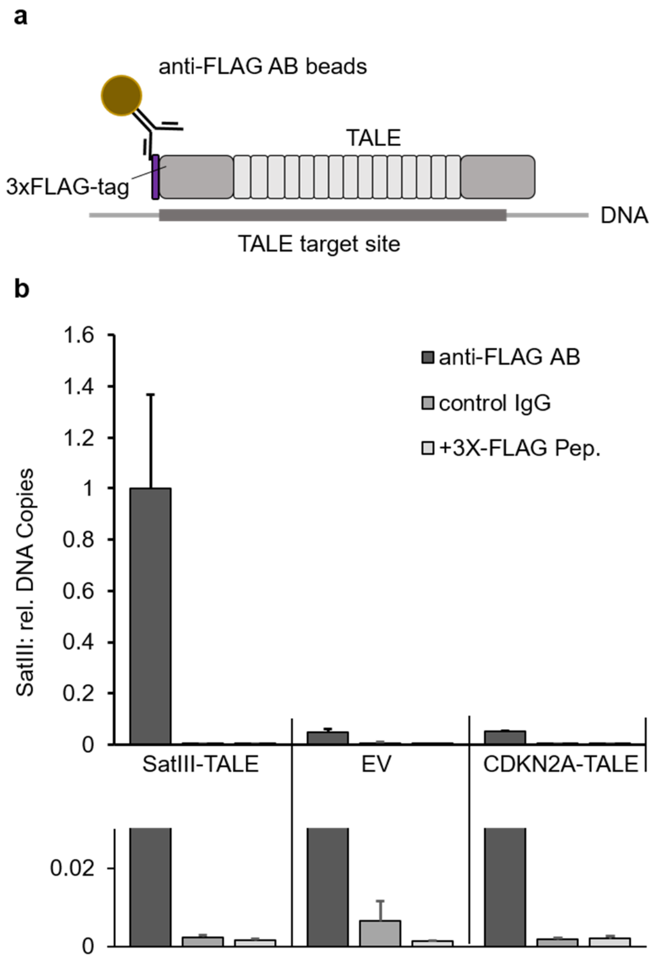

Figure 24 Chromatin immunoprecipitation to investigate TALE affinities in a natural chromatin context: **a** Schematic overview of the performed chromatin immunoprecipitation. SatIII-TALE fused to a N-terminal a 3xFLAG-tag for precipitation by anti-FLAG antibody (anti-FLAG AB) coated magnetic beads. SatIII-TALE binding to its corresponding genomic target site inside the chromatin, results in isolation of SatIII DNA, which was quantified by qPCR from technical duplicates. **b** Relative DNA copies of SatIII DNA depending on different constructs and binding conditions. Either the SatIII-TALE targeting SatIII DNA, an empty vector (EV) or the CDKN2A-TALE targeting CDKN2A gene were transfected in HEK293T cells. The nuclear extract was incubated with either anti-FLAG AB coated beads, control IgG coated beads or anti-FLAG AB coated beads together with an 3X-FLAG Peptide (3X-FLAG Pep.). Amount of SatIII DNA was analysed using qPCR. Enlarged diagram under the main diagram displays measured relative SatIII DNA copies in the low range.

Beside the SatIII-TALE, an established CDKN2A-TALE[251] was expressed to analyse the TALE dependence of the measured SatIII DNA amount. The sample with the CDKN2A-TALE showed a lower number of DNA copies, indicating that the measured values are related to the amount of DNA bound by the SatIII-TALE protein. In addition, every sample was incubated with Dynabeads coated with the control antibody IgG mouse, which is not able to bind to the FLAG Tag. The control showed low relative DNA copies, indicating negligible unspecific DNA binding to the beads. As an additional control, the probes were treated with 3X-FLAG peptides in a competitive fashion during bead binding. Here, the measured low numbers of DNA copies illustrate again, that the measured DNA amount only results from a specific TALE-DNA interaction. Together, the ChIP assay showed the specific binding of the SatIII-TALE to its target site in the natural chromatin context.

9.2 Identification of non-canoncial amino acid (ncAA) Incorporation Sites

For the click-mediated enrichment, an amber-site should be introduced in the TALE constructs, leading to an incorporation of a clickable non-canonical amino acid (ncAA) by the tRNA^{Pyl}/PylRS-AF pair.

Besides the TALE protein, the TALE entry vectors bear an mCherrry-^{Y39TAG}GFP fusion transfection control[252] (Fig. 25a), enabling fluorescent identification of cells transfected with the TALE plasmid *via* the mCherry signal and the tRNA^{Pyl}/PylRS-AF plasmid through the GFP fluorescence, since the expression of GFP requires suppression of the amber codon by added ncAA. Furthermore, it showed successful incorporation of the ncAA by the tRNA^{Pyl}/PylRS-AF pair and its amber suppression fidelity (Fig. 25b). The PylRS-AF is based on the PylRS of *Methanosarcina mazei* with two mutated key residues (Y306A and Y384F) in its hydrophobic pocket, thereby accepting bulky side-chain moieties such as *t*-butyloxycarbonyl (Boc)- or *trans*-cyclooctene ncAAs, which results in an increased incorporation efficiency[230,252–254].

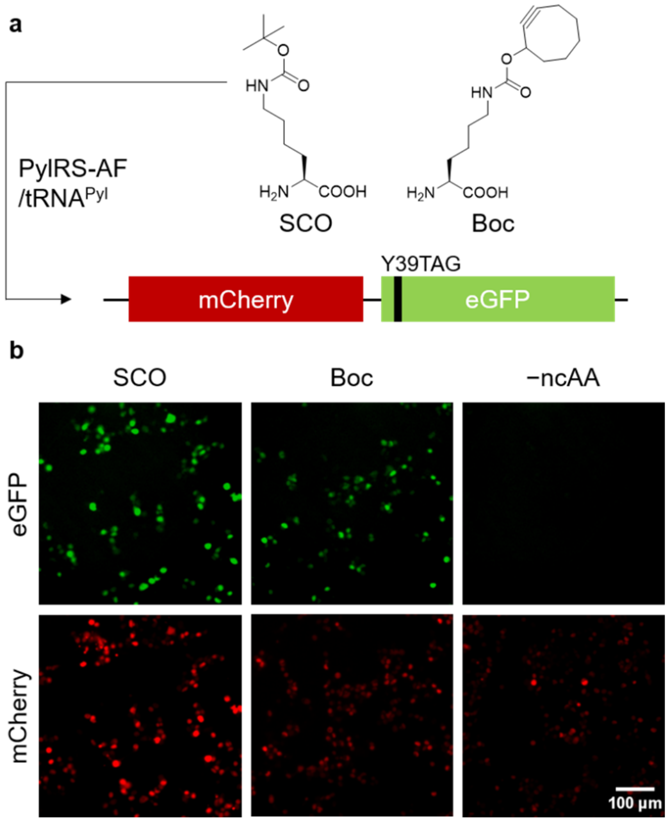

Figure 25 Fidelity of amber suppression using PylRS-AF/tRNA^{Pyl} pair: **a** Non canonical amino acids (ncAA) are incorporated at position Y39 of GFP located downstream of mCherry in the reporter construct. The successful incorporation of the ncAA leads to GFP expression and GFP fluorescent signal. **b** Fluorescent images (10x) of HEK293T cells, expressing the mCherrry-^{Y39TAG}GFP fusion transfection control and the tRNA^{Pyl}/PylRS-AF. The cells were either treated with cyclooctyne-lysine (SCO), Boc-lysine (Boc) or no ncAA was added (–ncAA).

The GFP fluorescence signal indicates a good incorporation efficiency of the ncAA Boc-lysine (Boc) and the clickable ncAA cyclooctyne-lysine (SCO), whereas no GFP signal was detected without ncAA, showing a high fidelity of the PylRS-AF. The similar mCherry fluorescence in each sample indicates similar transfection levels (Fig. 25b and Fig. S25).

For the validation of the ncAA incorporation sites, several amber codon positions in the NTR of the well-established hey2-TALE[178,255] and in the linker region between the FLAG-Tag, and the TALE protein were tested using the luciferase activator assay (Fig. 26a) and fluorescent microscopy (Fig. S27 and Fig. S29). Through the installation of clickable ncAAs in the N-terminal region of TALE proteins at these amber codon positions, chromatin segments can be subsequently isolated. From crystal structures of TALE-DNA complexes several possible amber codon positions in the TALE NTR for ncAA incorporation were identified (Fig. 26b). These positions are surfaced exposed and do not participate in secondary structure formation and DNA binding[179]. Empiric testing of various sites is required due to context effects of amber suppression[256].

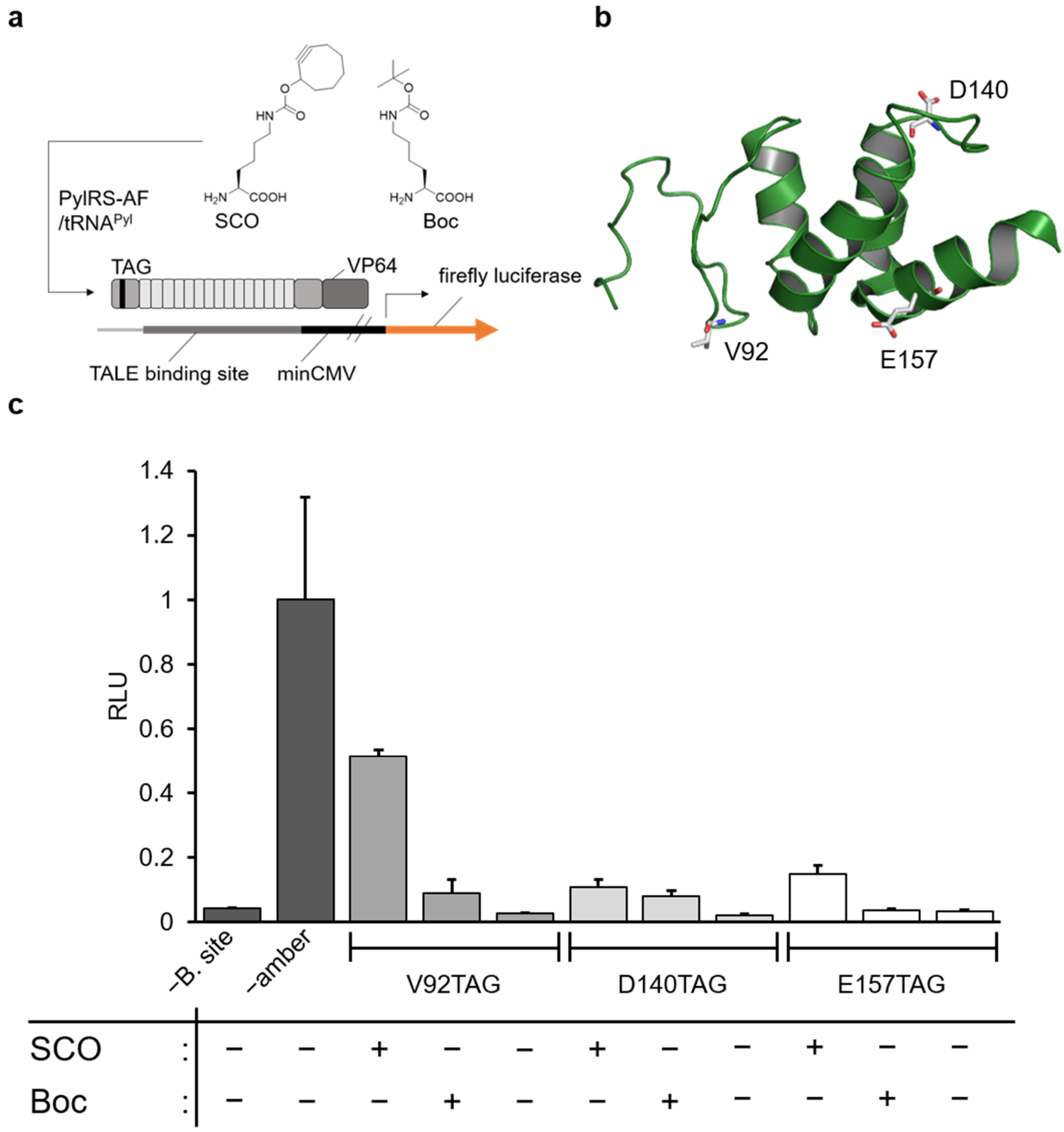

Figure 26 *In vivo* reporter activation assay for studying non-canonical amino acid (ncAA) incorporation efficiency into TALEs: **a** ncAAs are incorporated into different positions of the TALE N-terminal region (NTR). TALE is fused with a VP64 domain driving transcription of a luciferase reporter, which is under control of the minimal CMV promoter (minCMV). Thereby TALE binding to its corresponding binding site induces the expression of the luciferase reporter. Assaying luciferase activity allows assessing site-dependence of ncAA incorporation efficiency and expression levels. **b** ncAA incorporation sites in TALE NTR with low perturbative potential and good solvent accessibility (3UGM pdb[179]). **c** Relative luminescence units (RLU) from biological triplicates show incorporation efficiency of ncAA Boc or SCO into position V92, D140 and E157 of the hey2-TALE fused to VP64. –B. site: No TALE binding site in the luciferase reporter; –amber: Positive control, TALE-VP64 without amber codon.

In comparison to the other amber sites D140 and E157, the amber site V92 showed the highest RLU values using the ncAA SCO. Interestingly relatively low RLU values were observed for the incorporation of Boc-lysine, which is not consistent with earlier *in vitro* studies[257]. At this point, it is negligible since Boc-lysine incorporation is not needed for further experiments. Overall, the samples without ncAAs showed the lowest RLU values, indicating again a high fidelity of the PylRS-AF also for the amber position V92 in the NTR of the hey2-TALE (Fig. 26c).

Since the amber suppression was performed in the hey2-TALE[178,255] context, the luciferase assay was repeated with the most promising amber site V92 in the chosen SatIII context.

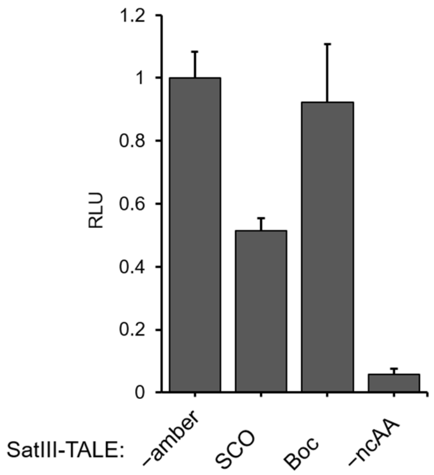

Figure 27 *In vivo* reporter activation assay for studying non-canonical amino acid (ncAA) incorporation efficiency into SatIII-TALE: Relative luminescence units (RLU) from biological duplicates show incorporation efficiency of ncAA Boc or SCO into position V92 of the SatIII-TALE fused to VP64. –amber: TALE-VP64 without amber codon.

In the SatIII context, the incorporation of the ncAA SCO in the NTR of the SatIII-TALE was highly efficient as well (Fig. 27). In contrast to the hey2 context, the incorporation of the ncAA Boc-lysine led to expression levels that are comparable to the wild type construct lacking an amber site, indicating position V92 as being generally promising for ncAA incorporation.

For imaging studies, fluorescently labelled TALEs were used in a variety of mammalian cell lines, providing a solid basis for the design and validation of TALEs selective target binding *in vivo*. Specifically, a new entry vector was generated by exchanging the VP64

domain by mCherry and removing of the mCherry-^{Y39TAG}GFP fusion transfection control (Fig. 28a).
However, with simultaneous incorporation of ncAA SCO or Boc-lysine, the SatIII-TALE fused to mCherry showed nearly no expression in the fluorescent imaging. The high mCherry fluorescence signal of the wild type construct, lacking an amber site, illustrates a good transfection and expression efficiency of the SatIII-TALE mCherry fusion construct, indicating a relatively low incorporation efficiency of the ncAAs at positions V92 in the SatIII-TALE mCherry fusion contruct (Fig. 28b and Fig. S26).

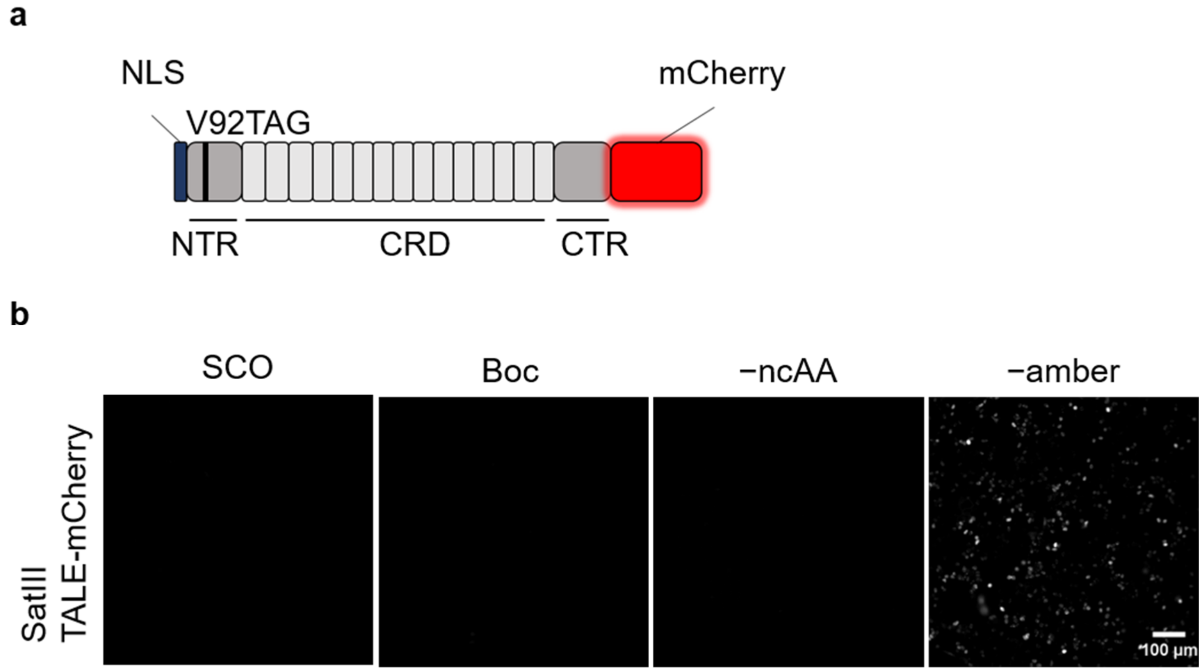

Figure 28 Incorporation efficiency at position V92 and expression efficiency of the SatIII-TALE: **a** General design of fusion constructs consisting of the TALE including a nuclear localization signal (NLS), amber codon at position V92 and mCherry as fluorescent protein. **b** fluorescent images (10x) of HEK293T cells, expressing SatIII-TALE^{V92TAG}-mCherry and tRNA^{Pyl}/PylRS-AF. Images were taken in the RFP channel showing insufficient incorporation of ncAA Boc or SCO and expression of SatIII-TALE-mCherry fusion construct. –amber: SatIII-TALE-mCherry without amber codon.

Since the luciferase activator assay has a higher sensitivity as fluorescent imaging, the expression levels were probably too low for fluorescent imaging based detection. However, the observed low suppression efficiency showed the need for investigation of new amber codon positions in the TALE NTR (Fig. 29).

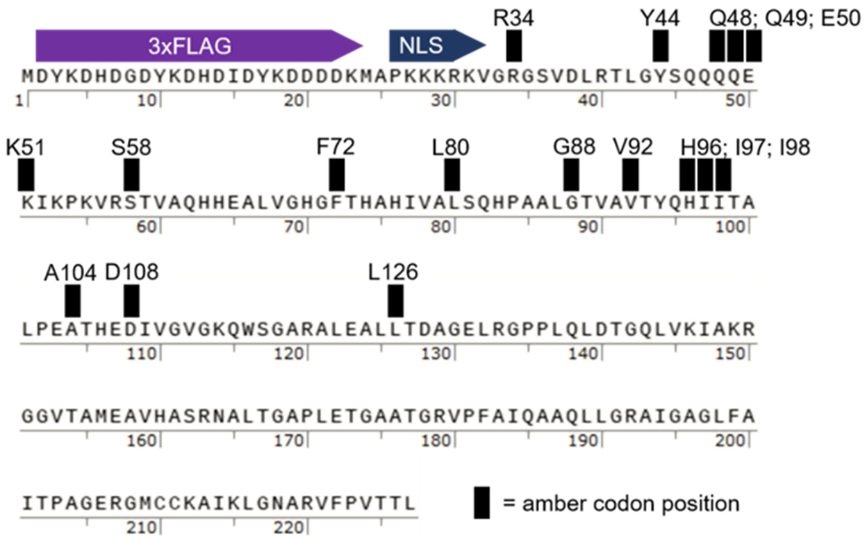

Figure 29 Schematic overview of non-canonical amino acid (ncAA) incorporation sites in TALE N-terminal region (NTR): Amino acid sequence of the SatIII-TALE NTR with amber tested amber codon positions (black blocks), 3xFLAG-tag (purple arrow) and nuclear localization signal (NLS, dark blue arrow).

Specifically, several new amber codon positions were chosen based on empiric rules on suppression efficiency[256] and crystal structures[179] (Fig. 29). The incorporation efficiency and TALE expression levels were identified by fluorescent imaging. Since the PylRS-AF contains a cryptic NLS, a nuclear export signal (NES) was introduced to facilitate the cytosolic localization and to increase the incorporation efficiency during translation[258].

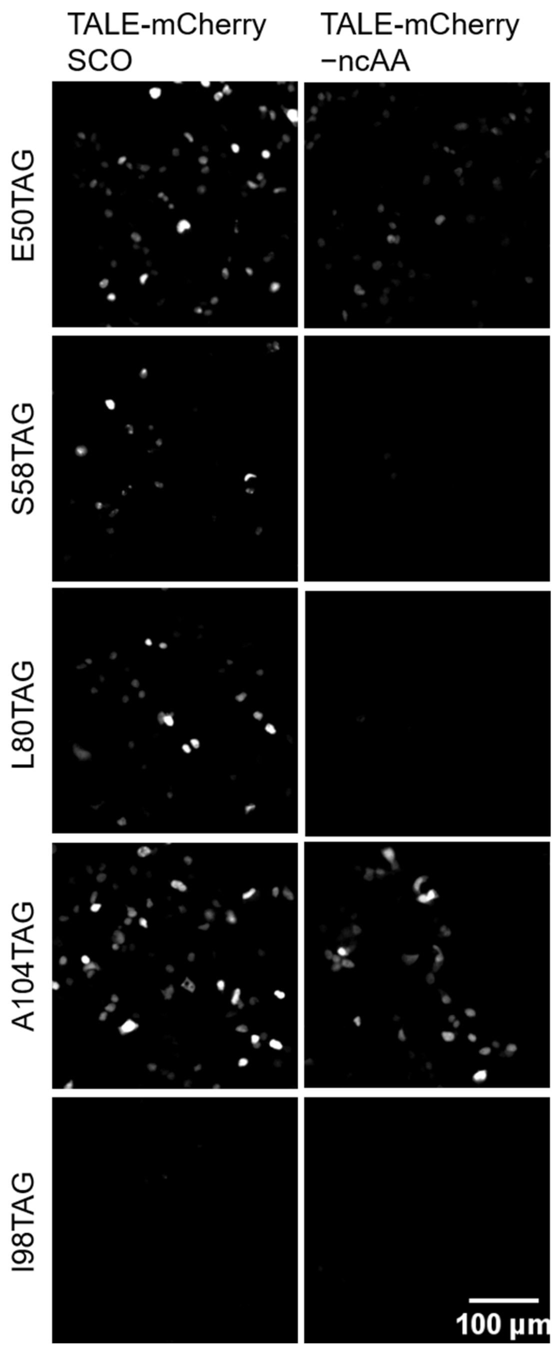

Figure 30 Fluorescent imaging for studying non-canonical amino acid (ncAA) incorporation efficiency into SatIII-TALE: Fluorescent images (10x) of HEK293T cells, expressing SatIII-TALE mCherry fusion construct and $tRNA^{Pyl}$/PylRS-AF^{NES}. Images were taken in the RFP channel showing incorporation of SCO at different positions and expression of SatIII-TALE-mCherry fusion construct.

From a total of sixteen different analysed amber codon positions, the positions E50, K51, S58, F72, L80, G88, and I97 showed good expression levels with a relatively high amber suppression fidelity (Fig. 30 and Fig. S27). Other amber codon positions like A104, showed relatively high expression levels in both cases, with and without ncAA, illustrating the position dependence of the amber suppression fidelity. The amber codon position I98, showed no expression of the TALE protein, indicating exemplary strong position dependence of the incorporation efficiency (Fig. 30). Together, these results show the strong need of empiric testing of various amber codon positions due to the context effects of amber suppression.

Since SatIII DNA belongs to the tandem repeats, a specific fluorescent pattern showing small foci in the nucleus of the cell, was expected[259]. Specifically, the localization of the TALE proteins with promising amber codons were analyzed by fluorescent imaging.

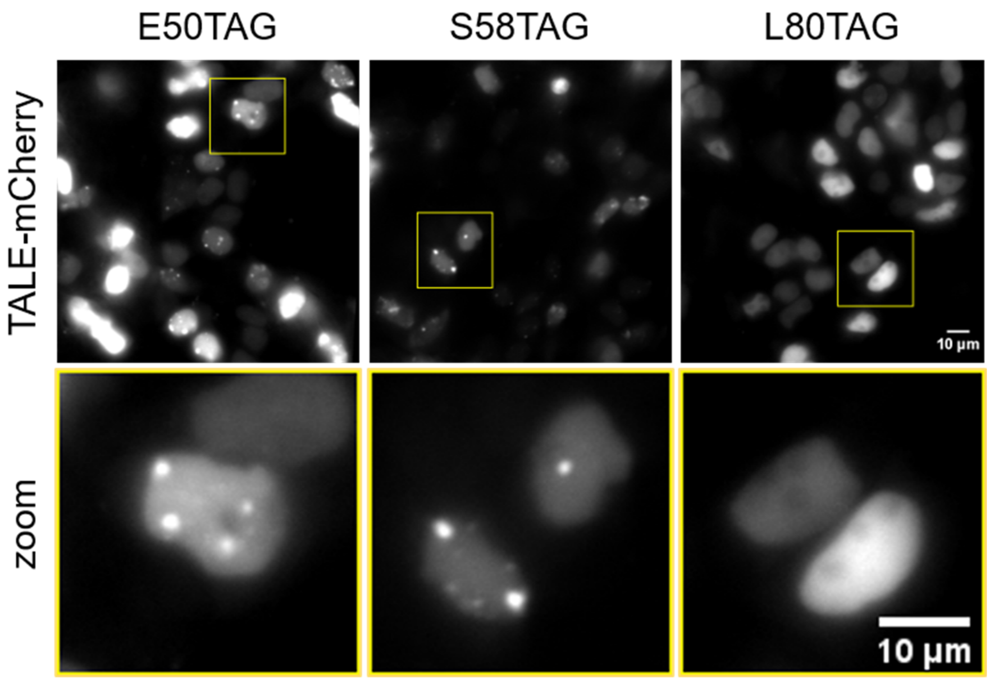

Figure 31 Fluorescent imaging for studying non-canonical amino acid (ncAA) incorporation efficiency into SatIII-TALE and its localization: Fluorescent images (60x) of HEK293T cells, expressing SatIII-TALE mCherry fusion contruct and $tRNA^{Pyl}$/PylRS-AF^{NES}. Images were taken in the RFP channel showing incorporation of SCO at different positions and expression of SatIII-TALE-mCherry fusion constructs. Furthermore, foci in the nucleus showing specific localization of the SatIII-TALE-mCherry fusion construct indicate specific DNA binding at genomic SatIII tandem repeats.

From the seven amber codon positions, which showed good incorporation efficiency (E50, K51, S58, F72, L80, G88, and I97), the expected foci in the nucleus could be detected only for the four positions, E50, K51, S58 and G88 (Fig. 31 and Fig. S28). Together with earlier studies[259] it can assumed that the foci in the nucleus are showing the binding of TALE to the SatIII DNA. In contrast, other amber codon positions, like L80, showed homogenous distribution of the expressed TALE-mCherry fusion construct in the nucleus, indicating the incorporation of a ncAA leads to the loss of the TALE DNA interaction.

In summary, from the sixteen analyzed amber codon positions, seven showed a good incorporation and expression efficiency, while only four of them showed the TALE DNA interaction and were therefore further characterized.

9.3 Characterization of ncAA Incorporation Sites

Since the clickable ncAA needs to be accessible for the tetrazine-biotin molecule for later biotinylation, the accessibility of the incorporated ncAA was investigated. HEK239T cells, transfected with the ^{TAG}SatIII-TALE mCherry plasmid and the PylRS-AF^{NES}/tRNA^{Pyl} pair, were fixed and permeabilized using methanol and treated with tetrazine-FAM (fluorescein) after expression and incorporation of the ncAA SCO[252]. The tetrazine-FAM reacts with SCO *via* the strain-promoted inverse electron demand Diels-Alder cycloaddition (SPIEDAC) (Fig. 32b). This resulted in a co-localization of the fluorescent signal of the SatIII-TALE mCherry fusion construct and the tetrazine-FAM molecule (Fig. 32c).

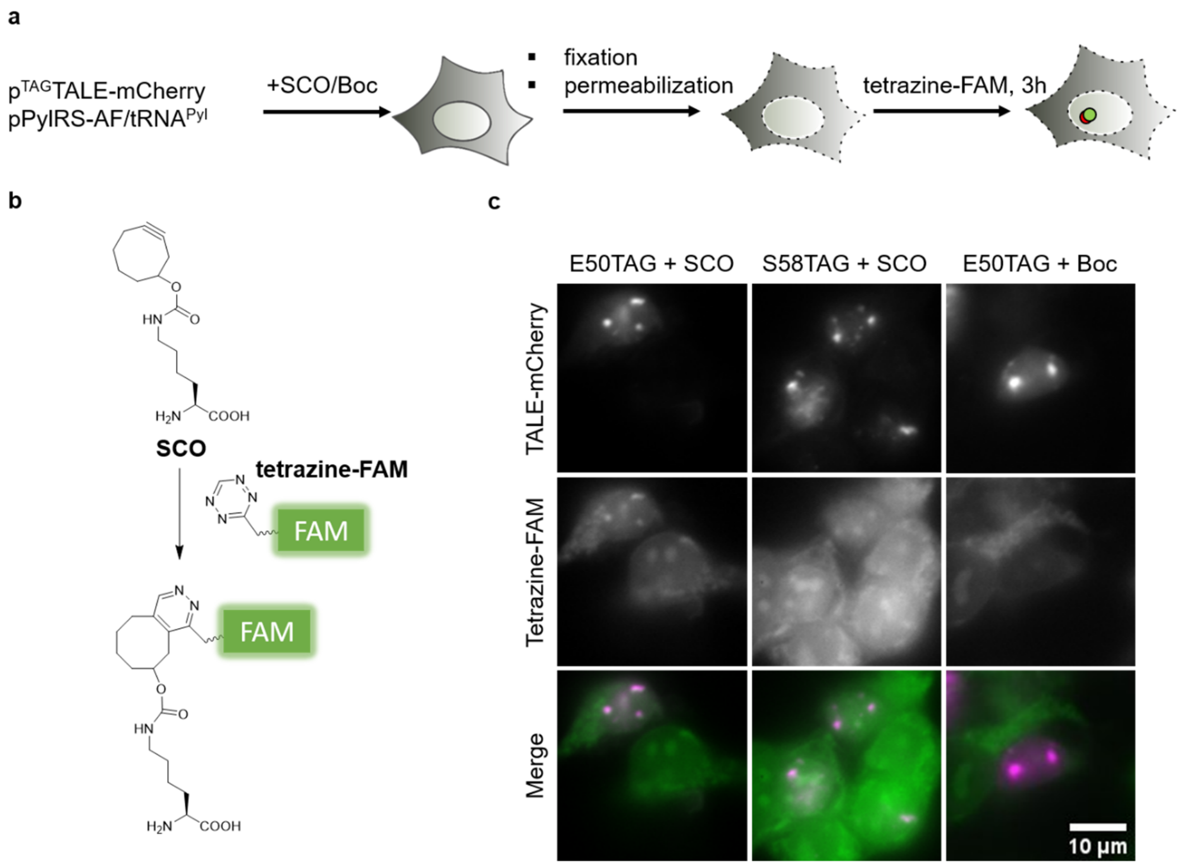

Figure 32 Fluorescent imaging for studying accessibility of incorporated non-canonical amino acid (ncAA): **a** Schematic overview of fluorescent labelling of the SatIII-TALE by click reaction between SCO and tetrazine-FAM. **b** Reaction scheme of copper-free click reaction between SCO and tetrazine-FAM. **c** Fluorescent images (60x) of HEK293T cells, expressing SatIII-TALE mCherry fusion contructs and tRNA^{Pyl}/PylRS-AF^{NES}. Images were taken in the RFP channel, showing incorporation of SCO or Boc at different positions and expression of the SatIII-TALE-mCherry fusion construct. Foci in the nucleus showing specific localization of the SatIII-TALE-mCherry fusion construct indicating specific DNA binding. Images taken in the GFP channel showing FAM signal after click reaction between SCO and tetrazine-FAM. Merge images show the co-localization of SCO bearing SatIII-TALE-mCherry (magenta) and tetrazine-FAM (green), indicating successful labelling.

The expected co-localization was observed for the amber codon positions E50 and S58, while position E50 showed slightly more specific labelling of the SCO bearing SatIII-TALE mCherry fusion construct with tetrazine-FAM (Fig. 32c). Since the click-mediated enrichment requires formaldehyde crosslinking of chromatin binding proteins and DNA, the accessibility must be given under formaldehyde fixation conditions. Specifically, the accessibility of the incorporated ncAA SCO under methanol fixation was compared to the accessibility under formaldehyde fixation.

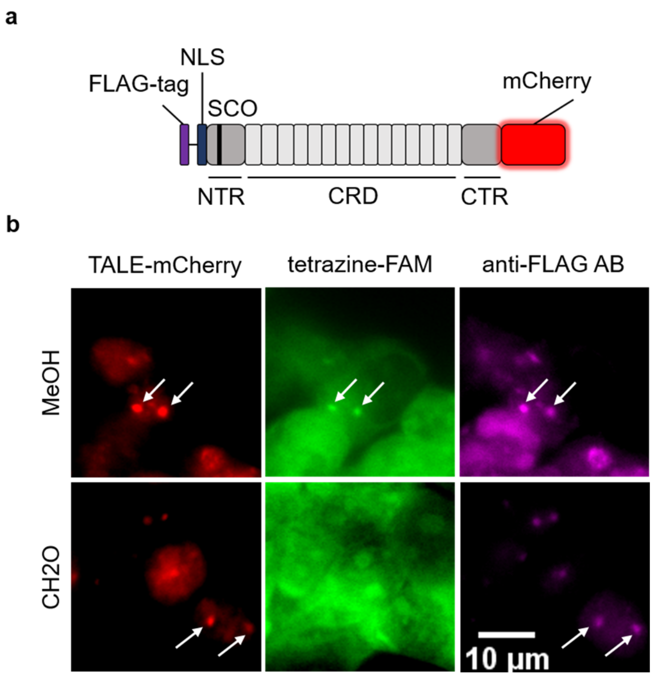

Figure 33 Fluorescent imaging for studying accessibility of incorporated non-canonical amino acid (ncAA) under usage of different fixatives: **a** General design of fusion constructs consisting of the SatIII-TALE including an N-terminal 3xFLAG-tag, nuclear localization signal (NLS), amber codon at position E50 and mCherry as fluorescent protein. **b** Fluorescent images (60x) of HEK293T cells either fixed with methanol or formaldehyde and expressing SatIII-TALE^{E50TAG} mCherry fusion construct and tRNA^{Pyl}/PylRS-AF^{NES}. Images were taken in the RFP channel, showing incorporation of SCO at position E50 and expression of the SatIII-TALE-mCherry fusion construct. Foci in the nucleus (indicated by white arrows) showing specific localization of the SatIII-TALE-mCherry fusion construct, showing specific DNA binding. Images taken in the GFP channel showing click reaction between SCO and tetrazine-FAM. Images taken in the Cy7 channel show immunostaining of the SatIII-TALE with an primary anti-FLAG antibody (anti-FLAG AB) and a secondary Cy7 antibody.

In comparison to methanol fixation, the ncAA SCO showed no accessibility in the formaldehyde fixed cells. Methanol fixation can reshape the chromatin structure, change the protein localization and can lead to protein precipitation[260–263]. Hence, it can lead to a better accessibility of the genomic DNA and proteins, explaining the accessibility of the incorporated ncAA SCO under methanol fixation. To validate the accessibility dependence of the fluorescent intensity, the cells were treated with an anti-FLAG antibody, which binds to the N-terminal FLAG-tag and were co-stained with a Cy7 labelled secondary antibody (Fig. 33). The accessibility of the FLAG-Tag was already demonstrated by the previously performed immunoprecipitations (Fig. 24 and

Fig. 35). The fluorescent signal of the FLAG-tag stained cells was comparable for both fixation methods, indicating that the fluorescent intensity depends on the accessiblity and not on the fixation method (Fig. 33b).

Since formaldehyde crosslinking is required for the click-mediated enrichment, and methanol fixation could lead to undesired re-localization of proteins, additional amber codon positions were investigated. Five new amber codon positions were introduced inside or next to the FLAG-tag due to its good accessibility. In addition, three amber codons were introduced in the linker region between the TALE protein and the mCherry fluorophore (Fig. 34a).

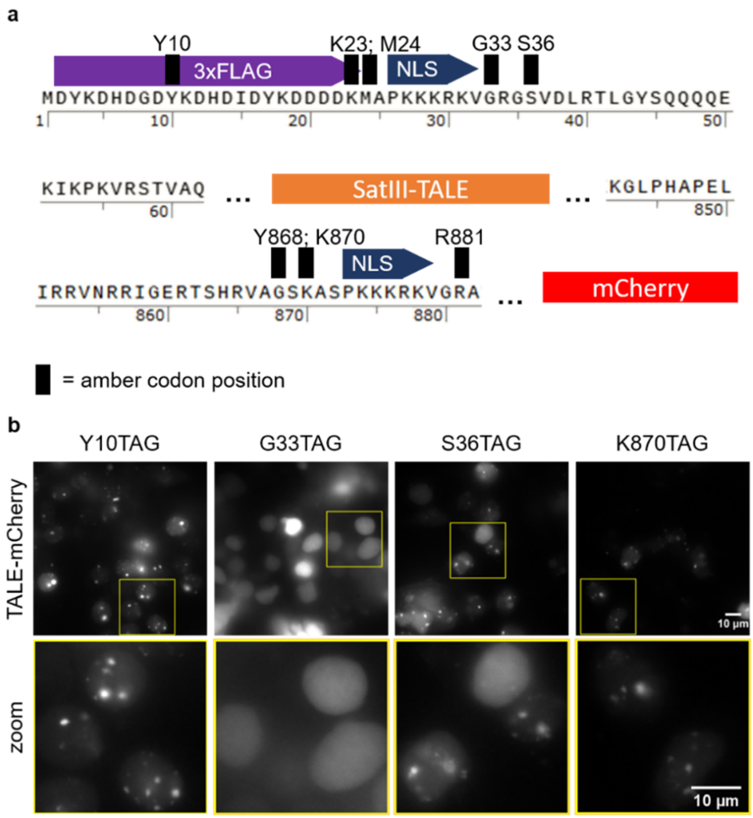

Figure 34 Schematic overview and analysis by fluorescent microscopy of non-canonical amino acid (ncAA) incorporation sites in the TALE N-terminal region (NTR) and the linker region between TALE and mCherry: **a** Part of the amino acid sequence of the SatIII-TALE NTR and C-terminal region (CTR) with tested amber codon positions (black blocks), 3xFLAG-tag (purple arrow), nuclear localization signal (NLS, dark blue arrow), central repeat domain (CRD) of the SatIII-TALE (orange block) and mCherry (red block). **b** Fluorescent images (60x) of HEK293T cells, expressing SatIII-TALE mCherry fusion constructs and tRNA^{Pyl}/PylRS-AF^{NES}. Images were taken in the RFP channel showing incorporation of SCO at different positions and expression of SatIII-TALE-mCherry fusion construct. Furthermore, foci in the nuclei show a specific localization of the SatIII-TALE-mCherry fusion construct indicating specific DNA binding.

Three (Y10, S36 and K870) of the eight tested amber codon positions showed valid incorporation and expression efficiency as well as the expected foci, indicating the specific TALE DNA interaction in the SatIII context (Fig. 34b and Fig. S29). Two amber codon positions, Y10 and K23, are located inside the FLAG-tag, near a second start codon that is in the reading frame. This could lead to the expression of a shortened construct, which does not require ncAA incorporation. Consequently, the shown expression of the SatIII-TALE carrying the amber codon at position Y10 or K23 does not necessarily show a correlation with the ncAA incorporation. The amber position G33 showed homogenous nuclear distribution of the expressed TALE (Fig. 34b), like the previously tested position L80 (Fig. 31), indicating a disruption of the TALE DNA interaction due to the ncAA incorporation. The amber codon position S36, located in the linker region between the FLAG-tag and the TALE protein, and the position K870, located in the linker region between the TALE protein and the mCherry fluorophore showed valid expression and incorporation efficiency, whereas the positions S36 showed a higher expression level (Fig. 34b).

Furthermore, the ncAA incorporation efficiency was analyzed in comparison to the wild type construct by fluorescent imaging. The relative incorporation efficiency is shown for the three amber codon positions S36, E50 and S58 (Fig. 35), using the ncAA trans-cyclooct-2-en – L – lysine (TCO).

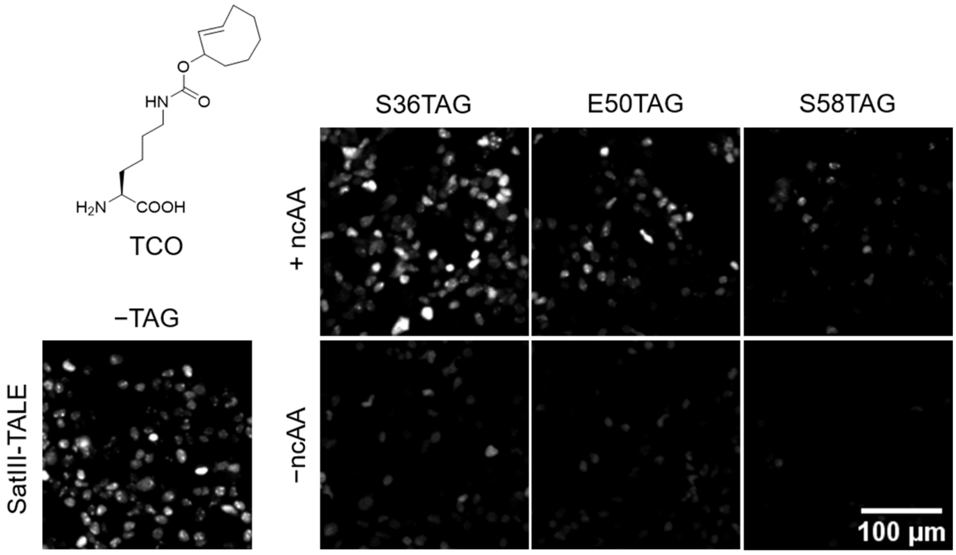

Figure 35 Fluorescent imaging for studying amber suppression efficiency: Fluorescent images (10x) of HEK293T cells, expressing the SatIII-TALE-mCherry fusion constructs with either no amber codon or with an amber codon at position S36, E50 or S58 and the $tRNA^{Pyl}$/$PylRS\text{-}AF^{NES}$ pair. –amber: SatIII-TALE without amber codon; +ncAA: Expression of SatIII-TALE after addition of the ncAA TCO; –ncAA: Expression of SatIII-TALE without adding TCO.

In comparison to the amber codon positions E50 and S58, which showed the highest incorporation efficiency in the second amber codon screen (Fig. 30) but insufficient accessibility under formaldehyde crosslinking conditions (Fig. 33), the amber codon positions S36 showed a higher fluorescent signal, thereby showing a higher incorporation efficiency. With the increasing expression level, the background expression, in absence of an ncAA, also increased slightly. However, the background expression was observed to be relatively low in comparison to the high expression by adding TCO. Furthermore, the wild type SatIII-TALE mCherry fusion construct, not carrying an amber codon, showed similar fluorescent intensities like the S36TAG carrying SatIII-TALE mCherry fusion construct, indicating expression levels of this amber suppressed fusion construct comparable to the wild type construct. This in turn shows a relative high incorporation efficiency of the ncAA TCO at position S36, therefore this amber codon position was further characterized.

Accordingly, the needed accessibility under formaldehyde fixation was analyzed for the amber codon position S36, using the ncAA TCO with a potentially higher reaction rate[264]. HEK293T cells, transfected with the ^{S36TAG}SatIII-TALE-mCherry plasmid and the PylRS-AF^{NES}/tRNA^{Pyl} pair were fixed and permeabilized under formaldehyde conditions. The accessibility was analyzed using the SPIEDAC reaction between tetrazine-FAM and the ncAA TCO (Fig. 36a), resulting in a co-localization of the fluorescent signal of the SatIII-TALE mCherry fusion construct and the tetrazine-FAM molecule (Fig. 36b).

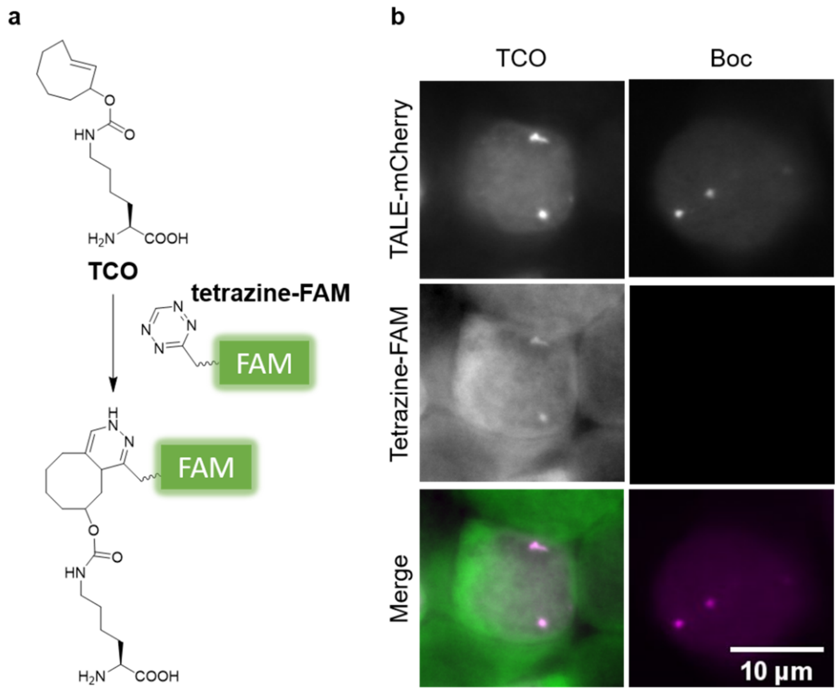

Figure 36 Fluorescent microscopy for studying accessibility of incorporated TCO at position S36 under formaldehyde fixation: **a** Reaction scheme of copper-free click reaction between TCO and tetrazine-FAM. **b** Fluorescent images (60x) of HEK293T cells, expressing SatIII-TALE^{S36TAG} mCherry fusion construct and tRNA^{Pyl}/PylRS-AF^{NES}. Images were taken in the RFP channel, showing incorporation of TCO or Boc at position S36 and expression of SatIII-TALE-mCherry fusion construct. Foci in the nucleus showing specific localization of the SatIII-TALE-mCherry fusion construct indicating specific DNA binding. Images taken in the GFP channel showing click reaction between TCO and tetrazine-FAM. Merge images show the co-localization of SatIII-TALE-mCherry (magenta) and tetrazine-FAM (green), indicating successful labelling and good accessibility of incorporated TCO.

The position S36 directly showed efficient ncAA incorporation, good expression levels and an accessibility using formaldehyde fixation (Fig. 36b) comparable to the accessibility of the ncAA at amber codon position E50 under methanol fixation conditions (Fig. 33b). Since the method requires the biotinylation of the TALE protein, the accessibility assay was repeated using tetrazine-biotin together with Cy7 labelled streptavidin instead of tetrazine-FAM (Fig. 37a).

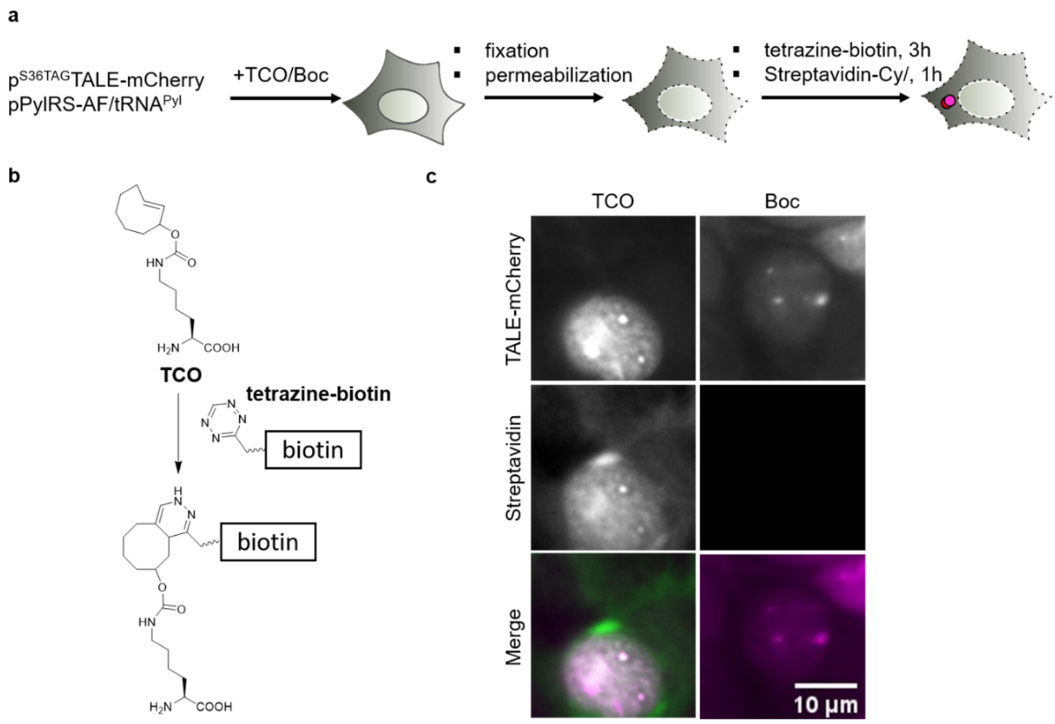

Figure 37 TALE biotinylation by click reaction between TCO and tetrazine-biotin: **a** Schematic overview of biotinylation of the SatIII-TALE by click reaction between TCO and tetrazine-biotin. **b** Reaction scheme of copper-free click reaction between TCO and tetrazine-biotin. **c** Fluorescent images (60x) of HEK293T cells, expressing ^{S36TAG}SatIII-TALE mCherry fusion construct and tRNA^{Pyl}/PylRS-AF^{NES}. Images were taken in the RFP channel, showing incorporation of TCO or Boc at different positions and expression of SatIII-TALE-mCherry fusion construct. Foci in the nuclei are showing specific localization of the SatIII-TALE-mCherry fusion construct indicating specific DNA binding. Images taken in the Cy7 channel are indicating a successful click reaction between TCO and tetrazine-biotin, due to co-localization of Cy7 labelled streptavidin. Merge images show the co-localization of SatIII-TALE-mCherry (magenta) and streptavidin (green), indicating successful biotinylation.

Fluorescent imaging showed the expected co-localization of the TALE protein with the Cy7 labelled streptavidin (Fig. 37c), indicating the successful reaction between tetrazine-biotin and the clickable incorporated ncAA TCO at the N-terminal region of the TALE protein (Fig. 37b). The achieved high accessibility of the cyclooctene group in the SatIII-TALE demonstrates the power of amber suppression for internal tagging.

9.4 Kinetics of Click-mediated Biotin Labelling with ncAA

To further improve the click reaction-based functionalization of TALE proteins in mammalian cells, the reaction rate of three commercially available clickable amino acids were compared. HEK239T cells, transfected with the ^{S36TAG}SatIII-TALE mCherry plasmid and the tRNA^{Pyl}/PylRS-AF^{NES} pair were fixed with formaldehyde, permeabilized and treated with tetrazine-biotin after expression and incorporation of the three ncAAs SCO, TCO and endo-Bicyclo [6.1.0] nonyne - Lysine (BCN) (Fig. 38a). Afterwards, the biotinylated TALE protein was visualized with Cy7-streptavidin at different time points during the reaction. Earlier *in vitro* studies have revealed that the ncAA BCN with a second order rate constant of 1.6 x 10^4 M^{-1} s^{-1} has the highest reaction rate compared to TCO and SCO. With a still very high second order rate constant of 1.3 x 10^4 M^{-1} s^{-1} , the ncAA TCO showed a high reaction rate, whereas the ncAA SCO showed the lowest reaction rate with a second order rate constant of 670 M^{-1} s^{-1}[253].

Interestingly, the respective fluorescent image analysis showed the fastest reaction between the incorporated ncAA TCO and tetrazine-biotin, with clearly visible co-localization after only 5 minutes of incubation time (Fig. 38b). In comparison, the first co-localization of tetrazine-biotin and BCN was observed after 3 hours.

BCN has shown cross reactivity with the thiols of cysteines[265], leading to reduced reactivity, whereas the used TCO showed a high stability in the presence of thiols[253]. These findings suggest that BCN may not be suitable for a cysteine-containing environment. However, it was shown that low concentrations of β-mercaptoethanol can enhances the biorthogonality of BCN for labelling reactions. Nevertheless, a more precise understanding on how β-mercaptoethanol could reduce the background labelling for purified proteins would be important for utilizing this approach for labelling in mammalian cells.[265]

Consistent with the previous *in vitro* study, slowest reaction was observed between the ncAA SCO and tetrazine-biotin with barely detectable co-localization after 3 hours. Based on these results, one can conclude that the most efficient click reaction in cells can be achieved by using the ncAA TCO.

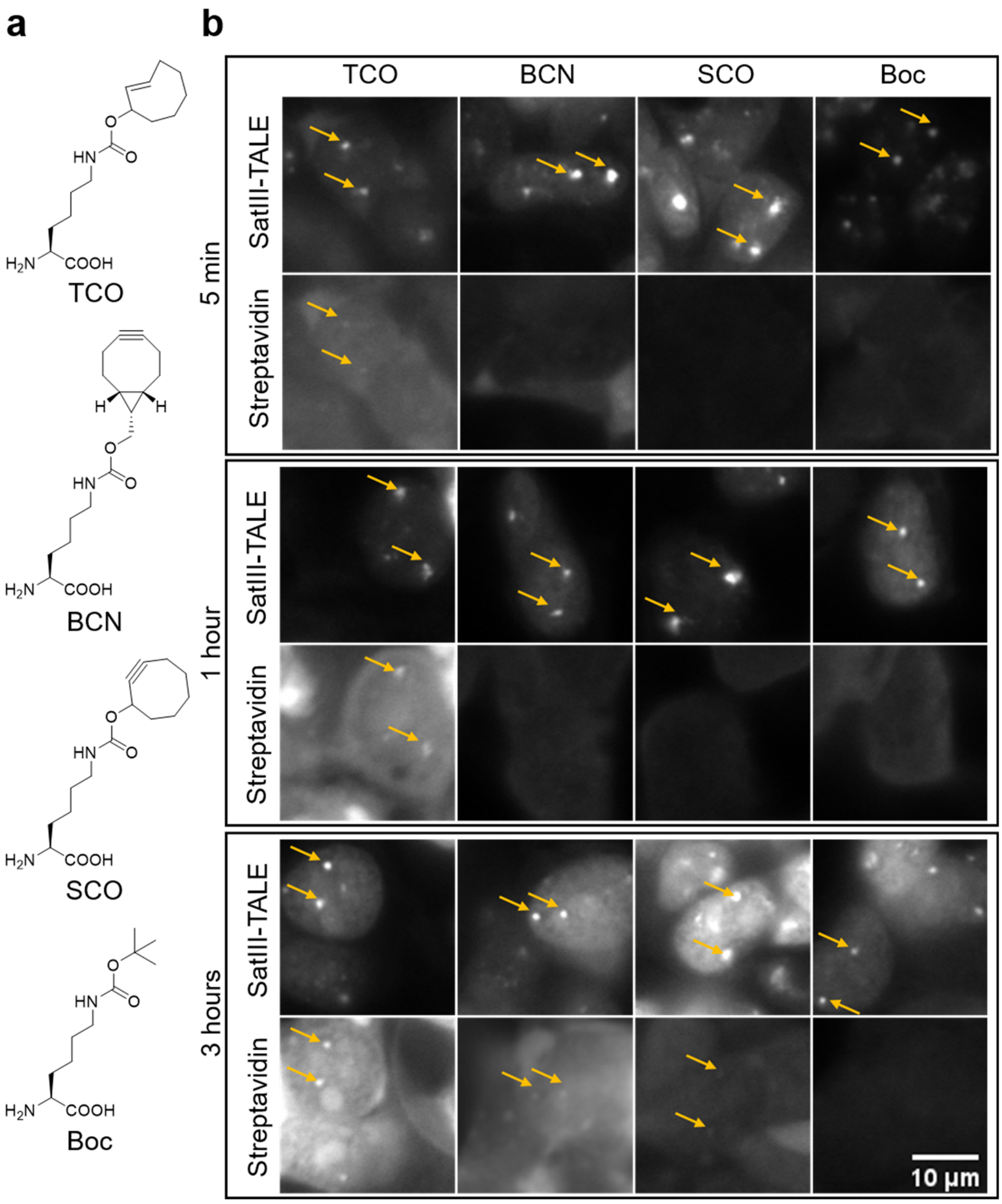

Figure 38 Visualization of differences in reaction rates of three different clickable amino acids: **a** Chemical strucutres of the used non-canonical amino acids (ncAA), TCO, BCN, SCO and Boc-lysine **b** Fluorescent images (60x) of HEK293T cells, expressing ^{S36TAG}SatIII-TALE mCherry fusion construct and tRNA^{Pyl}/PylRS-AF^{NES}. Images were taken in the RFP channel, showing incorporation of TCO, BCN, SCO or Boc at position S36 and expression of the SatIII-TALE-mCherry fusion construct. Foci in the nuclei show specific localization of the SatIII-TALE-mCherry fusion construct indicating specific DNA binding. Images in the Cy7 channel show click reaction between TCO, BCN, SCO or Boc and tetrazine-biotin after 5 min, 1 h and 3 h by co-localization of Cy7 labelled streptavidin.

9.5 Click-mediated Enrichment of user-defined Genomic Loci

The click-mediated enrichment was validated by the isolation of the SatIII locus, using streptavidin-conjugated beads after nuclear extraction. HEK293T cells were transfected with the ^{S36TAG}SatIII-TALE and the tRNA^{Pyl}/PylRS-AF^{NES} pair and treated with the ncAA TCO or Boc-lysine, as a non-binding control. After TALE expression and simultaneous incorporation of TCO the TALEs bound locus specific *in vivo*. Crosslinking of the construct and other chromatin proteins to the DNA was achieved by formaldehyde treatment. Afterwards, the TALE was biotinylated *in situ* by adding tetrazine-biotin to the permeabilized cells. After chromatin purification, the crosslinked complex was enriched on streptavidin-conjugated beads. The performed chromatin purification, whereby only nuclear extract is isolated, showed, in comparison to the well-established genome isolation using the QIAmp Mini Kit, similarly high DNA yields (Fig. S33). Both methods resulted in nearly equal DNA copy numbers of the measured SatIII DNA, indicating a sufficient isolation efficiency of the used chromatin purification method. After enrichment and stringent washing, the enrichment of the SatIII-locus was analyzed by qPCR and the composition of the enriched SatIII DNA protein complex was investigated by MS-based approaches (Fig. 39).

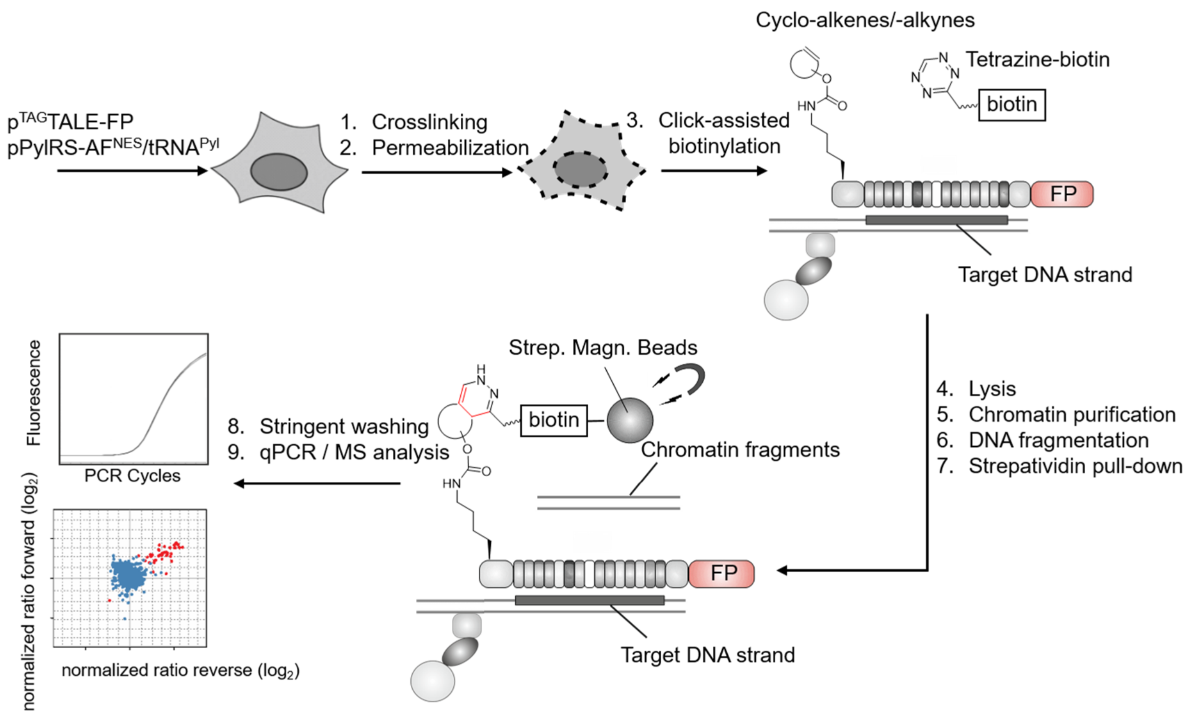

Figure 39 Workflow for Click-mediated biotinylation and enrichment.

For the enrichment, four different commercially available streptavidin-conjugated beads were tested in a blocked and unblocked state by using either 0.1 % BSA or not (Fig. 40). The DNA copy numbers for the M270 and the MyOneC1 beads were comparable between the TCO treated samples and the non-binding Boc-lysine samples under both blocking conditions, thereby showing high unspecific binding (Fig. 40a). In contrast, the other two types of beads, M280 and MyOneT1, only showed an increased DNA copy number for the clickable TCO samples, indicating a specific enrichment of the SatIII-DNA protein complex in comparison to the nonbinding Boc-lysine samples, which only differs in the added ncAA. Comparing blocked and the unblocked samples of the M280 and MyOneT1 beads, blocked MyOneT1 beads showed the highest enrichment as well as the lowest unspecific binding (Fig. 40b). Consequently, the MyOneT1 beads were found to be the preferred choice for further experiments. In addition, a click-mediated enrichment was performed with TCO bearing SatIII-TALEs, while a non tetrazine-biotin treated sample served as control (Fig. 40c). The qPCR results showed a clear enrichment only for the tetrazine-biotin treated samples, meaning the click-mediated enrichment depends on the successful click reaction between TCO and tetrazine-biotin. Together, these results show a new sensitive and selective methods for targeted isolation of user-defined genomic loci based on copper free click-chemistry.

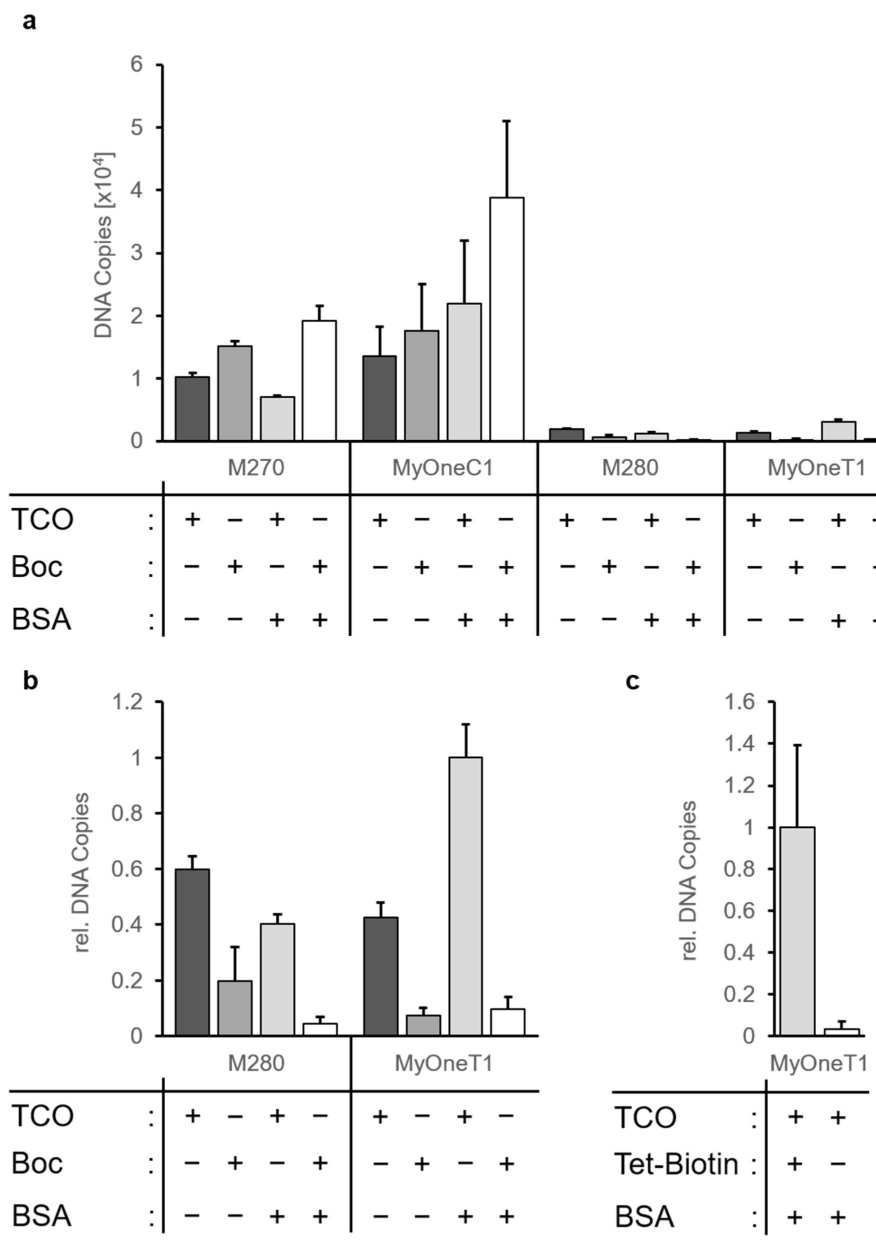

Figure 40 qPCR analysis of click-mediated enrichment of the SatIII locus: **a** The amount of SatIII DNA bound by the SatIII-TALE with incorporated non-canonical amino acid (ncAA) TCO or Boc were analysed after click-mediated enrichment using tetrazine-biotin and different streptavidin coated magnetic beads (M270, MyOneC1, M280, MyOneT1) either blocked with 0.1 % BSA or unblocked. **b** Relative DNA copies of SatIII DNA bound by the SatIII-TALE with incorporated ncAA TCO or Boc after click-mediated enrichment using tetrazine-biotin and streptavidin coated M280 or MyOneT1 magnetic beads either blocked with 0.1 % BSA or unblocked. **c** Relative DNA copies of SatIII DNA bound by the biotinylated SatIII-TALE (+tetrazine-biotin (Tet-biotin)) or non-biotinylated TALE (–Tet-biotin) after click-mediated enrichment using streptavidin coated MyOneT1 magnetic beads blocked with 0.1 % BSA. All results are from technical duplicates.

After showing an enrichment of the SatIII-locus based on qPCR analysis, the enrichment was further investigated using MS-based approaches. HEK293T cells and HeLa cells were transfected with the ^{S36TAG}SatIII-TALE mCherry fusion construct and the tRNA^{Pyl}/PylRS-AF^{NES} pair, while the ncAA TCO was added. As controls, non tetrazine-biotin treated cells as well as cells expressing either the ^{S36TAG}SatIII-TALE mCherry fusion construct with incorporated non-binding Boc-lysine or only mCherry from an empty vector (EV) were used. The last one also expresses the tRNA^{Pyl}/PylRS-AF^{NES} pair and was treated with the ncAA TCO (Fig. S24). Since the SatIII-locus play a major role in stress response, the enrichment was investigated under heat shock and non-heat shock conditions. The click-mediated enrichment was followed by extensive washing and on bead digestion, before applying the peptides to electrospray ionization mass spectrometry (ESI-MS/MS) measurements. The enrichments were done in either technical or biological triplicates to allow label-free quantification (LFQ). For the label-free quantification, the measured intensities were normalized to a common background, which is present in all samples. For each experiment, the calculated mean of LFQ intensities were normalized to the positive control expressing the biotinylated ^{S36TAG}SatIII-TALE fusion construct after incorporation of TCO and tetrazine-biotin addition, under heat shock conditions.

In all three MS-based analyses of the click-mediated enrichment, the TCO carrying ^{S36TAG}SatIII-TALE mCherry expressing samples showed the highest LFQ intensities compared to the corresponding controls, indicating a successful enrichment of the SatIII-TALE in MS-based approaches (Fig. 41).

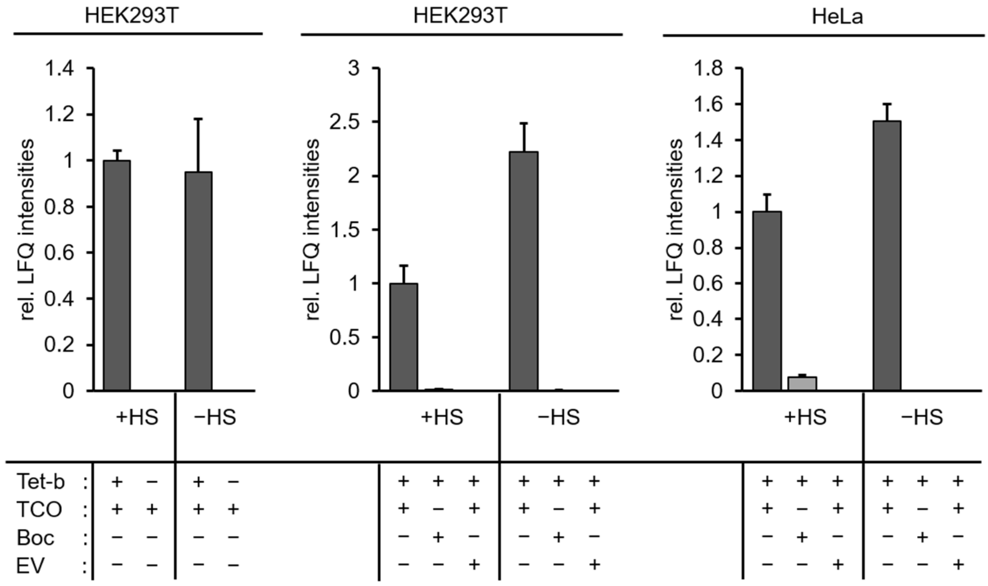

Figure 41 MS analysis of click-mediated enrichment of the SatIII-TALE: Mean of label free quantification (LFQ) intensities after MS-based analysis in HEK293T cells or HeLa cells under heat shock (1 h at 42 °C/44 °C) or non-heat shock (1 h at 37 °C) conditions. In the first setting (left diagram) HEK293T cells, expressing ^{S36TAG}SatIII-TALE mCherry fusion construct and tRNA^{Pyl}/PylRS-AF^{NES}, were treated either with or without tetrazine-biotin (Tet-b.). The means of the LFQ intensities were calculated from technical triplicates and normalized to the Tet-b. treated sample under heat shock conditions (1h 42 °C). In the other two settings, either HEK293T cells (middle diagram) or HeLa cells (right diagram) were expressing the ^{S36TAG}SatIII-TALE mCherry fusion construct with incorporated TCO and the tRNA^{Pyl}/Pyl-RS-AF^{NES} pair and were treated with tetrazine-biotin. As controls, cells expressing either the ^{S36TAG}SatIII-TALE mCherry fusion construct with incorporated non-binding Boc-lysine or only mCherry from an empty vector (EV), whereby the last one was also transfected with the tRNA^{Pyl}/PylRS-AF^{NES} pair and treated with TCO, were used. In both settings, the means of the LFQ intensities were calculated from biological triplicates and normalized to the TCO incorporated ^{S36TAG}SatIII-TALE mCherry expressing sample under heat shock conditions (1 h 44 °C).

In the first setting (left diagram) HEK293T cells were not treated with tetrazine biotin as control, leading to a non-biotinylated TCO carrying SatIII-TALE. This showed the nonspecific binding of the TCO-^{S36TAG}SatIII-TALE mCherry fusion construct to the streptavidin-conjugated beads. Under these conditions, the SatIII-TALE was found to be undetectable in the proteomics analysis, indicating a relatively low nonspecific binding and the biotinylation dependence of the enrichment. In the other two settings (middle and right diagram) the relatively low nonspecific binding was visualized by the ^{S36TAG}SatIII-TALE mCherry expressing sample with incorporated Boc-lysine, which showed in all cases relatively low LFQ intensities near at detectable levels. Further, cells were transfected with an empty vector plasmid, only expressing mCherry, and the $tRNA^{Pyl}$/$PylRS\text{-}AF^{NES}$ pair and were treated with the ncAA TCO. This served as a control for later proteomics analysis to identify the protein compositions at the SatIII-locus. Since these samples did not express the SatIII-TALE, it was also not detectable in the MS analysis, excluding a cross contamination.

In the first setting (left diagram) heat shock and non-heat shock conditions showed similar LFQ intensities, whereas in the other two settings (middle and right diagram) the non-heat shock condition showed increased LFQ intensities, compared to the heat shock samples. The heat shock in the first setting was performed for 1 hour at 42 °C and in the other two settings for 1 hour at 44°C. The increased heat shock temperature in the last two settings could result in an increased stress level of the cells, which in turn could lead to a reduced expression of the SatIII-TALE protein. The reduced expression would result in a decreased amount of SatIII-TALE compared to the non-heat shock samples, explaining the decreased LFQ intensities in the heat shock samples of the last two settings.

Together with the qPCR analysis (Fig. 40), this showed the successful enrichment of the SatIII-TALE bound to its target SatIII locus. This indeed is the first time that a user-defined chromatin locus was isolated using copper-free click chemistry, which shows the huge variety of genetic code expansion and provides a robust technique for purifying genomic loci based on click-mediated biotinylation. Biotinylation is a preferred tagging method in several advanced chromatin enrichment methods, often allowing sufficient enrichment in a single high-stringency capture step. The established alternative biotinylation using copper free click chemistry may enable highly specific biotinylation with only a defined, constant background of amber codon carrying genes.

9.6 Heat shock response

The heat shock response of the chosen SatIII locus was further investigated by fluorescent imaging and qPCR analyses. Specifically, the SatIII-TALE fused to mCherry was transfected into HEK239T and HeLa cells in combination with amber suppression, to reduce the TALE expression levels and increase the signal to noise ratio. After heat shock the endogenous HSF1 proteins were visualized by immunostaining in fixed and permeabilized cells. Since an accumulation of HSF1 and SatIII DNA in nSB is published[266], a co-localization of the TALE signal and the HSF1 detecting antibody was expected.

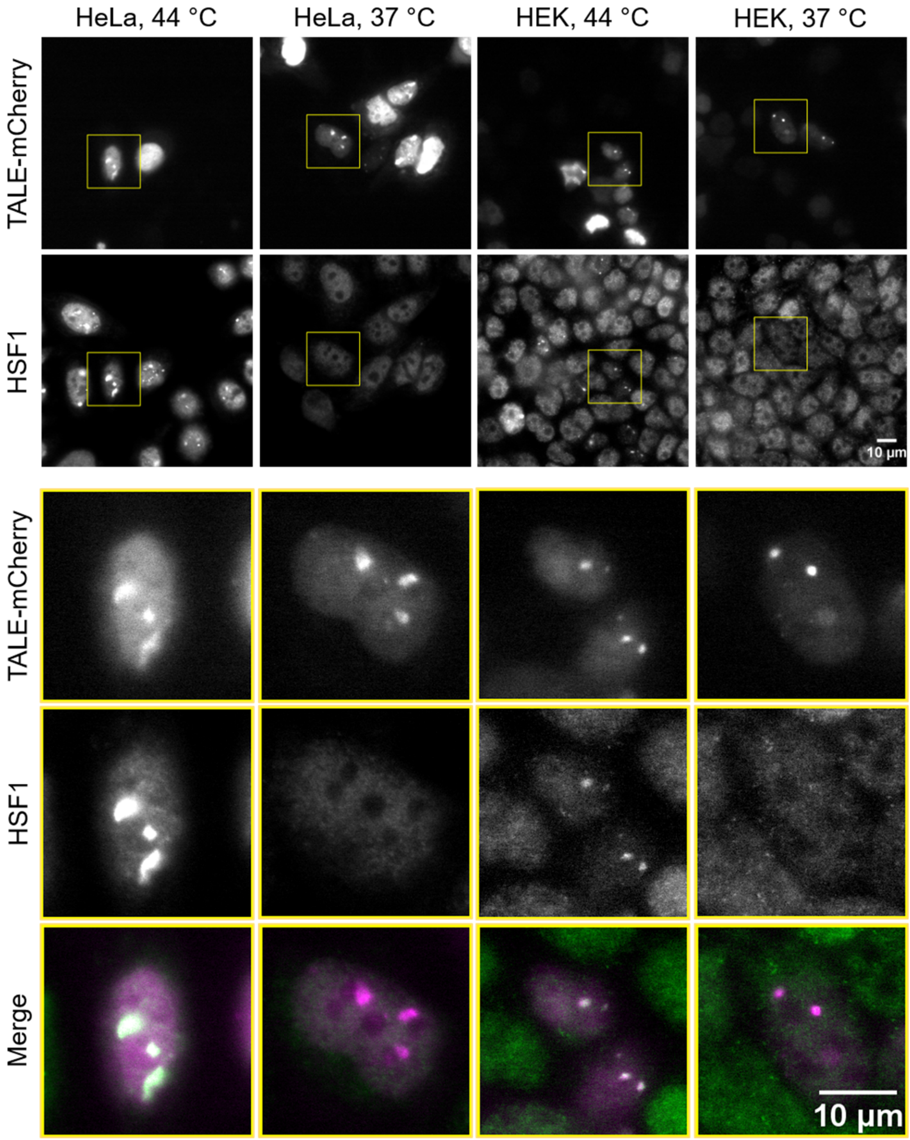

Figure 42 SatIII-TALE co-localization with HSF1 after heat shock: Fluorescent images (60x) of HEK293T and HeLa cells after 1 hour incubation at 44 °C (heat shock) or 37 °C. Images were taken in the RFP channel, showing incorporation of TCO at position S36 and expression of the SatIII-TALE-mCherry fusion construct. Foci in the nuclei show specific localization of the SatIII-TALE-mCherry fusion construct. Images in the GFP channel showing immunostaining of endogenous HSF1 with a primary anti-HSF1 antibody and a secondary FITC labelled antibody. Merge images show the co-localization of SatIII-TALE-mCherry (magenta) and endogenous HSF1 (green), indicating a co-localization of HSF1 and the SatIII-TALE at SatIII DNA upon heat shock.

In both cell lines the expected co-localization of the SatIII-TALE and the endogenous HSF1 was observed (Fig. 42). In comparison, HeLa cells showed a slightly stronger heat shock response under the same heat shock conditions. However, further experiments were performed with HEK293T cells, due to the clear heat shock response in and the higher transfection efficiencies as well as higher cell density and DNA yields. As additional validation an immunoprecipitation against endogenous HSF1 was performed, with qPCR based quantification of SatIII DNA from heat shocked and non-heat shocked cells.

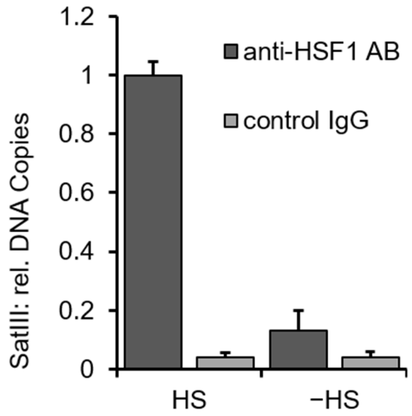

Figure 43 Immunoprecipitation for studying SatIII heat shock (HS) response: Diagram shows relative DNA Copies of SatIII DNA depending on HS from biological triplicates. As control beads were coated with control IgG. Immunoprecipitation was performed using HSF1 antibody (HSF1 AB) against endogenous HSF1 after HS (1 hour, 44 °C) or no HS (1 hour, 37 °C).

The high DNA copy numbers of the heat shock sample compared to the non-heat shock sample confirm a strong accumulation of HSF1 at the SatIII locus upon heat shock (Fig. 43). The low levels of the non-heat shock samples were found to be comparable to the SatIII DNA levels of the nonspecific bead binding samples (control IgG), indicating a cellular stress dependence of the SatIII DNA HSF1 interaction, induced by high temperature.

9.7 Enrichment and Proteomic Analysis of Repetitive Targets

The successful immobilization and enrichment of the SatIII-TALE amber mutant bound to the corresponding DNA using click-mediated biotinylation and streptavidin-conjugated beads enabled the combination of this enrichment strategy with mass spectrometry-based proteomics analysis. For this purpose, nuclear extracts from the SatIII-TALE or empty vector transfected HEK293T and HeLa cells treated with TCO or Boc-lysine, also expressing $tRNA^{Pyl}$ and PylRS, were prepared. The Boc-lysine treated samples served as a control for non-specific bead binding, whereas the empty vector control, only expressing mCherry, treated with TCO displayed the off-target amber suppression within the whole genome. The enrichments were done in biological triplicates to allow label-free quantification (LFQ) and statistical testing. Raw data was analyzed using label-free quantification, and the resulting quantification of all identified proteins was visualized in a volcano plot by plotting the false discovery rate (–Log scale) against the observed enrichment (Log_2 Ratio).

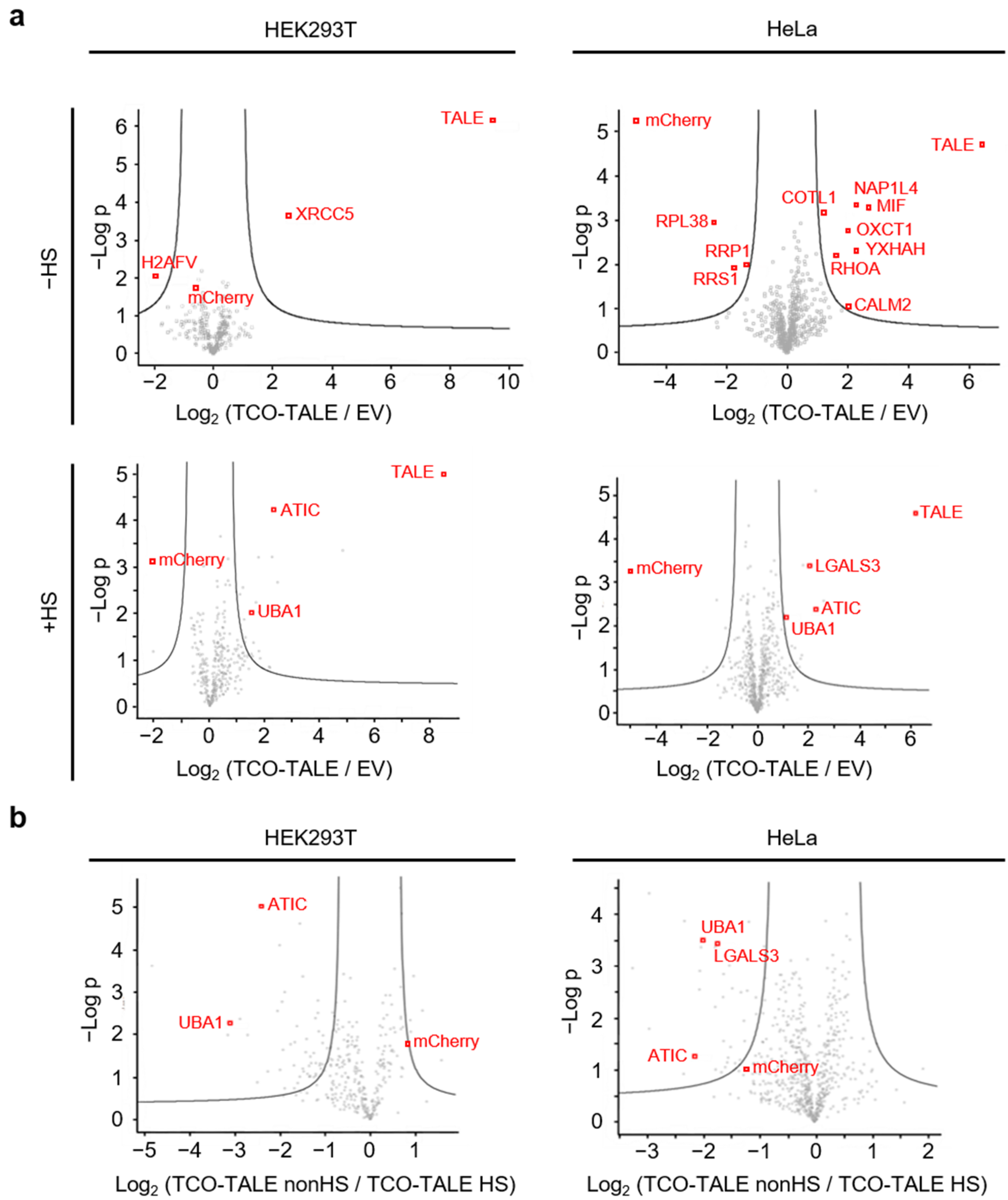

Figure 44 Mass spectrometry analysis of the SatIII-locus based enrichment: Enriched proteins were identified by proteomics analysis of biological triplicates after click-mediated enrichment using SatIII-TALE with incorporated non-canonical amino acid (ncAA) TCO together with tetrazine-biotin and streptavidin-conjugated beads. **a** Volcano plots depicting the enrichment and significance of the identified proteins for the SatIII locus for both cell lines HEK293T and HeLa under heat shock and non-heat shock conditions. **b** Volcano plots depicting the enrichment and significance of the identified proteins depending on heat shock (HS).

Most of the observed proteins, either in the TCO treated sample or in the control samples were nuclear proteins, indicating an efficient chromatin purification (Tab. S2 and Tab. S6). In both cell lines a 100-fold enrichment of the cyclooctene-functionalized SatIII-TALE protein compared to the empty vector control was observed (Fig. 44a). Overall, in the Boc-lysine treated samples a low number of proteins were identified, indicating an overall low non-specific binding background (Tab. S2 and Tab. S6). As expected, the number of identified proteins in the empty vector control were higher compared to the Boc-lysine treated samples. Even though the amber-codon is the least abundant stop codon, 24 % of the proteins in the human genome carry an amber-stop codon. By transfecting the cells with the $tRNA^{Pyl}$/PylRS pair and the empty vector, the added ncAA TCO can get incorporated in these proteins, suggesting that these proteins, which can get also enriched using the click-mediated enrichment, represent the overall off target amber suppression (Tab. S2 and Tab. S6).

Both cell lines showed an overlap in the significant enriched proteins in the heat-shock samples, whereas they did not overlap in the non-heat shock samples (Fig. 44a). The difference in the protein patterns between heat shock and non-heat shock samples indicates a heat shock response of both cell lines. Proteins, like UBA1 and ATIC, were significantly enriched only in the heat shock samples of both cell lines, suggesting a heat shock related function of these proteins (Fig. 44b, Tab. S3, Tab. S4, Tab. S5 and Tab. S7, Tab. S8,Tab. S9).

UBA1 is the canonical Ubiquitin E1 activating enzyme and is involved in proteostasis[267] by catalyzing the first step of the ubiquitin conjugation cascade, which marks cellular proteins for degradation through the ubiquitin-proteasome system. This gene complements an X-linked mouse temperature-sensitive defect in DNA synthesis, and thus may function in DNA repair.[268,269] Although there are no published relations between the SatIII locus and UBA1, cellular stress induced by heat shock is directly related to protein degradation and DNA repair, suggesting a connection between UBA1 and the SatIII locus, which is involved in the highly conserved and regulated heat shock response. Furthermore, with LGALS3 another potentially interesting protein was significantly identified from the heat shocked HeLa cell samples (Fig. 44 and Tab. S7, Tab. S8, Tab. S9). It was shown that Galectin-3 (LGALS3) interacts with transcription factors, such as the cAMP response element binding protein (CREBBP)[270], which is also known to be recruited to nSB similar to HSF1[134]. Additionally, it is demonstrated that the recruitment of CREBBP to nSBs is SatIII dependent[134]. Together this illustrates a direct association between CREBBP and SatIII as well as CREBBP and LGALS3, suggesting a direct or indirect interaction between SatIII and LGALS3. These findings demonstrate the potential of click-mediated enrichment of user-defined genomic loci combined with proteomic analysis for the identification of protein-protein and protein-DNA interactions and for studying their effects on the chromatin landscape. However, other heat shock factors like HSF1 or BRD4 could not be enriched. This could be a consequence of the transient transfection that causes very heterogeneous expression levels in the cells and a lower transfection efficiency. Pervious, fluorescent imaging has shown that HSF1 is not accumulated in the nSBs in every cell (Fig. 42). In combination with moderate transient transfection rates of multiple plasmids and the heterogeneous expression levels, this could lead to a small cell sub-population, showing both the expression of the TALE constructs and the HSF1 accumulation, thereby being potentially not sufficient for proteomics analysis. Previous studies with TALE-based telomere enrichment did not identify shelterin proteins, suggesting that the TALE binding might compete with the binding of these telomere proteins. In this work, however, HSF1 is not retrieved, as the fluorescent imaging indicates that the SatIII-TALE itself does not introduce a bias by outcompetition of HSF1 (Fig. 42). Furthermore the recruitment of HSF1 shown by qPCR in the presence of the SatIII-TALE (Fig. 43), also suggest that the absence of HSF1 is not an intrinsic limitation of TALE-capture, but either due to insufficient ionization of HSF1 or insufficient enrichment. Comprehensive identification of protein-protein or protein-DNA interactions using click-mediated enrichment in combination with proteomic analyses will probably benefit from cells stably expressing the amber suppression machinery. In addition, the overexpressed TALE could lead to a bead blocking effect. Since the overexpression can cause a huge fraction of non-DNA bound TALE protein still bound to the beads, the capturing efficiency might be reduced. This could be overcome by further reducing the expression levels of the TALE protein. Nevertheless, a very low amount of the heat shock factor BRD4 could be detected in one of the heat shocked biological triplicates in HeLa cells, which could indicate an insufficient quantity of SatIII DNA protein complex at the beads. This is further indicated by the amount of the starting material used ($3x10^6$ HEK293T cells and 10^7 HeLa cells), which is relatively low compared to other purification and enrichment methods of specific chromatin loci[138].

In addition, the significant enriched ATIC, showing a significant heat shock response, is not related to cellular stress or to the SatIII locus so far, which could indicate that some enriched proteins are possible contaminants. Also the mCherry fluorophore, strongly overexpressed by the EV, was found to enrich in the negative controls, indicating that the washing conditions were not sufficient to remove highly abundant proteins which bind nonspecifically to the beads. Consequently, the method still requires further optimization of binding/washing conditions or should be combined with a second orthogonal enrichment step.

9.8 Enrichment and Proteomic Analyses of TALE-TET fusion constructs targeting Repetitive Loci

The click-mediated enrichment in combination with proteomics analysis could be also applicable for detecting readers of cytosine modifications in the genome. The growing evidence that the oxidized 5mC derivates 5hmC, 5fC and 5caC represent epigenetic marks, raises the question with which proteins these nucleobases interact and how they interact in the natural chromatin setting, i.e. in the presence of nucleosomes and the multitude of additional chromatin proteins that may selectively induce or prevent interactions[271–273]. So far, most of the *in vitro* studies are focused on interaction analysis of single, selected proteins and “naked” DNA[274–277]. Besides the found interaction partners of oxidized 5mC derivates, the effect of these nucleobases on the local chromatin landscape remains unclear. These studies cannot reveal indirect protein recruitment and release, chromatin opening or the influence on writing and erasing of histone posttranslational modifications (PTM). Even perturbation editing strategies like global TET overexpression or inhibition by small molecules combined with downstream chromatin analysis are often poorly resolved and cannot reveal effects of local 5mC oxidation[278]. The combination of TALE-TET fusion constructs, which could introduce oxidized 5mC derivates locus specific *in vivo*, with robust click-mediated enrichment could enable studying epigenetic changes in the local chromatin landscape *in vivo* with potential increased sensitivity and selectivity. For first experiments in this direction, different TALE proteins against several repetitive DNA loci were fused to the TET2 catalytic domain (TET2CD) to introduce oxidized 5mC derivates at user-defined genomic loci *in vivo*. Specifically, a new TALE entry vector was generated by exchanging the C-terminal fused mCherry fluorophore with the TET2CD using Gibson cloning[279]. Afterwards TALE proteins against the Alu, Line1, α-Sat, SatII, SatIII and telomere locus were assembled into the entry vector, resulting in amber codon carrying TALEs, C-terminally fused to TET2CD. The selective binding of these TALEs to their specific genomic loci was exhibited by a click-mediated enrichment followed by qPCR analysis.

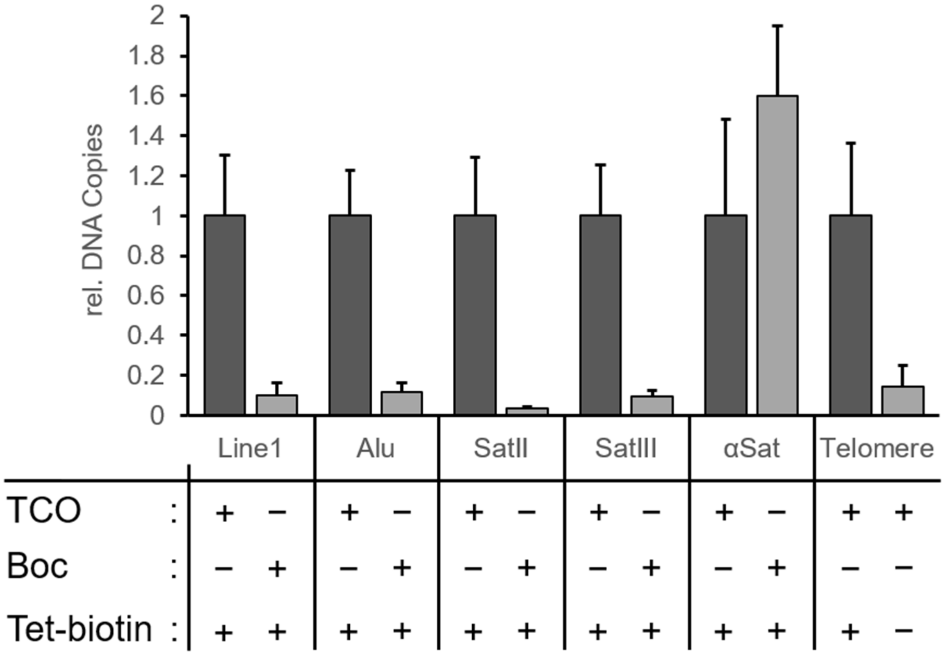

Figure 45 qPCR analysis of click-mediated enrichment of different genomic loci: Relative DNA copies of six different genomic loci (Line1, Alu, SatII, SatIII, αSat and Telomere) bound by the corresponding TALE with incorporated non-canonical amino acid (ncAA) after click-mediated enrichment using tetrazine-biotin and streptavidin coated magnetic beads from technical triplicates. For the loci Line1, Alu, SatII, SatIII and αSat TALE-TET fusion constructs were used with incorporated ncAA TCO or Boc. For the Telomere locus a biotinylated (+tetrazine-biotin (TET-biotin)) or non-biotinylated (–Tet-biotin) TALE-mCherry construct was used. The DNA copy numbers were normalized to the respective positive sample.

Five of six TALE constructs, Line1, Alu, SatII, telomeres and the already established SatIII-TALE, showed an enrichment of the selected genomic loci in the qPCR analysis (Fig. 45). This indicates that the C-terminal TET2CD of the Alu, Line1, SatII and SatIII-TALEs does not interfere with the TALE binding. The good selectivity, which is comparable between these five TALEs, shows a valid binding affinity of the designed TALEs.

Since the TALE binding affinity depends on the chromatin accessibility as well as on the length and the GC content of the target sequence, changing the target sequence inside the genomic regions for the αSat-locus could potentially lead to an effective isolation of α-Sat loci.

Next the nuclear extracts of HEK293T cells, transfected with the new TALE-TET2CD fusion constructs as well as the telomere-TALE, were analyzed by the established click-mediated enrichment in combination with mass spectrometry-based proteomics. To further reduce the overall background of the off-target amber suppression and to increase sensitivity, an immunoprecipitation step was added to the protocol, which was followed by the click-mediated enrichment.

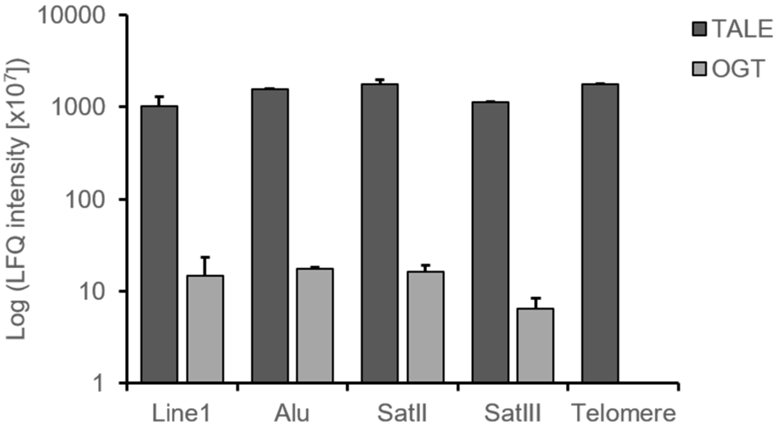

Figure 46 Mass spectrometry-based analysis of the enrichment of different genomic loci: LFQ intensities are shown for different TALE constructs targeting different genomic loci and for the TET2 interaction partner OGT from technical duplicates. TALEs targeting Line1, Alu, SatII and SatIII were fused to TET2CD and the telomere-TALE was fused to mCherry.

The LFQ intensities showed that all loci are obtained with comparable levels of enriched TALE protein. Furthermore, only for the four loci Line1, Alu, SatII and SatIII, where the TALE proteins was fused to TET2CD, the known TET2 interaction partner O-linked β-N-acetylglucosamine (O-GlcNAc) transferase (OGT)[280] was identified, whereas for the telomere-TALE sample, not carrying the TET2CD domain, no OGT peptide could be found (Fig. 46 and Tab. S10). This illustrates the potential of the click-mediated enrichment in combination with targeted proteomics for the identification of specific interaction partners as well as the huge variety of usable target sequences. To study the effects of 5mC oxidation on the chromatin landscape, additional experiments are needed that could show the successful target specific oxidation of 5mC as well as changes in the protein pattern between active and inactive TET2CD carrying samples.

10 Summary and Outlook

In the course of this work, the first ever click-mediated enrichment of specific genomic loci based on copper-free click chemistry could be established. This click-mediated enrichment is based on TALE proteins, which have shown high selectivity in the natural chromatin landscape *in vivo* as well as full programmability, allowing the targeting of different genomic loci. A successful TALE targeting of five different genomic loci, Line1, Alu, SatII, SatIII and telomere, was shown. For the click-mediated biotinylation, a non-canonical amino acid (ncAA) was introduced at the N-terminal region of the TALE constructs using genetic code expansion. This showed, a position depended fidelity and incorporation efficiency of amber suppression, providing new insights into the position dependence of ncAA incorporation using amber suppression. Additionally, the accessibility and thereby the successful biotinylation of the incorporated ncAA was validated by the click-reaction between the ncAA TCO and tetrazine-biotin. This enabled the click-mediated enrichment of SatIII locus through streptavidin-conjugated beads with high sensitivity and selectivity. In combination with proteomics analysis, this method allowed detection of changes in the protein composition at the SatIII-locus in the natural chromatin setting upon heat shock.

Click-mediated enrichment enables a robust isolation method of user-defined genomic loci and the identification of changes in the protein composition in the chromatin landscape. Since the introduced trans-cyclooctene (TCO) is very small, it has only a minimal effect on the protein structure, making it a viable alternative to epitope tagging, especially for proteins that are not N- or C-terminally taggable. In contrast to the antibody-protein affinity method, click-mediated enrichment relies on the formation of a covalent bond and a streptavidin-biotin interaction for enrichment, which allows for stringent purification and enrichment. This is beneficial for analysis techniques that are sensitive to contaminations, such as comprehensive PTM identification, crosslinking-MS, and chromatin immunoprecipitation purposes. The biotinylation using copper-free click chemistry is an alternative biotinylation method, which only provides a low nonspecific biotinylation in the chromatin context, thereby decreasing the nonspecific biotinylated proteome. This shows that the principle of click-mediated enrichment of specific genomic loci has great potential for both proteomics and genomics analyses.

Furthermore, the designed TALE-TET fusion construct showed in combination with the click-mediated biotinylation, the specific enrichment of the five different genomic loci, Line1, Alu, SatII, SatIII and telomere. The proteomics analyses of these constructs have shown the specific detection of a TET interaction partner, thereby providing the basis for a robust technique for purifying genomic loci based on click-mediated enrichment with targeted mC oxidation. This will lead to new perspectives for simple and accurate analysis to study how hmC, fC and caC influence the local chromatin landscape *in vivo* and potential discovery of repelled 5mC readers and direct and indirect oxi-5mC readers. Furthermore, an improved version of the click-mediated enrichment could be applied for studying single gene loci, which would give insights into the impact of 5mC oxidation effects on cancer-related misregulations and its dependence on promoter and cell type.

11 Materials and Methods

11.1 Materials

Table 1 Lab Equipment

Type	Model	Supplier
3-in1 pH glass electrode	LE410	Mettler Toledo
Agarose Gel Electrophoresis System	Midicell Primo EC330 kuroGEL MiniPlus 10	ThermoEC vwr
Agarose gel staining bath	Steel chamber 18/10	Bochem
Biological Safety Cabinet	NU S440 500E	Nuaire
Bunsen Burner	1010	Usbeck
Calculator	FX-82SX Plus	Casio
Camera	PowerShot G10	Canon
Camera Chamber	BDAdigital	Biometra
Centrifugal vaccum concentrator	Concentrator plus	Eppendorf
Centrifuges	5415R/5810R/5424/5427R/5804R Sprout Mini Centrifuge Sorvall Lynx 6000	Eppendorf Heathrow Scientific Thermo Scientific
CO_2 Incubator	HeraCell 150 Cell Expert	Thermo Electron Corp. Eppendorf
Conversion lens adapter	LA-DC58K	Canon
Cryo Container	5100-0001	Nalgene
ddH_2O	Purelab flex2	ELGA
Electric transformation	Eporator	Eppendorf

Freezer	Profi Line GG4010 Premium GGU 1500	Liebherr
Freezer	−80 °C Ultra Low Temperature Freezer U725-G Innova	New Brunswick Scientific
Freezer	−152 °C Ultra Low	Sanyo
Fridge	Profi Line FKU 1800	Liebherr
Heating Block	AccuBlock Digital Dry Bath Thermocell Cooling & Heating Block Thermostat plus	Labnet Biozym Eppendorf
Hemocytometer	718605 (Neubauer)	Brand
Ice Machine	AF20	Scotsman
Incubator	100-800	Memmert
Incubator – Shaker	I26	New Brunswick Scientific
Magnetic stand	MagRack 6	GE Healthcare
Magnetic Stirrer	MR Hei-Standard MR Hei-Mix S Thermo Variomag Mono Stir CB 161	Heidolph Heidolph Thermo Scientific Stuart
Microscope 1	IX81	Olympus
Microscope 1 Camera System	EM-CCD	Hamamatsu
Microscope 1 Lamp	MT20	Olympus
Microscope 1 Objectives	10x ULPSAPO 60x PLAPO/TIRF	Olympus
Microscope 2	IX81	Olympus
Microscope 2 Camera System	ORCA-R^2 – C106000	Hamamatsu
Microscope 2 Lamp	IX2-UCB	Olympus
Microscope 2 Objective	60x UPlanSApo	Olympus
Microscope 3	EVOS XL Imaging System	Life Technologies

Microscope 3 Objectives	4x Amep 4632 10x Amep 4633 20x Amep 4634	Life Technologies
Microscope 4	Eclipse TE200	Nikon
Microscope 4 Objective	10x 20x	Nikon
Microwave	ED 8525.3S	Exquisit
Multichannel Pipettes	Research 10/200 µL (8 channel)	Eppendorf
PCR Cycler	SimpliAmp T Personal Thermocycler MyCycler™ Thermal Cycler System	Life Technologies Biometra Bio-Rad
PCR workstation	PCR workstation pro	Peqlab/vwr
pH-Meter	Five easy	Mettler-Toledo
Pipetboy	Accu-jet Pipetboy	Brand IBS Integra Biosciences
Pipettes	Research Plus 1000/100/10/2.5 µL	Eppendorf
Plate reader	Infinite M1000	Tecan
Power Supply	EV233 PowerPac basic	Consort Bio-Rad
qPCR Cycler	CFX 384 Touch Real-Time PCR Detection System	Bio-Rad
Rotor	Fiberlite F14-6x250y	Thermo Scientific
Scale	3500-2NM AX224 PM400	Kern PLJ Sartorius Mettler
Sonicator	Bioruptor Pico	Diagenode
Spectrometer for concentration determination of DNA	Nanodrop 2000	Thermo Scientific

Thermomixer	Thermomixer comfort Thermomixer F1.5 Thermomixer C	Eppendorf Eppendorf Eppendorf
Tube Revolver	Tube Revolver	Thermo Scientific
UV Protection	EN 166-3F	Bollé
UV Table	UVstar 312 nm	Biometra
UV-Vis Spectral Photometer	NanoDrop2000	Thermo Scientific
Vacuum Manifold	QIAvac 24 Plus	Qiagen
Vacuum Pump	VNC2 Vacusafe comfort	Vacuubrand IBS Integra Biosciences
Vortex Mixer	Vortex-Genie 2	Scientific Industries
Waterbath	3047	Köttermann

Table 2 Software and Tools

Name	Purpose	Developer/Distributor
BioDoc Analyze 2.1	Imaging of agarose gels	Jena Bioscience
CFX Manager	Analysis and presentation of data from qPCR	Bio-Rad
Chemdraw 18.0	Chemical structure and reaction scheme design	Perkin Elmer
Citavi 6	Citation	Swiss Academic Software
CorelDRAW X6	Figure design	Corel
Excel	Data analysis and presentation	Microsoft
ExPASy	Bioinformatic tools (UniProt KB, BLAST, Compute pI/MW)	Swiss Institute of Bioinformatics
ImageJ	Image editing and data analysis	National Institute of Health
NanoDrop 2000 Software 1.6.198	Data analysis of DNA concentration measurements	Thermo Scienctific
Origin 2018	Data analysis and presentation	OriginLab
Pymol	Protein structure design	Schroedinger
SnapGene	Analysis of data from Sanger sequencing, design of plasmid maps	GSL Biotech
Word	Data presentation and writing of manuscript	Microsoft

Table 3 Services

Service	Product	Company
Synthesis	Oligonucleotides	Sigma Aldrich/Merck
Analysis	Sanger Sequencing	GATC/Eurofins Microsynth

Table 4 Disposables and Glass Ware

Product	Manufacturer/Distributor
µ-Dish 35 mm, high, glass bottom	ibidi
1.5 mL Bioruptor Pico Mircotubes	Diagenode
35 mm Dish, 10 mm glass diameter	Matek
384 well Lightcycler plate PP	Sarstedt
96 well plates transparent	Carl Roth
96 well plates white	Sarstedt
Adhesive clear qPCR seals	Biozym
Biosphere Tip 200 µL	Sarstedt
Cell Scraper 39 cm, 25 cm, 16 cm	Sarstedt
Conical plastic tubes, 15 mL	Sarstedt
Conical plastic tubes, 50 mL	Sarstedt
CryoPure 2 mL	
Disposable glass Pasteur pipettes, sealed point, pre-marked, 230 mm	vwr
Electroporation cuvettes 1 mm	Carl Roth
ELISA-Platte weiß 96 Well	Sarstedt
epT.I.P.S. LoRetention 0.1 -10 µL	eppendorf

Erlenmayer flasks (2 L, 1 L, 500 mL, 100 mL, 25 mL)	vwr
Filter tips, low retention (2-100µL)	vwr
Filtropur BT50 500 mL, 0.22 µm	Sarstedt
Filtropur V50 0.2, 500 mL Vacuum Filter	Sarstedt
Glass beads	VWR
Gloves Nitrile	VWR
Multiply Pro 0.2 mL reaction tube	Sarstedt
MµLTIGUARD 100-1000 µL low retention filter tips	Sorenson
MµLTIGUARD 1-10 µL low retention filter tips	Sorenson
MµLTIGUARD 1-200 µL low retention filter tips	Sorenson
NORM-JECT single-use syringes (20 mL, 5 mL)	Henke-Sass, Wolf
Nunc LabTek II 8-well Chamber Slide	Thermo
Nunc sealing tape, breathable, sterile	Thermo Fisher Scientific
Omnifix single-use syringes (50 mL, 20 mL, 10 mL)	B.Braun
Omnifix-F single-use syringes (1 mL)	B.Braun
Parafilm PM-996	Bemis
Petrischale 92x16 mm	Sarstedt
Pierce C18 Tips 100 µL bed	Thermo
Pipette tips (10 µL, 200 µL, 1000 µL) Sarstedt	Sarstedt
Pipette tips 0,1 – 20 µL, PP, CE-IVD	Brand

Protein LoBind Tubes	eppendorf
qPCR seals	Biozym
Reaction tubes 1.5 mL	Sarstedt
Reaction tubes 2.0 mL	Sarstedt
Round bottom flask with standard ground joint (250 mL, 100 mL)	Duran
Scalpel	B.Braun
Schott flasks (10 mL, 25 mL, 1000 mL, 500 mL, 250 mL, 100 mL, 50 mL)	Duran
Schott flasks (1000 mL, 500 mL, 250 mL, 100 mL, 50 mL)	vwr
Serological pipette 10 mL	Sarstedt
Serological pipette 25 mL	Sarstedt
Sterican single-use needles 0.80 x 120 mm, 21 G x 4 ¾''	B.Braun
Sterican single-use needles 0.90 x 40 mm, 20 G x 1 ½''	B.Braun
Sterican single-use needles 0.90 x 70 mm, 20 G x 2 ¾''	B.Braun
Sterican single-use needles 1.20 x 40 mm, 18 G x 1 ½''	B.Braun
Syringe filter 0.2 µM	Sarstedt
TC-Platte 6 Well, Standard	Sarstedt
TC-Platte 96 Well, Standard	Sarstedt
TC-Platte 96 Well, Standard	Sarstedt
TC-Schale 35, 60, 100, Standard	Sarstedt

Table 5 Commercial Kits and Master Mixes

Name	Type	Manufacturer/Distributor
1.33x Gibson master mix	5x isothermal buffer, T5 exonuclease 1.0 U/µL, Phusion DNA polymerase 2 U/µL, Taq DNA ligase 40 U/µL	AG Summerer
GeneJET Gel extraction Kit	Purification of PCR products and DNA from agarose gels	Thermo Scientific
GeneJET PCR purification Kit	Purification of PCR products and DNA from reaction mixes	Thermo Scientific
GeneJET Plasmid Miniprep Kit	Plasmid DNA purification	Thermo Scientific
GoTaq qPCR Master Mix	qPCR Master Mix	Promega
Invitrogen™ PureLink™ HiPure Plasmid FP	MaxiPrep Kit for Plasmid DNA purification	Invitrogen
NucleoBond® Xtra Maxi Plus	MaxiPrep Kit for Plasmid DNA purification	Macherey Nagel
Nucleospin Gel and PCR Clean-up	Purification of PCR products and DNA from reaction mixes and agarose gels	Macherey Nagel
NucleoSpin Plasmid Easy Pure	Plasmid DNA purification	Macherey Nagel
Pierce BCA Protein Assay Kit	Protein concentration determination	Thermo Scientific
QIAamp DNA Mini Kit	Purification of gDNA	Qiagen

Table 6 Consumables

Name	Use	Manufacutrer/Distributor
10 % FBS	Supplement for DMEM	PAN Biotech
2-Log DNA Ladder (0.1-10 kb)	Standard DNA ladder for agarose gels	NEB
3x-FLAG Peptide	Peptide for IP Elution	Merck
Avidin from egg white	Biotin blocking reagent	VWR
Bright-Glo	Luciferase assay master mix	Promega
Complete Mini Protease Inhibitor Cocktail	Protease Inhibitor	Merck
Complete Protease Inhibitor Cocktail	Protease Inhibitor	Merck
DMEM	Medium for HEK293T and HeLa cells	PAN Biotech
DPBS	Wash buffer for Luciferase assay	PAN Biotech
Dynabeads 270 Streptavidin	Magnetic Streptavidin Beads	Invitrogen
Dynabeads M280 Streptavidin	Magnetic Streptavidin Beads	Invitrogen
Dynabeads MyOne Streptavidin C1	Magnetic Streptavidin Beads	Invitrogen
Dynabeads MyOne Streptavidin T1	Magnetic Streptavidin Beads	Invitrogen
Dynabeads Protein G	Magentic Protein G Beads for IP	Invitrogen
GoTag qPCR Master Mix	Convenient Master Mixes for qPCR and RT-qPCR	Promega

LB agar (Lennox)	Solid medium for *E.coli*	Carl Roth
LB-medium (Lennox)	Liquid medium for *E.coli*	Carl Roth
Lipofectamin 2000	Transfection reagent for HEK293T cells	Thermo Fisher Scientific
Low Molecular Weight DNA Ladder (25 bp to 766 bp)	DNA ladder for high percentage agarose gels	NEB
Opti MEM	Transfection Medium for HEK293T cells	Gibco
Penicillin/Streptavidin solution	Antibiotics for cell medium	PAN Biotech
Tetrazine-5-FAM	Click Reagent for Fluorescent Labelling	Jenabioscience
Tetrazine-PEG$_4$-Biotin	Click Reagent for biotinylation	Jenabioscience
Trypsin / EDTA	For the dissociation of cell monolayers	PAN Biotech
X-tremeGENE 9	Transfection reagent for HeLa cells	Merck

Table 7 Chemicals

Name	CAS	Distributor
1,4-Dithiothreitol (DTT)	3483-12-3	Carl Roth
2-Propanol	67-63-0	Fisher Scientific
37 % Formaldehyde	50-00-0	Merck
5-Brom-4-chlor-3-indoxyl-β-D-galactopyranosid (X-Gal)	7240-90-6	Thermo Fisher Scientific
Acetic Acid	64-19-7	Carl Roth
Acetonitrile	75-05-8	Sigma Aldrich
Adenosintriphosphat, 10 mM solution	56-65-5	NEB
Agarose	9012-36-6	Biozym
Albumin, Bovine Serum (BSA)	9048-46-8	Cell Signaling Technology
Boric acid	10043-35-3	Carl Roth
Bromphenol blue	115-39-9	Sigma Aldrich
Carbenicillin disodium salt	4800-94-6	Carl Roth
Chloracetamide	79-07-2	Acros
Chloramphenicol	56-75-7	Carl Roth
Comassie Brilliant Blue G250	6104-58-1	Carl Roth
D(+)-Biotin	58-85-5	Carl Roth
dATP 100 mM	-	Thermo Fisher Scientific
dCTP 100 mM	-	Thermo Fisher Scientific
dGTP 100 mM	-	Thermo Fisher Scientific
Dimethyl sulfoxide (DMSO)	67-68-5	Carl Roth
dNTP solution mix, 10 mM	-	NEB
dTTP 100 mM	-	Thermo Fisher Scientific
endo BCN - L - Lysine	1493802-96-2	SiChem

Ethanol 96 %	64-17-5	Fisher Scientific
Ethanol, absolute	64-17-5	Sigma Aldrich
Ethidium bromide	1239-45-8	Sigma Aldrich
ethylene glycol-bis(β-aminoethyl ether)-*N,N,N′,N′*-tetraacetic acid (EGTA)	67-42-5	Sigma Aldrich
Ethylenediaminetetraacetate (EDTA)	60-00-4	Carl Roth
Formic acid	64-18-6	Carl Roth
Glucose	50-99-7	Merck
Glycerole	56-81-5	Carl Roth
Glycine	56-40-6	Carl Roth
Hydrochloric acid (1 M)	7647-01-0	vwr
Hydrochloric acid (37 %)	7647-01-0	vwr
IGEPAL CA-630	9002-93-1	Sigma Aldrich
Kanamycinsulfate	25389-94-0	Carl Roth
Lithium chloride	7447-41-8	Sigma Aldrich
Magnesium chloride hexadydrate	7791-18-6	Acros Organics
Magnesium sulfate heptahydrate	10034-99-8	Merck
Methanol	67-56-1	Sigma Aldrich
Nε-(tert-butoxycarbonyl)-L-lysine (Boc)	2418-95-3	VWR
Polyethylene glycol 8000 (PEG-8000)	25322-68-3	Merck
Poly-L-lysine hydrobromide (PLL)	25988-63-0	Sigma Aldrich
SCO - L - Lysine - HCO2H-salt	1309581-49-4	SiChem
Sodium chloride	7647-14-5	Carl Roth
sodium deoxycholate	302-95-4	Sigma Aldrich

Sodium dihydrogen phosphate monohydrate	10049-21-5	Merck
Sodium dodecyl sulfate (SDS)	151-21-3	Carl Roth
Sodium hydroxide	1310-73-2	Fisher Scientific
Sodium lauroyl sarcosinate	137-16-6	AppliChem
Tetracycline hydrochloride	64-75-5	Carl Roth
trans-Cyclooct-2-en – L - Lysine (TCO*A)	1801936-26-4	SiChem
Trifluoroacetic acid (TFA)	76-05-1	Sigma Aldrich
Tris(hydroxymethyl)aminomethane	77-86-1	Sigma Aldrich
Triton-X	9002-93-1	Fluka
Trizma base (Tris)	77-86-1	Carl Roth
Tryptone	91079-40-2	Merck
Tween20	9005-64-5	Fisher Scientific
Urea	57-13-6	Carl Roth
Water, nuclease-free	7732-18-5	Qiagen
Xylencyanol	2650-17-1	Carl Roth
Yeast extract	8013-01-2	Carl-Roth
β-Nicotinamide adenine dinucleotide hydrate (NAD)	53-84-9	Sigma Aldrich

Table 8 Buffers

Name	Components
5x isothermal reaction buffer	25 % PEG-8000, 500 mM Tris-HCl pH 7.5, 50 mM $MgCl_2$, 50 mM DTT, 1 mM dATP, 1 mM dTTP, 1 mM dCTP, 1mM dGTP, 5 mM NAD
Alkylation solution	50 mM chloracetamide in Denaturing/Reducing buffer
Cam Stock	34 mg/mL chloramphenicol in ethanol
Carb Stock	50 mg/mL Carbenicillin salt in 1:1 ethanol:water
Cell Lysis Buffer (CLB)	10 mM Tris-HCl, pH 8.0, 1 mM EDTA, 0.5% IGEPAL CA-630, 1 x protease inhibitors
CutSmart Buffer	50 mM KOAc, 20 mM Tris-acetate, 10 mM Mg(OAc)2, 100 µg/ml BSA, pH = 7.9
Denaturing/Reducing Buffer	8 M urea in 50 mM Tris pH = 7.5, 1 mM DTT
Dynabeads blocking solution	0.01 % Tween-20, 0.1 % BSA in DPBS
Dynabeads washing solution	0.01 % Tween-20 in DPBS
Enrichment solution	1 % Triton X-100 in MLB
HEK293T lysis buffer	100 mM NaH2PO4, 0.2 % Triton X-100
High Salt Buffer (HSB)	20 mM Tris-HCl, pH 8.0, 2 mM EDTA, 500 mM NaCl, 1% Triton X-100, 0.1% SDS
IP elution solution	500 µg/mL 3xFLAG peptide in TBS+IGEPAL
Kan Stock	50 mg/mL kanamycin sulfate in water
LB Medium	10 g/L tryptone, 5 g/L yeast extract, 10 g/L NaCl, pH = 7

LiCl Buffer	10 mM Tris-HCl, pH 8.0, 1 mM EDTA, 0.25 M LiCl, 0.5% IGEPAL CA-630, 0.5% sodium deoxycholate
Low Salt Buffer (LSB)	20 mM Tris-HCl, pH 8.0, 2 mM EDTA, 150 mM NaCl, 1% Triton X-100, 0.1% SDS
Modified Lysis Buffer (MLB)	10 mM Tris-HCl, pH 8.0, 1 mM EDTA, 0.5 mM EGTA, 150 mM NaCl, 0.1% sodium deoxycholate, 0.1% SDS, 1 x protease inhibitors
NEB1	10 mM bis-Tris-propane-HCl, 10 mM MgCl2, 1 mM DTT, pH = 7
NEB2	50 mM NaCl, 10 mM Tris-HCl, 10 mM MgCl2, 1 mM DTT, pH = 7.9
NEB3	100 mM NaCl, 50 mM Tris-HCl, 10 mM MgCl2, 1 mM DTT, pH = 7.9
NEB4	50 mM KOAc, 20 mM Tris-acetate, 10 mM Mg(OAc)2, 1 mM DTT, pH = 7.9
Nuclear Lysis Buffer (NLB)	10 mM Tris-HCl, pH 8.0, 1 mM EDTA, 0.5 M NaCl, 1% Triton X-100, 0.5% sodium deoxycholate, 0.5% lauroylsarcosine sodium salt, 1 x protease inhibitors
Permeabilization solution	0.25 % Triton X-100 in DPBS
PLL coating solution	0.01 % PLL in DPBS
Purple loading dye	2.5 % Ficoll-400, 10 mM EDTA, 3.33 mM Tris-HCl, 0.08% SDS, 0.02 % Dye 1, 0.001 % Dye 2, pH = 8
SOC	0.58 g/l NaCl, 2.03 g/l MgCl2 hexahydrate, 2.46 g/l MgSO4 heptahydrate, 5 g/l yeast extract, 20 g/l tryptone, 1 M glucose, pH = 7.5
Spec stock	100 mg/mL spectinomycin in water
Stage tip Buffer A	0.1 % formic acid in water

Stage tip Buffer B	0.1 % formic acid in 20 % water/80 % acetonitril
Stop crosslinking solution	1.25 M Gylcine
T4 DNA ligase buffer	50 mM Tris-HCl, 10 mM MgCl2, 1 mM ATP, 10 mM DTT, pH = 7.5
TBE Buffer	10.78 g/l Tris base, 5.50 g/l boric acid, 0.585 g/l EDTA, pH = 8.3
TBS	50 mM Tris-HCl, pH 7.5, 150 mM NaCl
TBS + IGEPAL	50 mM Tris-HCl, pH 7.5, 150 mM NaCl, 0.1% IGEPAL CA-630
Tet stock	12.5 mg/mL tetracycline in ethanol

Table 9 Enzymes

Name	Distributor
AscI	NEB
BglII	NEB
BsaI	NEB
BsmBI	NEB
DpnI	NEB
LysC	NEB
NruI	NEB
PacI	NEB
Pfu DNA Polymerase	Promega
Phusion Polymerase	NEB
PlasmidSafe nuclease	Biozym
Proteinkinase K	Roche
Q5 Polymerase	NEB
RNase A	Thermo Fisher Scientific
SacII	NEB
SalI	NEB
SpeI	NEB
T4 ligase	NEB
T5 exonuclease	NEB
Taq DNA ligase	NEB
Taq Polymerase	NEB
Trypsin MS Grade	NEB

Table 10 Antibodies

Antibody	Source	Supplier
monoclonal anti-FLAG M2	mouse	Sigma Aldrich
HSF1 #4356	rabbit	Cell Signaling
secondary goat anti-rabbit FITC	goat	Invitrogen
secondary goat anti-mouse Alexa Fluor 750	goat	Invitrogen

Table 11 Strains and Cell Lines

Type	Host
GH371	*E. coli*
HEK293T	*H. sapiens*
HeLa	*H. sapines*

Table 12 Oligonucleotides

Name	Description	Sequence
o1899	hey2-TALE binding site fw for hybridization and restriction (SalI and SpeI)	TTTTGTCGACTCTTCCGTTTCCACATCTACTAGTTTTT
o1900	hey2-TALE binding site rv for hybridization and restriction (SalI and SpeI)	AAAAACTAGTAGATGTGGAAACGGAAGAGTCGACAAAA
o2481	SatIII-TALE binding site fw for hybridization and restriction (SalI and SpeI)	TTTTGTCGACTGATTCCATTCCATTCCATTACTAGTTTTT
o2482	SatIII-TALE binding site rv for hybridization and restriction (SalI and SpeI)	AAAAACTAGTAATGGAATGGAATGGAATCAGTCGACAAAA
o2851	Gibson Primer linearization of pDaS273 fw	GATAAAAAACCGCTGAATACCCTGA
o2852	Gibson Primer linearization of pDaS273 rv	CATGGTGGCAAGCTTCC
o2471	Gibson Primer mCherry into pAnW750 fw	AAACGCAAAGTTGGGCGCGCCGTGAGCAAGGGCGAGGAGCTGTTC
o2472	Gibson Primer mCherry into pAnW750 rv	GAACGTCGTACGGGTAGTTAATCTTGTACAGCTCGTCCATGCCGAG

o2853	Gibson Primer NES Insert fw	CACGGAAGCTTGCCACCATGGCCTGCCCCGTGCCCCTGCAGCTGCCCCCCCTGGAGAGACTGACCCTGGACGATAAAAAACCGCTGAATAC
o2854	Gibson Primer NES Insert fw	GTATTCAGCGGTTTTTTATCGTCCAGGGTCAGTCTCTCCAGGGGGGGCAGCTGCAGGGGCACGGGGCAGGCCATGGTGGCAAGCTTCCGTG
o2108	Gibson Primer transfection control into pAnW750 fw	GTGCCACCTGACGTCGACGGATCGGGACGTTACATAACTTACGGTAAATGG
o2109	Gibson Primer transfection control into pAnW750 rv	GTCAACGCGTATATCTGGCCCGTACATCGATGTCTGCTCGAAGCGGC
o3387	Insert GG Cassette deletion on pAnW1272 fw	GGAGGTGGCGGTGGCAGCGGG
o3388	Insert GG Cassette deletion on pAnW1272 rv	CGCGCCCGCTGCCACCGCCACCTCCGC
o2843	Quick Change Primer A104TAG fw	GGCGTTGCCAGAGTAGACACACGAAGACAT
o2844	Quick Change Primer A104TAG rv	TCTTCGTGTGTCTACTCTGGCAACGCCGTG
o2845	Quick Change Primer D108TAG fw	GACACACGAATAGATCGTTGGCGTCGGCAA
o2846	Quick Change Primer D108TAG rv	CCGACGCCAACGATCTATTCGTGTGTCGCC
o1993	Quick Change Primer D140TAG fw	GGTCCGCCGTTACAGTTGTAGACAGGCCAACTTGTGAAG
o1994	Quick Change Primer D140TAG rv	GCAATCTTCACAAGTTGGCCTGTCTACAACTGTAACGGC

o1995	Quick Change Primer E157TAG fw	GGCGGCGTGACCGCAATGTAGGCAGTGCATGCATCGCGC
o1996	Quick Change Primer E157TAG rv	GCATTGCGCGATGCATGCACTGCCTACATTGCGGTCACG
o2817	Quick Change Primer E50TAG fw	CAGCAGCAGCAATAGAAGATCAAACCGAAG
o2818	Quick Change Primer E50TAG rv	CACCTTCGGTTTGATCTTCTATTGCTGCTG
o2829	Quick Change Primer F72TAG fw	GGTGGGCCATGGGTAGACACACGCGCACAT
o2830	Quick Change Primer F72TAG rv	TGCGCGTGTGTCTACCCATGGCCCACCAGT
o3218	Quick Change Primer G33TAG fw	GAAGAGGAAGGTGTAGCGCGGATCTGTGGA
o3219	Quick Change Primer G33TAG rv	AGATCCACAGATCCGCGCTACACCTTCCTC
o2835	Quick Change Primer G88TAG fw	CCCGGCAGCGTTATAGACCGTCGCTGTCAC
o2836	Quick Change Primer G88TAG rv	ACAGCGACGGTCTATAACGCTGCCGGGTGT
o2837	Quick Change Primer H96TAG fw	CTGTCACGTATCAGTAGATAATCACGGCGT
o2838	Quick Change Primer H96TAG rv	CCGTGATTATCTACTGATACGTGACAGCGA
o2839	Quick Change Primer I97TAG fw	CGTATCAGCACTAGATCACGGCGTTGCCAG
o2840	Quick Change Primer I97TAG rv	GCAACGCCGTGATCTAGTGCTGATACGTGA
o2841	Quick Change Primer I98TAG fw	CGTATCAGCACATATAGACGGCGTTGCCAG
o2842	Quick Change Primer I98TAG rv	GCAACGCCGTCTATATGTGCTGATACGTGA

o3205	Quick Change Primer K23TAG fw	GATGACGATGACTAGATCGCCCCCAAGAAG
o3206	Quick Change Primer K23TAG rv	CTTCTTCTTGGGGGCGATCTAGTCATCGTC
o2819	Quick Change Primer K51TAG fw	CAGCAGCAGCAAGAGTAGATCAAACCGAAG
o2820	Quick Change Primer K51TAG rv	CACCTTCGGTTTGATCTACTCTTGCTGCTG
o3232	Quick Change Primer K870TAG fw	GTTGCCGGATCCTAGGCTAGCCCGAAAAAG
o3233	Quick Change Primer K870TAG rv	TTTCTTTTTCGGGCTAGCCTAGGATCCGGC
o2847	Quick Change Primer L126TAG fw	CCTGGAGGCCTTGTAGACGGATGCGGGGG A
o2848	Quick Change Primer L126TAG rv	CCCGCATCCGTCTACAAGGCCTCCAGGGCG
o2833	Quick Change Primer L80TAG fw	CGCACATCGTTGCGTAGAGCCAACACCCGG
o2834	Quick Change Primer L80TAG rv	GGTGTTGGCTCTACGCAACGATGTGCGCGT
o3207	Quick Change Primer M24TAG fw	GACGATGACAAGTAGGCCCCCAAGAAGAAG
o3208	Quick Change Primer M24TAG rv	CCTCTTCTTCTTGGGGGCCTACTTGTCATC
o2813	Quick Change Primer Q48TAG fw	CTACAGTCAGCAGTAGCAAGAGAAGATCAA
o2814	Quick Change Primer Q48TAG rv	ATCTTCTCTTGCTACTGCTGACTGTAGCCG
o2815	Quick Change Primer Q49TAG fw	CAGTCAGCAGCAGTAGGAGAAGATCAAACC
o2816	Quick Change Primer Q49TAG rv	TTGATCTTCTCCTACTGCTGCTGACTGTAG
o2809	Quick Change Primer R34TAG fw	CTGTGGATCTATAGACGCTCGGCTACAGTC

o2810	Quick Change Primer R34TAG rv	TGTAGCCGAGCGTCTATAGATCCACAGATC
o3240	Quick Change Primer R881TAG fw	GAAACGCAAAGTTGGGTAGGCCGTGAGCAA
o3241	Quick Change Primer R881TAG rv	CCCTTGCTCACGGCCTACCCAACTTTGCGT
o3224	Quick Change Primer S36TAG fw	GAAGGTGGGCCGCGGATAGGTGGATCTAC G
o3225	Quick Change Primer S36TAG rv	GTGCGTAGATCCACCTATCCGCGGCCCACC
o2825	Quick Change Primer S58TAG fw	CCGAAGGTGCGTTAGACAGTGGCGCAGCAC
o2826	Quick Change Primer S58TAG rv	CTGCGCCACTGTCTAACGCACCTTCGGTTT
o1991	Quick Change Primer V92TAG fw	GGGACCGTCGCTTAGACGTATCAGCACATA ATCACGGCG
o1992	Quick Change Primer V92TAG rv	GATTATGTGCTGATACGTCTAAGCGACGGTC CCTAACGC
o3197	Quick Change Primer Y10TAG fw	GACCATGACGGTGATTAGAAAGATCATGAC
o3198	Quick Change Primer Y10TAG rv	GATGTCATGATCTTTCTAATCACCGTCATG
o2811	Quick Change Primer Y44TAG fw	CTACGCACGCTCGGCTAGAGTCAGCAGCAG
o2812	Quick Change Primer Y44TAG rv	CTGCTGACTCTAGCCGAGCGTGCGTAGATC
o3228	Quick Change Primer Y868TAG fw	CATCGCGTTGCCTAGTCCAAGGCTAGCCCG
o3229	Quick Change Primer Y868TAG rv	TTTCGGGCTAGCCTTGGACTAGGCAACGCG

o736	Sequencing Primer fw for Golden Gate Assembly in pAnW750	TTGGCGTCGGCAAACAGTGG
o2040	Sequencing Primer mCherry in pAnW750	TCCTGCCATGGATGCAGT
o2270	Sequencing Primer NES in pAnW1410	GGATAGCGGTTTGACTCACG
o1953	Sequencing Primer N-terminal amber codons	GGACTACAAAGACCATGACG
o2086	Sequencing Primer rv for Golden Gate Assembly in pAnW750	GACTCTTCTGATCAATTCCG
o1978	Sequencing Primer TALE binding site in pAnW755	GGTCATAACAGCAGCTTCAG
o2112	Sequencing Primer Transfection control in pAnW750	GAAGCATTTATCAGGGTTATTG
o3799	qPCR Primer αSat fw	CTCAGAAACTTCTTTGTGATGTGT
o3800	qPCR Primer αSat rv	TATTCCCTTTTCCAACGAAGGC
o3749	qPCR Primer Alu fw	AGTTCGAGACCAGCCTGGC
o3750	qPCR Primer Alu rv	CGGGTTCAAGCGATTCTCC
o3655	qPCR Primer Line1 fw	GCTACGGGAGGACATTCAAA
o3656	qPCR Primer Line1 rv	TTCAGCTCCATCAGCTCCTT
o3802	qPCR Primer SatII fw	CATCGAATGGAAATGAAAGGAGTC
o3803	qPCR Primer SatII rv	ACCATTGGATGATTGCAGTCAA
o2419	qPCR Primer SatIII fw	AATCAACCCGAGTGCAATCGAATGGAATCG
o2420	qPCR Primer SatIII rv	TCCATTCCATTCCTGTACTCGG
o2807	qPCR Primer Telomere fw	GGTTTTTGAGGGTGAGGGTGAGGGTGAGGGTGAGGGT
o2808	qPCR Primer Telomere rv	TCCCGACTATCCCTATCCCTATCCCTATCCCTATCCCTA

Table 13 Plasmids

Name	Description	Supplier	Resistance
pAnW750	Golden-Gate entry plasmid with CMV promoter and C-terminal VP64 domain	AddGene	Carb
pAnW755	Luciferase reporter plasmid with minimal CMV promoter (CMV) and firefly luciferase gene	Oxford Genetics	Kan
pAnW781	Luciferase reporter plasmid with 1297-TALE binding site	this work	Kan
pAnW803	Golden-Gate entry plasmid with CMV promoter, C-terminal VP64 domain and V92TAG	this work	Carb
pAnW891	Golden-Gate entry plasmid with CMV promoter, C-terminal VP64 domain and mCherry-GFP fusion construct with Y39TAG as transfection control	this work	Carb
pAnW917	Golden-Gate entry plasmid with CMV promoter, C-terminal VP64 doamin, transfection control and V92TAG	this work	Carb
pAnW919	Golden-Gate entry plasmid with CMV promoter, C-terminal VP64 doamin, transfection control and D140TAG	this work	Carb
pAnW921	Golden-Gate entry plasmid with CMV promoter, C-terminal VP64 doamin, transfection control and E157TAG	this work	Carb
pAnW996	1297-TALE with V92TAG, C-terminal VP64 domain and CMV promoter; additional transfection control under CMV promoter	this work	Carb
pAnW997	1297-TALE with D140TAG, C-terminal VP64 domain and CMV promoter; additional transfection control under CMV promoter	this work	Carb

pAnW999	1297-TALE with E157TAG, C-terminal VP64 domain and CMV promoter; additional transfection control under CMV promoter	this work	Carb
pAnW1000	1297-TALE without amber codon and with C-terminal VP64 domain and CMV promoter; additional transfection control under CMV promoter	this work	Carb
pAnW1031	SatIII-TALE without amber codon and with C-terminal VP64 domain and CMV promoter; additional transfection control under CMV promoter	this work	Carb
pAnW1032	Scrambled (sc) SatIII-TALE without amber codon and with C-terminal VP64 domain and CMV promoter; additional transfection control under CMV promoter	this work	Carb
pAnW1054	SatIII-TALE with V92TAG, C-terminal VP64 domain and CMV promoter; additional transfection control under CMV promoter	this work	Carb
pAnW1183	Luciferase reporter plasmid with SatIII-TALE binding site	this work	Kan
pAnW1272	Golden-Gate entry plasmid with CMV promoter, C-terminal mCherry	this work	Carb
pAnW1273	Golden-Gate entry plasmid with CMV promoter, C-terminal mCherry and V92TAG	this work	Carb
pAnW1274	SatIII-TALE without amber codon and with, C-terminal mCherry and CMV promoter	this work	Carb
pAnW1275	SatIII-TALE with V92TAG, C-terminal mCherry and CMV promoter	this work	Carb

pAnW1276	CDKN2A-TALE without amber codon and with, C-terminal mCherry and CMV promoter	this work	Carb
pAnW1360	Golden-Gate entry plasmid with R34TAG, CMV promoter, C-terminal mCherry	this work	Carb
pAnW1361	Golden-Gate entry plasmid with Y44TAG, CMV promoter, C-terminal mCherry	this work	Carb
pAnW1362	Golden-Gate entry plasmid with Q48TAG, CMV promoter, C-terminal mCherry	this work	Carb
pAnW1363	Golden-Gate entry plasmid with Q49TAG, CMV promoter, C-terminal mCherry	this work	Carb
pAnW1364	Golden-Gate entry plasmid with E50TAG, CMV promoter, C-terminal mCherry	this work	Carb
pAnW1365	Golden-Gate entry plasmid with K51TAG, CMV promoter, C-terminal mCherry	this work	Carb
pAnW1367	Golden-Gate entry plasmid with S58TAG, CMV promoter, C-terminal mCherry	this work	Carb
pAnW1369	Golden-Gate entry plasmid with F72TAG, CMV promoter, C-terminal mCherry	this work	Carb
pAnW1370	Golden-Gate entry plasmid with L80TAG, CMV promoter, C-terminal mCherry	this work	Carb
pAnW1371	Golden-Gate entry plasmid with G88TAG, CMV promoter, C-terminal mCherry	this work	Carb
pAnW1372	Golden-Gate entry plasmid with H96TAG, CMV promoter, C-terminal mCherry	this work	Carb
pAnW1373	Golden-Gate entry plasmid with I97TAG, CMV promoter, C-terminal mCherry	this work	Carb
pAnW1374	Golden-Gate entry plasmid with I98TAG, CMV promoter, C-terminal mCherry	this work	Carb
pAnW1375	Golden-Gate entry plasmid with A104TAG, CMV promoter, C-terminal mCherry	this work	Carb

pAnW1376	Golden-Gate entry plasmid with D108TAG, CMV promoter, C-terminal mCherry	this work	Carb
pAnW1377	Golden-Gate entry plasmid with L126TAG, CMV promoter, C-terminal mCherry	this work	Carb
pAnW1410	PylRS-AF + nuclear export signal (NES) and $tRNA^{Pyl}$	this work	Carb
pAnW1411	SatIII-TALE with R34TAG, C-terminal mCherry and CMV promoter	this work	Carb
pAnW1412	SatIII-TALE with Y44TAG, C-terminal mCherry and CMV promoter	this work	Carb
pAnW1413	SatIII-TALE with Q48TAG, C-terminal mCherry and CMV promoter	this work	Carb
pAnW1414	SatIII-TALE with Q49TAG, C-terminal mCherry and CMV promoter	this work	Carb
pAnW1415	SatIII-TALE with E50TAG, C-terminal mCherry and CMV promoter	this work	Carb
pAnW1416	SatIII-TALE with K51TAG, C-terminal mCherry and CMV promoter	this work	Carb
pAnW1417	SatIII-TALE with S58TAG, C-terminal mCherry and CMV promoter	this work	Carb
pAnW1418	SatIII-TALE with F72TAG, C-terminal mCherry and CMV promoter	this work	Carb
pAnW1419	SatIII-TALE with L80TAG, C-terminal mCherry and CMV promoter	this work	Carb
pAnW1420	SatIII-TALE with G88TAG, C-terminal mCherry and CMV promoter	this work	Carb
pAnW1421	SatIII-TALE with H96TAG, C-terminal mCherry and CMV promoter	this work	Carb
pAnW1422	SatIII-TALE with I97TAG, C-terminal mCherry and CMV promoter	this work	Carb
pAnW1423	SatIII-TALE with I98TAG, C-terminal mCherry and CMV promoter	this work	Carb

pAnW1424	SatIII-TALE with A104TAG, C-terminal mCherry and CMV promoter	this work	Carb
pAnW1425	SatIII-TALE with D108TAG, C-terminal mCherry and CMV promoter	this work	Carb
pAnW1426	SatIII-TALE with L126TAG, C-terminal mCherry and CMV promoter	this work	Carb
pAnW1788	Golden-Gate entry plasmid with Y10TAG, CMV promoter, C-terminal mCherry	this work	Carb
pAnW1795	Golden-Gate entry plasmid with K23TAG, CMV promoter, C-terminal mCherry	this work	Carb
pAnW1796	Golden-Gate entry plasmid with M24TAG, CMV promoter, C-terminal mCherry	this work	Carb
pAnW1797	Golden-Gate entry plasmid with G33TAG, CMV promoter, C-terminal mCherry	this work	Carb
pAnW1800	Golden-Gate entry plasmid with S36TAG, CMV promoter, C-terminal mCherry	this work	Carb
pAnW1802	Golden-Gate entry plasmid with Y868TAG, CMV promoter, C-terminal mCherry	this work	Carb
pAnW1803	Golden-Gate entry plasmid with K870TAG, CMV promoter, C-terminal mCherry	this work	Carb
pAnW1806	Golden-Gate entry plasmid with R881TAG CMV promoter, C-terminal mCherry	this work	Carb
pAnW1807	SatIII-TALE with Y10TAG, C-terminal mCherry and CMV promoter	this work	Carb
pAnW1808	SatIII-TALE with K23TAG, C-terminal mCherry and CMV promoter	this work	Carb
pAnW1809	SatIII-TALE with M24TAG, C-terminal mCherry and CMV promoter	this work	Carb
pAnW1810	SatIII-TALE with G33TAG, C-terminal mCherry and CMV promoter	this work	Carb
pAnW1811	SatIII-TALE with S36TAG, C-terminal mCherry and CMV promoter	this work	Carb

pAnW1812	SatIII-TALE with Y868TAG, C-terminal mCherry and CMV promoter	this work	Carb
pAnW1813	SatIII-TALE with K870TAG, C-terminal mCherry and CMV promoter	this work	Carb
pAnW1814	SatIII-TALE with R881TAG, C-terminal mCherry and CMV promoter	this work	Carb
pAnW1817	Telomere-TALE with S36TAG, C-terminal mCherry and CMV promoter	this work	Carb
pAnW1872	empty vector control, only CMV promoter and mCherry	this work	Carb
pDaS0273	PylRS-AF/tRNA^{Pyl}	AG Summerer	Carb
pLeM1933	αSat-TALE with S36TAG, C-terminal TET2CD and CMV promoter	AG Summerer	Carb
pLeM1934	Alu-TALE with S36TAG, C-terminal TET2CD and CMV promoter	AG Summerer	Carb
pLeM1935	SatII-TALE with S36TAG, C-terminal TET2CD and CMV promoter	AG Summerer	Carb
pLeM1936	SatIII-TALE with S36TAG, C-terminal TET2CD and CMV promoter	AG Summerer	Carb
pLeM1937	Line1-TALE with S36TAG, C-terminal TET2CD and CMV promoter	AG Summerer	Carb
pLeM1952	Alu-TALE with S36TAG, C-terminal TET2CD inactive and CMV promoter	AG Summerer	Carb
pLeM1953	SatII-TALE with S36TAG, C-terminal TET2CD inactive and CMV promoter	AG Summerer	Carb
pLeM1958	SatIII-TALE with S36TAG, C-terminal TET2CD inactive and CMV promoter	AG Summerer	Carb
pLeM1959	Line1-TALE with S36TAG, C-terminal TET2CD inactive and CMV promoter	AG Summerer	Carb

Table 14 TALE Proteins

TALE	RVD Sequence	Target Sequence	Supplier
hey2-TALE	HD NG NG HD HD NN NG NG NG HD HD NI HD NI NG HD	TCTTCCGTTTCCACATCT	AG Summerer[255]
CDKN2A-TALE	HD HD NG HD HD NG NG HD HD NG NG NN HD HD NI NI HD NN HD NG NN NN HD NG	TCCTCCTTCCTTGCCAACGCTGGCT	AG Summerer[251]
αSat-TALE	NG NG NG NI NG NN NG NN NI NI NN NI NG NI NG	TTTTATGTGAAGATATT	this work
SatII-TALE	NN NI NG NG HD HD NI NG NG HD HD NI NG NG HD HD NI NG NG	TGATTCCATTCCATTCCATT	this work
sc SatIII-TALE	NG NG HD HD NI NG NG NN NI NG NG HD NI HD NG NG NI HD HD	TGATTCCATTCCATTCCATT	this work
SatIII-TALE	NN NI NG NG HD HD NI NG NG HD HD NI NG NG HD HD NI NG	TGATTCCATTCCATTCCATT	this work
Line1-TALE	HD HD NG NI NG NG HD NN NN HD HD NI NG HD NG NG NN NN HD NG HD HD NG HD	TCCTATTCGGCCATCTTGGCTCCTCC	this work
Alu-TALE	NN NG NI NI NG HD HD HD NI NN HD NI HD NG NG NG NN	TGTAATCCCAGCACTTTGG	this work
Telomere-TALE	NI NI HD HD HD NG NI NI HD HD HD NG NI NI	TAACCCTAACCCTAA	AG Summerer[281]

11.2 Methods

11.2.1 Preparation of Chemical-competent GH371 *E. coli* bacteria

20 mL LB-Medium were inoculated with a single *E. coli* colony and grown at 200 rpm and at 37 °C overnight. 800 mL LB-Medium were inoculated with 8 mL of the previous culture and grown at 200 rpm and at 37 °C to OD_{600} of 0.5. The culture was cooled on ice for 30 min. The culture was distribute in 50 mL reaction tubes and centrifuged at 4 °C for 10 min at 4000 rpm. The supernatant was discarded and each pellet was resuspended in 10 mL ice-cold 100 mM $MgCl_2$ on ice. The cell-suspension was centrifuged at 4 °C for 15 min at 4000 rpm. The supernatant was discarded and each pellet was resuspended in 40 mL ice-cold 50 mM $CaCl_2$ and incubated 30 min on ice. The cell-suspension was centrifuged at 4 °C for 15 min at 4000 rpm. The supernatant was discarded and each pellet was resuspended in 2 mL ice-cold 50 mM $CaCl_2$ + 15 % glycerol on ice. The cell suspension were aliquoted on ice and freezed in liquid nitrogen and stored at −80 °C.

11.2.2 Preparation of Electrocompetent GH371 *E. coli* bacteria

25 mL LB-Medium were inoculated with a single *E. coli* colony and grown at 200 rpm and at 37 °C overnight. 500 mL LB-Medium were inoculated with 5 mL of the previous culture and grown at 140 rpm and at 37 °C to OD_{600} of 0.4. The culture was distributed in 50 mL reaction tubes and centrifuged at 4 °C for 15 min at 3500 rpm. The supernatant was discarded and each pellet was resuspended in 20 mL ice-cold double distilled water on ice. The cell-suspension was centrifuged at 4 °C for 15 min at 3500 rpm. The supernatant was discarded and each pellet was resuspended in 10 mL ice-cold double distilled water on ice. The cell-suspension was centrifuged at 4 °C for 20 min at 3500 rpm. The supernatant was discarded and each pellet was resuspended in 6 mL ice-cold double distilled water + 10 % glycerol on ice. The cell-suspension was centrifugde at 4 °C for 20 min at 4000 rpm. The supernatant was discarded and each pellet was resuspended in 600 µL ice-cold double distilled water + 10 % glycerol on ice. The cell suspension were aliquoted on ice and freezed in liquid nitrogen and stored at −80 °C.

11.2.3 Transformation by Heat Shock

An appropriate amount of plasmid were added to 25 µL of chemical competent GH731 cells and incubated on ice for 30 min. The heat shock was performed at 42 °C for 45 sec. The solution was cooled on ice for 2 min and then mixed with 500 µL SOC-medium. The cell-suspension was incubated at 37 °C and 700 rpm for 1 h. An appropriate amount of the cell-suspension was pipetted onto LB-Agar plates supplemented with antibiotics and distributed using glass beads. Plates were incubated at 37 °C overnight.

11.2.4 Transformation by Electroporation

An appropriate amount of plasmid were added to 25 µL of electro-competent GH731 cells and transferred into an electroporation cuvette. The electroporation was performed at 1800 V in an electroporator for 3 sec. The solution was cooled on ice for 2 min and then mixed with 500 µL SOC-medium. The cell-suspension was incubated at 37 °C and 700 rpm for 1 h. An appropriate amount of the cell-suspension was pipetted onto LB-Agar plates supplemented with antibiotics and distributed using glass beads. Plates were incubated at 37 °C overnight.

11.2.5 Plate Culture

Either bacterica were streaked onto LB-Agar plates supplemented with antibiotics or a bacterical suspension in SOC-Medium were pipetted onto LB-Agar plates supplemented with antibiotics and distributed using glass beads. Plates were incubated at 37 °C overnight.

11.2.6 Liquid culture

LB-Medium were inoculated with a single *E. coli* colony and grown at 175 rpm and at 37 °C overnight in a 15 mL reaction tube.

11.2.7 TALE Assembly by Golden Gate Reactions

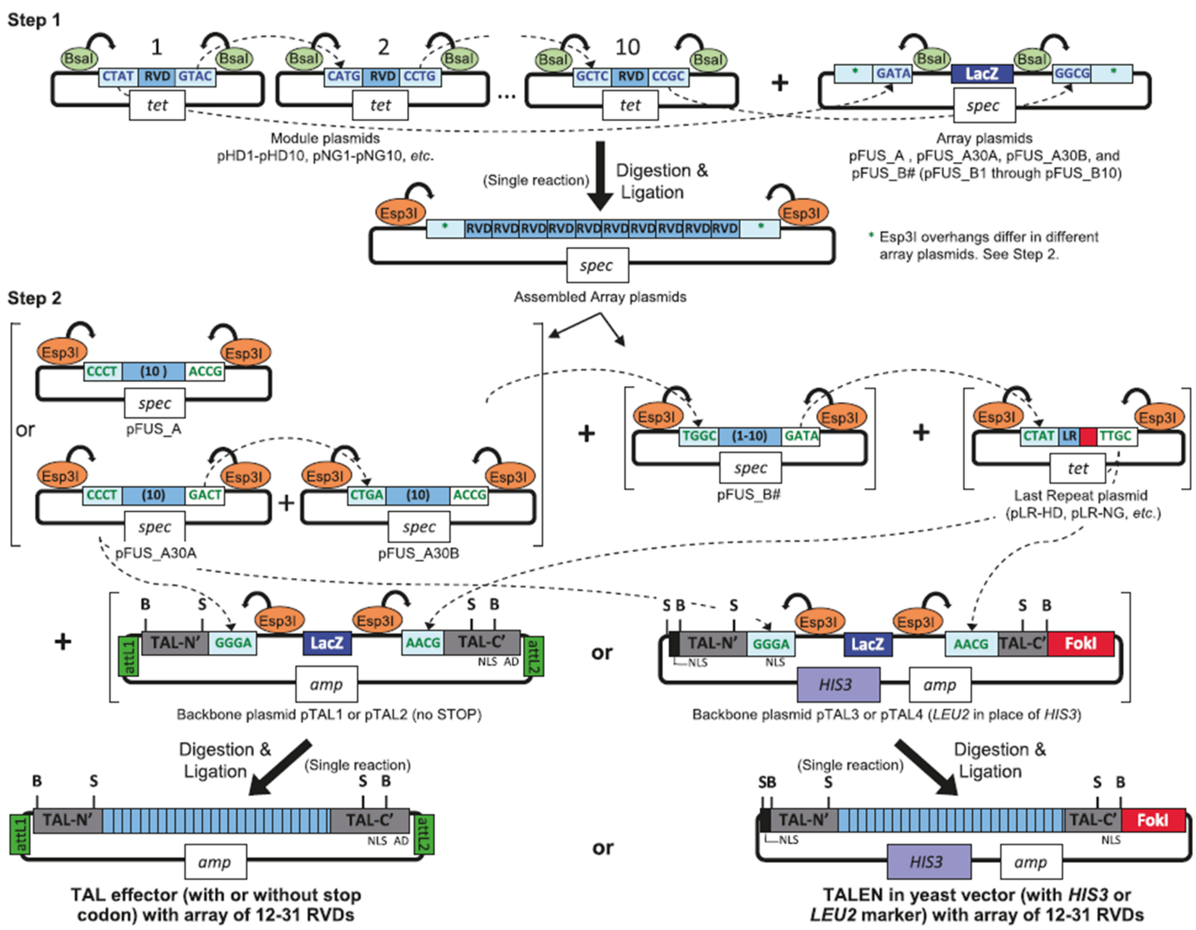

Figure 47 Golden Gate assembly of custom TAL effectors using module, array, last repeat and entry vector plasmids: In a first step modules containing the desired RVDs are released by using type IIS restriction endonucleases BsaI creating unique cohesive ends for ordered single-reaction assembly into array plasmids. Those arrays are subsequently released using BsmBI assembled in order in a second step into a entry vector plasmid to create full length constructs with custom repeat arrays NLS, nuclear localization signal(s); AD, transcriptional activation domain; tet, tetracycline resistance; spec, spectinomycin resistance; amp, ampicillin resistance; attL1 and attL2, recombination sites for Gateway cloning; B, BamHI, and S, SphI, useful for subcloning custom repeat arrays. (adapted from[183])

TALE genes for αSat, SatII, SatIII, Line1, Alu and Telomere loci were assembled according to a previous published protocol[183]. In the first Golden Gate 1 reaction the module plasmids were assembled according to their target sequence into a pFUSA for the positions 1–10. In the second reaction the module plasmids were assembled into a pFUSBx vector for the left positions of their target sequences, whereas x determines the number of positions and thereby the used vector. All non-circular plasmid DNA was removed by adding 5 nmol ATP and 5 Un Plasmid-safe Nuclease and incubating the mixture for 1 h at 37 °C. 2.5 µL of the reactions mixture was transformed in GH371 *E.coli* cells and a blue/white screening was performed. The white colonies were used for a colony PCR to validate the correct assembly of module plasmids with agarose gel electrophoresis. An overnight culture was started with a correct colony and the plasmid was purified and sequenced.

Table 15 Golden Gate 1 reagent concentrations in 25 µL

Reagent	Volume [µL]
each pM (150 ng/µL)	0.5
pFUS vector (75 ng/µL)	0.5
T4 ligase buffer (10x)	2.5
BsaI (10 Un/µL)	1
T4 DNA ligase (400 Un/µL)	1
ddH_2O	to 25

Table 16 Golden Gate 1 reaction conditions

T [°C]	t [s]	Cycles
37	300	15
16	600	
50	300	1
80	300	1

In the Golden Gate 2 reaction the pFUSA and pFUSBx vectors were assemebled with their specific last repeat plasmid (pLR) into a cloned entry vector. 2.5 µL of the reactions mixture was transformed in GH371 *E.coli* cells and a blue/white screening was performed. An overnight culture was started with three white colonies and the plasmid was purified and sequenced.

Table 17 Golden Gate 2 reagent concentrations in 25 µL

Reagent	Volume [µL]
each assembled pFUS vector (150 ng/µL)	0.5
pLR (150 ng/µL)	0.5
entry vector (75 ng/µL)	0.5
T4 ligase buffer (10x)	2.5
BsmBI (10 Un/µL)	1
T4 DNA ligase (400 Un/µL)	1
ddH_2O	to 25 µL

Table 18 Golden Gate 2 reaction conditions

T [°C]	t [s]	Cycles
37	600	10
16	900	
37	900	1
80	300	1

11.2.8 Blue/White Screening

The foreign DNA was ligated into a lacZ gene containing plasmid, whereby the lacZ gene was disrupted. A sufficient amount of the reaction mixture was transformed into GH371 *E.coli* cells and plated onto LB-Agar plates, supplemented with the corresponding antibiotic and 50 µg/mL X-Gal. The white colonies were used for an overnight culture and the plasmid was purified and sequenced.

11.2.9 Colony PCR

A single *E. coli* colony was resuspeneded in 20 µL water and kept on ice. The PCR reaction was pipetted as followed (Tab. 19) on ice, with the polymerase added last. The product formation was analysed by agarose gel electrophoresis.

Table 19 Colony PCR reagent concentrations

Reagent	Volume [µL]
bacterial colony suspension	1
primer, forward (10 µM)	1
primer, reverse (10 µM)	1
10x Thermo Pol buffer	5
dNTPs (10mM each)	1.25
ddH_2O	40.25
Taq polymerase	0.5

Table 20 Colony PCR reaction conditions

T [°C]	t [s]	Cycles
95	120	1
95	30	
55	30	35
68	180	
68	300	1

11.2.10 Agarose Gel Electrophoresis

Agarose was dissolved in 0.5x TBE Buffer by heating. The solution was poured into the gel casting chamber. By adding a comb, wells were created. After solidification, the gel was transferred into the running chamber, filled with 0.5x TBE Buffer. The samples were mixed with a loading dye and loaded into the gel. The electrophoresis was performed at 5V/cm for 60 min. The gel was stained with ethidium bromide and the DNA was visualized by UV light.

11.2.11 Purification of DNA by Agarose Gel Electrophoreses

The agarose gel eletrophoreses was performed with 100 µL of a PCR reaction, which were loaded on an agarose gel with big sample wells, and the electrophoresis and staining was performed as described. Within a short UV illumination the position of the PCR amplicon were marked. The single DNA band were cut out and the DNA were recovered by using the Gel purification kit according to manufacture’s guidelines. The DNA was finally eluted with 50 µL ddH_2O. The DNA concentration and purity was determined on a Nanodrop 2000.

11.2.12 Site-directed Mutagenesis (Quickchange PCR reactions)

To introduce site-directed mutations into a plasmid, forward and revers primers were designed to exhibit melting temperatures (T_m) of ≥ 78 °C and a GC content of above 40 %. The length of the primers was varied according to the melting temperature, but was usually around 30 bp. The primers were designed to have overlaps on one sites of 3 bp. The PCR reaction was performed as indicated below.

Table 21 Quickchange PCR reagent concentrations in 50 µL

Reagent	Volume [µL]
template plasmid	50–100 ng
dNTPs (10 mM)	1.5
forward primer (10 µM)	2.5
revers primer (10 µM)	2.5
Pfu 10x buffer	5
Pfu Polymerase	1
ddH_2O	to 50

Table 22 Quickchange PCR reaction conditions

T [°C]	t [s]	Cycle
95	30	
95	30	18
55	60	
68	120/kb	
4	∞	

The template plasmid was removed by adding 1 µL DpnI (20 Un/µL) and incubating the mixture for 1 h at 37 °C and heat inactivated at 80 °C for 20 min. 2.5 µL of the reaction mixture was transformed in 25 µL of GH371 *E.coli* cells. An overnight culture was started with three colonies and the plasmid was purified and sequenced.

11.2.13 Cassette Mutagenesis

4 µM complementary oligonucleotide pairs bearing the mutation were hybridized in 100 µL 1x CutSmart buffer at 95 °C for 10 min and cooled down to room temperature for 30 min. The corresponding sticky ends of the target-vector restriction sites were directly created by choosing explicit overlaps. 30 µL of the target-vector was digested by incubating the plasmid for 1 h at 37 °C with the corresponding restriction enzymes in 1x buffer. The reaction was purified with the PCR purification kit. 5 µL digested vector and 5 µL paired oligonucleotides were ligated in 20 µL 1x T4 ligase buffer using 400 Un T4 DNA ligase for 2 hours at room temperature. 2.5 µL of the crude reaction mixture was transformed into 25 µL GH371 *E.coli* cells. An overnight culture was started with three single colonies and the plasmid was purified and sequenced.

11.2.14 Gibson Assembly

DNA inserts were amplified by PCR reaction with primers creating 20 bp overlapping ends and the target-vector was linearized by restriction enzymes. 5 µL equally distributed fragments were mixed with 15 µL 1.33x Gibson master mix and incubated for 1 h at 50 °C. 2.5 µL of the crude reaction mixture was transformed into 25 µL GH371 *E.coli* cells. An overnight culture was started with three single colonies and the plasmid was purified and sequenced.

11.2.15 Isolation of plasmid DNA

A cell suspension from a liquid culture was centrifuged at 4000 rpm for 10 min and the plasmid was isolated and purified using the “Nucleospin Plasmid Easy Pure” Kit according to the manufacture’s guidelines. The DNA was finally eluted with 50 µL ddH_2O. The DNA concentration and purity was determined on a Nanodrop 2000.

11.2.16 DNA Sequencing

The sequencing was performed using either the “Lightrun night express” service by GATC/Eurofins or the “Barcode Economy Run” service by Mircosynth. For GATC up to 500 ng DNA was mixed with 2.5 µL 10 µM primer and filled up with ddH_2O to 10 µL. For Microsynth 12 µL ddH_2O containing up to 1200 ng DNA were sent together with a second tube containing 20 µL of 10 µM sequencing primer.

11.2.17 Cultivation of Mammalian cells

Both cell lines HEK293T and HeLa cells were maintained in DMEM media supplemented with 1 % penicillin/streptomycin, 10 % FBS and 1 % L-Glutamine at 37 °C, a CO_2 level of 5 % and a humidity of ≥95 %. Usually they were cultured on standard 10 cm tissue-culture plates with 10 mL medium. For 6 cm plates 5 mL medium, for 3.5 cm plates 2 mL and for 96 well plates 200 µL medium were used.

11.2.18 Generation and Usage of Cryoconserved Cell Cultures

Cryo cultures were used for long-term storage of mammalian cell lines and stored at –150 °C. The medium of a 70 % confluent tissue-culture plate was discarded and the cells were washed once with DPBS. 2 mL 37 °C-prewarmed trypsin-EDTA were added to the cells and incubated 5 min at 37 °C. The cells were resuspended in 10 mL 37 °C-prewarmed medium and centrifuged at 1500 rpm for 4 min at 4 °C temperature. The medium was discarded and the pellet was resuspended in 1 mL cold freezing medium (growth medium with 5 % DMSO). The cell suspension was transferred to cryotubes, which were placed into an isopropanol bath and stored at –80 °C for 24 h. Afterwards the cryotubes were stored at –150 °C until needed.

To start a new cultivation batch a cryotube was shortly incubated in a 37 °C water bath until it was fully thawed. Then the cell suspension was transferred to 5 mL growth medium and centrifuged for at 1500 for 5 min at room temperature. The cell pellet was resuspended in 10 mL growth medium and transferred to a 10 cm standard tissue-culture plate.

11.2.19 Passaging of HEK293T cells

Before passaging, HEK293T cells were cultured till they reached a confluence of 70 %. The medium was discarded and the cells were washed carefully with 1 mL DPBS. 2 mL 37 °C-prewarmed trypsin-EDTA were added to the cells and incubated 5 min at 37 °C. The cells were resuspended in 10 mL 37 °C-prewarmed medium and the cell concentration was determined using a hemocytometer. The needed amount of cells were transferred to a new tissue-culture plate and a sufficient amount of medium was added.

11.2.20 Passaging of HeLa cells

Before passaging, HeLa cells were cultured till they reached a confluence of 70 %. The medium was discarded and the cells were washed carefully with 5 mL DPBS. 2 mL 37 °C-prewarmed trypsin-EDTA were added to the cells and incubated 8 min at 37 °C. The cells were resuspended in 10 mL 37 °C-prewarmed medium and the cell concentration was determined using a hemocytometer. The needed amount of cells were transferred to a new tissue-culture plate and a sufficient amount of medium was added.

11.2.21 Transient transfection and amber suppression

Before transfection, HEK293T and HeLa cells were cultured till they reached a confluence of 70 %. 3 µL of the transfection reagent (Lipofectamin 2000 for HEK293T and X-tremeGene 9 for HeLa cells) was diluted in 100 µL Opti-MEM medium. Then this mixture was added to 1 µg of prepared plasmid mix and incubated for 20 min at room temperature. Afterwards the mixture was added to the cells drop wise and the transfected cells were further cultured for 24 h.
For amber suppression, the needed ncAA was added to the cells dropwise to a final concentration of 250 µM after the transfection mixture was added to the cells. Afterwards the cells were further cultured for 24 h.

11.2.22 Luciferase Assay

1.6 x 10^4 cells were cultured in a 96 well plate overnight prior transfection. Opti-MEM and Lipofectamin 2000 were mixed according to the manufacturer's protocol. 25 ng of the luciferase reporter plasmid (encoding the TALE binding site and a minCMV promoter upstream of a firefly luciferase gene) and 175 ng of the TALE plasmid (encoding the TALE-VP64 fusion constructs). Transfection mix was added to each plasmid pair and incubated for 20 minutes at RT. The solution was added to the wells of the 96 well plate and incubated at 37 °C and 5 % CO_2 for 48 hr. Each well was then washed with 20 µl of DPBS. 40 µl of lysis buffer (100 mM NaH_2PO_4 and 0.2 % Triton X-100) was added to each well and mixed vigorously. The plate was then incubated on ice for 20 min. After incubation, 20 µL of the lysis solution from each well was combined with each 90 µL of Bright-Glo in a second 96 well plate. The plate was quickly spun down and the luminescence was immediately measured on a TECAN M1000 plate reader (wavelength 380-600 nM). Ratio of luminescence from each sample to that of a sample transfected with TALE-VP64 and the luciferase reporter plasmid bearing the TALE binding-site was plotted as relative luminescence.

11.2.23 Live cell imaging

For microscopy, the medium of the transfected cells was changed to HEPES buffered imaging medium, not containing phenol red. For fluorescent live cell imaging, an Olympus IX-81 microscope with a 10x ULPSAPO and a 60x PLAPO/TIRF objective and a MT20 lamp (Olympus), as well as an 60x UPlanSApo objective and a IX2-UCB lamp, were used. For detection, an EM-CCD camera (C9100-13, Hamamatsu) or an ORCA-R2 – C106000 camera (Hamamatsu) and a standard filter set were used.

11.2.24 Formaldehyde fixation of mammalian cells

For the fixation of HEK293T and HeLa cells 37 % Formaldehyde were added drop wise to the cell medium to a final concentration of 4 % and incubated 20 min at 37 °C. Then, the cells were washed once with a sufficient amount of DPBS and were covered with DPBS for microscopy.

11.2.25 Permeabilization of mammalian cells

Fixed cells were covered with a sufficient amount of 0.25 % Triton X-100 in DPBS and incubated for 15 min at RT. The cells were washed once with DPBS and treated further according to the experimental gain.

11.2.26 Methanol fixation of mammalian cells

For the fixation of HEK293T cells the medium was discarded and the cells were carefully washed once with DPBS. Ice cold methanol was added drop wise to the cells and incubated 5 min at –20 °C. Then, the cells were washed once with a sufficient amount of DPBS and were covered with DPBS for microscopy.

11.2.27 PLL coating

Tissue-culture plates were coated with PLL by adding a sufficient amount of 0.01 % PLL to the plates. After 1 h incubation at 37 °C the plates were washed once with DPBS and were directly used for passaging of cells.

11.2.28 Heat shock HEK293T cells

After 24 h of transfection HEK293T cells plated on PLL coated plates were incubated for 1 h at 44 °C and directly fixed afterwards.

11.2.29 Heat shock HeLa cells

After 24 h of transfection HeLa cells were incubated for 1 h at 44 °C and directly fixed afterwards.

11.2.30 Immunostaining

Fixed and permeabilizied cells were covered with a sufficient amount of blocking buffer (1 % BSA, 0.05 % Tween20 in DBPS) and incubated for 30 min at RT. After discarding the blocking buffer, 500 µL of primary antibody, diluted in blocking buffer according to the manufacture's guidelines, were added to the cells and incubated for 2 hours at RT. To remove the excess antibody the cells were washed three times with DPBS. Afterwards, 500 µL of the secondary antibody, diluted in blocking buffer according to the manufacture's guidelines were added to the cells and incubated one hour at RT. The cells were washed two times with DPBS-T and once with DPBS. For microscopy experiments, the cells were covered with DPBS.

11.2.31 Streptavidin staining of Biotin labelled Mammalian Cells for Fluorescence Microscopy

Fixed and permeabilized cells were covered with 100 µM tetrazine-biotin solution in DBPS and incubated 5 min to 3 hours at 37 °C. The cells were washed three times with DPBS. For the fluorescent staining the Cy7-streptavidin compound was diluted 1:1000 and 500 µL were added to the cells and incubated for 1 h at RT. The cells were washed three times with DPBS and were covered with 1 mL DPBS for microscopy.

11.2.32 Crosslinking of mammalian cells and biotin Labelling

37 % formaldehyde was added to 1 % final concentration into the culture medium of the target cells and incubated at 37 °C for 10 min. The crosslinking reaction was stopped by adding 1.25 M glycine solution to 127 mM final concentration and an incubation at room temperature for 10 min. The solution was discarded and the cells were washed with 3 mL DPBS. The cells were permeabilized by adding 3 mL 0.25 % Triton X-100 in DPBS and incubated at room temperature for 10 min. After washing the cells with 3 mL DBPS, 10 mL 0.001 % avidin in DBPS was added to cells and incubated one hour at room temperature. Again three washing steps were performed with 3 mL DPBS and 10 mL 0.001 % biotin in DPBS was added and the cells were incubated one hour at room temperature. The cells were washed once with 3 mL DPBS before 10 mL 100 µM tetrazine-biotin in DPBS were added and the cells were incubated over night at 4 °C. Next day the cells were collected by centrifugation at 2000 rpm and 4 °C for 8 min. The cell pellet was washed once with 10 mL DPBS and stored at −80 °C.

11.2.33 Image analysis

Microscopic images were analyzed and processed with ImageJ (NIH, Bethesda) and prepared for presentation using PowerPoint. Image manipulations were restricted to background subtraction, adjustment of brightness levels, cropping, scaling and false color-coding using LUT tables.

11.2.34 Isolation of genomic DNA

The genomic DNA was isolated from adherent HEK239T cells by using the QIAamp DNA Mini Kit according to the manufacture's guidelines in the protocol "DNA Purification from Blood or Fluids (Spin Protocol)". Therefore the cells were detached from TC-plates by trypsinization and collected by centrifugation at 1000 rpm and 4 °C for 5 min. The cell pellet was resuspended in 200 µL DPBS and 20 µL proteinase K from the Kit were added. For the final elution 200 µL ddH_2O were added to the column and incubated for 5 min at RT.

11.2.35 Chromatin Purification

2 x 10^7 cells, which were crosslinked as described before, were suspended in 10 mL cell lysis buffer (CLB) and incubated on ice for 10 min. The cell suspension was centrifuged at 2000 rpm and 4 °C for 8 min and the supernatant was discarded. The cell pellet was again suspended in 10 mL nuclear lysis buffer (NLB) and incubated on ice for 10 min, while the cell suspension was vortexed every 3 minutes. After centrifugation at 2000 rpm and 4 °C for 8 min the supernatant was discarded and the pellet was washed with 10 mL DPBS. The suspension was centrifuged at 2000 rpm and 4 °C for 10 min and the chromatin containing pellet was suspended in 800 µL modified lysis buffer 3 (MLB3). The chromatin was sheared by sonication using the Bioruptor Pico (Fig. S31 and Fig. S32).

Table 23 Sonication conditions using HEK293T cells

Step	On	Off	Cycle
1	5	90	7
2	10	90	7
3	20	90	6

Table 24 Sonication conditions using HeLa cells

Step	On	Off	Cycle
1	30	30	10

The solution was centrifuged at 13000 rpm and 4 °C for 10 min and the chromatin containing supernatant was collected.

11.2.36 Preparation of Dynabeads conjugated with antibody

30 µL Dynabeads-Protein G were transferred in a protein low binding 1.5 mL tube placed in a magnet rack. After discarding the supernatant the beads were washed twice with 1 mL 0.01 % Tween-20 in DBPS. The beads were resuspended in 300 µL DBPS with 0.01 % Tween-20, 0.1 % BSA and 3 µg antibody and rotated overnight at 4 °C. The beads were centrifuged briefly and the tube was placed in a magent rack to discard the supernatant. After washing the beads three times with 1 mL DPBS they were used for chromatin immunoprecipitation.

11.2.37 Chromatin immunoprecipitation for qPCR

160 µL fragmented chromatin, which corresponds to chromatin extracted from 4 x 10^6 cells were mixed with 340 µL of 1.47 % Triton X-100 in MLB3 and added to the Dynabeads conjugated with the antibody. After a rotation step at 4 °C overnight, the tube was placed in a magnet rack and the supernatant was discarded. The beads were washed twice with 900 µL Low Salt Buffer (LSB), High Salt Buffer (HSB), LiCl Buffer and TBS with 0.1 % IGEPAL. The DNA was eluted by reverse crosslinking and purified.

11.2.38 Protein Concentration determination

The Protein Concentration was determined by using the Pierce “BCA Protein Assay” Kit according to the manufacture’s guidelines. The volume of the sample and standards was decreased to 12.5 µL and accordingly the volume of the working reagent was adjusted. After a 30 min incubation step at 37 °C the plate was cooled down to room temperature and the absorbance was measured with the Tecan plate reader.

11.2.39 Click-mediated Enrichment

For protein enrichment from purified chromatin an equal amount of each chromatin fraction depending on the protein concentration was mixed with 2.125 fold MLB3 + 1 % Triton X-100 and the total volume was adjusted to each sample with MLB3. The solution was added to blocked streptavidin beads and incubated shaking overnight at RT. The beads were washed two times each with LSB, HSB and LiCl Buffer. The last washing step was performed either two times with TBS + IGEPAL for qPCR analysis or three times with DPBS for proteomics analysis. The beads were further treated depending on analysis method.

11.2.40 Reverse crosslinking

10 µL of fragmented chromatin or beads after click-mediated enrichment were suspended in 85 µL ddH_2O and 4 µL 5 M NaCl and incubated at 65 °C overnight. After adding 1 µL of 10 mg/mL RNase A and an incubation step at 37 °C for 45 min, 2 µL of 0.5 M EDTA (pH 8.0), 8 µL of 0.5 M Tris-HCl (pH 6.8) and 1 µL Proteinase K were added and incubated at 45 °C for 1.5 h. In case of the reverse crosslinking from bead bound proteins, the beads were separated by a magnetic rack and the supernatant containing the DNA were kept for purification. In both cases the DNA was purified using PCR purification kit according to the manufacture's guidelines.

11.2.41 Purification of DNA

To purify DNA, the Nucleospin Gel and PCR Clean-up from Macherey Nagel was used according to the manufacture's guidelines. The DNA was finally eluted with 50 µL ddH_2O.

11.2.42 Quantitative PCR (qPCR)

After a reverse crosslink of either the beads from the click-mediated enrichment or fragmented chromatin 4 µL of the purified DNA were pipetted in a PCR workstation into a 384 well plate. A reaction mixture containing the 2x GoTaq master mix, forward primer, reverse primer and ddH_2O was prepared and added to the sample without mixing. The plate was tightly sealed and centrifuged at RT for 1 min at 2500 rpm. Afterwards the qPCR was performed on the CFX384 Touch real-time PCR detection system.

Table 25 qPCR reaction concentrations

Locus	Reagent	Volume [µL]
SatII	2x GoTaq master mix	5
	Forward primer 10 µM (o3802)	0.5
	Reverse primer 10 µM (o3803)	0.5
SatIII	2x GoTaq master mix	5
	Forward primer 10 µM (o2419)	0.1
	Reverse primer 10 µM (o2420)	0.1
	ddH_2O	0.8
Line1	2x GoTaq master mix	5
	Forward primer 10 µM (o3655)	0.1
	Reverse primer 10 µM (o3656)	0.1
	ddH_2O	0.8
Alu	2x GoTaq master mix	5
	Forward primer 10 µM (o3749)	0.2
	Reverse primer 10 µM (o3750)	0.2
	ddH_2O	0.6
Telomere	2x GoTaq master mix	5
	Forward primer 10 µM (o2807)	0.27
	Reverse primer 10 µM (o2808)	0.9

Table 26 qPCR reaction conditions for SatII Locus

T [°C]	t [s]	Cycles
95	1202	1
95	30	40
50	30	
72	30	
65	30	1
65–95 (0.5 °C/Cycle)	5	60

Table 27 qPCR reaction conditions for SatIII Locus

T [°C]	t [s]	Cycles
95	120	1
95	15	40
56	60	
65	30	
65–95 (0.5 °C/Cycle)	5	60

Table 28 qPCR reaction conditions for Line1 Locus

T [°C]	t [s]	Cycles
95	180	1
95	30	40
60	45	
65	30	1
65–95 (0.5 °C/Cycle)	5	60

Table 29 qPCR reaction conditions for Alu Locus

T [°C]	t [s]	Cycles
95	600	1
95	15	40
56	45	
65	30	1
65–95 (0.5 °C/Cycle)	5	60

Table 30 qPCR reaction conditions for Telomere Locus

T [°C]	t [s]	Cycles
95	120	1
95	15	18
54	120	
95	15	30
58	60	
65–95 (0.5 °C/Cycle)	5	60

11.2.43 On Bead digest

The detergent free beads were resuspended in 50 µL Denaturing/Reducing Buffer and incubated shaking for 30 min at RT. After adding 5.55 µL of Alkylation Buffer the beads were incubated shaking for 30 min at RT. The first digestion step was performed by adding 2 µg of LysC solved in nuclease free water and an shaking incubation for 1 hour at 37 °C. For the second digestion step 165 µL Tris pH 7.5 containing 1 µg trypsin were added to the bead solution and shaked again for 1 hour at 37 °C. The supernatant was separated from the beads using a magnetic rack and 2µg of trypsin solved in 50 mM acetic acid were added to the supernatant. The reaction mixture was incubated shaking overnight at 37 °C. For proteomic analysis the digestion was stopped by adding 2 µL TFA and the peptides were purified using stage tips.

11.2.44 Stage Tip purification

The peptides after tryptic digest were desalted using 100 µL Stage tips from Pierce. The tips were activated with 100 µL methanol and washed once with 100 µL Buffer B and two times with 100 µL Buffer A. The sample was loaded on the tip step wise and the tip was washed again once with 100 µL Buffer A. Then, the peptides were eluted twice with 20 µL Buffer B for 1 min. The peptide solution were dryed in a speedvac for 1.5 hours at 30 °C. Then, the solid was send for proteomic analysis.

12 Supporting Information

12.1 Transfections

Table S1 Transfections

Experiment	Cell Line	Sample	Plasmids	DNA amount	Cell number	Plate
Figure 23	HEK293T				$5x10^5$	3.5 cm
		SatIII-TALE	pAnW1031 pDaS273 pAnW1183	1000 1000 150		
		sc SatIII-TALE	pAnW1032 pDaS273 pAnW1183	1000 1000 150		
Figure 24	HEK293T				$3x10^6$	10 cm
		SatIII-TALE	pAnW1417 pAnW140	6000 6000		
		EV	pAnW1272 pAnW1410	6000 6000		
		CDKN2A-TALE	pAnW1276 pAnW1410	6000 6000		
Figure 25	HEK293T				$3x10^6$	3.5 cm
		SatIII-TALE V92TAG & transfection control	pAnW996 pDaS273	1000 1000		
Figure 26	HEK293T				$1.6x10^4$	96 Well
		–B. site hey2-TALE	pAnW755 pAnW1000 pDaS273	25 175 175		
		hey2-TALE –amber	pAnW781 pAnW1000 pDaS273	25 175 175		
		hey2-TALE V92TAG	pAnW781 pAnW996 pDaS273	25 175 175		
		hey2-TALE D140TAG	pAnW781 pAnW997 pDaS273	25 175 175		
		hey2-TALE E157TAG	pAnW781 pAnW999 pDaS273	25 175 175		

Figure 27	HEK293T				$5x10^5$	3.5 cm
		SatIII-TALE –amber	pAnW1031 pDaS273	1000 1000		
		SatIII-TALE V92TAG	pAnW1054 pDaS273	1000 1000		
Figure 28	HEK293T				$4x10^4$	LabTek 8 Well
		SatIII-TALE V92TAG	pAnW1275 pDaS273	300 300		
		SatIII-TALE –amber	pAnW1274 pDaS273	300 300		
Figure 30	HEK293T				$4x10^4$	LabTeK 8 Well
		SatIII-TALE R34TAG	pAnW1411 pAnW1410	300 300		
		SatIII-TALE Y44TAG	pAnW1412 pAnW1410	300 300		
		SatIII-TALE Q48TAG	pAnW1413 pAnW1410	300 300		
		SatIII-TALE Q49TAG	pAnW1414 pAnW1410	300 300		
		SatIII-TALE E50TAG	pAnW1415 pAnW1410	300 300		
		SatIII-TALE K51TAG	pAnW1416 pAnW1416	300 300		
		SatIII-TALE S58TAG	pAnW1417 pAnW1410	300 300		
		SatIII-TALE F72TAG	pAnW1418 pAnW1410	300 300		
		SatIII-TALE L80TAG	pAnW1419 pAnW1410	300 300		
		SatIII-TALE G88TAG	pAnW1420 pAnW1410	300 300		
		SatIII-TALE H96TAG	pAnW1421 pAnW1410	300 300		
		SatIII-TALE I97TAG	pAnW1422 pAnW1410	300 300		
		SatIII-TALE I98TAG	pAnW1423 pAnW1410	300 300		
		SatIII-TALE A104	pAnW1424 pAnW1410	300 300		
		SatIII-TALE D108	pAnW1425 pAnW1410	300 300		
		SatIII-TALE L126	pAnW1426 pAnW1410	300 300		
Figure 31	HEK293T				$4x10^4$	LabTek 8 Well

		SatIII-TALE	pAnW1415	300		
		E50TAG	pAnW1410	300		
		SatIII-TALE	pAnW1416	300		
		K51TAG	pAnW1410	300		
		SatIII-TALE	pAnW1417	300		
		S58TAG	pAnW1410	300		
		SatIII-TALE	pAnW1418	300		
		F72TAG	pAnW1410	300		
		SatIII-TALE	pAnW1419	300		
		L80TAG	pAnW1410	300		
		SatIII-TALE	pAnW1420	300		
		G88TAG	pAnW1410	300		
		SatIII-TALE	pAnW1422	300		
		I97TAG	pAnW1410	300		
Figure 32	HEK293T				$4x10^4$	LabTek 8 Well
		SatIII-TALE	pAnW1274	300		
		–amber	pAnW1410	300		
		SatIII-TALE	pAnW1415	300		
		E50TAG	pAnW1410	300		
		SatIII-TALE	pAnW1417	300		
		S58TAG	pAnW1410	300		
Figure 33	HEK293T				$4x10^4$	LabTek 8 Well
		SatIII-TALE	pAnW1415	300		
		E50TAG	pAnW1410	300		
Figure 34	HEK293T				$4x10^4$	LabTek 8 Well
		SatIII-TALE	pAnW1807	300		
		Y10TAG	pAnW1410	300		
		SatIII-TALE	pAnW1808	300		
		K23TAG	pAnW1410	300		
		SatIII-TALE	pAnW1809	300		
		M24TAG	pAnW1410	300		
		SatIII-TALE	pAnW1810	300		
		G33TAG	pAnW1410	300		
		SatIII-TALE	pAnw1811	300		
		S36TAG	pAnW1410	300		
		SatIII-TALE	pAnW1812	300		
		Y868TAG	pAnW1410	300		
		SatIII-TALE	pAnW1813	300		
		K870TAG	pAnW1410	300		
		SatIII-TALE	pAnW1814	300		
		R881	pAnW1410	300		
Figure 35	HEK293T				$4x10^5$	3.5 cm
		SatIII-TALE	pAnW1272	1000		
		–TAG	pAnW1410	1000		

		SatIII-TALE	pAnW1811	1000		
		S36TAG	pAnW1410	1000		
		SatIII-TALE	pAnW1415	1000		
		E50	pAnW1410	1000		
		SatIII-TALE	pAnW1417	1000		
		S58	pAnW1410	1000		
Figure 36	HEK293T				$5x10^5$	3.5 cm
		SatIII-TALE	pAnW1811	1000		
		S36TAG	pAnW1410	1000		
Figure 37	HEK293T				$5x10^5$	3.5 cm
		SatIII-TALE	pAnw1811	1000		
		S36TAG	pAnW1410	1000		
Figure 38	HEK293T				$4x10^5$	3.5 cm
		SatIII-TALE	pAnW1811	1000		
		S36TAG	pAnW1410	1000		
Figure 40	HEK293T				$2.5x10^6$	10 cm
		SatIII-TALE	pAnW1811	6000		
		S36TAG	pAnW1410	6000		
Figure 41	HeLa				$1.5x10^6$	10 cm
		SatIII-TALE	pAnW1811	4500		
		S36TAG	pAnW1410	4500		
		EV	pAnW1872	4500		
			pAnW1410	4500		
Figure 41	HEK293T				$7x10^5$	6 cm
		SatIII-TALE	pAnW1811	6000		
		S36TAG	pAnW1410	6000		
		EV	pAnW1872	6000		
			pAnW1410	6000		
Figure 42	HeLa				$1.5x10^5$	3.5 cm
		SatIII-TALE	pAnW1811	1000		
		S36TAG	pAnW1410	1000		
	HEK293T				$4x10^5$	3.5 cm
		SatIII-TALE	pAnW1811	1000		
		S36TAG	pAnW1410	1000		
Figure 43	HeLa				$1.5x10^6$	10 cm
		SatIII-TALE	pAnW1811	4500		
		S36TAG	pAnW1410	4500		
Figure 44	HeLa				$1.5x10^6$	10 cm
		SatIII-TALE	pAnW1811	4500		
		S36TAG	pAnW1410	4500		
		EV	pAnW1872	4500		
			pAnW1410	4500		

Figure 44	HEK293T				$7x10^5$	6 cm
		SatIII-TALE	pAnW1811	6000		
		S36TAG	pAnW1410	6000		
		EV	pAnW1872	6000		
			pAnW1410	6000		
Figure 45	HEK293T				$7x10^5$	6 cm
		Line1-TALE	pLeM1937	2000		
		S36TAG & TET	pAnW1410	2000		
		Alu-TALE	pLeM1934	2000		
		S36TAG & TET	pAnW1410	2000		
		SatII-TALE	pLeM1935	2000		
		S36TAG & TET	pAnW1410	2000		
		SatIII-TALE	pLeM1936	2000		
		S36TAG & TET	pAnW1410	2000		
		αSat-TALE	pLeM1933	2000		
		S36TAG & TET	pAnW1410	2000		
		Telomere-TALE	pAnW1817	2000		
		S36TAG	pAnW1410	2000		
Figure 46	HEK293T				$2.5x10^6$	10 cm
		Line1-TALE	pLeM1959	6000		
		S36TAG & TET inactive	pAnW1410	6000		
		Alu-TALE	pLeM1952	6000		
		S36TAG & TET inactive	pAnW1410	6000		
		SatII-TALE	pLeM1953	6000		
		S36TAG & TET inactive	pAnW1410	6000		
		SatIII-TALE	pLeM195	6000		
		S36TAG & TET inactive	pAnW1410	6000		
		Telomere-TALE	pAnW1817	6000		
		S36TAG	pAnW1410	6000		

12.2 Plasmid Maps

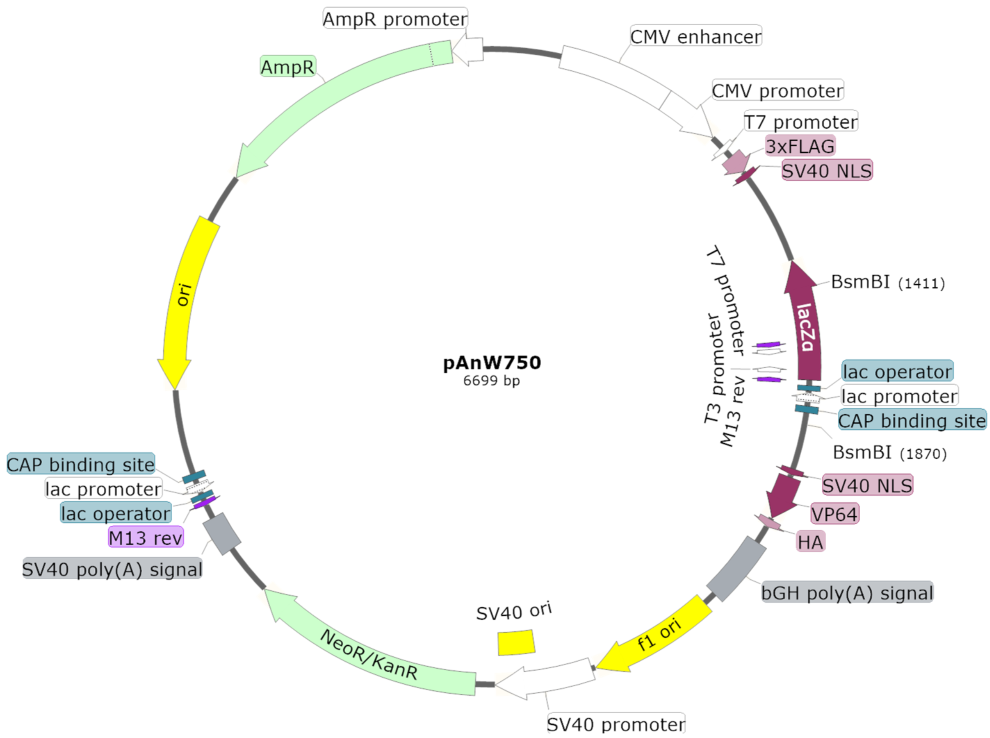

Figure S1 Golden-Gate entry plasmid with CMV promoter and C-terminal VP64 domain.

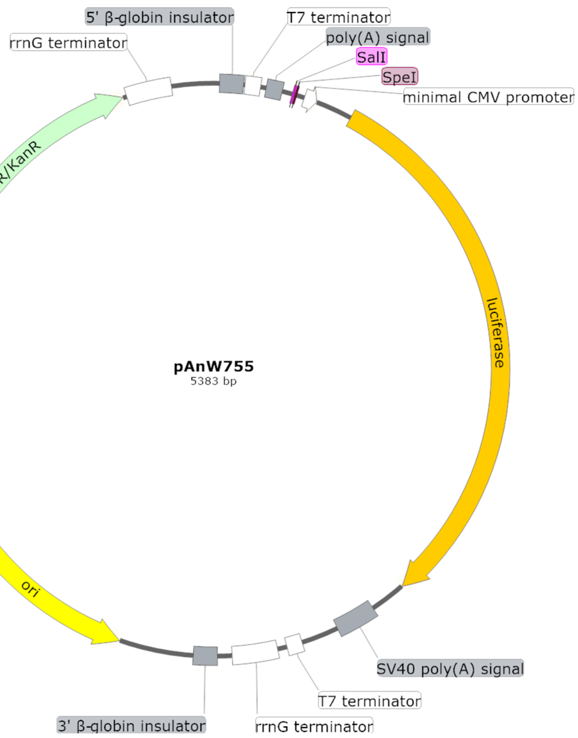

Figure S2 Luciferase reporter plasmid with minimal CMV promoter (CMV) and firefly luciferase gene.

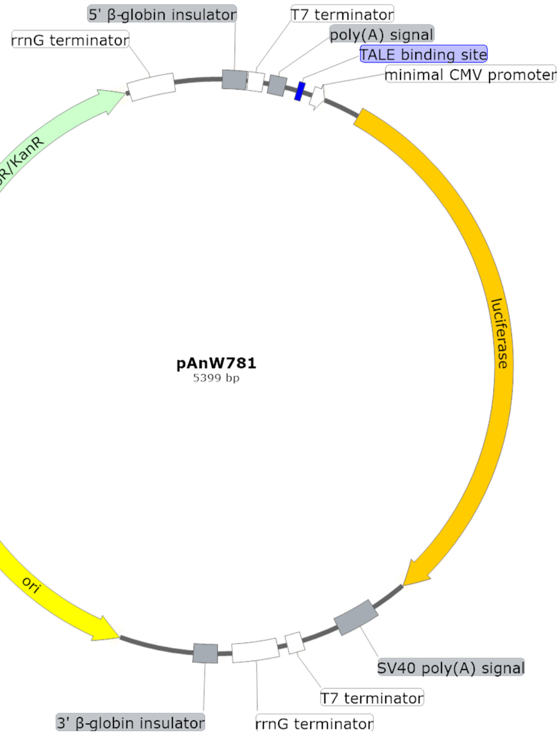

Figure S3 Exemplary luciferase reporter plasmid with TALE binding site.

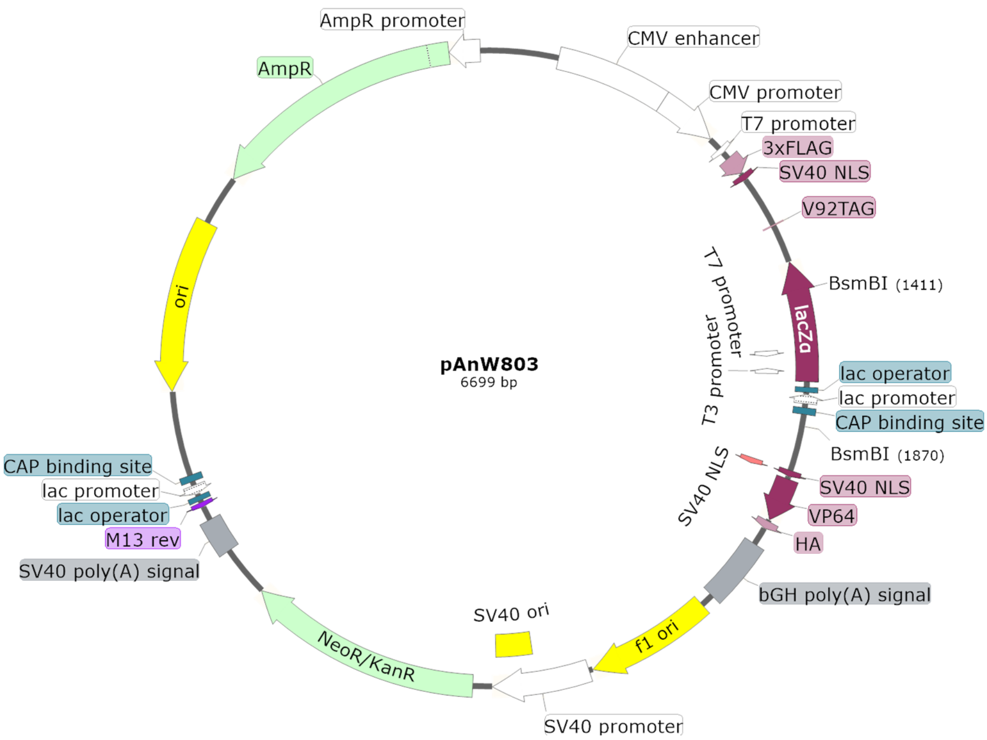

Figure S4 Exemplary Golden-Gate entry plasmid with CMV promoter, C-terminal VP64 domain and N-terminal amber codon (V92TAG).

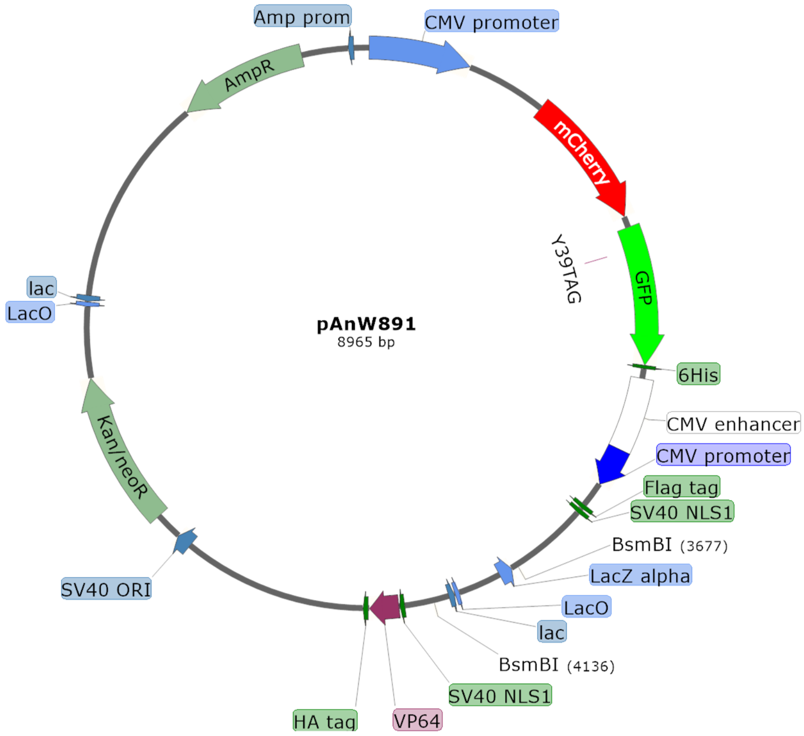

Figure S5 Golden-Gate entry plasmid with CMV promoter, C-terminal VP64 domain and mCherry-GFP fusion construct with Y39TAG as transfection control.

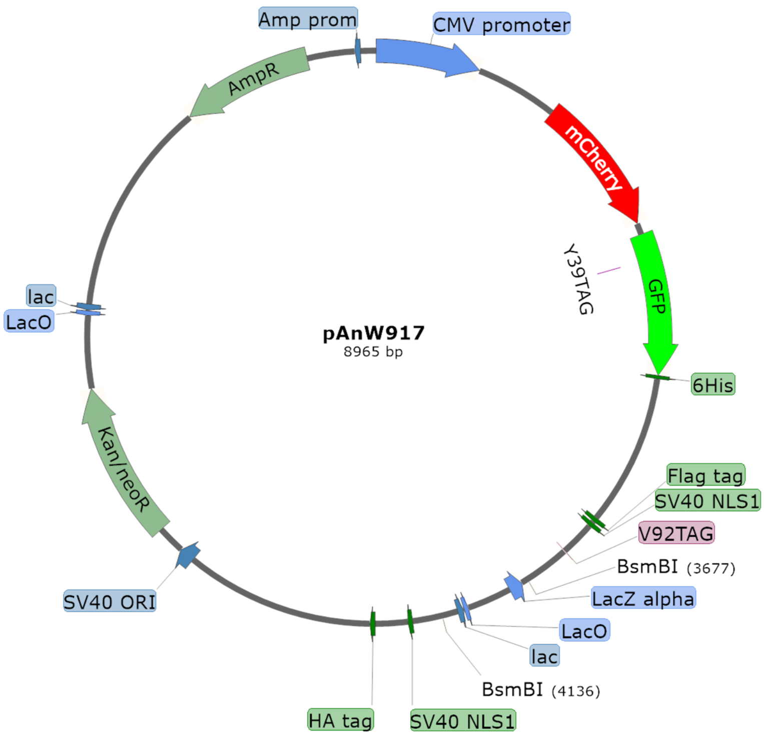

Figure S6 Exemplary Golden-Gate entry plasmid with CMV promoter, C-terminal VP64 doamin, transfection control and N-terminal amber codon (V92TAG).

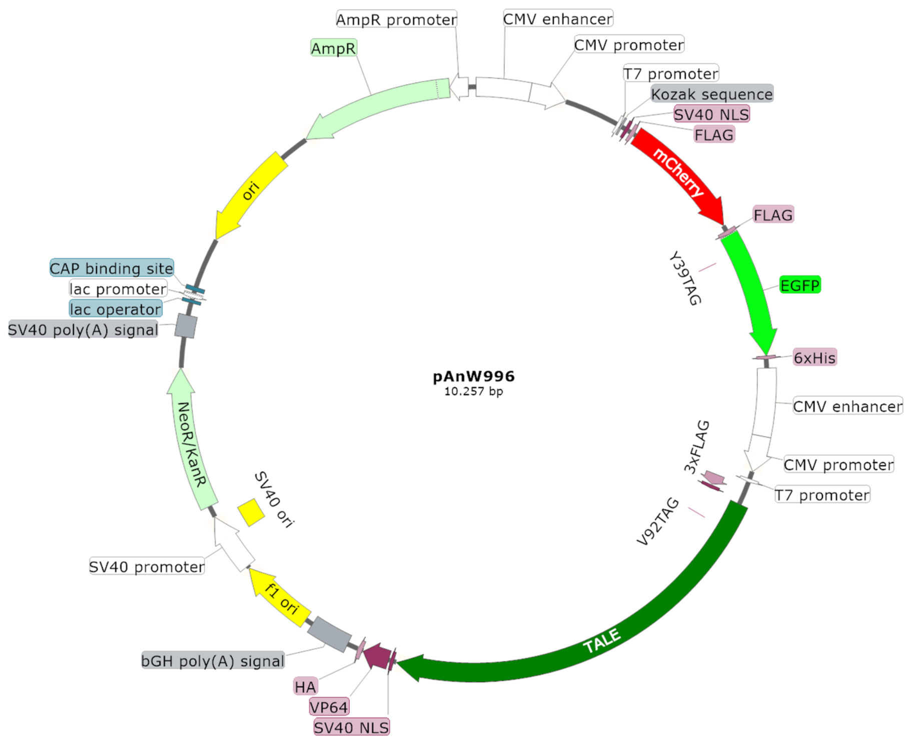

Figure S7 Exemplary plasmid map for TALE with amber codon (V92TAG), C-terminal VP64 domain and CMV promoter; additional transfection control under CMV promoter.

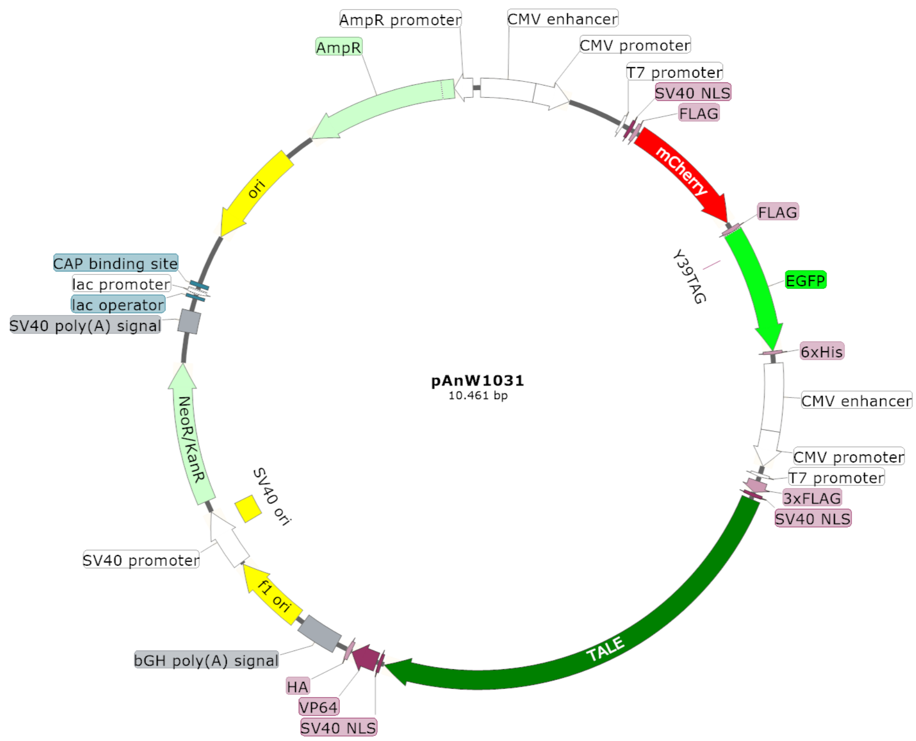

Figure S8 Exemplary plasmid map for TALE without amber codon and with C-terminal VP64 domain and CMV promoter; additional transfection control under CMV promoter.

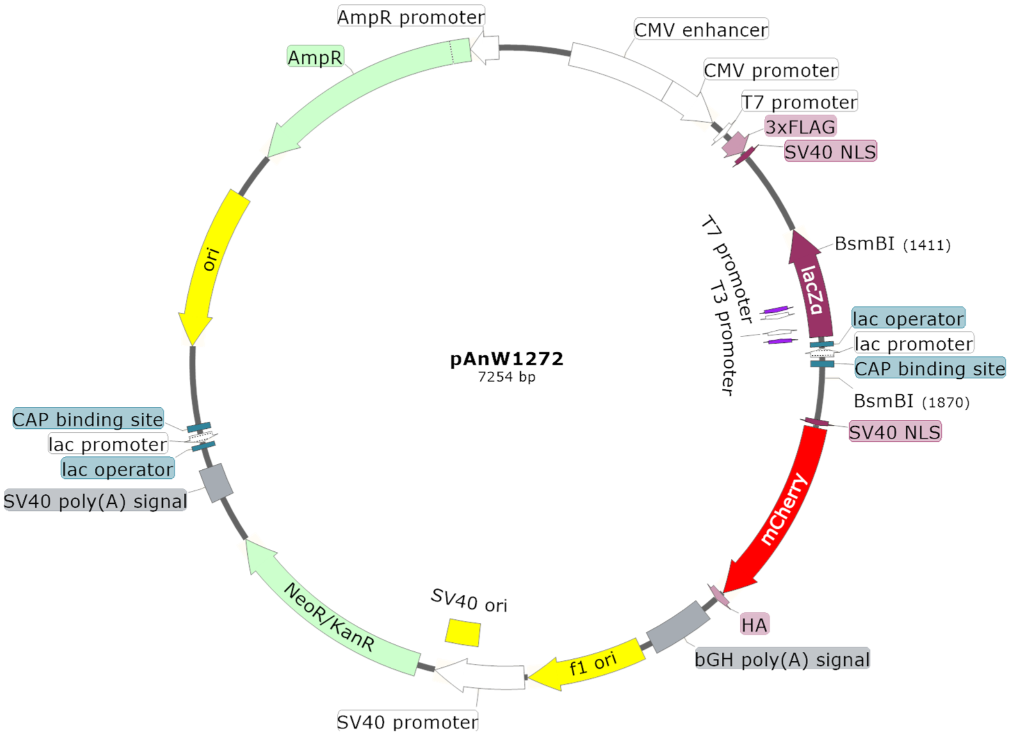

Figure S9 Golden-Gate entry plasmid with CMV promoter, C-terminal mCherry.

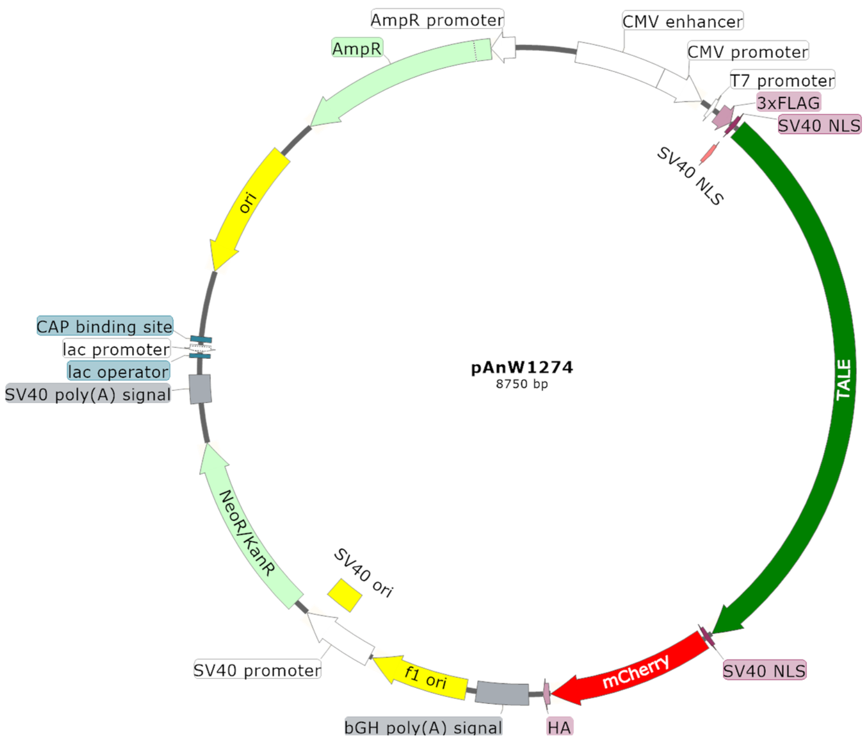

Figure S10 Exemplary plasmid map of TALE without amber codon and with, C-terminal mCherry and CMV promoter.

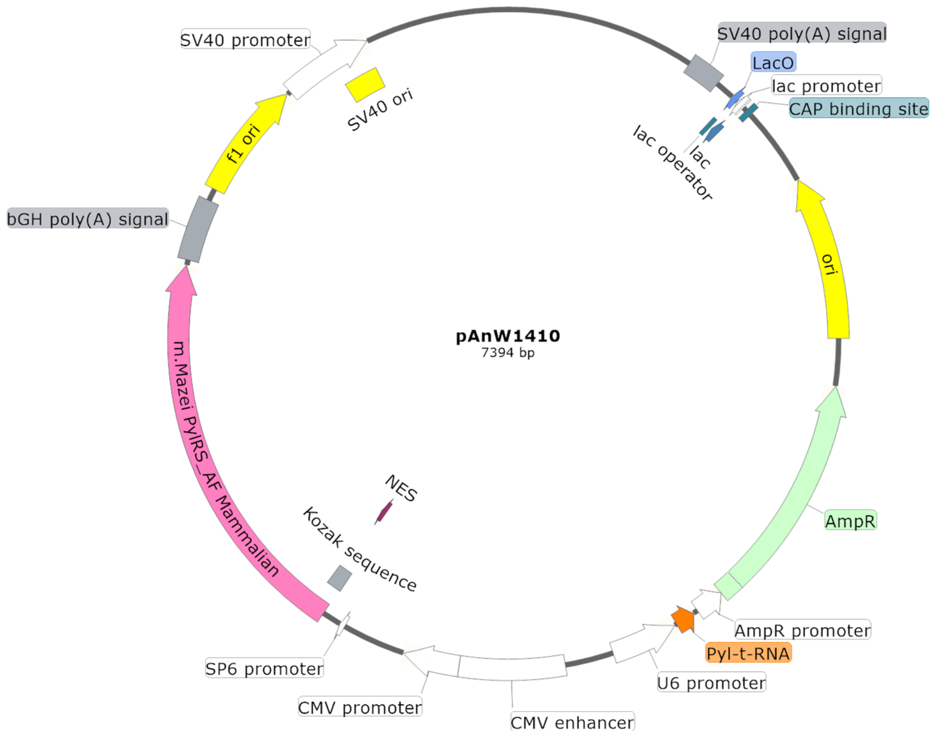

Figure S11 Plasmid map for PylRS-AF + nuclear export signal (NES) and tRNA^{Pyl}.

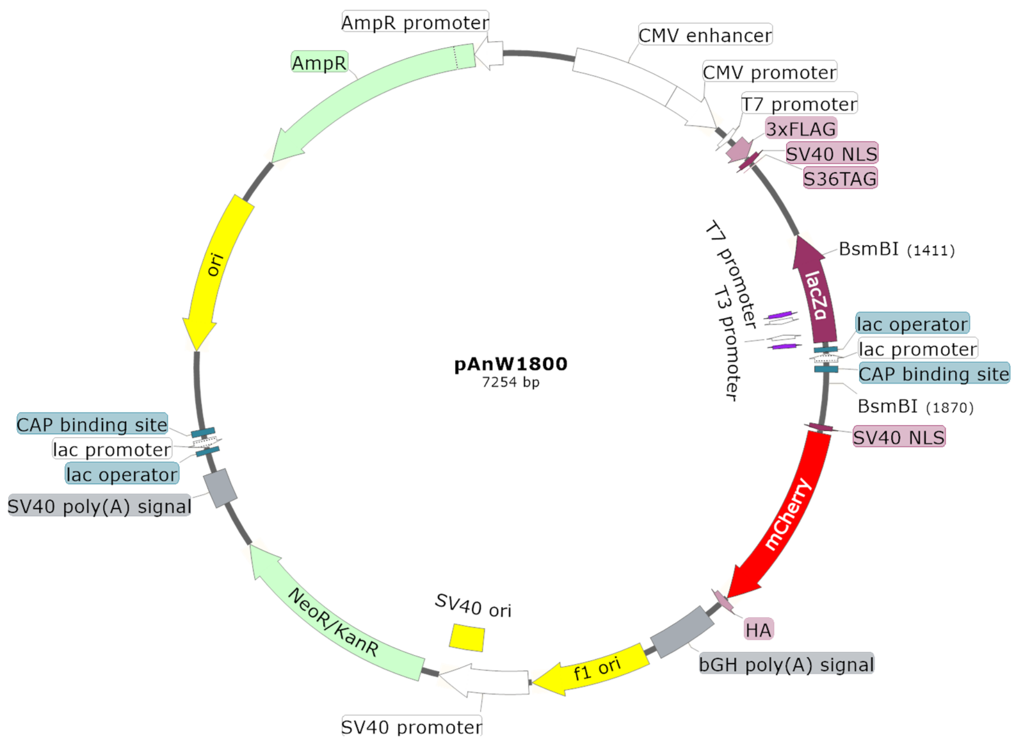

Figure S12 Exemplary Golden-Gate entry plasmid with amber codon (S36TAG), CMV promoter, C-terminal mCherry.

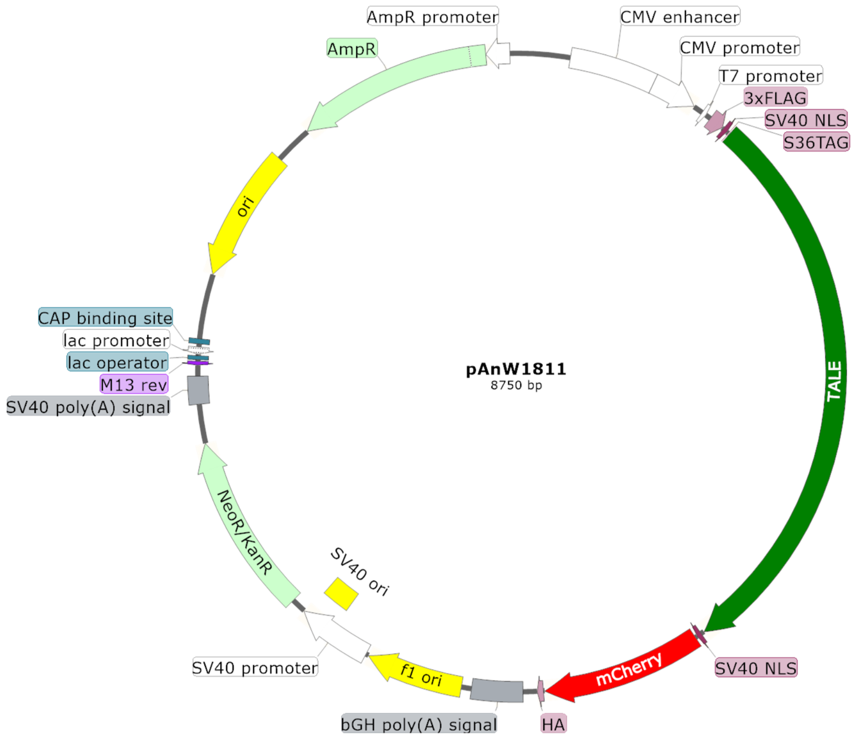

Figure S13 Exemplary plasmid map for TALE with amber codon (S36TAG), C-terminal mCherry and CMV promoter.

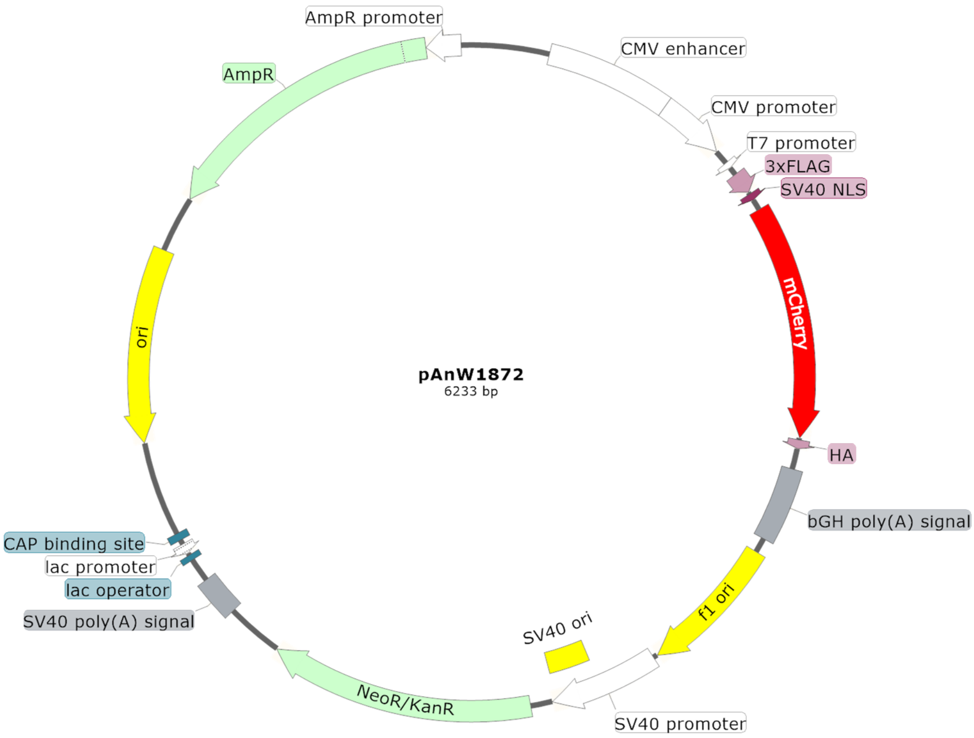

Figure S14 Plasmid map for empty vector control, only CMV promoter and mCherry.

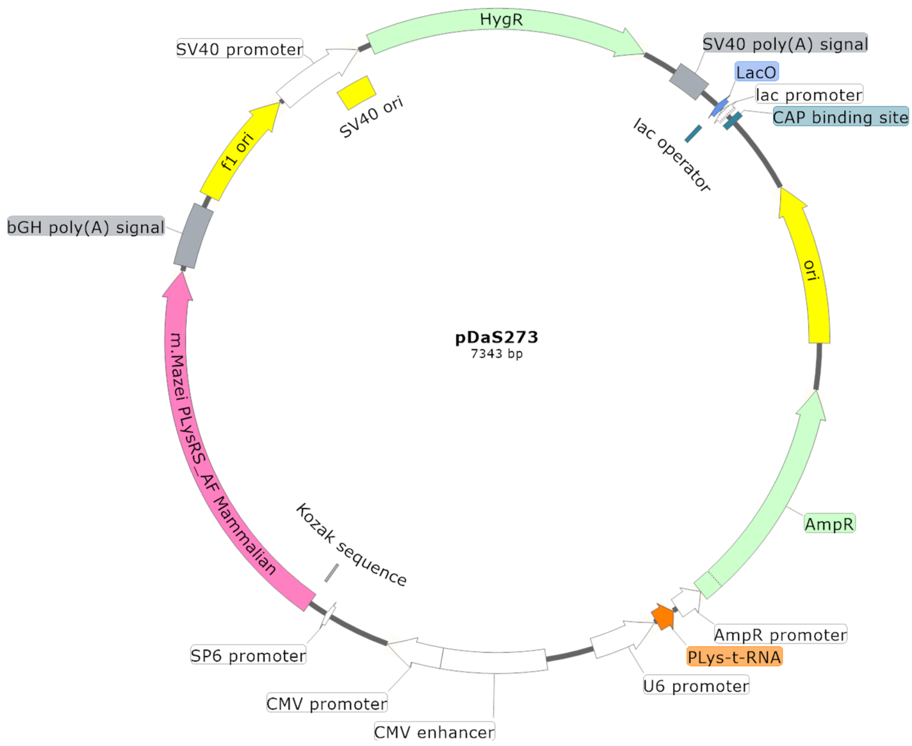

Figure S15 Plasmid map for PylRS-AF and tRNA^{Pyl}.

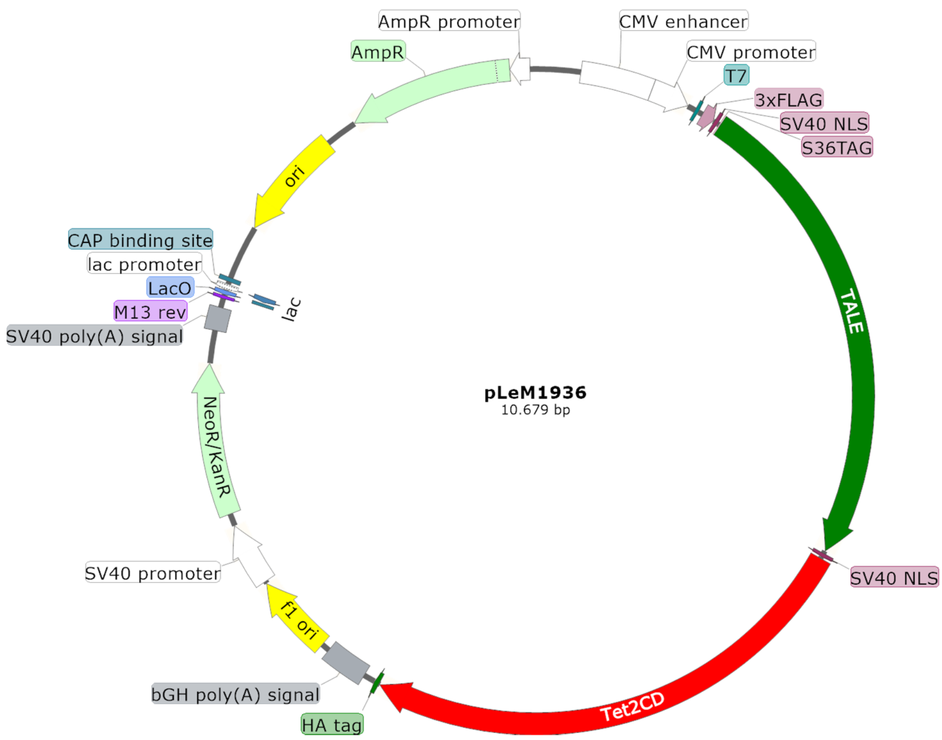

Figure S16 Exemplary plasmid map for TALE with amber codon (S36TAG), C-terminal TET2CD and CMV promoter.

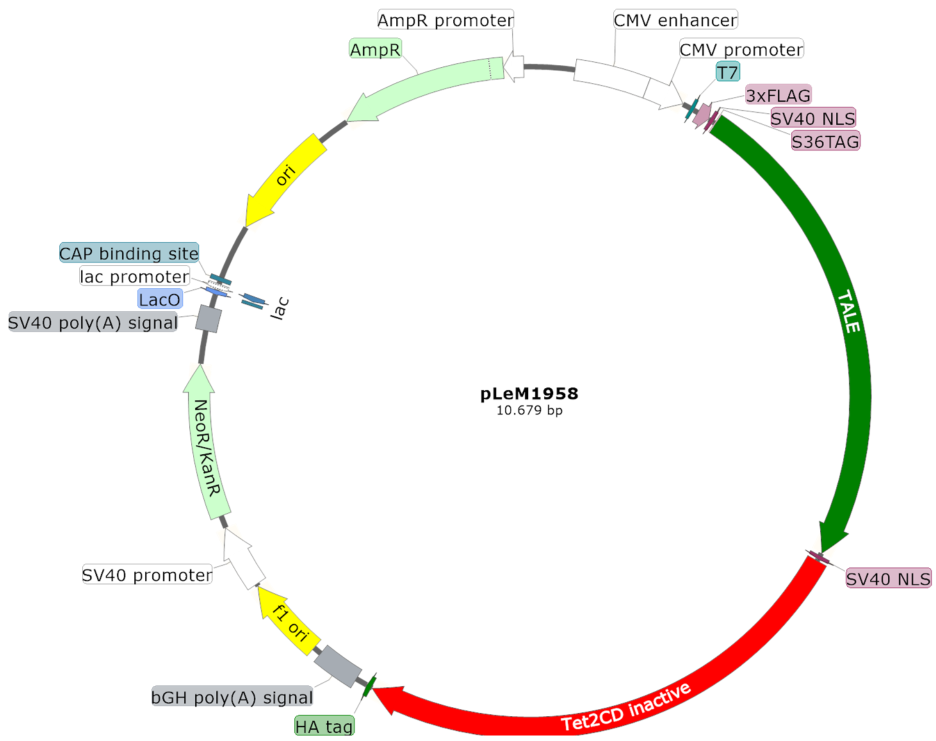

Figure S17 Exemplary plasmid map for TALE with amber codon (S36TAG), C-terminal TET2CD inactive and CMV promoter.

12.3 Sequences for TALE design

TTCCATTCCATTCCTGTACTCGGGTTGATTCCATTCCATTCCATTCCAATCCATGCCATTCC
ACTCGTGTTGATTCCATTCTTTCCATTCCATTCAAGTTGAATCCATTCCATTGCATTCCATT
CATTCGATTCCATTCGATTGCACTCGGGTTGATT

Figure S18 SatIII Sequence with SatIII-TALE binding site (blue).

CTTCTGTCTAGTTTTTATGTGAAGATATTCCCTTTTCCAACGAAGGCCTCAAAGCGCTCCAA
ATATCCACTTGCAGATTCTACAAAAAGAGTGTTTCAAAACTGCTCTATCAAAAGAAAGGTTC
AACTCTGTGAGTTGAATGCACACATCACAAAGAAGTTTCTGAGAATG

Figure S19 αSat consensus sequence with αSat-TALE binding site (blue)[282].

TTTTTTTTTTTTTTTTTTTTTTTTTTTTTTTATTATACTCTAAGTTTTAGGGTACATGTGCA
CATTGTGCAGGTTAGTTACATATGTATACATGTGCCATGCTGGTGCGCTGCACCCACTAATG
TGTCATCTAGCATTAGGTATATCTCCCAATGCTATCCCTCCCCCCTCCCCCGACCCCACCAC
AGTCCCCAGAGTGTGATATTCCCCTTCCTGTGTCCATGTGATCTCATTGTTCAATTCCCACC
TATGAGTGAGAATATGCGGTGTTTGGTTTTTTGTTCTTGCGATAGTTTACTGAGAATGATGG
TTTCCAATTTCATCCATGTCCCTACAAAGGATATGAACTCATCATTTTTTATGGCTGCATAG
TATTCCATGGTGTATATGTGCCACATTTTCTTAATCCAGTCTATCATTGTTGGACATTTGGG
TTGGTTCCAAGTCTTTGCTATTGTGAATAGTGCCGCAATAAACATACGTGTGCATGTGTCTT
TATAGCAGCATGATTTATACTCATTTGGGTATATACCCAGTAATGGGATGGCTGGGTCAAAT
GGTATTTCTAGTTCTAGATCCCTGAGGAATCGCCACACTGACTTCCACAATGGTTGAACTAG
TTTACAGTCCCACCAACAGTGTAAAAGTGTTCCTATTTCTCCGCATCCTCTCCAGCACCTGT
TGTTTCCTGACTTTTTAATGATTGCCATTCTAACTGGTGTGAGATGATATCTCATAGTGGTT
TTGATTTGCATTTCTCTGATGGCCAGTGATGATGAGCATTTCTTCATGTGTTTTTTGGCTGC
ATAAATGTCTTCTTTTGAGAAGTGTCTGTTCATGTCCTTCACCCACTTTTTGATGGGGTTGT
TTGTTTTTTTCTTGTAAATTTGTTTGAGTTCATTGTAGATTCTGGATATTAGCCCTTTGTCA
GATGAGTAGGTTGCGAAAATTTTCTCCCATGTTGTAGGTTGCCTGTTCACTCTGATGGTAGT
TTCTTTTGCTGTGCAGAAGCTCTTTAGTTTAATTAGATCCCATTTGTCAATTTTGTCTTTTG
TTGCCATTGCTTTTGGTGTTTTGGACATGAAGTCCTTGCCCACGCCTATGTCCTGAATGGTA
ATGCCTAGGTTTTCTTCTAGGGTTTTTATGGTTTTAGGTTTAACGTTTAAATCTTTAATCCA
TCTTGAATTGATTTTTGTATAAGGTGTAAGGAAGGGATCCAGTTTCAGCTTTCTACATATGG
CTAGCCAGTTTTCCCAGCACCATTTATTAAATAGGGAATCCTTTCCCCATTGCTTGTTTTTC
TCAGGTTTGTCAAAGATCAGATAGTTGTAGATATGCGGCATTATTTCTGAGGGCTCTGTTCT

GTTCCATTGATCTATATCTCTGTTTTGGTACCAGTACCATGCTGTTTTGGTTACTGTAGCCT
TGTAGTATAGTTTGAAGTCAGGTAGTGTGATGCCTCCAGCTTTGTTCTTTTGGCTTAGGATT
GACTTGGCAATGCGGGCTCTTTTTTGGTTCCATATGAACTTTAAAGTAGTTTTTTCCAATTC
TGTGAAGAAAGTCATTGGTAGCTTGATGGGGATGGCATTGAATCTGTAAATTACCTTGGGCA
GTATGGCCATTTTCACGATATTGATTCTTCCTACCCATGAGCATGGAATGTTCTTCCATTTG
TTTGTGTCCTCTTTTATTTCCTTGAGCAGTGGTTTGTAGTTCTCCTTGAAGAGGTCCTTCAC
ATCCCTTGTAAGTTGGATTCCTAGGTATTTTATTCTCTTTGAAGCAATTACGAATGGGAGTT
CACCCATGATTTGGCTCTCTGTTTGTCTGTTGTTGGTGTATAAGAATGCTTGTGATTTTTGT
ACATTGATTTTGTATCCTGAGACTTTGCTGAAGTTGCTTATCAGCTTAAGGAGATTTTGGGC
TGAGACGATGGGGTTTTCTAGATATACAATCATGTCGTCTGCAAACAGGGACAATTTGACTT
CCTCTTTTCCTAATTGAATACCCTTTATTTCCTTCTCCTGCCTGATTGCCCTGGCCAGAACT
TCCAACACTATGTTGAATAGGAGCGGTGAGAGAGGGCATCCCTGTCTTGTGCCGGTTTTCAA
AGGGAATGCTTCCAGTTTTTGCCCATTCAGTATGATATTGGCTGTGGGTTTGTCATAGATAG
CTCTTATTATTTTGAAATACGTCCCATCAATACCTAATTTATTGAGAGTTTTTAGCATGAAG
GGTTGTTGAATTTTGTCAAAGGCTTTTTCTGCATCTATTGAGATAATCATGTGGTTTTTGTC
TTTGGCTCTGTTTATATGCTGGATTACATTTATTGATTTGCGTATATTGAACCAGCCTTGCA
TCCCAGGGATGAAGCCCACTTGATCATGGTGGATAAGCTTTTTGATGTGCTAATGGATTCGG
TTTGCCAGTATTTTATTGAGGATTTTTGCATCAATGTTCATCAAGGATATTGGTCTAAAATT
CTCTTTTTTGGTTGTGTCTCTGCCCGGCTTTGGTATCAGAATGATGCTGGCCTCATAAAATG
AGTTAGGGAGGATTCCCTCTTTTTCTATTGATTGGAATAGTTTCAGAAGGAATGGTACCAGT
TCCTCCATGTACCTCTGGTAGAATTCGGCTGTGAATCCATCTGGTCCTGGACTCTTTTTGGT
TGGTAAACTATTGATTATTGCCACAATTTCAGAGCCTGTTATTGGTCTATTCAGAGATTCAA
CTTCTTCCTGGTTTAGTCTTGGGAGAGTGTATGTGTCGAGGAATGTATCCATTTCTTCTAGA
TTTTCTAGTTTATTTGCGTAGAGGTGTTTGTAGTATTCTCTGATGGTAGTTTGTATTTCTGT
GGGATCGGTGGTGATATCCCCTTTATCATTTTTTATTGTGTCTATTTGATTCTTCTCTCTTT
TTTTCTTTATTAGTCTTGCTAGCGGTCTATCAATTTTGTTGATCCTTTCAAAAAACCAGCTC
CTGGATTCATTGATTTTTTGAAGGGTTTTTTGTGTCTCTATTTCCTTCAGTTCTGCTCTGAT
TTTAGTTATTTCTTGCCTTCTGCTAGCTTTTGAATGTGTTTGCTCTTGCTTTTCTAGTTCTT
TTAATTGTGATGTTAGGGTGTCAATTTTGGATCTTTCCTGCTTTCTCTTGTAGGCATTTAGT
GCTATAAATTTCCCTCTACACACTGCTTTGAATGCGTCCCAGAGATTCTGGTATGTGGTGTC
TTTGTTCTCGTTGGTTTCAAAGAACATCTTTATTTCTGCCTTCATTTCGTTATGTACCCAGT
AGTCATTCAGGAGCAGGTTGTTCAGTTTCCATGTAGTTGAGCGGCTTTGAGTGAGATTCTTA
ATCCTGAGTTCTAGTTTGATTGCACTGTGGTCTGAGAGATAGTTTGTTATAATTTCTGTTCT
TTTACATTTGCTGAGGAGAGCTTTACTTCCAACTATGTGGTCAATTTTGGAATAGGTGTGGT
GTGGTGCTGAAAAAAAGGTATATTCTGTTGATTTGGGGTGGAGAGTTCTGTAGATGTCTATT

AGGTCTGCTTGGTGCAGAGCTGAGTTCAATTCCTGGGTATCCTTGTTGACTTTCTGTCTCGT
TGATCTGTCTAATGTTGACAGTGGGGTGTTAAAGTCTCCCATTATTAATGTGTGGGAGTCTA
AGTCTCTTTGTAGGTCACTCAGGACTTGCTTTATGAATCTGGGTGCTCCTGTATTGGGTGCA
TAAATATTTAGGATAGTTAGCTCCTCTTGTTGAATTGATCCCTTTACCATTATGTAATGGCC
TTCTTTGTCTCTTTTGATCTTTGTTGGTTTAAAGTCTGTTTTATCAGAGACTAGGATTGCAA
CCCCTGCCTTTTTTTGTTTTCCATTGGCTTGGTAGATCTTCCTCCATCCTTTTATTTTGAGC
CTATGTGTGTCTCTGCACGTGAGATGGGTTTCCTGAATACAGCACACTGATGGGTCTTGACT
CTTTATCCAACTTGCCAGTCTGTGTCTTTTAATTGCAGAATTTAGTCCATTTATATTTAAAG
TTAATATTGTTATGTGTGAATTTGATCCTGTCATTATGATGTTAGCTGGTGATTTTGCTCAT
TAGTTGATGCAGTTTCTTCCTAGTCTCAATGGTCTTTACATTTTGGCATGATTTTGCAGCGG
CTGGTACCGGTTGTTCCTTTCCATGTTTAGCGCTTCCTTCAGGAGCTCTTTTAGGGCAGGCC
TGGTGGTGACAAAATCTCTCAACATTTGCTTGTCTATAAAGTATTTTATTTCTCCTTCACTT
ATGAAGCTTAGTTTGGCTGGATATGAAATTCTGGGTTGAAAATTCTTTTCTTTAAGAATGTT
GAATATTGGCCCCCACTCTCTTCTGGCTTGTAGGGTTTCTGCCGAGAGATCCACTGTTAGTC
TGATGGGCTTTCCTTTGAGGGTAACCCGACCTTTCTCTCTGGCTGCCCTTAACATTTTTTCC
TTCATTTCAACTTTGGTGAATCTGACAATTATGTGTCTTGGAGTTGCTCTTCTCGAGGAGTA
TCTTTGTGGCGTTCTCTGTATTTCCTGAATCTGAACGTTGGCCTGCCTTGCTAGATTGGGGA
AGTTCTCCTGGATAATATCCTGCAGAGTGTTTTCCAACTTGGTTCCATTCTCCACATCACTT
TCAGGTACACCAATCAGACGTAGATTTGGTCTTTTCACATAGTCCCATATTTCTTGGAGGCT
TTGCTCATTTCTTTTTATTCTTTTTTCTCTAAACTTCCCTTCTCGCTTCATTTCATTCATTT
CATCTTCCATTGCTGATACCCTTTCTTCCAGTTGATCGCATCGGCTCCTGAGGCTTCTGCAT
TCTTCACGTAGTTCTCGAGCCTTGGTTTTCAGCTCCATCAGCTCCTTTAAGCACTTCTCTGT
ATTGGTTATTCTAGTTATACATTCTTCTAAATTTTTTTCAAAGTTTTCAACTTCTTTGCCTT
TGGTTTGAATGTCCTCCCGTAGCTCAGAGTAATTTGATCGTCTGAAGCCTTCTTCTCTCAGC
TCGTCAAAATCATTCTCCATCCAGCTTTGTTCTGTTGCTGGTGAGGAACTGCGTTCCTTTGG
AGGAGGAGAGGCGCTCTGCGTTTTAGAGTTTCCAGTTTTTCTGTTCTGTTTTTTCCCCATCT
TTGTGGTTTTATCTACTTTTGGTCTTTGATGATGGTGATGTACAGATGGGTTTTCGGTGTAG
ATGTCCTTTCTGGTTGTTAGTTTTCCTTCTAACAGACAGGACCCTCAGCTGCAGGTCTGTTG
GAATACCCTGCCGTGTGAGGTGTCAGTGTGCCCCTGCTGGGGGGTGCCTCCCAGTTAGGCTG
CTCGGGGGTCAGGAGTCAGGGACCCACTTGAGGAGGCAGTCTGTCTGCCCGTTCTCAGATCT
CCAGCTGCGTGCTGGGAGAACCACTGCTCTCTTCAAAGCTGTCAGACAGGGACACTTAAGTC
TGCAGAGGTTACTGCTGCCTTTTTGTTTGTCTGTGCCCTGCCCCCAGAGGTGGAGCCTACAG
AGGCAGGCAGGCCTCCTTGAGCTGTGGTGGGCTCCACCCAGTTCGAGCTTCCCGGCTGCTTT
GTTTACCTAAGCAAGCCTGGGCAATGGCGGGCGCCCCTCCCCCAGCCTCGTTGCCGCCTTGC
AGTTTGATCTCAGACTGCTGTGCTAGCAATCAGCGAGATTCCGTGGGCGTAGGACCCTCCGA

GCCAGGTGTGGGATATAGTCTCGTGGTGCGCCGTTTCTTAAGCCGGTCTGAAAAGCGCAATA
TTCGGGTGGGAGTGACCCGATTTTCCAGGTGCGACCGTCACCCCTTTCTTTGACTCAGAAAG
GGAACTCCCTGACCCCTTGCGCTTCCCAGGTGAGGCAATGCCTCGCCCTGCTTCGGCTCGCG
CACGGTGCGCACACACACTGGCCTGCGCCCACTGTCTGGCACTCCCTAGTGAGATGAACCCG
GTACCTCAGATGGAAATGCAGAAATCACCGTCTTCTGCGTCGCTCACGCTGGGAGCTGTAGA
CCGGAGCTGTTCCTATTCGGCCATCTTGGCTCCTCCCCC

Figure S20 Line1 sequence with Line1-TALE binding site (blue).

GGCCGGGCGCGGTGGCTCACGCCTGTAATCCCAGCACTTTGGGAGGCCGAGGCGGGCGGATC
ACCTGAGGTCAGGAGTTCGAGACCAGCCCGGCCAACACGGTGAAACCCCGTCTCTACTAAAA
ATACAAAAATTAGCCGGGCGTGGTGGCGCGCCTGTAATCCCAGCTACTCGGGAGGCTGAG
GCAGGAGAATCGCTTGAACCCGGGAGGCGGAGGTTGCAGTGAGCCGAGATCGCGCCACTGCA
CTCCAGCCTGGGCGACAGAGCGAGACTCCGTCTC

Figure S21 Alu sequence with Alu-TALE binding site (blue).

ATTCCATTCGATGATGACCCCTTTCATTTCCATTCAATGAGGANTCCATTCGAGACCATTCG
ATGATTGCATTCAATTCATTCGATGACGANTCCATTCGGGTCCATTCGATGATGCTCACACT
GGATTTCATTCCATAATTCTATTCG

Figure S22 SatII conesus sequence with SatII-TALE binding site (blue)[283].

CCTAACCCTAACCCTAACCCTAACCCTAACCCTAACCCTAACCCTAACCCTAACCCTAACCC
TAACCCTAACCCTAACCCTAACCCTAACCCTAACCCTAACCCTAACCCTAACCCTAACCCTA
ACCCTAACCCTAACCCTAACCCTAACCCTAACCCTAACCCTAACCCTAACCCTAACCCTAAC
CCTAACCCTAACCCTAACCCTAACCCTAACCCTAACCCTAACCCTAA

Figure S23 Telomere sequence with Telomere-TALE binding sites (blue)[284].

12.4 Open reading frames (ORF) of plasmids used in proteomics analysis

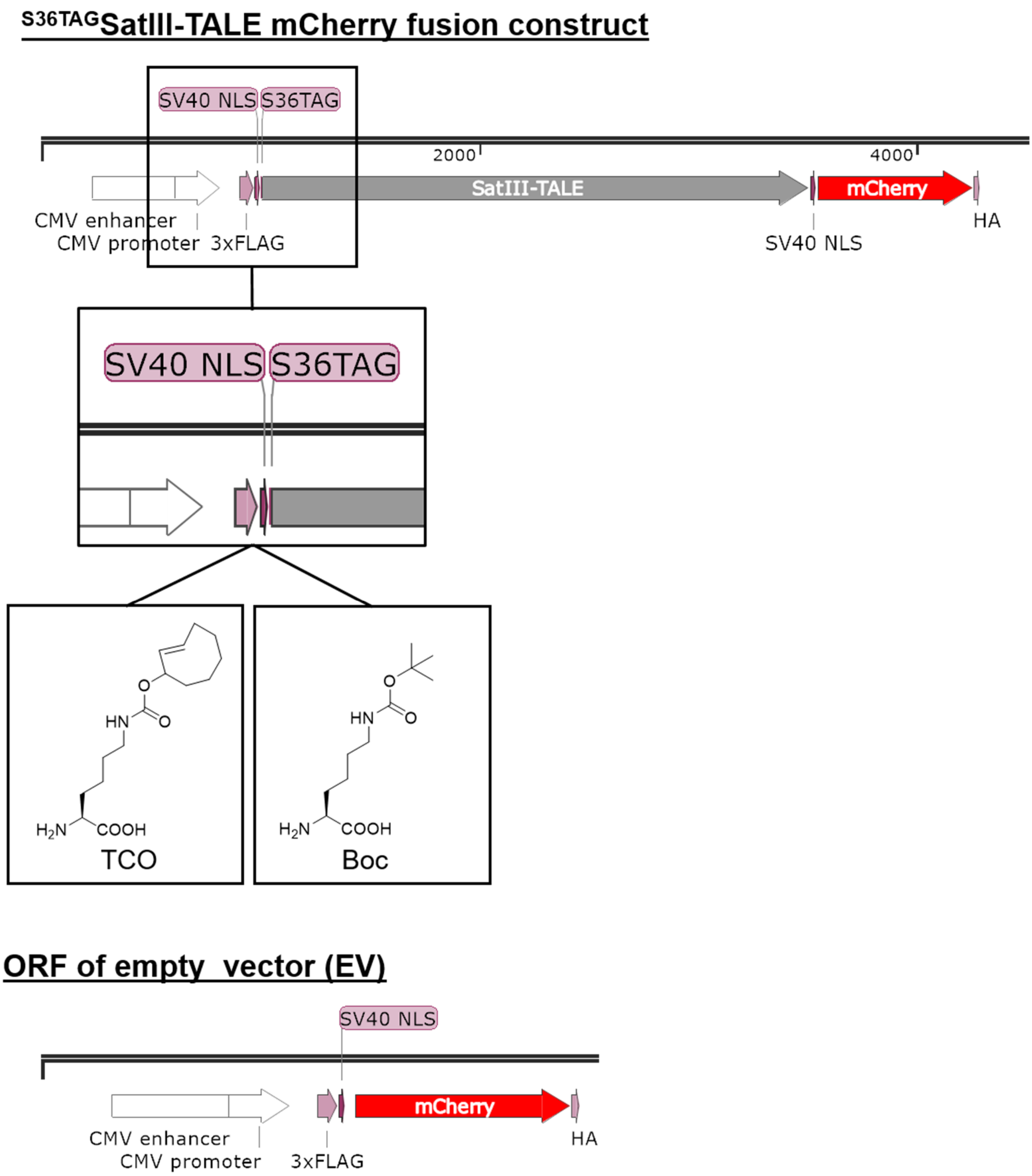

Figure S24 ORF of plasmids used in proteomics analysis: ^{S36TAG}SatIII-TALE mCherry fusion construct with either incorporated ncAA TCO as positive control or Boc as a non-binding control, which visualize the non-spoecifi9c binding to the beads. The empty vector (EV) expresses only mCherry, whereby always TCO is added and the tRNA^{Pyl}/PylRS-AF^{NES} pair is cotransfected.

12.5 Protein Lists from Proteomics Analyses

Table S2 List of identified proteins from HEK cells with mean of LFQ intensities from biological triplicates.

Gene names	mean (LFQ int.) TCO HS	mean (LFQ int.) Boc HS	mean (LFQ int.) EV HS	mean (LFQ int.) TCO nonHS	mean (LFQ int.) Boc nonHS	mean (LFQ int.) EV nonHS
HIST1H2AJ	7.27E+08	3.26E+08	9.42E+08	1.15E+09	4.51E+08	1.93E+09
TUBA1B	4.14E+08	8.56E+07	3.11E+08	3.37E+08	5.55E+07	3.73E+08
EEF1A1P5	4.09E+08	1.12E+08	3.55E+08	3.25E+08	6.83E+07	2.66E+08
HIST1H2BN	4.05E+08	2.59E+08	6.51E+08	7.91E+08	3.40E+08	1.28E+09
HIST1H4A	3.25E+08	1.65E+08	4.93E+08	6.07E+08	2.20E+08	9.82E+08
HIST2H3PS2	2.55E+08	9.18E+07	3.25E+08	4.81E+08	1.54E+08	8.67E+08
EEF2	2.47E+08	4.08E+07	1.94E+08	1.86E+08	4.94E+06	1.51E+08
VIM	2.40E+08	1.73E+08	2.54E+08	3.01E+08	9.41E+07	3.31E+08
HIST1H1C	2.37E+08	1.44E+08	3.72E+08	3.83E+08	1.15E+08	6.51E+08
TUBB	1.94E+08	9.22E+07	1.88E+08	1.54E+08	5.20E+07	1.52E+08
HSPA8	1.85E+08	7.55E+07	1.48E+08	1.36E+08	2.95E+06	1.15E+08
HSPA1B	1.78E+08	8.03E+07	1.47E+08	1.27E+08	1.75E+07	1.07E+08
CKB	1.68E+08	5.84E+07	1.31E+08	9.73E+07	3.95E+06	7.77E+07
HSP90AB1	1.67E+08	3.66E+07	1.27E+08	1.23E+08	1.33E+07	8.83E+07
PGK1	1.63E+08	8.89E+06	1.31E+08	1.20E+08	1.77E+06	8.51E+07
ENO1	1.44E+08	2.93E+07	1.01E+08	1.02E+08	1.24E+07	7.84E+07
HNRNPK	1.40E+08	4.88E+07	1.50E+08	1.31E+08	1.64E+07	1.20E+08
NPM1	1.35E+08	5.43E+07	1.39E+08	1.50E+08	4.11E+07	1.48E+08
RPL4	1.29E+08	2.41E+07	1.34E+08	1.43E+08	1.38E+07	1.87E+08
PKM	1.19E+08	2.03E+07	8.51E+07	5.88E+07	3.43E+06	4.14E+07
RPL7A	1.17E+08	3.14E+07	1.19E+08	1.33E+08	1.51E+07	1.62E+08
ITGA6	1.09E+08	3.05E+08	0.00E+00	0.00E+00	1.09E+09	0.00E+00
HNRNPA1	9.81E+07	1.47E+07	9.60E+07	9.10E+07	1.11E+07	7.67E+07
HNRNPH1	9.65E+07	9.57E+06	9.78E+07	1.06E+08	0.00E+00	9.92E+07
HNRNPU	9.04E+07	1.92E+07	1.08E+08	7.23E+07	1.87E+07	9.45E+07
NCL	8.98E+07	2.54E+07	1.05E+08	1.02E+08	1.41E+07	9.75E+07
HNRNPA2B1	8.77E+07	1.80E+07	8.97E+07	7.83E+07	5.49E+06	7.13E+07
ACTG1	8.66E+07	6.05E+07	8.61E+07	7.36E+07	3.70E+07	8.28E+07
FASN	8.26E+07	2.79E+06	7.81E+07	8.05E+07	2.03E+06	7.79E+07
GAPDH	8.17E+07	2.55E+07	6.16E+07	5.95E+07	1.33E+07	4.97E+07
PPIA	8.16E+07	0.00E+00	6.04E+07	5.53E+07	0.00E+00	4.72E+07
RPL6	8.04E+07	7.88E+06	7.46E+07	8.22E+07	1.70E+06	1.03E+08
HNRNPC	7.55E+07	0.00E+00	7.82E+07	8.05E+07	0.00E+00	7.60E+07
ALDOA	7.47E+07	1.20E+07	4.72E+07	4.93E+07	0.00E+00	3.54E+07
DDX21	7.24E+07	5.49E+06	9.40E+07	1.06E+08	7.66E+06	1.28E+08
PARP1	6.83E+07	7.62E+06	6.78E+07	8.26E+07	2.44E+06	8.05E+07
HSPD1	6.72E+07	5.99E+07	5.61E+07	3.39E+07	2.48E+06	2.31E+07
HNRNPM	6.50E+07	2.95E+07	7.63E+07	7.11E+07	1.29E+07	5.90E+07
RPL3	6.19E+07	0.00E+00	6.43E+07	6.26E+07	0.00E+00	7.38E+07
RPS3	5.84E+07	5.16E+06	5.49E+07	5.85E+07	0.00E+00	5.95E+07
SFPQ	5.84E+07	1.03E+07	5.05E+07	6.93E+07	4.36E+06	6.61E+07
PTBP1	5.83E+07	0.00E+00	5.94E+07	6.16E+07	0.00E+00	5.27E+07
DDX5	5.67E+07	1.04E+07	6.05E+07	6.57E+07	7.02E+06	6.51E+07
UBB	5.56E+07	1.19E+07	4.82E+07	4.89E+07	8.95E+06	6.27E+07
EIF4A1	5.44E+07	2.51E+06	4.65E+07	3.96E+07	0.00E+00	3.27E+07
RPL7	5.33E+07	8.10E+06	5.66E+07	5.94E+07	0.00E+00	7.20E+07
RPS4X	5.07E+07	0.00E+00	5.01E+07	4.65E+07	0.00E+00	5.12E+07
SRP72	5.06E+07	0.00E+00	0.00E+00	0.00E+00	0.00E+00	0.00E+00
RPL18	5.05E+07	2.01E+07	5.89E+07	5.27E+07	0.00E+00	7.24E+07
PRDX1	4.91E+07	1.75E+07	4.18E+07	4.01E+07	4.65E+06	3.14E+07
CLTC	4.58E+07	0.00E+00	3.78E+07	4.30E+07	0.00E+00	4.04E+07
RPL13	4.44E+07	1.66E+07	4.22E+07	4.70E+07	0.00E+00	5.11E+07
PABPC1	4.40E+07	0.00E+00	3.93E+07	4.11E+07	0.00E+00	3.61E+07
YWHAE	4.32E+07	0.00E+00	3.98E+07	3.31E+07	0.00E+00	2.58E+07
RPS8	4.27E+07	2.39E+06	3.45E+07	4.28E+07	6.16E+06	5.55E+07
LDHB	4.21E+07	3.21E+06	3.07E+07	2.82E+07	0.00E+00	2.04E+07
MTHFD1	4.20E+07	1.64E+06	3.60E+07	3.43E+07	0.00E+00	2.82E+07
PFN1	4.17E+07	0.00E+00	3.75E+07	2.85E+07	0.00E+00	2.34E+07
PCBP2	4.09E+07	4.29E+06	3.27E+07	3.57E+07	0.00E+00	3.41E+07
PHGDH	4.05E+07	9.56E+06	3.06E+07	2.93E+07	0.00E+00	2.26E+07
RPS2	4.05E+07	0.00E+00	3.30E+07	3.91E+07	0.00E+00	4.41E+07
SRSF7	3.95E+07	0.00E+00	4.32E+07	4.84E+07	0.00E+00	5.08E+07
DDX3X	3.86E+07	5.40E+06	3.19E+07	3.21E+07	0.00E+00	3.05E+07
EEF1G	3.73E+07	6.54E+06	2.66E+07	2.30E+07	0.00E+00	1.82E+07
RPS6	3.58E+07	6.98E+06	3.64E+07	3.48E+07	0.00E+00	4.39E+07
RPS11	3.37E+07	0.00E+00	2.96E+07	3.67E+07	0.00E+00	4.59E+07
RPL8	3.36E+07	1.56E+07	3.09E+07	3.10E+07	7.76E+06	4.16E+07
RPS3A	3.34E+07	7.03E+06	3.43E+07	3.09E+07	0.00E+00	3.49E+07
PCBP1	3.32E+07	3.60E+06	3.34E+07	3.24E+07	1.73E+06	2.98E+07
RPL14	3.31E+07	1.30E+07	3.40E+07	2.99E+07	8.56E+06	4.58E+07
RAN	3.29E+07	0.00E+00	3.14E+07	3.26E+07	0.00E+00	2.59E+07
RPL23A	3.26E+07	1.64E+07	4.04E+07	3.44E+07	5.76E+06	4.70E+07
TCP1	3.21E+07	0.00E+00	2.40E+07	1.38E+07	0.00E+00	1.14E+07
TRIM28	3.20E+07	0.00E+00	3.67E+07	3.54E+07	5.91E+06	3.45E+07
CCT8	3.13E+07	1.60E+06	2.59E+07	1.94E+07	0.00E+00	1.32E+07
IGF2BP1	3.11E+07	0.00E+00	2.79E+07	2.50E+07	0.00E+00	2.07E+07
HSP90AA1	2.99E+07	4.29E+06	2.62E+07	2.38E+07	0.00E+00	1.73E+07
KPNB1	2.95E+07	0.00E+00	2.11E+07	2.27E+07	0.00E+00	1.80E+07
RPL13A	2.95E+07	1.16E+07	3.38E+07	2.81E+07	2.70E+06	3.58E+07
CFL1	2.91E+07	0.00E+00	2.02E+07	2.32E+07	0.00E+00	1.90E+07
CCT4	2.88E+07	0.00E+00	2.27E+07	1.64E+07	0.00E+00	1.17E+07
PAICS	2.85E+07	0.00E+00	2.06E+07	1.70E+07	0.00E+00	1.46E+07
SERBP1	2.82E+07	0.00E+00	2.13E+07	2.40E+07	0.00E+00	2.34E+07
TUBB4B	2.81E+07	1.19E+07	2.79E+07	2.82E+07	2.89E+06	2.73E+07
GSTP1	2.80E+07	0.00E+00	1.70E+07	1.58E+07	0.00E+00	7.62E+06

CCT3	2.79E+07	0.00E+00	2.12E+07	1.72E+07	0.00E+00	1.32E+07
CCT6A	2.71E+07	0.00E+00	2.23E+07	1.80E+07	0.00E+00	1.21E+07
HNRNPD	2.69E+07	6.69E+06	2.50E+07	1.39E+07	0.00E+00	2.02E+07
RPS9	2.68E+07	0.00E+00	2.37E+07	2.46E+07	0.00E+00	3.17E+07
UBA1	2.66E+07	0.00E+00	9.71E+06	2.99E+06	0.00E+00	1.87E+06
MATR3	2.66E+07	0.00E+00	2.69E+07	3.30E+07	0.00E+00	3.14E+07
MYH9	2.65E+07	0.00E+00	1.71E+07	2.69E+07	0.00E+00	2.67E+07
RUVBL1	2.53E+07	0.00E+00	2.27E+07	2.01E+07	0.00E+00	1.73E+07
RPL23	2.48E+07	0.00E+00	3.65E+07	3.46E+07	0.00E+00	3.56E+07
NAP1L1	2.45E+07	0.00E+00	1.69E+07	1.49E+07	0.00E+00	1.29E+07
RPL17	2.44E+07	1.08E+07	2.74E+07	2.18E+07	2.74E+06	3.03E+07
DHX9	2.40E+07	0.00E+00	2.66E+07	2.51E+07	0.00E+00	2.48E+07
STIP1	2.38E+07	0.00E+00	1.70E+07	1.42E+07	0.00E+00	1.30E+07
LDHA	2.38E+07	0.00E+00	1.60E+07	1.70E+07	0.00E+00	1.36E+07
CCT2	2.33E+07	0.00E+00	1.39E+07	8.98E+06	0.00E+00	5.13E+06
RPS26	2.32E+07	0.00E+00	2.21E+07	1.45E+07	0.00E+00	1.23E+07
ACLY	2.29E+07	0.00E+00	1.88E+07	1.72E+07	0.00E+00	1.46E+07
LMNB1	2.27E+07	0.00E+00	2.65E+07	2.44E+07	0.00E+00	2.55E+07
SND1	2.23E+07	0.00E+00	1.92E+07	1.78E+07	0.00E+00	1.41E+07
HSPA9	2.23E+07	1.85E+07	1.66E+07	1.21E+07	4.11E+06	9.48E+06
RBMX	2.18E+07	1.35E+07	3.24E+07	2.94E+07	0.00E+00	3.32E+07
GNB2L1	2.17E+07	0.00E+00	2.00E+07	1.77E+07	0.00E+00	1.55E+07
RPS7	2.15E+07	0.00E+00	8.50E+06	1.09E+07	0.00E+00	2.16E+07
RPL27A	2.12E+07	0.00E+00	2.13E+07	2.20E+07	3.95E+06	2.74E+07
RPL24	2.12E+07	5.52E+06	2.69E+07	2.40E+07	6.61E+06	2.88E+07
TUFM	2.08E+07	6.09E+06	1.67E+07	1.32E+07	0.00E+00	1.34E+07
XRCC6	2.04E+07	0.00E+00	1.87E+07	1.84E+07	0.00E+00	1.37E+07
AHCY	1.96E+07	0.00E+00	1.70E+07	1.45E+07	0.00E+00	1.29E+07
RPL28	1.94E+07	0.00E+00	2.09E+07	2.22E+07	0.00E+00	2.83E+07
HNRNPR	1.94E+07	0.00E+00	1.79E+07	1.72E+07	0.00E+00	1.49E+07
CCT7	1.94E+07	0.00E+00	1.13E+07	7.00E+06	0.00E+00	3.64E+06
RPL19	1.89E+07	0.00E+00	1.79E+07	1.95E+07	0.00E+00	2.51E+07
HNRNPL	1.89E+07	0.00E+00	2.35E+07	2.20E+07	0.00E+00	2.03E+07
RPL15	1.81E+07	0.00E+00	1.98E+07	1.95E+07	0.00E+00	3.08E+07
RPL27	1.78E+07	5.48E+06	2.26E+07	2.00E+07	0.00E+00	2.58E+07
NONO	1.75E+07	0.00E+00	2.23E+07	2.19E+07	0.00E+00	2.22E+07
EEF1B2	1.75E+07	0.00E+00	1.39E+07	1.57E+07	0.00E+00	8.58E+06
SLC25A5	1.72E+07	0.00E+00	1.88E+07	1.64E+07	0.00E+00	1.66E+07
RPL18A	1.70E+07	0.00E+00	1.73E+07	2.08E+07	0.00E+00	2.22E+07
NME1-NME2	1.68E+07	0.00E+00	1.57E+07	1.21E+07	0.00E+00	6.85E+06
RPL9	1.66E+07	0.00E+00	1.05E+07	5.49E+06	0.00E+00	1.40E+07
EIF5A	1.61E+07	0.00E+00	8.34E+06	8.75E+06	0.00E+00	3.13E+06
FLNA	1.61E+07	0.00E+00	1.46E+07	1.51E+07	0.00E+00	1.26E+07
HNRNPA3	1.60E+07	0.00E+00	1.94E+07	1.57E+07	0.00E+00	1.66E+07
ATP5A1	1.55E+07	0.00E+00	1.33E+07	7.42E+06	0.00E+00	7.43E+06
H2AFY	1.55E+07	0.00E+00	1.87E+07	2.58E+07	0.00E+00	3.59E+07
PRPF19	1.53E+07	0.00E+00	1.30E+07	1.56E+07	0.00E+00	1.67E+07
SUPT16H	1.51E+07	0.00E+00	1.63E+07	1.92E+07	0.00E+00	1.88E+07
RPS16	1.50E+07	0.00E+00	1.43E+07	1.87E+07	7.12E+06	2.16E+07
HNRNPAB	1.48E+07	0.00E+00	1.18E+07	1.27E+07	0.00E+00	1.11E+07
RPL35	1.47E+07	9.76E+06	1.10E+07	9.31E+06	3.70E+06	1.81E+07
EEF1D	1.46E+07	0.00E+00	1.00E+07	6.80E+06	0.00E+00	7.06E+06
RPS27	1.45E+07	0.00E+00	1.15E+07	1.71E+07	0.00E+00	1.88E+07
RPS23	1.44E+07	0.00E+00	1.61E+07	1.79E+07	0.00E+00	2.39E+07
DDX17	1.44E+07	0.00E+00	1.73E+07	1.96E+07	0.00E+00	1.88E+07
RPL10A	1.41E+07	0.00E+00	1.22E+07	1.08E+07	0.00E+00	9.74E+06
PHB	1.40E+07	0.00E+00	1.22E+07	3.21E+06	0.00E+00	7.64E+06
CCT5	1.36E+07	0.00E+00	5.28E+06	0.00E+00	0.00E+00	0.00E+00
RPS10	1.32E+07	0.00E+00	4.17E+06	5.76E+06	0.00E+00	2.46E+06
SUMO2	1.30E+07	0.00E+00	1.68E+07	0.00E+00	0.00E+00	5.95E+06
LRRC59	1.30E+07	0.00E+00	8.28E+06	8.18E+06	0.00E+00	2.49E+06
EPRS	1.29E+07	0.00E+00	1.20E+07	1.24E+07	0.00E+00	1.22E+07
XRCC5	1.28E+07	0.00E+00	9.64E+06	1.15E+07	0.00E+00	0.00E+00
RPL11	1.25E+07	0.00E+00	1.37E+07	1.42E+07	0.00E+00	8.98E+06
RPS14	1.24E+07	0.00E+00	1.60E+07	1.59E+07	1.75E+06	1.76E+07
RPS13	1.23E+07	2.35E+06	1.11E+07	1.12E+07	8.37E+05	1.15E+07
HNRNPDL	1.21E+07	0.00E+00	1.37E+07	1.19E+07	0.00E+00	1.08E+07
DNAJA1	1.21E+07	0.00E+00	8.86E+06	1.11E+07	0.00E+00	1.03E+07
RPS17	1.20E+07	0.00E+00	0.00E+00	4.23E+06	0.00E+00	3.27E+06
MDH2	1.20E+07	0.00E+00	5.59E+06	4.30E+06	0.00E+00	0.00E+00
PRKDC	1.19E+07	0.00E+00	1.24E+07	1.52E+07	0.00E+00	1.53E+07
U2AF2	1.19E+07	0.00E+00	1.45E+07	1.39E+07	0.00E+00	1.42E+07
G3BP1	1.19E+07	0.00E+00	3.09E+06	2.84E+06	0.00E+00	4.84E+06
HNRNPF	1.19E+07	0.00E+00	1.41E+07	1.07E+07	0.00E+00	1.15E+07
CALM2	1.17E+07	0.00E+00	0.00E+00	7.02E+06	0.00E+00	0.00E+00
KHSRP	1.16E+07	0.00E+00	1.24E+07	1.16E+07	1.15E+06	8.98E+06
SRSF2	1.16E+07	0.00E+00	1.37E+07	1.52E+07	0.00E+00	9.73E+06
HMGB1	1.14E+07	0.00E+00	8.45E+06	9.18E+06	0.00E+00	8.79E+06
RPS24	1.13E+07	0.00E+00	1.73E+07	1.23E+07	0.00E+00	1.45E+07
RPL12	1.12E+07	0.00E+00	1.19E+07	9.99E+06	0.00E+00	8.61E+06
ILF3	1.12E+07	0.00E+00	1.22E+07	1.26E+07	0.00E+00	1.10E+07
ATIC	1.10E+07	0.00E+00	0.00E+00	0.00E+00	0.00E+00	0.00E+00
RPS18	1.10E+07	0.00E+00	1.07E+07	1.01E+07	0.00E+00	1.03E+07
RBM14	1.09E+07	0.00E+00	1.38E+07	1.60E+07	0.00E+00	1.58E+07
SRSF1	1.09E+07	0.00E+00	1.50E+07	1.52E+07	0.00E+00	1.51E+07
YBX3	1.08E+07	0.00E+00	8.92E+06	5.45E+06	0.00E+00	4.82E+06
ILF2	1.06E+07	0.00E+00	4.03E+06	2.22E+06	0.00E+00	0.00E+00
SSRP1	1.05E+07	0.00E+00	1.22E+07	1.38E+07	0.00E+00	1.37E+07
RPSA	1.01E+07	0.00E+00	8.82E+06	6.87E+06	0.00E+00	5.33E+06
RANBP1	1.00E+07	0.00E+00	4.29E+06	7.12E+06	0.00E+00	4.35E+06
HNRNPA0	9.90E+06	0.00E+00	8.30E+06	8.82E+06	0.00E+00	1.67E+07
PA2G4	9.72E+06	0.00E+00	6.49E+06	5.97E+06	0.00E+00	4.14E+06
SRSF3	9.68E+06	0.00E+00	1.17E+07	8.53E+06	0.00E+00	8.33E+06
IARS	9.66E+06	0.00E+00	6.29E+06	8.16E+06	0.00E+00	7.15E+06
ERH	9.66E+06	0.00E+00	0.00E+00	0.00E+00	0.00E+00	0.00E+00
VDAC2	9.39E+06	0.00E+00	8.91E+06	5.79E+06	0.00E+00	7.29E+06
TPI1	9.25E+06	0.00E+00	5.42E+06	8.05E+06	0.00E+00	6.37E+06
FUBP1	9.16E+06	0.00E+00	8.75E+06	7.82E+06	0.00E+00	6.01E+06
RPL32	8.67E+06	0.00E+00	3.18E+06	9.23E+06	0.00E+00	9.28E+06
FKBP4	8.65E+06	0.00E+00	2.53E+06	0.00E+00	0.00E+00	0.00E+00
SRSF6	8.60E+06	0.00E+00	1.16E+07	1.17E+07	0.00E+00	1.17E+07
RUVBL2	8.46E+06	0.00E+00	7.58E+06	5.82E+06	0.00E+00	6.45E+06

KHDRBS1	8.37E+06	0.00E+00	1.22E+07	1.02E+07	0.00E+00	7.93E+06
RPS12	8.22E+06	0.00E+00	3.70E+06	0.00E+00	0.00E+00	1.97E+06
PRDX6	8.20E+06	0.00E+00	3.61E+06	5.64E+06	0.00E+00	4.42E+06
FUS	8.09E+06	0.00E+00	8.82E+06	9.63E+06	0.00E+00	8.82E+06
DDX39B	7.99E+06	0.00E+00	8.33E+06	5.35E+06	0.00E+00	6.01E+06
TMPO	7.96E+06	1.28E+06	9.59E+06	9.43E+06	0.00E+00	9.02E+06
CSE1L	7.93E+06	0.00E+00	8.24E+06	5.66E+06	0.00E+00	0.00E+00
HNRNPH3	7.90E+06	0.00E+00	9.29E+06	6.95E+06	0.00E+00	6.62E+06
DNAJA2	7.79E+06	0.00E+00	0.00E+00	6.71E+06	0.00E+00	4.41E+06
ELAVL1	7.78E+06	0.00E+00	4.33E+06	7.09E+06	0.00E+00	5.91E+06
RPL5	7.78E+06	0.00E+00	5.18E+06	4.43E+06	0.00E+00	7.68E+06
PHB2	7.77E+06	0.00E+00	7.58E+06	3.80E+06	0.00E+00	3.96E+06
TXN	7.69E+06	0.00E+00	2.15E+06	1.91E+06	0.00E+00	3.43E+06
SSB	7.63E+06	0.00E+00	2.15E+06	0.00E+00	0.00E+00	0.00E+00
EIF3C	7.60E+06	0.00E+00	6.32E+06	6.29E+06	0.00E+00	5.98E+06
CSDE1	7.58E+06	0.00E+00	5.98E+06	5.37E+06	0.00E+00	2.00E+06
RARS	7.58E+06	0.00E+00	1.41E+06	9.23E+05	0.00E+00	0.00E+00
CDC2	7.57E+06	0.00E+00	7.64E+06	7.79E+06	0.00E+00	4.20E+06
NOP2	7.51E+06	0.00E+00	1.03E+07	1.20E+07	0.00E+00	1.70E+07
U2AF1	7.43E+06	0.00E+00	7.39E+06	1.01E+07	0.00E+00	9.37E+06
MIF	7.41E+06	0.00E+00	8.59E+06	3.73E+06	0.00E+00	1.67E+06
EIF3A	7.27E+06	0.00E+00	3.51E+06	4.20E+06	0.00E+00	4.27E+06
RPS20	7.23E+06	0.00E+00	6.67E+06	5.97E+06	0.00E+00	5.24E+06
RPS5	7.17E+06	0.00E+00	5.84E+06	6.55E+06	0.00E+00	5.00E+06
GDI2	7.14E+06	0.00E+00	4.55E+06	0.00E+00	0.00E+00	1.77E+06
PRDX2	7.11E+06	0.00E+00	5.04E+06	4.60E+06	0.00E+00	5.36E+06
EIF2S3	6.95E+06	0.00E+00	1.83E+06	1.73E+06	0.00E+00	3.29E+06
TPM3	6.91E+06	0.00E+00	5.74E+06	5.96E+06	0.00E+00	5.12E+06
RANGAP1	6.90E+06	0.00E+00	6.18E+06	7.37E+06	0.00E+00	4.00E+06
ABCE1	6.90E+06	0.00E+00	3.37E+06	5.77E+06	0.00E+00	5.40E+06
RCC1	6.87E+06	0.00E+00	9.18E+06	5.95E+06	0.00E+00	4.94E+06
ST13	6.86E+06	0.00E+00	5.31E+06	4.28E+06	0.00E+00	2.90E+06
PTGES3	6.70E+06	0.00E+00	1.56E+06	0.00E+00	0.00E+00	0.00E+00
VCP	6.70E+06	0.00E+00	4.49E+06	2.71E+06	0.00E+00	2.12E+06
MARS	6.63E+06	0.00E+00	5.44E+06	5.44E+06	0.00E+00	6.25E+06
FARSB	6.61E+06	0.00E+00	0.00E+00	0.00E+00	0.00E+00	0.00E+00
IPO5	6.55E+06	0.00E+00	3.83E+06	4.77E+06	0.00E+00	1.16E+06
YWHAZ	6.48E+06	0.00E+00	5.85E+06	1.46E+06	0.00E+00	2.42E+06
EIF3D	6.42E+06	0.00E+00	3.83E+06	4.44E+06	0.00E+00	6.88E+06
IMPDH2	6.34E+06	0.00E+00	4.41E+06	4.41E+06	0.00E+00	2.96E+06
SYNCRIP	6.34E+06	0.00E+00	2.78E+06	2.65E+06	0.00E+00	1.04E+06
KPNA2	6.28E+06	0.00E+00	6.99E+06	2.35E+06	0.00E+00	3.45E+06
PPP2R1A	6.28E+06	0.00E+00	0.00E+00	1.01E+06	0.00E+00	0.00E+00
CLIC1	6.22E+06	0.00E+00	0.00E+00	0.00E+00	0.00E+00	0.00E+00
EIF5	6.22E+06	0.00E+00	1.53E+06	0.00E+00	0.00E+00	0.00E+00
YARS	6.20E+06	0.00E+00	2.46E+06	3.22E+06	0.00E+00	1.19E+06
RPS25	6.20E+06	0.00E+00	2.69E+06	3.81E+06	0.00E+00	5.81E+06
MCM3	6.13E+06	0.00E+00	5.39E+06	3.33E+06	0.00E+00	1.76E+06
FBL	6.10E+06	0.00E+00	5.46E+06	7.19E+06	0.00E+00	1.24E+07
HSPA4	6.09E+06	0.00E+00	4.60E+06	3.12E+06	0.00E+00	3.00E+06
HDLBP	6.05E+06	0.00E+00	1.62E+06	3.62E+06	0.00E+00	2.96E+06
SNRNP200	6.05E+06	0.00E+00	6.07E+06	4.54E+06	0.00E+00	7.16E+06
RPS15A	6.04E+06	0.00E+00	9.68E+06	6.99E+06	0.00E+00	6.92E+06
MCM5	5.98E+06	0.00E+00	3.76E+06	4.51E+06	0.00E+00	5.11E+06
TKT	5.91E+06	0.00E+00	4.86E+06	4.81E+06	0.00E+00	4.25E+06
BANF1	5.88E+06	0.00E+00	2.10E+06	3.16E+06	0.00E+00	7.27E+06
NACA	5.85E+06	0.00E+00	5.27E+06	4.48E+06	0.00E+00	3.94E+06
RBBP4	5.83E+06	0.00E+00	3.21E+06	5.46E+06	0.00E+00	3.45E+06
RPL21	5.77E+06	0.00E+00	6.62E+06	8.64E+06	0.00E+00	1.10E+07
EIF4G1	5.74E+06	0.00E+00	1.35E+06	1.77E+06	0.00E+00	0.00E+00
UCHL1	5.73E+06	0.00E+00	3.52E+06	2.91E+06	0.00E+00	1.49E+06
ALYREF	5.73E+06	0.00E+00	4.01E+06	4.77E+06	0.00E+00	7.49E+06
CAD	5.69E+06	0.00E+00	3.11E+06	3.39E+06	0.00E+00	2.95E+06
DDX1	5.68E+06	0.00E+00	4.04E+06	3.46E+06	0.00E+00	3.71E+06
PDLIM1	5.56E+06	0.00E+00	5.09E+06	4.59E+06	0.00E+00	1.38E+06
SNRPD3	5.53E+06	0.00E+00	7.30E+06	5.24E+06	0.00E+00	5.33E+06
TLN1	5.46E+06	0.00E+00	1.74E+06	0.00E+00	0.00E+00	1.26E+06
LARS	5.35E+06	0.00E+00	3.57E+06	5.54E+06	0.00E+00	4.10E+06
EIF4A3	5.31E+06	0.00E+00	6.80E+06	6.34E+06	0.00E+00	5.68E+06
RPN1	5.18E+06	0.00E+00	3.85E+06	3.30E+06	0.00E+00	1.10E+06
RPL10	5.17E+06	0.00E+00	6.42E+06	4.42E+06	0.00E+00	9.14E+06
RPA1	5.14E+06	0.00E+00	0.00E+00	0.00E+00	0.00E+00	0.00E+00
MKI67	5.12E+06	0.00E+00	5.38E+06	8.25E+06	0.00E+00	1.01E+07
DIS3	5.06E+06	0.00E+00	5.97E+06	6.15E+06	0.00E+00	5.35E+06
ASNS	5.06E+06	0.00E+00	4.09E+06	0.00E+00	0.00E+00	0.00E+00
SRRM2	5.05E+06	0.00E+00	7.13E+06	7.30E+06	0.00E+00	9.64E+06
AKR1B1	5.04E+06	0.00E+00	1.29E+06	1.29E+06	0.00E+00	0.00E+00
DYNC1H1	4.92E+06	0.00E+00	7.33E+05	0.00E+00	0.00E+00	1.41E+06
EIF4H	4.88E+06	0.00E+00	2.17E+06	2.95E+06	0.00E+00	2.32E+06
HIST2H2BE	4.82E+06	0.00E+00	0.00E+00	6.82E+06	0.00E+00	3.41E+07
RPL36	4.68E+06	0.00E+00	2.12E+06	2.91E+06	0.00E+00	6.31E+06
COPA	4.61E+06	0.00E+00	2.85E+06	4.19E+06	0.00E+00	4.28E+06
BUB3	4.54E+06	0.00E+00	4.95E+06	5.61E+06	0.00E+00	3.36E+06
UBE2M	4.50E+06	0.00E+00	2.92E+06	1.26E+06	0.00E+00	1.16E+06
RPL30	4.50E+06	0.00E+00	2.16E+06	0.00E+00	0.00E+00	0.00E+00
ETF1	4.29E+06	0.00E+00	2.20E+06	0.00E+00	0.00E+00	0.00E+00
ACP1	4.26E+06	0.00E+00	4.18E+06	2.55E+06	0.00E+00	2.32E+06
TUBA1C	4.24E+06	0.00E+00	0.00E+00	0.00E+00	0.00E+00	0.00E+00
RPL26	4.23E+06	0.00E+00	2.24E+06	2.01E+06	0.00E+00	5.89E+06
TUBB2B	4.17E+06	0.00E+00	1.48E+06	9.98E+05	0.00E+00	2.77E+06
ANXA2	4.17E+06	0.00E+00	2.63E+06	1.12E+06	0.00E+00	2.24E+06
RBM39	4.15E+06	0.00E+00	4.02E+06	4.12E+06	0.00E+00	4.36E+06
SEPT2	4.11E+06	0.00E+00	0.00E+00	0.00E+00	0.00E+00	0.00E+00
ALDH18A1	4.10E+06	0.00E+00	3.03E+06	3.75E+06	0.00E+00	3.78E+06
SF3B3	4.08E+06	0.00E+00	1.45E+06	2.58E+06	0.00E+00	2.48E+06
FHL1	4.06E+06	0.00E+00	1.07E+06	2.49E+06	0.00E+00	3.85E+06
SNRPD1	4.05E+06	0.00E+00	4.03E+06	4.38E+06	0.00E+00	5.70E+06
RPL34	4.04E+06	0.00E+00	8.96E+06	4.45E+06	0.00E+00	1.23E+07
VCL	4.03E+06	0.00E+00	3.35E+06	2.01E+06	0.00E+00	1.42E+06
SNRPD2	4.00E+06	0.00E+00	4.02E+06	3.14E+06	0.00E+00	4.63E+06
ESD	3.98E+06	0.00E+00	3.95E+06	3.36E+06	0.00E+00	0.00E+00
PDCD5	3.97E+06	0.00E+00	0.00E+00	0.00E+00	0.00E+00	0.00E+00

HSD17B4	3.97E+06	0.00E+00	2.24E+06	1.29E+06	0.00E+00	0.00E+00
NOP56	3.95E+06	0.00E+00	4.78E+06	5.58E+06	0.00E+00	6.41E+06
ARCN1	3.93E+06	0.00E+00	1.25E+06	1.54E+06	0.00E+00	0.00E+00
SRSF10	3.92E+06	0.00E+00	4.04E+06	4.92E+06	0.00E+00	5.80E+06
GART	3.90E+06	0.00E+00	0.00E+00	0.00E+00	0.00E+00	0.00E+00
FSCN1	3.89E+06	0.00E+00	0.00E+00	0.00E+00	0.00E+00	1.04E+06
HSPH1	3.87E+06	0.00E+00	1.33E+06	0.00E+00	0.00E+00	0.00E+00
TNPO1	3.86E+06	0.00E+00	2.99E+06	3.85E+06	0.00E+00	2.72E+06
LUC7L2	3.84E+06	0.00E+00	4.53E+06	2.81E+06	0.00E+00	3.78E+06
IMMT	3.83E+06	0.00E+00	2.31E+06	1.37E+06	0.00E+00	3.57E+06
ANP32A	3.81E+06	0.00E+00	1.92E+06	9.81E+05	0.00E+00	0.00E+00
MYH10	3.74E+06	0.00E+00	1.36E+06	1.57E+06	0.00E+00	2.73E+06
THRAP3	3.74E+06	0.00E+00	3.04E+06	6.10E+06	0.00E+00	6.13E+06
SUB1	3.73E+06	0.00E+00	3.57E+06	3.81E+06	0.00E+00	2.76E+06
EIF3B	3.73E+06	0.00E+00	1.20E+06	2.07E+06	0.00E+00	2.65E+06
RPLP0	3.67E+06	0.00E+00	1.41E+06	0.00E+00	0.00E+00	0.00E+00
DKC1	3.65E+06	0.00E+00	5.91E+06	1.77E+06	0.00E+00	5.38E+06
PLS3	3.60E+06	0.00E+00	0.00E+00	0.00E+00	0.00E+00	0.00E+00
FLNB	3.60E+06	0.00E+00	9.95E+05	1.39E+06	0.00E+00	8.49E+05
MCM7	3.59E+06	0.00E+00	1.14E+06	2.49E+06	0.00E+00	1.09E+06
ATAD3A	3.55E+06	0.00E+00	3.28E+06	4.06E+06	0.00E+00	3.96E+06
FABP5	3.51E+06	0.00E+00	0.00E+00	9.63E+05	0.00E+00	0.00E+00
PGD	3.49E+06	0.00E+00	0.00E+00	0.00E+00	0.00E+00	0.00E+00
LMNB2	3.49E+06	0.00E+00	4.48E+06	4.80E+06	0.00E+00	3.05E+06
H1FX	3.46E+06	0.00E+00	2.85E+06	4.98E+06	0.00E+00	7.15E+06
EBNA1BP2	3.43E+06	0.00E+00	4.00E+06	5.79E+06	0.00E+00	7.62E+06
AIFM1	3.41E+06	0.00E+00	0.00E+00	0.00E+00	0.00E+00	0.00E+00
VDAC3	3.40E+06	0.00E+00	9.95E+05	1.14E+06	0.00E+00	0.00E+00
PPP1CC	3.34E+06	0.00E+00	0.00E+00	2.55E+06	0.00E+00	0.00E+00
XPO1	3.33E+06	0.00E+00	0.00E+00	0.00E+00	0.00E+00	0.00E+00
MYL6	3.32E+06	0.00E+00	0.00E+00	0.00E+00	0.00E+00	0.00E+00
EDC4	3.30E+06	0.00E+00	0.00E+00	3.36E+06	0.00E+00	3.76E+06
CBX3	3.30E+06	0.00E+00	1.72E+06	2.68E+06	0.00E+00	4.07E+06
STRAP	3.28E+06	0.00E+00	2.46E+06	2.37E+06	0.00E+00	1.12E+06
CAND1	3.25E+06	0.00E+00	1.63E+06	0.00E+00	0.00E+00	0.00E+00
EIF3I	3.25E+06	0.00E+00	2.32E+06	2.18E+06	0.00E+00	2.11E+06
KIF5B	3.23E+06	0.00E+00	1.17E+06	1.25E+06	0.00E+00	1.07E+06
FAU	3.22E+06	0.00E+00	0.00E+00	0.00E+00	0.00E+00	0.00E+00
HACD3	3.18E+06	0.00E+00	0.00E+00	2.67E+06	0.00E+00	1.36E+06
CNN3	3.17E+06	0.00E+00	7.71E+05	0.00E+00	0.00E+00	0.00E+00
RCC2	3.13E+06	0.00E+00	1.26E+06	3.89E+06	0.00E+00	3.78E+06
TOP1	3.11E+06	0.00E+00	1.44E+06	4.79E+06	0.00E+00	2.86E+06
TOP2A	3.10E+06	0.00E+00	1.11E+06	3.87E+06	0.00E+00	4.45E+06
RTCB	3.09E+06	0.00E+00	3.89E+06	2.14E+06	0.00E+00	2.33E+06
PEBP1	3.07E+06	0.00E+00	0.00E+00	0.00E+00	0.00E+00	0.00E+00
ABCF2	3.05E+06	0.00E+00	1.05E+06	1.03E+06	0.00E+00	2.07E+06
MYBBP1A	3.04E+06	0.00E+00	2.61E+06	2.70E+06	0.00E+00	5.25E+06
LRPPRC	2.98E+06	0.00E+00	5.92E+05	9.90E+05	0.00E+00	0.00E+00
GNL3	2.95E+06	0.00E+00	0.00E+00	4.00E+06	0.00E+00	1.33E+07
TPR	2.93E+06	0.00E+00	2.46E+06	4.07E+06	0.00E+00	4.39E+06
NUP93	2.90E+06	0.00E+00	2.11E+06	2.18E+06	0.00E+00	2.76E+06
DCTN2	2.90E+06	0.00E+00	0.00E+00	0.00E+00	0.00E+00	0.00E+00
LMNA	2.88E+06	0.00E+00	1.24E+06	2.84E+06	0.00E+00	3.55E+06
CBR1	2.84E+06	0.00E+00	0.00E+00	0.00E+00	0.00E+00	0.00E+00
ARF1	2.80E+06	0.00E+00	0.00E+00	0.00E+00	0.00E+00	1.19E+06
CS	2.78E+06	0.00E+00	0.00E+00	0.00E+00	0.00E+00	0.00E+00
LTA4H	2.76E+06	0.00E+00	1.17E+06	0.00E+00	0.00E+00	0.00E+00
MCM4	2.76E+06	0.00E+00	0.00E+00	0.00E+00	0.00E+00	0.00E+00
GMPS	2.72E+06	0.00E+00	0.00E+00	1.77E+06	0.00E+00	0.00E+00
C1QBP	2.63E+06	0.00E+00	4.23E+06	0.00E+00	0.00E+00	0.00E+00
BTF3	2.57E+06	0.00E+00	0.00E+00	0.00E+00	0.00E+00	0.00E+00
EIF3G	2.55E+06	0.00E+00	1.42E+06	1.17E+06	0.00E+00	1.01E+06
RPLP2	2.53E+06	0.00E+00	0.00E+00	0.00E+00	0.00E+00	0.00E+00
UPF1	2.47E+06	0.00E+00	0.00E+00	6.48E+05	0.00E+00	0.00E+00
DNAJC7	2.45E+06	0.00E+00	2.23E+06	2.52E+06	0.00E+00	2.30E+06
DDX6	2.45E+06	0.00E+00	0.00E+00	7.37E+05	0.00E+00	8.43E+05
MCM2	2.42E+06	0.00E+00	0.00E+00	0.00E+00	0.00E+00	0.00E+00
PSMA7	2.39E+06	0.00E+00	0.00E+00	0.00E+00	0.00E+00	0.00E+00
GLO1	2.39E+06	0.00E+00	8.26E+05	0.00E+00	0.00E+00	0.00E+00
STUB1	2.32E+06	0.00E+00	0.00E+00	1.14E+06	0.00E+00	0.00E+00
NOP58	2.30E+06	0.00E+00	2.57E+06	1.41E+06	0.00E+00	5.13E+06
FXR1	2.22E+06	0.00E+00	1.31E+06	1.38E+06	0.00E+00	0.00E+00
SNRNP70	2.21E+06	0.00E+00	0.00E+00	0.00E+00	0.00E+00	0.00E+00
SMC4	2.19E+06	0.00E+00	0.00E+00	1.05E+06	0.00E+00	2.06E+06
STAU1	2.15E+06	0.00E+00	9.74E+05	0.00E+00	0.00E+00	2.42E+06
COPB2	2.12E+06	0.00E+00	0.00E+00	0.00E+00	0.00E+00	0.00E+00
MCM6	2.11E+06	0.00E+00	3.48E+06	1.24E+06	0.00E+00	0.00E+00
SMC2	2.10E+06	0.00E+00	1.49E+06	1.40E+06	0.00E+00	2.32E+06
PRMT1	2.09E+06	0.00E+00	0.00E+00	0.00E+00	0.00E+00	0.00E+00
EIF4B	2.07E+06	0.00E+00	2.10E+06	1.10E+06	0.00E+00	3.85E+06
RNH1	2.04E+06	0.00E+00	2.82E+06	1.97E+06	0.00E+00	1.89E+06
NUDC	2.02E+06	0.00E+00	0.00E+00	0.00E+00	0.00E+00	0.00E+00
RPL31	2.02E+06	0.00E+00	0.00E+00	0.00E+00	0.00E+00	1.89E+06
PCCA	2.00E+06	5.06E+06	1.47E+06	7.10E+05	0.00E+00	8.93E+05
PSMA5	2.00E+06	0.00E+00	0.00E+00	0.00E+00	0.00E+00	0.00E+00
SUGT1	1.98E+06	0.00E+00	0.00E+00	0.00E+00	0.00E+00	0.00E+00
ADSL	1.96E+06	0.00E+00	0.00E+00	0.00E+00	0.00E+00	0.00E+00
YWHAG	1.96E+06	0.00E+00	0.00E+00	0.00E+00	0.00E+00	0.00E+00
DHX15	1.95E+06	0.00E+00	7.88E+05	0.00E+00	0.00E+00	6.45E+05
VARS	1.95E+06	0.00E+00	0.00E+00	1.18E+06	0.00E+00	1.28E+06
RPL22	1.90E+06	0.00E+00	4.49E+06	3.20E+06	0.00E+00	3.04E+06
PARK7	1.90E+06	0.00E+00	0.00E+00	0.00E+00	0.00E+00	0.00E+00
AIMP1	1.89E+06	0.00E+00	0.00E+00	0.00E+00	0.00E+00	0.00E+00
GSPT1	1.88E+06	0.00E+00	0.00E+00	0.00E+00	0.00E+00	0.00E+00
SMC1A	1.87E+06	0.00E+00	1.01E+06	9.73E+05	0.00E+00	1.50E+06
CENPV	1.86E+06	0.00E+00	3.29E+06	1.44E+06	0.00E+00	5.66E+06
PSMA4	1.86E+06	0.00E+00	6.73E+05	0.00E+00	0.00E+00	0.00E+00
HMGB3	1.86E+06	0.00E+00	0.00E+00	0.00E+00	0.00E+00	0.00E+00
CHORDC1	1.80E+06	0.00E+00	0.00E+00	0.00E+00	0.00E+00	0.00E+00
EIF5B	1.80E+06	0.00E+00	0.00E+00	1.06E+06	0.00E+00	0.00E+00
PDCD6IP	1.80E+06	0.00E+00	0.00E+00	0.00E+00	0.00E+00	0.00E+00
MRI1	1.79E+06	0.00E+00	0.00E+00	0.00E+00	0.00E+00	0.00E+00

DDX18	1.79E+06	0.00E+00	0.00E+00	2.22E+06	0.00E+00	2.99E+06
EFTUD2	1.79E+06	0.00E+00	1.96E+06	0.00E+00	0.00E+00	1.24E+06
MAP4	1.76E+06	0.00E+00	9.68E+05	1.78E+06	0.00E+00	9.92E+05
PABPC4	1.75E+06	0.00E+00	0.00E+00	0.00E+00	0.00E+00	0.00E+00
PABPN1	1.73E+06	0.00E+00	0.00E+00	0.00E+00	0.00E+00	0.00E+00
ZC3HAV1	1.72E+06	0.00E+00	2.19E+06	2.10E+06	0.00E+00	2.21E+06
PRDX5	1.71E+06	0.00E+00	0.00E+00	0.00E+00	0.00E+00	0.00E+00
DENR	1.71E+06	0.00E+00	0.00E+00	0.00E+00	0.00E+00	0.00E+00
GCN1L1	1.67E+06	0.00E+00	0.00E+00	7.48E+05	0.00E+00	2.48E+06
DARS	1.65E+06	0.00E+00	1.94E+06	8.50E+05	0.00E+00	2.53E+06
CACYBP	1.65E+06	0.00E+00	0.00E+00	0.00E+00	0.00E+00	9.21E+05
GLRX3	1.65E+06	0.00E+00	0.00E+00	0.00E+00	0.00E+00	0.00E+00
PCNA	1.64E+06	0.00E+00	0.00E+00	0.00E+00	0.00E+00	0.00E+00
MAT2A	1.61E+06	0.00E+00	0.00E+00	0.00E+00	0.00E+00	0.00E+00
RSL1D1	1.59E+06	0.00E+00	4.18E+06	2.65E+06	0.00E+00	7.07E+06
MCCC1	1.59E+06	4.84E+06	0.00E+00	0.00E+00	1.53E+06	2.46E+06
TARDBP	1.54E+06	0.00E+00	1.73E+06	0.00E+00	0.00E+00	0.00E+00
MDH1	1.52E+06	0.00E+00	0.00E+00	0.00E+00	0.00E+00	0.00E+00
SAFB	1.45E+06	0.00E+00	0.00E+00	0.00E+00	0.00E+00	0.00E+00
LSM12	1.43E+06	0.00E+00	9.50E+05	9.16E+05	0.00E+00	0.00E+00
EEF1E1	1.42E+06	0.00E+00	0.00E+00	0.00E+00	0.00E+00	0.00E+00
QARS	1.41E+06	0.00E+00	0.00E+00	0.00E+00	0.00E+00	0.00E+00
GTF2I	1.39E+06	0.00E+00	1.23E+06	1.50E+06	0.00E+00	0.00E+00
EIF2S2	1.38E+06	0.00E+00	0.00E+00	0.00E+00	0.00E+00	0.00E+00
FEN1	1.37E+06	0.00E+00	0.00E+00	0.00E+00	0.00E+00	0.00E+00
EIF1	1.35E+06	0.00E+00	0.00E+00	0.00E+00	0.00E+00	0.00E+00
DFFA	1.34E+06	0.00E+00	0.00E+00	0.00E+00	0.00E+00	0.00E+00
HSPA5	1.33E+06	0.00E+00	0.00E+00	0.00E+00	0.00E+00	0.00E+00
PRPF8	1.27E+06	0.00E+00	7.22E+05	7.71E+05	0.00E+00	0.00E+00
SNRPE	1.26E+06	0.00E+00	0.00E+00	0.00E+00	0.00E+00	0.00E+00
PC	1.25E+06	1.93E+06	5.05E+05	8.07E+05	1.77E+06	2.26E+06
ABCF1	1.25E+06	0.00E+00	0.00E+00	0.00E+00	0.00E+00	0.00E+00
RPL35A	1.24E+06	0.00E+00	6.51E+06	1.69E+06	0.00E+00	5.17E+06
SNRPA1	1.22E+06	0.00E+00	1.55E+06	8.13E+05	0.00E+00	1.11E+06
IPO7	1.21E+06	0.00E+00	7.58E+05	0.00E+00	0.00E+00	1.15E+06
AARS	1.20E+06	0.00E+00	0.00E+00	0.00E+00	0.00E+00	0.00E+00
PSMG1	1.20E+06	0.00E+00	0.00E+00	0.00E+00	0.00E+00	0.00E+00
CORO1C	1.18E+06	0.00E+00	0.00E+00	0.00E+00	0.00E+00	0.00E+00
RPS19	1.18E+06	0.00E+00	9.97E+05	1.57E+06	0.00E+00	0.00E+00
ETFA	1.18E+06	0.00E+00	0.00E+00	0.00E+00	0.00E+00	0.00E+00
PYGL	1.15E+06	0.00E+00	0.00E+00	0.00E+00	0.00E+00	0.00E+00
HSPB1	1.15E+06	0.00E+00	0.00E+00	1.14E+06	0.00E+00	0.00E+00
ADSS	1.15E+06	0.00E+00	0.00E+00	0.00E+00	0.00E+00	0.00E+00
YTHDF2	1.14E+06	0.00E+00	9.53E+05	0.00E+00	0.00E+00	1.18E+06
FTSJ3	1.14E+06	0.00E+00	0.00E+00	2.58E+06	0.00E+00	2.71E+06
YWHAB	1.11E+06	0.00E+00	3.98E+05	0.00E+00	0.00E+00	0.00E+00
ATP5B	1.11E+06	0.00E+00	0.00E+00	0.00E+00	0.00E+00	0.00E+00
SLC25A3	1.10E+06	0.00E+00	0.00E+00	0.00E+00	0.00E+00	0.00E+00
RRS1	1.09E+06	0.00E+00	0.00E+00	1.50E+06	0.00E+00	5.03E+06
WDR1	1.09E+06	0.00E+00	0.00E+00	0.00E+00	0.00E+00	0.00E+00
ACAT1	1.09E+06	0.00E+00	0.00E+00	0.00E+00	0.00E+00	0.00E+00
IRS4	1.07E+06	0.00E+00	0.00E+00	0.00E+00	0.00E+00	0.00E+00
AGL	1.05E+06	0.00E+00	0.00E+00	0.00E+00	0.00E+00	0.00E+00
BOLA2	1.05E+06	0.00E+00	7.50E+05	0.00E+00	0.00E+00	0.00E+00
ACTN4	1.04E+06	0.00E+00	0.00E+00	0.00E+00	0.00E+00	0.00E+00
TXNDC17	1.03E+06	0.00E+00	0.00E+00	0.00E+00	0.00E+00	0.00E+00
RPS21	1.02E+06	0.00E+00	1.09E+06	0.00E+00	0.00E+00	0.00E+00
CPNE3	9.96E+05	0.00E+00	0.00E+00	8.79E+05	0.00E+00	0.00E+00
EIF4G2	9.91E+05	0.00E+00	0.00E+00	0.00E+00	0.00E+00	0.00E+00
SHMT2	9.78E+05	0.00E+00	0.00E+00	0.00E+00	0.00E+00	0.00E+00
EIF3L	9.59E+05	0.00E+00	0.00E+00	0.00E+00	0.00E+00	0.00E+00
NOLC1	9.49E+05	0.00E+00	4.26E+06	4.95E+06	0.00E+00	3.04E+06
PPM1G	9.47E+05	0.00E+00	0.00E+00	0.00E+00	0.00E+00	0.00E+00
EIF3E	9.45E+05	0.00E+00	9.09E+05	7.92E+05	0.00E+00	0.00E+00
ATP2A2	9.21E+05	0.00E+00	7.29E+05	0.00E+00	0.00E+00	0.00E+00
GTPBP1	9.18E+05	0.00E+00	0.00E+00	0.00E+00	0.00E+00	0.00E+00
C14orf166	9.04E+05	0.00E+00	0.00E+00	0.00E+00	0.00E+00	0.00E+00
PSMD3	8.81E+05	0.00E+00	4.10E+05	0.00E+00	0.00E+00	0.00E+00
CPSF6	8.78E+05	0.00E+00	3.91E+05	0.00E+00	0.00E+00	0.00E+00
PCMT1	8.77E+05	0.00E+00	0.00E+00	0.00E+00	0.00E+00	0.00E+00
HSP90AB4P	8.72E+05	0.00E+00	0.00E+00	0.00E+00	0.00E+00	0.00E+00
DRG1	8.58E+05	0.00E+00	0.00E+00	0.00E+00	0.00E+00	0.00E+00
TXLNA	8.51E+05	0.00E+00	0.00E+00	8.48E+05	0.00E+00	0.00E+00
PSMC5	8.51E+05	0.00E+00	0.00E+00	0.00E+00	0.00E+00	0.00E+00
RRP1B	8.41E+05	0.00E+00	0.00E+00	0.00E+00	0.00E+00	2.74E+06
STMN1	8.39E+05	0.00E+00	0.00E+00	0.00E+00	0.00E+00	0.00E+00
TAGLN2	8.06E+05	0.00E+00	0.00E+00	0.00E+00	0.00E+00	0.00E+00
SSBP1	8.02E+05	0.00E+00	0.00E+00	0.00E+00	0.00E+00	0.00E+00
SF1	7.94E+05	0.00E+00	0.00E+00	0.00E+00	0.00E+00	0.00E+00
MPST	7.91E+05	0.00E+00	0.00E+00	0.00E+00	0.00E+00	0.00E+00
RBM25	7.83E+05	0.00E+00	0.00E+00	0.00E+00	0.00E+00	3.99E+05
CKAP5	7.80E+05	0.00E+00	0.00E+00	0.00E+00	0.00E+00	0.00E+00
SRP68	7.77E+05	0.00E+00	0.00E+00	0.00E+00	0.00E+00	0.00E+00
RDH11	7.76E+05	0.00E+00	0.00E+00	0.00E+00	0.00E+00	0.00E+00
CAP1	7.74E+05	0.00E+00	6.04E+05	0.00E+00	0.00E+00	0.00E+00
DAZAP1	7.73E+05	0.00E+00	0.00E+00	0.00E+00	0.00E+00	0.00E+00
TRIM25	7.70E+05	0.00E+00	0.00E+00	0.00E+00	0.00E+00	0.00E+00
SRRT	7.68E+05	0.00E+00	0.00E+00	0.00E+00	0.00E+00	0.00E+00
API5	7.59E+05	0.00E+00	0.00E+00	0.00E+00	0.00E+00	0.00E+00
HSPE1	7.32E+05	0.00E+00	0.00E+00	0.00E+00	0.00E+00	0.00E+00
NIFK	7.27E+05	0.00E+00	7.81E+05	1.93E+06	0.00E+00	4.47E+06
HADHA	7.26E+05	0.00E+00	0.00E+00	0.00E+00	0.00E+00	0.00E+00
CSTF2	7.25E+05	0.00E+00	0.00E+00	0.00E+00	0.00E+00	0.00E+00
LRRC47	7.24E+05	0.00E+00	0.00E+00	0.00E+00	0.00E+00	0.00E+00
DDX46	7.21E+05	0.00E+00	6.25E+05	7.04E+05	0.00E+00	1.29E+06
RAB8A	7.12E+05	0.00E+00	0.00E+00	0.00E+00	0.00E+00	0.00E+00
SEPT7	7.11E+05	0.00E+00	0.00E+00	0.00E+00	0.00E+00	0.00E+00
EIF2S1	6.90E+05	0.00E+00	0.00E+00	0.00E+00	0.00E+00	0.00E+00
NSUN2	6.75E+05	0.00E+00	0.00E+00	0.00E+00	0.00E+00	0.00E+00
PSMD11	6.68E+05	0.00E+00	0.00E+00	0.00E+00	0.00E+00	0.00E+00
DSP	6.65E+05	0.00E+00	0.00E+00	0.00E+00	0.00E+00	3.58E+06
CAPRIN1	6.61E+05	0.00E+00	0.00E+00	0.00E+00	0.00E+00	0.00E+00

TMPO	6.59E+05	0.00E+00	0.00E+00	0.00E+00	0.00E+00	0.00E+00
AK2	6.49E+05	0.00E+00	0.00E+00	0.00E+00	0.00E+00	0.00E+00
LUC7L3	6.48E+05	0.00E+00	0.00E+00	0.00E+00	0.00E+00	6.77E+05
PSMC6	6.38E+05	0.00E+00	0.00E+00	0.00E+00	0.00E+00	0.00E+00
PSPC1	6.26E+05	0.00E+00	8.53E+05	0.00E+00	0.00E+00	0.00E+00
PSMD1	6.21E+05	0.00E+00	0.00E+00	0.00E+00	0.00E+00	0.00E+00
ANP32E	6.11E+05	0.00E+00	0.00E+00	0.00E+00	0.00E+00	0.00E+00
CHCHD3	6.07E+05	0.00E+00	0.00E+00	0.00E+00	0.00E+00	0.00E+00
PUF60	6.07E+05	0.00E+00	0.00E+00	0.00E+00	0.00E+00	0.00E+00
EIF3H	5.97E+05	0.00E+00	0.00E+00	0.00E+00	0.00E+00	0.00E+00
XRN2	5.93E+05	0.00E+00	0.00E+00	0.00E+00	0.00E+00	3.28E+05
ACACA	5.90E+05	2.48E+06	1.11E+06	1.10E+06	5.99E+06	2.49E+06
EXOSC4	5.81E+05	0.00E+00	0.00E+00	0.00E+00	0.00E+00	0.00E+00
RAB7A	5.73E+05	0.00E+00	0.00E+00	0.00E+00	0.00E+00	0.00E+00
NUDT21	5.65E+05	0.00E+00	0.00E+00	0.00E+00	0.00E+00	0.00E+00
DNAJB1	5.62E+05	0.00E+00	0.00E+00	0.00E+00	0.00E+00	0.00E+00
ACO2	5.60E+05	0.00E+00	0.00E+00	0.00E+00	0.00E+00	0.00E+00
DYNC1LI1	5.55E+05	0.00E+00	0.00E+00	0.00E+00	0.00E+00	0.00E+00
SF3B1	5.54E+05	0.00E+00	0.00E+00	0.00E+00	0.00E+00	0.00E+00
CKMT1B	5.48E+05	0.00E+00	0.00E+00	0.00E+00	0.00E+00	0.00E+00
NDUFS3	5.28E+05	0.00E+00	0.00E+00	0.00E+00	0.00E+00	0.00E+00
COPB1	5.04E+05	0.00E+00	0.00E+00	0.00E+00	0.00E+00	0.00E+00
TBL3	4.96E+05	0.00E+00	0.00E+00	0.00E+00	0.00E+00	1.07E+06
NAA15	4.95E+05	0.00E+00	0.00E+00	0.00E+00	0.00E+00	0.00E+00
RANBP2	4.87E+05	0.00E+00	0.00E+00	0.00E+00	0.00E+00	1.68E+06
ZNF326	4.85E+05	0.00E+00	0.00E+00	0.00E+00	0.00E+00	0.00E+00
DNAJC9	4.81E+05	0.00E+00	0.00E+00	0.00E+00	0.00E+00	0.00E+00
ATP5C1	4.73E+05	0.00E+00	0.00E+00	0.00E+00	0.00E+00	5.75E+05
PYCR1	4.67E+05	0.00E+00	0.00E+00	0.00E+00	0.00E+00	0.00E+00
CSTB	4.61E+05	0.00E+00	0.00E+00	0.00E+00	0.00E+00	0.00E+00
CCDC124	4.58E+05	0.00E+00	0.00E+00	0.00E+00	0.00E+00	0.00E+00
PFDN2	4.54E+05	0.00E+00	0.00E+00	0.00E+00	0.00E+00	0.00E+00
NCAPG	4.50E+05	0.00E+00	0.00E+00	0.00E+00	0.00E+00	0.00E+00
NUP205	4.49E+05	0.00E+00	0.00E+00	0.00E+00	0.00E+00	0.00E+00
PRDX4	4.32E+05	0.00E+00	0.00E+00	0.00E+00	0.00E+00	0.00E+00
PRPF4	4.24E+05	0.00E+00	0.00E+00	0.00E+00	0.00E+00	0.00E+00
SRP54	4.23E+05	0.00E+00	3.16E+05	0.00E+00	0.00E+00	0.00E+00
EDF1	4.23E+05	0.00E+00	0.00E+00	0.00E+00	0.00E+00	0.00E+00
SRM	4.19E+05	0.00E+00	0.00E+00	0.00E+00	0.00E+00	0.00E+00
TARS	3.90E+05	0.00E+00	0.00E+00	0.00E+00	0.00E+00	0.00E+00
SPTAN1	3.88E+05	0.00E+00	0.00E+00	0.00E+00	0.00E+00	4.30E+05
CPSF7	3.85E+05	0.00E+00	0.00E+00	4.28E+05	0.00E+00	2.81E+05
CKAP4	3.85E+05	0.00E+00	0.00E+00	0.00E+00	0.00E+00	0.00E+00
CDKN2A	3.78E+05	0.00E+00	0.00E+00	0.00E+00	0.00E+00	0.00E+00
DCTN1	3.76E+05	0.00E+00	0.00E+00	0.00E+00	0.00E+00	6.25E+05
IPO4	3.57E+05	0.00E+00	0.00E+00	0.00E+00	0.00E+00	0.00E+00
CLUH	3.55E+05	0.00E+00	0.00E+00	0.00E+00	0.00E+00	0.00E+00
EIF3F	3.54E+05	0.00E+00	0.00E+00	0.00E+00	0.00E+00	0.00E+00
NUDT5	3.52E+05	0.00E+00	0.00E+00	0.00E+00	0.00E+00	0.00E+00
PRRC2C	3.50E+05	0.00E+00	0.00E+00	0.00E+00	0.00E+00	0.00E+00
SDHA	3.35E+05	0.00E+00	0.00E+00	0.00E+00	0.00E+00	0.00E+00
NSF	3.29E+05	0.00E+00	0.00E+00	0.00E+00	0.00E+00	0.00E+00
RPRD1A	3.18E+05	0.00E+00	0.00E+00	0.00E+00	0.00E+00	0.00E+00
ARPC1B	3.17E+05	0.00E+00	0.00E+00	0.00E+00	0.00E+00	0.00E+00
PSMA3	3.17E+05	0.00E+00	0.00E+00	0.00E+00	0.00E+00	0.00E+00
PRMT5	3.05E+05	0.00E+00	0.00E+00	0.00E+00	0.00E+00	0.00E+00
PSMC1	3.04E+05	0.00E+00	0.00E+00	0.00E+00	0.00E+00	0.00E+00
HSPA4L	2.85E+05	0.00E+00	0.00E+00	0.00E+00	0.00E+00	0.00E+00
TIAL1	2.83E+05	0.00E+00	0.00E+00	0.00E+00	0.00E+00	0.00E+00
TBCB	2.76E+05	0.00E+00	0.00E+00	0.00E+00	0.00E+00	0.00E+00
TRIP13	2.74E+05	0.00E+00	0.00E+00	0.00E+00	0.00E+00	0.00E+00
MTA2	2.58E+05	0.00E+00	0.00E+00	0.00E+00	0.00E+00	0.00E+00
PGRMC1	2.46E+05	0.00E+00	0.00E+00	0.00E+00	0.00E+00	0.00E+00
TBCE	2.44E+05	0.00E+00	0.00E+00	0.00E+00	0.00E+00	0.00E+00
AAMP	2.37E+05	0.00E+00	0.00E+00	0.00E+00	0.00E+00	0.00E+00
SF3A3	2.37E+05	0.00E+00	0.00E+00	0.00E+00	0.00E+00	0.00E+00
BAZ1B	2.28E+05	0.00E+00	0.00E+00	0.00E+00	0.00E+00	0.00E+00
ZYX	2.25E+05	0.00E+00	0.00E+00	0.00E+00	0.00E+00	0.00E+00
CNOT1	2.23E+05	0.00E+00	0.00E+00	0.00E+00	0.00E+00	0.00E+00
HELLS	2.14E+05	0.00E+00	0.00E+00	0.00E+00	0.00E+00	0.00E+00
SRSF9	2.14E+05	0.00E+00	0.00E+00	0.00E+00	0.00E+00	7.25E+05
PSMC2	2.08E+05	0.00E+00	0.00E+00	0.00E+00	0.00E+00	0.00E+00
MTHFD2	2.07E+05	0.00E+00	0.00E+00	0.00E+00	0.00E+00	0.00E+00
PPP1CA	2.07E+05	0.00E+00	0.00E+00	0.00E+00	0.00E+00	0.00E+00
DDX19A	2.06E+05	0.00E+00	0.00E+00	0.00E+00	0.00E+00	0.00E+00
SEC61A1	1.98E+05	0.00E+00	0.00E+00	0.00E+00	0.00E+00	0.00E+00
ATP1A3	1.96E+05	0.00E+00	0.00E+00	0.00E+00	0.00E+00	0.00E+00
SARNP	1.94E+05	0.00E+00	0.00E+00	0.00E+00	0.00E+00	0.00E+00
DSG2	1.93E+05	0.00E+00	0.00E+00	0.00E+00	0.00E+00	0.00E+00
DNMT1	1.87E+05	0.00E+00	0.00E+00	0.00E+00	0.00E+00	0.00E+00
NUP155	1.65E+05	0.00E+00	0.00E+00	0.00E+00	0.00E+00	0.00E+00
CTPS1	1.64E+05	0.00E+00	0.00E+00	0.00E+00	0.00E+00	0.00E+00
GEMIN5	1.58E+05	0.00E+00	0.00E+00	0.00E+00	0.00E+00	0.00E+00
CTBP2	1.51E+05	0.00E+00	0.00E+00	0.00E+00	0.00E+00	0.00E+00
RRP15	1.47E+05	0.00E+00	0.00E+00	0.00E+00	0.00E+00	0.00E+00
DDX23	1.32E+05	0.00E+00	0.00E+00	0.00E+00	0.00E+00	0.00E+00
CA2	1.13E+05	0.00E+00	0.00E+00	0.00E+00	0.00E+00	0.00E+00
DHX30	1.09E+05	0.00E+00	0.00E+00	0.00E+00	0.00E+00	0.00E+00
FKBP3	1.06E+05	0.00E+00	0.00E+00	0.00E+00	0.00E+00	0.00E+00
ADAR	0.00E+00	0.00E+00	1.34E+06	0.00E+00	0.00E+00	0.00E+00
ANKHD1	0.00E+00	0.00E+00	2.14E+05	0.00E+00	0.00E+00	0.00E+00
BCLAF1	0.00E+00	0.00E+00	8.31E+05	1.77E+06	0.00E+00	9.05E+05
BOP1	0.00E+00	0.00E+00	0.00E+00	0.00E+00	0.00E+00	1.34E+06
BRIX1	0.00E+00	0.00E+00	0.00E+00	0.00E+00	0.00E+00	2.49E+06
CDC37	0.00E+00	0.00E+00	1.58E+06	0.00E+00	0.00E+00	0.00E+00
CDC5L	0.00E+00	0.00E+00	0.00E+00	0.00E+00	0.00E+00	9.61E+05
CDC73	0.00E+00	0.00E+00	1.32E+05	0.00E+00	0.00E+00	0.00E+00
COPZ1	0.00E+00	0.00E+00	7.14E+05	0.00E+00	0.00E+00	0.00E+00
DDX27	0.00E+00	0.00E+00	7.58E+05	8.11E+05	0.00E+00	2.06E+06
DDX47	0.00E+00	0.00E+00	8.72E+05	0.00E+00	0.00E+00	1.69E+06
DDX50	0.00E+00	0.00E+00	0.00E+00	0.00E+00	0.00E+00	3.82E+05
DDX54	0.00E+00	0.00E+00	0.00E+00	1.02E+06	0.00E+00	1.11E+06

DEK	0.00E+00	0.00E+00	7.64E+05	0.00E+00	0.00E+00	0.00E+00
DNTTIP2	0.00E+00	0.00E+00	0.00E+00	0.00E+00	0.00E+00	2.95E+05
DSC1	0.00E+00	6.85E+05	0.00E+00	0.00E+00	0.00E+00	0.00E+00
DSG1	0.00E+00	0.00E+00	0.00E+00	0.00E+00	0.00E+00	1.59E+06
EIF2A	0.00E+00	0.00E+00	1.42E+05	0.00E+00	0.00E+00	0.00E+00
EXOSC10	0.00E+00	0.00E+00	0.00E+00	3.44E+05	0.00E+00	0.00E+00
EZR	0.00E+00	0.00E+00	2.95E+05	0.00E+00	0.00E+00	0.00E+00
FDPS	0.00E+00	0.00E+00	0.00E+00	0.00E+00	0.00E+00	0.00E+00
FUBP3	0.00E+00	0.00E+00	0.00E+00	0.00E+00	0.00E+00	6.19E+05
GNB2	0.00E+00	0.00E+00	0.00E+00	0.00E+00	0.00E+00	3.23E+05
GPATCH4	0.00E+00	0.00E+00	0.00E+00	0.00E+00	0.00E+00	3.85E+05
GRWD1	0.00E+00	0.00E+00	5.57E+05	0.00E+00	0.00E+00	0.00E+00
GTPBP4	0.00E+00	0.00E+00	2.25E+06	2.30E+06	0.00E+00	1.00E+07
H2AFV	0.00E+00	0.00E+00	0.00E+00	0.00E+00	0.00E+00	9.83E+06
H2AFY2	0.00E+00	0.00E+00	1.19E+06	1.16E+06	0.00E+00	4.24E+06
HEATR1	0.00E+00	0.00E+00	0.00E+00	0.00E+00	0.00E+00	0.00E+00
HMGB2	0.00E+00	0.00E+00	6.89E+05	0.00E+00	0.00E+00	0.00E+00
HNRNPH2	0.00E+00	0.00E+00	0.00E+00	0.00E+00	0.00E+00	0.00E+00
HP1BP3	0.00E+00	0.00E+00	0.00E+00	0.00E+00	0.00E+00	7.27E+05
LBR	0.00E+00	0.00E+00	0.00E+00	0.00E+00	0.00E+00	1.54E+06
MDC1	0.00E+00	0.00E+00	0.00E+00	0.00E+00	0.00E+00	5.29E+05
MSH6	0.00E+00	0.00E+00	0.00E+00	4.30E+05	0.00E+00	0.00E+00
NARS	0.00E+00	0.00E+00	5.13E+05	0.00E+00	0.00E+00	3.72E+05
NASP	0.00E+00	0.00E+00	2.04E+05	0.00E+00	0.00E+00	0.00E+00
NEK9	0.00E+00	0.00E+00	0.00E+00	0.00E+00	0.00E+00	3.67E+05
NHP2L1	0.00E+00	0.00E+00	2.68E+05	0.00E+00	0.00E+00	0.00E+00
NKRF	0.00E+00	0.00E+00	0.00E+00	0.00E+00	0.00E+00	1.05E+06
NSA2	0.00E+00	0.00E+00	0.00E+00	9.19E+05	0.00E+00	1.58E+06
NUMA1	0.00E+00	0.00E+00	2.82E+05	0.00E+00	0.00E+00	0.00E+00
PDCD11	0.00E+00	0.00E+00	0.00E+00	0.00E+00	0.00E+00	1.06E+06
PES1	0.00E+00	0.00E+00	0.00E+00	5.06E+05	0.00E+00	0.00E+00
PHIP	0.00E+00	0.00E+00	0.00E+00	0.00E+00	0.00E+00	1.81E+05
PNN	0.00E+00	0.00E+00	0.00E+00	1.03E+06	0.00E+00	1.20E+06
PPAN	0.00E+00	0.00E+00	0.00E+00	0.00E+00	0.00E+00	4.68E+05
PRDX3	0.00E+00	0.00E+00	1.52E+06	1.09E+06	0.00E+00	0.00E+00
PRPF4B	0.00E+00	0.00E+00	0.00E+00	0.00E+00	0.00E+00	1.68E+05
PSMC3	0.00E+00	0.00E+00	3.20E+05	0.00E+00	0.00E+00	0.00E+00
RBM28	0.00E+00	0.00E+00	0.00E+00	1.39E+06	0.00E+00	4.87E+06
RBM34	0.00E+00	0.00E+00	0.00E+00	0.00E+00	0.00E+00	4.03E+05
RBM4	0.00E+00	0.00E+00	3.77E+05	0.00E+00	0.00E+00	9.19E+05
RNF40	0.00E+00	0.00E+00	0.00E+00	0.00E+00	0.00E+00	4.18E+05
RPF2	0.00E+00	0.00E+00	9.88E+05	0.00E+00	0.00E+00	3.14E+06
RRM1	0.00E+00	0.00E+00	2.15E+05	0.00E+00	0.00E+00	0.00E+00
RRP1	0.00E+00	0.00E+00	1.09E+06	0.00E+00	0.00E+00	1.12E+06
RRP12	0.00E+00	0.00E+00	0.00E+00	6.42E+05	0.00E+00	0.00E+00
SAR1A	0.00E+00	0.00E+00	2.46E+05	0.00E+00	0.00E+00	0.00E+00
SART1	0.00E+00	0.00E+00	0.00E+00	0.00E+00	0.00E+00	2.43E+05
SF3A1	0.00E+00	0.00E+00	0.00E+00	3.88E+05	0.00E+00	0.00E+00
SF3B2	0.00E+00	0.00E+00	0.00E+00	5.66E+05	0.00E+00	0.00E+00
SMARCA5	0.00E+00	0.00E+00	0.00E+00	0.00E+00	0.00E+00	1.59E+06
SMC3	0.00E+00	0.00E+00	1.29E+06	1.98E+06	0.00E+00	1.97E+06
SMU1	0.00E+00	0.00E+00	1.42E+06	7.78E+05	0.00E+00	7.20E+05
SNRPN	0.00E+00	0.00E+00	1.77E+06	0.00E+00	0.00E+00	0.00E+00
SNW1	0.00E+00	0.00E+00	0.00E+00	2.86E+06	0.00E+00	2.07E+06
SRI	0.00E+00	0.00E+00	3.55E+05	0.00E+00	0.00E+00	0.00E+00
SRRM1	0.00E+00	0.00E+00	0.00E+00	0.00E+00	0.00E+00	2.97E+06
SRSF5	0.00E+00	0.00E+00	0.00E+00	0.00E+00	0.00E+00	1.12E+06
TRA2B	0.00E+00	0.00E+00	0.00E+00	0.00E+00	0.00E+00	1.67E+06
TRAP1	0.00E+00	0.00E+00	1.10E+06	0.00E+00	0.00E+00	0.00E+00
UBAP2L	0.00E+00	0.00E+00	2.00E+06	0.00E+00	0.00E+00	0.00E+00
USP10	0.00E+00	0.00E+00	0.00E+00	0.00E+00	0.00E+00	0.00E+00
UTP18	0.00E+00	0.00E+00	0.00E+00	5.01E+05	0.00E+00	0.00E+00
VPS35	0.00E+00	0.00E+00	0.00E+00	2.47E+05	0.00E+00	0.00E+00
WDR3	0.00E+00	0.00E+00	5.43E+05	0.00E+00	0.00E+00	0.00E+00
WDR36	0.00E+00	0.00E+00	0.00E+00	0.00E+00	0.00E+00	6.09E+05
YWHAQ	0.00E+00	0.00E+00	5.48E+05	0.00E+00	0.00E+00	0.00E+00
ZNF207	0.00E+00	0.00E+00	2.08E+05	0.00E+00	0.00E+00	0.00E+00

Table S3 Significantly enriched proteins from HEK293T cells in TCO nonHS compared to EV nonHS (p<0.05).

Gene names	−Log(P-value)	Difference	mean (LFQ int.) TCO nonHS	mean (LFQ int.) EV nonHS
TALE	6.1571	9.4744	30.6485	21.1742
XRCC5	3.6498	2.5623	23.4550	20.8927

Table S4 Significantly enriched proteins from HEK293T cells in TCO HS compared to EV HS (p<0.05).

Gene names	−Log(P-value)	Difference	mean (LFQ int.) TCO HS	mean (LFQ int.) EV HS
TALE	5.0052	8.4538	21.0326	29.4865
SRP72	3.3417	4.8058	20.6907	25.4965
CALM2	2.6634	2.4571	21.0134	23.4705
RPS17	2.0845	2.3806	21.1014	23.4819
ATIC	4.2048	2.3103	21.0834	23.3936
DNAJA2	3.2065	2.2473	20.6434	22.8908
RPS7	0.8251	2.1810	22.1661	24.3472
ILF2	0.8395	2.1467	21.1862	23.3328
RARS	1.0245	1.8326	21.0198	22.8524
RPS10	1.1821	1.7838	21.8644	23.6482
RPA1	2.0200	1.7770	20.4499	22.2269
PPP2R1A	3.1962	1.7637	20.8179	22.5816
FARSB	2.2285	1.6709	20.9333	22.6042
PTGES3	1.3638	1.5771	21.0928	22.6699
FKBP4	1.0679	1.5460	21.4970	23.0430
TLN1	1.1160	1.5051	20.6820	22.1871
UBA1	2.0283	1.4980	23.1555	24.6535
FSCN1	1.4742	1.2932	20.5964	21.8896
SEPT2	1.3737	1.2673	20.6868	21.9541
HACD3	1.8670	1.2416	20.3372	21.5787
PLS3	2.5475	1.1974	20.5674	21.7648
DCTN2	2.3973	1.0840	20.3750	21.4589

Table S5 Significantly enriched proteins from HEK293T cells in TCO HS compared to TCO nonHS (p<0.05).

Gene names	−Log(P-value)	Difference	mean (LFQ int.) TCO nonHS	mean (LFQ int.) TCO HS
SRP72	3.6090	-4.8272	20.6693	25.4965
CCT5	1.9813	-3.1499	20.2910	23.4409
UBA1	2.2693	-3.1099	21.5436	24.6535
FKBP4	2.3629	-2.8799	20.1631	23.0430
SUMO2	1.9880	-2.7137	20.9221	23.6358
RPL9	0.8796	-2.4921	21.4689	23.9610
ATIC	5.0387	-2.4331	20.9606	23.3936
PHB	1.1324	-2.2594	21.4375	23.6970
RPS12	2.5494	-2.0521	20.9159	22.9680
ETF1	4.1041	-1.9991	20.0298	22.0289
ILF2	1.1621	-1.9937	21.3391	23.3328
GDI2	2.7678	-1.9454	20.8205	22.7659
SSB	1.6407	-1.9238	20.9271	22.8508
RPS17	0.7358	-1.8922	21.5897	23.4819
PTGES3	2.9872	-1.8901	20.7798	22.6699
PPP2R1A	1.7731	-1.7619	20.8197	22.5816
G3BP1	1.2740	-1.6843	21.8200	23.5044
RPS10	0.7365	-1.6702	21.9780	23.6482
FARSB	1.8136	-1.6671	20.9371	22.6042
ASNS	2.1925	-1.6214	20.6383	22.2597
CCT7	0.8539	-1.6011	22.5215	24.1226
MDH2	1.0066	-1.5542	21.9268	23.4810
RARS	4.6079	-1.5500	21.3023	22.8524
EIF5	3.3600	-1.4849	21.0797	22.5646
EIF2S3	1.1965	-1.4829	21.2174	22.7003
UBE2M	1.1258	-1.4657	20.6319	22.0976
CCT2	1.5812	-1.4236	23.0176	24.4412
RPA1	1.8912	-1.4012	20.8257	22.2269
TXN	1.0709	-1.3884	21.4839	22.8723
TCP1	1.2631	-1.3436	23.5815	24.9251
TLN1	1.0073	-1.3345	20.8526	22.1871
ATP5A1	1.0072	-1.3331	22.5478	23.8809
VCP	1.0285	-1.3276	21.3452	22.6728
YWHAZ	1.4744	-1.3204	21.2984	22.6188
EIF4G1	1.3249	-1.2968	21.0690	22.3658
GART	1.5638	-1.2482	20.6450	21.8932

SYNCRIP	0.9951	-1.2476	21.3412	22.5888
RPLP0	2.3822	-1.2060	20.5922	21.7982
PDCD5	1.0251	-1.2016	20.7099	21.9115
AKR1B1	1.3296	-1.2010	21.0594	22.2604
PLS3	1.0730	-1.1999	20.5649	21.7648
CNN3	2.7982	-1.1554	20.4395	21.5949
CAND1	2.5046	-1.1521	20.4793	21.6314
SEPT2	2.0701	-1.1282	20.8260	21.9541
ANXA2	1.2738	-1.1100	20.8799	21.9899
ANP32A	1.3143	-1.1028	20.7578	21.8605
PGD	1.0432	-1.1006	20.6282	21.7288
HSPD1	1.1994	-1.0832	24.9081	25.9913
PKM	1.8016	-1.0507	25.7691	26.8198
TUBB2B	1.3030	-1.0466	20.9196	21.9663
DCTN2	1.9747	-1.0379	20.4211	21.4589
FSCN1	1.6734	-0.9477	20.9419	21.8896
PEBP1	1.6714	-0.8836	20.6585	21.5422
GSTP1	2.5126	-0.8247	23.9073	24.7320
CKB	2.4292	-0.7892	26.5273	27.3164

Table S6 List of identified proteins from HeLa cells with mean of LFQ intensities from biological triplicates.

Gene names	mean (LFQ int.) TCO HS	mean (LFQ int.) Boc HS	mean (LFQ int.) EV HS	mean (LFQ int.) TCO nonHS	mean (LFQ int.) Boc nonHS	mean (LFQ int.) EV nonHS
PPIA	3.98E+09	3.21E+09	2.64E+09	2.88E+09	3.22E+09	3.27E+09
KRT18	3.83E+09	3.03E+09	4.48E+09	4.98E+09	3.23E+09	4.75E+09
H3F3B	2.84E+09	1.22E+10	4.56E+09	2.51E+09	1.27E+10	3.15E+09
HIST1H2BN	2.53E+09	9.98E+09	3.35E+09	2.03E+09	1.05E+10	2.85E+09
HIST1H4A	2.25E+09	9.78E+09	2.98E+09	1.59E+09	9.78E+09	2.52E+09
CSE1L	2.08E+09	2.25E+09	2.09E+09	2.39E+09	1.56E+09	1.74E+09
C2orf16	1.92E+09	0.00E+00	1.76E+09	0.00E+00	0.00E+00	4.13E+09
EEF1A1P5	1.88E+09	1.34E+09	1.60E+09	1.81E+09	1.24E+09	1.70E+09
HIST1H1C	1.41E+09	7.02E+09	2.20E+09	9.84E+08	6.49E+09	1.13E+09
HIST1H2AJ	1.31E+09	5.58E+09	1.61E+09	1.06E+09	6.73E+09	1.82E+09
ACTB	1.25E+09	1.22E+09	1.62E+09	1.57E+09	1.52E+09	1.75E+09
TUBA1B	8.20E+08	5.73E+08	6.96E+08	8.48E+08	6.22E+08	1.06E+09
PKM	7.78E+08	4.41E+08	4.89E+08	5.10E+08	3.31E+08	4.71E+08
HSP90AB1	7.24E+08	5.11E+08	6.21E+08	6.74E+08	4.57E+08	5.51E+08
EEF2	6.64E+08	4.90E+08	5.64E+08	6.41E+08	4.35E+08	5.58E+08
LMNA	6.38E+08	7.81E+08	8.53E+08	8.57E+08	7.57E+08	7.23E+08
TUBB4B	6.10E+08	4.20E+08	5.24E+08	6.02E+08	4.30E+08	7.04E+08
NPM1	6.04E+08	9.66E+08	6.80E+08	5.83E+08	9.62E+08	5.62E+08
PGK1	5.64E+08	2.82E+08	4.24E+08	4.21E+08	2.21E+08	3.28E+08
RPS27A	5.47E+08	6.15E+08	4.69E+08	2.94E+08	5.42E+08	4.06E+08
PC	5.46E+08	6.28E+08	5.41E+08	5.75E+08	5.68E+08	4.95E+08
HNRNPU	5.34E+08	8.02E+08	6.04E+08	5.10E+08	7.32E+08	5.72E+08
RPL4	5.29E+08	1.48E+09	5.45E+08	4.24E+08	1.50E+09	5.65E+08
VIM	5.02E+08	4.44E+08	6.65E+08	7.48E+08	5.72E+08	7.50E+08
GAPDH	4.85E+08	3.27E+08	3.19E+08	4.43E+08	3.82E+08	4.52E+08
HSPA8	4.81E+08	3.88E+08	4.30E+08	4.32E+08	3.28E+08	3.92E+08
RPL6	4.68E+08	1.22E+09	5.20E+08	3.73E+08	1.19E+09	4.01E+08
RPS8	4.33E+08	9.53E+08	4.40E+08	3.56E+08	1.02E+09	4.54E+08
HNRNPA1	4.29E+08	4.67E+08	4.42E+08	4.13E+08	4.06E+08	3.67E+08
RPL7A	4.09E+08	9.90E+08	4.33E+08	3.19E+08	1.01E+09	3.60E+08
FASN	4.07E+08	3.06E+08	4.36E+08	4.67E+08	3.36E+08	5.07E+08
FLNA	3.93E+08	2.98E+08	4.52E+08	4.83E+08	3.03E+08	4.31E+08
MYH9	3.83E+08	3.21E+08	4.65E+08	5.47E+08	3.67E+08	5.03E+08
HNRNPA2B1	3.75E+08	3.97E+08	3.45E+08	3.35E+08	3.67E+08	3.13E+08
RPL7	3.70E+08	1.15E+09	4.09E+08	2.87E+08	1.17E+09	3.48E+08
RPS9	3.57E+08	7.65E+08	3.90E+08	3.13E+08	8.66E+08	3.92E+08
RPS3	3.56E+08	4.55E+08	3.77E+08	3.67E+08	5.32E+08	4.09E+08
RPL13	3.45E+08	8.84E+08	3.38E+08	2.54E+08	8.67E+08	3.09E+08
ENO1	3.40E+08	2.56E+08	2.47E+08	3.72E+08	3.04E+08	3.42E+08
RPL8	3.39E+08	6.88E+08	3.47E+08	2.56E+08	5.88E+08	2.70E+08
RPL3	3.36E+08	8.90E+08	4.00E+08	3.18E+08	9.34E+08	3.51E+08
DDX21	3.05E+08	6.36E+08	3.80E+08	3.05E+08	6.25E+08	3.27E+08
RAN	3.02E+08	2.71E+08	2.82E+08	3.17E+08	2.91E+08	2.97E+08
RPS2	2.99E+08	5.30E+08	3.19E+08	2.94E+08	6.70E+08	3.49E+08
PLEC	2.90E+08	1.81E+08	3.23E+08	3.59E+08	1.79E+08	3.12E+08
DDX5	2.79E+08	2.85E+08	2.96E+08	2.92E+08	2.91E+08	2.89E+08
RPL18	2.76E+08	7.32E+08	2.99E+08	2.09E+08	7.47E+08	2.76E+08
RPL15	2.72E+08	9.63E+08	3.00E+08	2.17E+08	9.39E+08	2.48E+08
HNRNPK	2.55E+08	2.74E+08	2.62E+08	2.50E+08	2.38E+08	2.21E+08
ALDOA	2.52E+08	1.53E+08	1.86E+08	2.22E+08	1.31E+08	1.55E+08
RPS4X	2.41E+08	4.11E+08	2.18E+08	1.93E+08	3.94E+08	2.25E+08
HNRNPC	2.39E+08	3.21E+08	2.37E+08	2.38E+08	3.49E+08	2.71E+08
RPL27A	2.37E+08	5.20E+08	2.12E+08	1.72E+08	4.77E+08	2.10E+08
LDHA	2.36E+08	1.35E+08	1.54E+08	1.78E+08	1.27E+08	1.31E+08
RPS11	2.34E+08	4.46E+08	2.47E+08	2.15E+08	4.70E+08	2.16E+08
NCL	2.30E+08	3.91E+08	2.15E+08	1.91E+08	3.58E+08	1.81E+08
RPS6	2.26E+08	5.33E+08	2.47E+08	1.94E+08	5.42E+08	2.51E+08
DHX9	2.23E+08	1.97E+08	2.29E+08	2.28E+08	1.76E+08	2.23E+08
RPL18A	2.22E+08	4.43E+08	2.46E+08	1.97E+08	4.50E+08	2.57E+08
NONO	2.20E+08	2.28E+08	2.71E+08	2.64E+08	1.98E+08	2.37E+08
RPL13A	2.15E+08	5.86E+08	2.39E+08	1.72E+08	6.03E+08	2.13E+08
ANXA2	2.10E+08	1.45E+08	1.60E+08	1.89E+08	1.28E+08	1.80E+08
RPL28	2.07E+08	4.59E+08	2.42E+08	1.83E+08	4.05E+08	1.89E+08
MKI67	1.97E+08	3.50E+08	2.55E+08	2.27E+08	3.34E+08	2.40E+08
PRDX1	1.96E+08	1.29E+08	1.46E+08	1.62E+08	1.16E+08	1.43E+08
TUBB	1.95E+08	1.38E+08	1.61E+08	1.98E+08	1.71E+08	2.86E+08
SLC25A5	1.90E+08	1.75E+08	2.04E+08	1.92E+08	1.69E+08	2.01E+08
PFN1	1.74E+08	1.21E+08	1.29E+08	1.32E+08	1.03E+08	1.13E+08
HNRNPL	1.70E+08	1.63E+08	1.70E+08	1.61E+08	1.45E+08	1.56E+08
HNRNPM	1.69E+08	1.52E+08	1.88E+08	1.86E+08	1.43E+08	1.83E+08
RPS3A	1.67E+08	3.06E+08	1.87E+08	1.66E+08	3.42E+08	1.92E+08
HNRNPH1	1.67E+08	1.43E+08	1.63E+08	1.58E+08	1.33E+08	1.43E+08
RPS16	1.67E+08	2.45E+08	1.64E+08	1.56E+08	2.82E+08	1.74E+08
HSPD1	1.62E+08	1.21E+08	1.21E+08	1.20E+08	8.41E+07	8.95E+07
EIF4A1	1.58E+08	1.13E+08	1.17E+08	1.23E+08	9.25E+07	1.20E+08
RPS18	1.55E+08	2.72E+08	1.74E+08	1.43E+08	2.93E+08	1.58E+08
PARP1	1.54E+08	1.98E+08	1.65E+08	1.50E+08	1.99E+08	1.44E+08
PCBP2	1.53E+08	1.22E+08	1.55E+08	1.44E+08	1.03E+08	1.30E+08
TUFM	1.52E+08	1.41E+08	1.32E+08	1.25E+08	9.03E+07	9.83E+07
LDHB	1.49E+08	8.14E+07	1.04E+08	1.05E+08	6.57E+07	7.93E+07
RPL23A	1.49E+08	3.72E+08	1.50E+08	1.01E+08	3.81E+08	1.14E+08
AHCY	1.48E+08	1.09E+08	1.30E+08	1.24E+08	9.66E+07	1.02E+08
RPL26	1.47E+08	3.47E+08	1.65E+08	1.45E+08	3.35E+08	1.28E+08
RPL32	1.45E+08	4.37E+08	1.49E+08	1.03E+08	3.31E+08	1.18E+08
TKT	1.39E+08	1.07E+08	1.07E+08	1.46E+08	1.21E+08	1.12E+08
RPL27	1.39E+08	3.24E+08	1.46E+08	1.04E+08	3.68E+08	1.19E+08
GNB2L1	1.34E+08	1.28E+08	1.11E+08	1.11E+08	1.32E+08	1.25E+08
EEF1G	1.30E+08	8.44E+07	9.89E+07	9.98E+07	7.28E+07	9.69E+07

RPL10	1.29E+08	3.06E+08	1.55E+08	1.23E+08	2.92E+08	1.37E+08
CSRP1	1.29E+08	1.07E+08	1.25E+08	1.16E+08	8.53E+07	1.02E+08
RPL17	1.26E+08	3.26E+08	1.53E+08	1.21E+08	4.30E+08	1.76E+08
RPL14	1.23E+08	2.94E+08	1.33E+08	1.01E+08	3.13E+08	1.77E+08
MTHFD1	1.22E+08	8.82E+07	1.26E+08	1.29E+08	8.13E+07	1.16E+08
RPS23	1.20E+08	2.49E+08	1.27E+08	1.02E+08	2.12E+08	9.88E+07
EPRS	1.20E+08	9.81E+07	1.41E+08	1.47E+08	1.03E+08	1.38E+08
ASS1	1.19E+08	7.81E+07	9.06E+07	1.24E+08	8.97E+07	9.49E+07
RPL11	1.19E+08	1.47E+08	1.25E+08	1.16E+08	1.27E+08	1.17E+08
H2AFY	1.14E+08	4.41E+08	1.66E+08	1.13E+08	5.38E+08	1.63E+08
ACACA	1.13E+08	1.52E+08	1.35E+08	1.76E+08	2.06E+08	2.02E+08
VDAC2	1.13E+08	9.85E+07	1.28E+08	1.34E+08	1.22E+08	1.37E+08
LMNB1	1.10E+08	1.29E+08	1.40E+08	1.46E+08	1.30E+08	1.26E+08
RPS14	1.09E+08	1.62E+08	1.19E+08	1.18E+08	1.84E+08	1.25E+08
SFPQ	1.08E+08	9.83E+07	1.12E+08	1.20E+08	9.87E+07	1.21E+08
DDX17	1.06E+08	1.13E+08	1.17E+08	1.12E+08	1.23E+08	1.16E+08
RPL35	1.06E+08	2.77E+08	1.22E+08	8.19E+07	2.73E+08	8.37E+07
RPL21	1.05E+08	2.40E+08	1.11E+08	1.03E+08	2.49E+08	1.24E+08
RPL5	1.03E+08	2.21E+08	1.08E+08	8.57E+07	1.89E+08	7.53E+07
RPL24	1.03E+08	2.35E+08	1.04E+08	8.72E+07	2.50E+08	1.44E+08
RPS26	1.02E+08	2.13E+08	1.18E+08	9.41E+07	2.61E+08	1.16E+08
RPL19	1.01E+08	3.16E+08	1.06E+08	7.37E+07	2.64E+08	8.20E+07
HNRNPA3	1.00E+08	1.16E+08	9.55E+07	9.48E+07	1.05E+08	9.41E+07
HSPB1	1.00E+08	8.02E+07	9.44E+07	8.68E+07	5.57E+07	8.09E+07
ATP2A2	1.00E+08	9.09E+07	1.15E+08	1.19E+08	9.30E+07	1.24E+08
HSP90AA1	1.00E+08	6.96E+07	8.61E+07	9.53E+07	6.52E+07	7.82E+07
RPL10A	9.92E+07	1.60E+08	9.37E+07	8.82E+07	1.73E+08	1.15E+08
CLTC	9.89E+07	5.63E+07	8.61E+07	9.81E+07	5.88E+07	1.04E+08
CFL1	9.80E+07	7.45E+07	6.78E+07	8.10E+07	7.93E+07	7.57E+07
PHGDH	9.67E+07	6.64E+07	9.27E+07	9.38E+07	5.91E+07	8.44E+07
RPS27	9.56E+07	1.55E+08	1.19E+08	1.07E+08	1.60E+08	1.04E+08
HMGB1	9.53E+07	1.59E+08	8.12E+07	6.18E+07	1.32E+08	5.30E+07
EIF5A	9.34E+07	9.10E+07	8.69E+07	7.46E+07	7.32E+07	7.81E+07
ZC3HAV1	9.22E+07	7.26E+07	9.30E+07	9.55E+07	6.75E+07	9.80E+07
PCBP1	9.12E+07	6.96E+07	8.50E+07	8.55E+07	5.64E+07	8.24E+07
EEF1D	9.04E+07	5.69E+07	6.77E+07	7.54E+07	4.74E+07	6.22E+07
PABPC1	8.92E+07	5.12E+07	6.97E+07	7.95E+07	4.76E+07	8.38E+07
HSPA1B	8.92E+07	7.03E+07	7.89E+07	7.36E+07	5.16E+07	6.38E+07
RPL34	8.84E+07	2.19E+08	1.02E+08	7.38E+07	1.75E+08	8.50E+07
DDX3X	8.82E+07	7.95E+07	8.66E+07	7.85E+07	7.13E+07	7.51E+07
RBMX	8.57E+07	1.34E+08	1.03E+08	9.53E+07	1.44E+08	1.07E+08
RRM1	8.56E+07	5.49E+07	7.09E+07	6.57E+07	3.97E+07	5.34E+07
MCCC1	8.40E+07	8.77E+07	7.11E+07	9.22E+07	7.94E+07	7.75E+07
ATP5A1	8.31E+07	7.25E+07	7.85E+07	9.14E+07	7.28E+07	8.24E+07
FBL	8.22E+07	1.61E+08	1.11E+08	8.61E+07	1.96E+08	1.09E+08
TRIM28	8.13E+07	7.96E+07	9.50E+07	1.00E+08	8.66E+07	1.09E+08
HSPA9	8.12E+07	6.58E+07	6.48E+07	7.40E+07	5.40E+07	5.80E+07
LRPPRC	8.00E+07	6.78E+07	8.05E+07	8.05E+07	4.70E+07	6.01E+07
FSCN1	7.94E+07	6.25E+07	7.27E+07	7.31E+07	4.64E+07	6.03E+07
MATR3	7.94E+07	7.66E+07	8.65E+07	8.87E+07	7.35E+07	8.41E+07
DSP	7.94E+07	7.61E+07	1.10E+08	1.16E+08	8.45E+07	1.37E+08
RPL35A	7.77E+07	1.41E+08	9.80E+07	7.77E+07	1.27E+08	7.81E+07
UBA1	7.74E+07	3.39E+07	3.67E+07	1.93E+07	7.34E+06	8.97E+06
HIST2H2BE	7.55E+07	3.06E+08	6.94E+07	4.42E+07	2.59E+08	1.27E+08
SUPT16H	7.54E+07	1.03E+08	8.32E+07	8.39E+07	1.15E+08	9.20E+07
PTBP1	7.29E+07	5.51E+07	6.54E+07	6.41E+07	4.50E+07	5.58E+07
SND1	6.99E+07	5.69E+07	6.93E+07	6.52E+07	5.82E+07	6.12E+07
RPL23	6.95E+07	1.17E+08	7.33E+07	6.53E+07	1.17E+08	8.57E+07
EIF2S3	6.95E+07	5.93E+07	6.19E+07	5.88E+07	5.04E+07	5.44E+07
PRPF19	6.86E+07	5.52E+07	6.49E+07	6.65E+07	5.99E+07	7.53E+07
EBNA1BP2	6.69E+07	1.83E+08	7.53E+07	5.06E+07	1.74E+08	5.86E+07
CDC2;CDK1	6.60E+07	5.59E+07	6.61E+07	7.04E+07	5.56E+07	5.64E+07
RPS7	6.60E+07	8.75E+07	7.24E+07	5.87E+07	1.01E+08	6.26E+07
HP1BP3	6.55E+07	3.26E+08	9.86E+07	6.45E+07	3.80E+08	7.41E+07
YWHAE	6.53E+07	4.06E+07	5.12E+07	5.72E+07	3.52E+07	4.37E+07
SRSF6	6.23E+07	8.80E+07	7.56E+07	6.64E+07	9.57E+07	6.86E+07
CBX3	6.06E+07	9.63E+07	6.07E+07	5.15E+07	1.13E+08	5.20E+07
HIST1H1B	5.90E+07	1.42E+08	4.50E+07	0.00E+00	1.28E+08	1.72E+07
CCT8	5.89E+07	3.48E+07	4.94E+07	5.57E+07	2.90E+07	4.33E+07
CCT6A	5.87E+07	3.66E+07	5.65E+07	6.01E+07	3.49E+07	4.63E+07
STIP1	5.80E+07	3.63E+07	4.66E+07	4.27E+07	2.31E+07	3.48E+07
RPL36A	5.76E+07	1.20E+08	6.31E+07	5.08E+07	9.52E+07	5.34E+07
SRSF3	5.75E+07	7.74E+07	6.18E+07	5.24E+07	6.41E+07	5.84E+07
TCP1	5.67E+07	3.76E+07	5.22E+07	5.85E+07	3.85E+07	4.92E+07
HNRNPR	5.66E+07	7.85E+07	5.06E+07	5.18E+07	8.45E+07	6.39E+07
RSL1D1	5.62E+07	1.51E+08	6.51E+07	5.00E+07	1.55E+08	5.99E+07
PCCA	5.59E+07	4.83E+07	5.20E+07	6.54E+07	3.98E+07	4.31E+07
HNRNPD	5.57E+07	5.57E+07	4.83E+07	4.31E+07	4.41E+07	4.14E+07
NOP2	5.51E+07	1.29E+08	7.00E+07	5.25E+07	1.36E+08	5.49E+07
CCT3	5.44E+07	3.31E+07	4.74E+07	5.03E+07	3.06E+07	5.40E+07
ACLY	5.43E+07	3.82E+07	4.71E+07	4.92E+07	3.33E+07	4.43E+07
RPS13	5.41E+07	8.60E+07	4.52E+07	4.02E+07	1.05E+08	5.76E+07
RPS10	5.32E+07	6.37E+07	4.44E+07	3.51E+07	5.65E+07	3.78E+07
BUB3	5.29E+07	4.61E+07	5.62E+07	5.68E+07	4.45E+07	4.56E+07
MYO1B	5.27E+07	4.36E+07	5.66E+07	6.25E+07	4.71E+07	7.06E+07
RPN1	5.22E+07	5.61E+07	5.62E+07	6.23E+07	6.24E+07	6.13E+07
RTCB	5.19E+07	4.72E+07	4.88E+07	5.02E+07	4.69E+07	4.80E+07
RCC2	5.18E+07	9.61E+07	5.50E+07	4.98E+07	9.95E+07	5.30E+07
RPS20	5.17E+07	6.37E+07	4.66E+07	4.67E+07	5.82E+07	3.75E+07
HNRNPF	5.16E+07	4.35E+07	5.08E+07	4.67E+07	4.04E+07	4.81E+07
XRCC6	5.10E+07	4.42E+07	4.49E+07	4.50E+07	4.48E+07	4.43E+07
DARS	5.06E+07	4.33E+07	5.46E+07	5.74E+07	4.59E+07	5.89E+07
RPL30	5.04E+07	8.06E+07	4.54E+07	3.87E+07	6.84E+07	4.03E+07
NOP58	5.01E+07	9.03E+07	6.25E+07	5.11E+07	8.86E+07	5.65E+07
PRKDC	4.97E+07	3.91E+07	6.01E+07	6.45E+07	4.61E+07	6.40E+07
FKBP4	4.97E+07	3.35E+07	4.09E+07	4.22E+07	2.47E+07	3.51E+07
NOP56	4.87E+07	9.06E+07	6.50E+07	5.71E+07	9.89E+07	5.59E+07
NSUN2	4.85E+07	4.82E+07	5.09E+07	5.74E+07	5.65E+07	5.71E+07
RBM14	4.80E+07	4.56E+07	6.06E+07	6.08E+07	4.46E+07	5.28E+07
SRSF1	4.78E+07	7.55E+07	6.15E+07	5.34E+07	8.98E+07	5.78E+07
DDX1	4.71E+07	4.49E+07	5.04E+07	5.06E+07	4.64E+07	5.96E+07
FUBP1	4.69E+07	3.60E+07	4.34E+07	4.43E+07	2.81E+07	3.16E+07

PGD	4.65E+07	2.82E+07	3.82E+07	3.72E+07	2.53E+07	3.06E+07
SDHA	4.65E+07	3.86E+07	3.71E+07	3.68E+07	2.57E+07	2.74E+07
FLNB	4.64E+07	3.19E+07	5.44E+07	5.93E+07	2.83E+07	5.08E+07
FEN1	4.55E+07	5.28E+07	5.26E+07	4.95E+07	5.95E+07	5.15E+07
IARS	4.50E+07	3.50E+07	4.81E+07	5.09E+07	4.03E+07	6.39E+07
PA2G4	4.48E+07	3.87E+07	3.58E+07	3.57E+07	3.46E+07	2.71E+07
PHB2	4.45E+07	3.88E+07	4.37E+07	5.02E+07	4.38E+07	4.91E+07
RNH1	4.42E+07	3.27E+07	5.67E+07	6.05E+07	3.97E+07	5.31E+07
DYNC1H1	4.42E+07	8.12E+06	4.50E+07	5.62E+07	1.89E+07	4.86E+07
SNRPD2	4.34E+07	4.99E+07	4.86E+07	4.57E+07	4.97E+07	4.18E+07
MSN	4.33E+07	3.28E+07	4.25E+07	4.91E+07	3.30E+07	4.10E+07
MYL6	4.32E+07	2.99E+07	3.96E+07	4.22E+07	3.20E+07	3.66E+07
TPM3	4.25E+07	3.07E+07	4.84E+07	5.22E+07	3.29E+07	3.99E+07
RARS	4.24E+07	3.32E+07	4.90E+07	5.04E+07	3.27E+07	4.69E+07
SRSF7	4.22E+07	5.43E+07	4.35E+07	3.88E+07	6.90E+07	4.01E+07
VCL	4.18E+07	2.11E+07	3.84E+07	4.48E+07	1.34E+07	3.11E+07
TXN	4.13E+07	3.28E+07	3.13E+07	3.31E+07	2.87E+07	2.90E+07
RPS15A	4.10E+07	6.75E+07	4.87E+07	5.41E+07	8.92E+07	7.69E+07
RPL22	4.06E+07	6.27E+07	3.90E+07	3.16E+07	6.44E+07	3.26E+07
TMPO	4.05E+07	5.10E+07	5.24E+07	4.50E+07	4.42E+07	4.21E+07
RPSA	4.04E+07	4.26E+07	3.14E+07	3.34E+07	4.25E+07	3.57E+07
ILF3	3.97E+07	3.85E+07	3.75E+07	3.74E+07	3.65E+07	3.70E+07
SNRNP70	3.94E+07	5.90E+07	4.26E+07	3.93E+07	5.52E+07	3.38E+07
TAGLN2	3.93E+07	2.44E+07	2.53E+07	2.74E+07	2.41E+07	2.60E+07
MCM6	3.92E+07	2.84E+07	3.88E+07	3.83E+07	2.78E+07	3.33E+07
KPNB1	3.90E+07	2.15E+07	3.33E+07	3.68E+07	1.38E+07	3.48E+07
CCT4	3.88E+07	2.28E+07	3.22E+07	3.63E+07	2.03E+07	3.07E+07
GTPBP4	3.87E+07	9.46E+07	5.19E+07	3.54E+07	1.13E+08	4.77E+07
RPL36	3.87E+07	1.08E+08	4.19E+07	2.74E+07	1.05E+08	3.66E+07
GNL3	3.85E+07	8.27E+07	5.60E+07	4.32E+07	1.14E+08	5.35E+07
HNRNPA0	3.82E+07	3.96E+07	4.33E+07	3.83E+07	3.94E+07	4.52E+07
RPS25	3.81E+07	4.85E+07	3.59E+07	2.94E+07	4.64E+07	3.58E+07
H1FX	3.79E+07	1.75E+08	5.07E+07	2.99E+07	1.74E+08	3.84E+07
TNPO1	3.77E+07	2.61E+07	4.18E+07	4.30E+07	2.57E+07	4.59E+07
CBX5	3.73E+07	6.33E+07	3.66E+07	3.49E+07	8.12E+07	4.32E+07
RCC1	3.71E+07	5.48E+07	3.77E+07	3.31E+07	6.45E+07	3.50E+07
MCM3	3.71E+07	3.13E+07	3.68E+07	3.74E+07	3.18E+07	3.66E+07
FUS	3.70E+07	4.25E+07	3.76E+07	3.43E+07	4.12E+07	3.34E+07
NUMA1	3.66E+07	5.11E+07	5.01E+07	5.24E+07	4.99E+07	4.70E+07
CLPB	3.62E+07	0.00E+00	0.00E+00	4.88E+07	3.94E+07	3.92E+07
RPL9	3.61E+07	5.28E+07	3.53E+07	3.96E+07	8.25E+07	6.19E+07
COPA	3.58E+07	2.67E+07	3.94E+07	4.15E+07	2.86E+07	4.68E+07
EPPK1	3.56E+07	2.77E+07	4.20E+07	5.02E+07	3.20E+07	4.38E+07
RPL37A	3.56E+07	6.63E+07	4.20E+07	3.01E+07	5.62E+07	3.35E+07
STRAP	3.53E+07	2.48E+07	2.94E+07	3.00E+07	2.53E+07	2.79E+07
CSDE1	3.53E+07	2.58E+07	3.30E+07	3.39E+07	2.31E+07	3.22E+07
BRIX1	3.51E+07	9.98E+07	4.25E+07	3.06E+07	1.09E+08	4.55E+07
RPL31	3.49E+07	6.89E+07	3.48E+07	3.23E+07	7.21E+07	3.10E+07
SRSF2	3.48E+07	4.92E+07	4.00E+07	3.20E+07	5.11E+07	3.77E+07
PAICS	3.42E+07	1.80E+07	2.77E+07	2.91E+07	9.21E+06	2.67E+07
XPO1	3.41E+07	2.49E+07	3.73E+07	4.00E+07	2.64E+07	4.71E+07
SNRPD3	3.39E+07	3.15E+07	2.96E+07	2.87E+07	2.93E+07	2.99E+07
DHX15	3.38E+07	3.10E+07	3.19E+07	3.34E+07	3.04E+07	3.64E+07
IQGAP1	3.35E+07	1.87E+07	2.93E+07	3.11E+07	1.72E+07	2.88E+07
RBBP7	3.34E+07	3.20E+07	3.67E+07	3.51E+07	3.08E+07	3.20E+07
WDR1	3.33E+07	2.52E+07	3.41E+07	3.32E+07	2.22E+07	2.96E+07
RPS24	3.33E+07	6.54E+07	3.26E+07	2.77E+07	8.06E+07	4.78E+07
ABCE1	3.30E+07	3.30E+07	3.34E+07	3.41E+07	3.68E+07	3.74E+07
DDX39A	3.27E+07	3.11E+07	2.93E+07	2.96E+07	3.15E+07	3.36E+07
MCM7	3.27E+07	2.75E+07	3.55E+07	3.77E+07	3.35E+07	3.91E+07
NOLC1	3.27E+07	7.00E+07	3.97E+07	3.22E+07	5.51E+07	2.76E+07
YBX1	3.26E+07	3.44E+07	2.77E+07	2.15E+07	3.07E+07	1.92E+07
NME2	3.25E+07	2.17E+07	2.61E+07	2.76E+07	2.02E+07	2.17E+07
EIF4G1	3.24E+07	2.40E+07	3.08E+07	2.95E+07	1.80E+07	2.71E+07
HSPA5	3.24E+07	2.14E+07	2.57E+07	3.05E+07	2.27E+07	2.80E+07
SERBP1	3.23E+07	5.23E+07	3.02E+07	2.63E+07	3.88E+07	2.50E+07
ALDH18A1	3.23E+07	2.82E+07	3.87E+07	3.86E+07	2.55E+07	2.97E+07
SLC25A6	3.12E+07	2.25E+07	2.63E+07	2.73E+07	2.01E+07	2.99E+07
GPI	3.12E+07	1.54E+07	1.62E+07	1.74E+07	7.69E+06	1.12E+07
EIF3D	3.08E+07	3.78E+07	3.29E+07	3.01E+07	4.18E+07	2.81E+07
SMARCA5	3.07E+07	4.01E+07	4.25E+07	3.95E+07	4.68E+07	3.57E+07
SUB1	3.07E+07	6.36E+07	2.98E+07	2.87E+07	6.88E+07	3.48E+07
HNRNPAB	3.07E+07	2.96E+07	2.79E+07	2.36E+07	2.74E+07	2.21E+07
EIF2S1	3.06E+07	3.30E+07	3.15E+07	2.84E+07	3.77E+07	2.89E+07
SNRNP200	3.03E+07	2.39E+07	3.14E+07	3.16E+07	2.58E+07	3.17E+07
LUC7L2	2.98E+07	3.56E+07	3.74E+07	3.07E+07	2.82E+07	2.50E+07
SMC1A	2.88E+07	2.90E+07	3.21E+07	3.76E+07	3.35E+07	3.53E+07
H1F0	2.87E+07	1.85E+08	5.47E+07	2.16E+07	1.73E+08	2.03E+07
TOP2A	2.86E+07	3.59E+07	3.46E+07	3.25E+07	4.07E+07	3.89E+07
FHL2	2.85E+07	2.58E+07	4.23E+07	3.91E+07	2.41E+07	3.68E+07
RPL12	2.84E+07	2.86E+07	2.60E+07	2.93E+07	2.61E+07	2.54E+07
HDLBP	2.84E+07	2.43E+07	3.10E+07	2.87E+07	2.51E+07	2.60E+07
HNRNPH3	2.83E+07	2.99E+07	2.82E+07	2.69E+07	2.85E+07	2.40E+07
EIF4A3	2.83E+07	3.39E+07	3.23E+07	2.92E+07	3.93E+07	3.09E+07
EIF3C	2.81E+07	2.40E+07	2.70E+07	2.82E+07	2.40E+07	2.73E+07
TPR	2.80E+07	1.83E+07	3.20E+07	3.92E+07	1.83E+07	2.90E+07
TOP1	2.76E+07	7.46E+07	3.18E+07	1.92E+07	7.20E+07	2.35E+07
APEX1	2.76E+07	4.42E+07	2.58E+07	2.34E+07	3.47E+07	2.02E+07
EIF3I	2.75E+07	2.30E+07	3.03E+07	2.97E+07	2.20E+07	2.40E+07
KHSRP	2.74E+07	1.95E+07	2.54E+07	2.61E+07	1.76E+07	2.26E+07
CPS1	2.74E+07	8.46E+06	8.03E+06	1.05E+07	1.68E+06	4.21E+06
CCT7	2.72E+07	1.67E+07	2.39E+07	2.67E+07	1.65E+07	2.39E+07
XRCC5	2.68E+07	2.19E+07	2.47E+07	2.31E+07	2.02E+07	2.57E+07
GSTM3	2.64E+07	1.35E+07	1.52E+07	1.18E+07	5.93E+06	1.24E+07
ACAT1	2.64E+07	2.13E+07	1.59E+07	1.05E+07	7.87E+06	8.11E+06
CCT2	2.63E+07	8.33E+06	2.03E+07	2.61E+07	1.29E+07	1.59E+07
MCM5	2.62E+07	2.02E+07	2.25E+07	2.34E+07	1.99E+07	2.76E+07
HNRNPDL	2.61E+07	2.03E+07	1.88E+07	1.79E+07	1.61E+07	1.71E+07
CMBL	2.60E+07	2.07E+07	2.68E+07	2.18E+07	9.94E+06	1.69E+07
ACP1	2.59E+07	1.95E+07	2.34E+07	2.31E+07	1.89E+07	2.53E+07
FABP5	2.59E+07	8.30E+06	1.34E+07	1.33E+07	3.00E+06	1.57E+07
TFRC	2.58E+07	1.87E+07	2.66E+07	2.76E+07	1.67E+07	2.18E+07

RANGAP1	2.58E+07	1.91E+07	2.87E+07	3.02E+07	1.85E+07	2.80E+07
DNMT1	2.57E+07	3.14E+07	3.35E+07	3.35E+07	4.09E+07	3.64E+07
PRDX2	2.57E+07	1.61E+07	2.06E+07	2.24E+07	1.73E+07	1.75E+07
RUVBL1	2.56E+07	1.73E+07	2.31E+07	2.57E+07	1.90E+07	2.61E+07
GEMIN5	2.56E+07	2.08E+07	2.90E+07	3.11E+07	2.02E+07	3.46E+07
U2AF2	2.56E+07	2.34E+07	2.19E+07	2.20E+07	2.09E+07	2.82E+07
EIF2S2	2.54E+07	2.47E+07	2.38E+07	2.03E+07	2.14E+07	1.92E+07
PRPF8	2.54E+07	1.78E+07	2.39E+07	2.73E+07	2.41E+07	2.69E+07
MIF	2.54E+07	1.82E+07	1.65E+07	1.71E+07	1.58E+07	0.00E+00
LRRC59	2.53E+07	2.64E+07	2.35E+07	2.50E+07	2.89E+07	3.22E+07
PRMT1	2.49E+07	2.13E+07	2.21E+07	2.30E+07	2.20E+07	2.42E+07
EEF1B2	2.45E+07	1.48E+07	1.58E+07	1.85E+07	1.51E+07	1.24E+07
PTGES3	2.44E+07	2.11E+07	1.28E+07	0.00E+00	8.28E+06	8.55E+06
RBM4	2.43E+07	2.32E+07	2.63E+07	2.27E+07	2.12E+07	2.33E+07
EIF3B	2.42E+07	1.98E+07	2.08E+07	2.11E+07	1.94E+07	2.16E+07
CKB	2.41E+07	1.59E+07	1.76E+07	1.70E+07	1.19E+07	1.40E+07
S100A11	2.41E+07	1.57E+07	1.82E+07	1.85E+07	8.10E+06	1.65E+07
ACAA2	2.40E+07	1.96E+07	1.97E+07	1.76E+07	9.09E+06	1.27E+07
VARS	2.40E+07	1.59E+07	2.31E+07	2.64E+07	1.72E+07	2.41E+07
MARS	2.38E+07	1.76E+07	2.58E+07	2.83E+07	1.96E+07	3.15E+07
CALM2	2.38E+07	1.70E+07	1.78E+07	2.11E+07	5.04E+06	5.80E+06
IPO5	2.38E+07	1.31E+07	2.05E+07	1.99E+07	2.72E+06	2.17E+07
DKC1	2.37E+07	4.31E+07	2.85E+07	2.30E+07	3.90E+07	2.16E+07
ACTN4	2.37E+07	6.05E+06	1.61E+07	1.97E+07	8.07E+06	1.45E+07
PRDX6	2.35E+07	1.66E+07	1.59E+07	2.08E+07	2.02E+07	2.10E+07
NAP1L4	2.35E+07	1.55E+07	1.56E+07	1.39E+07	2.94E+06	0.00E+00
SMC3	2.35E+07	2.10E+07	2.65E+07	3.01E+07	2.36E+07	2.26E+07
MTA2	2.34E+07	2.29E+07	2.76E+07	3.18E+07	2.62E+07	3.16E+07
DDX47	2.34E+07	3.37E+07	2.88E+07	2.22E+07	3.51E+07	2.61E+07
ESD	2.29E+07	1.69E+07	2.33E+07	2.10E+07	4.79E+06	1.80E+07
RPS5	2.28E+07	3.23E+07	2.44E+07	2.36E+07	3.17E+07	2.81E+07
CTTN	2.26E+07	8.30E+06	1.38E+07	9.76E+06	2.25E+06	5.04E+06
FXR1	2.26E+07	2.11E+07	2.82E+07	2.36E+07	2.13E+07	2.17E+07
IMPDH2	2.25E+07	1.68E+07	1.93E+07	2.63E+07	1.79E+07	2.04E+07
SF3B3	2.25E+07	1.49E+07	1.78E+07	1.83E+07	1.07E+07	1.80E+07
GMPS	2.21E+07	1.79E+07	1.88E+07	1.90E+07	1.73E+07	1.85E+07
RPS12	2.20E+07	1.88E+07	1.62E+07	1.26E+07	1.88E+07	1.90E+07
LARS	2.19E+07	1.48E+07	2.35E+07	2.36E+07	1.59E+07	2.70E+07
CCT5	2.18E+07	8.64E+06	1.77E+07	1.98E+07	6.75E+06	1.75E+07
GNB2	2.17E+07	1.52E+07	2.19E+07	2.18E+07	1.30E+07	2.01E+07
BZW1	2.16E+07	1.42E+07	1.95E+07	1.74E+07	1.22E+07	1.77E+07
HSD17B10	2.15E+07	1.42E+07	1.49E+07	1.39E+07	1.02E+07	7.96E+06
NAT10	2.15E+07	3.39E+07	2.96E+07	2.58E+07	3.70E+07	2.87E+07
HADHB	2.14E+07	1.67E+07	1.68E+07	1.32E+07	1.11E+07	8.37E+06
EIF2A	2.12E+07	1.63E+07	1.90E+07	1.64E+07	1.43E+07	1.80E+07
RANBP2	2.12E+07	1.62E+07	2.78E+07	2.79E+07	1.27E+07	3.14E+07
PPP1CA	2.12E+07	2.16E+07	2.31E+07	2.16E+07	2.17E+07	2.35E+07
TXNRD1	2.10E+07	1.08E+07	1.39E+07	1.67E+07	5.29E+06	1.42E+07
DNAJA1	2.09E+07	1.59E+07	2.30E+07	2.35E+07	1.97E+07	2.48E+07
UBE2M	2.08E+07	1.57E+07	1.92E+07	1.79E+07	1.36E+07	1.50E+07
ADAR	2.06E+07	1.72E+07	2.26E+07	2.37E+07	1.97E+07	2.60E+07
NCAPD3	2.06E+07	2.10E+07	2.84E+07	3.80E+07	2.82E+07	5.01E+07
SEC61A1	2.05E+07	2.92E+07	2.64E+07	1.30E+07	3.92E+07	2.19E+07
DDX18	2.05E+07	4.21E+07	2.32E+07	1.73E+07	5.16E+07	2.44E+07
SLC25A3	2.04E+07	1.94E+07	2.18E+07	2.18E+07	1.97E+07	1.93E+07
TRA2B	2.03E+07	2.95E+07	2.51E+07	1.91E+07	2.80E+07	2.69E+07
ERH	2.02E+07	2.15E+07	2.07E+07	1.81E+07	1.19E+07	1.70E+07
PES1	2.02E+07	3.45E+07	2.42E+07	2.08E+07	3.31E+07	2.03E+07
SORD	2.01E+07	1.42E+07	2.09E+07	1.93E+07	1.12E+07	2.16E+07
QARS	2.01E+07	9.80E+06	1.93E+07	1.91E+07	1.02E+07	1.55E+07
AARS	2.00E+07	1.26E+07	1.95E+07	1.85E+07	9.04E+06	1.28E+07
TUBA1C	1.93E+07	1.36E+07	1.56E+07	1.85E+07	1.41E+07	2.33E+07
TRAP1	1.92E+07	1.54E+07	1.38E+07	1.33E+07	7.10E+06	6.18E+06
RUVBL2	1.92E+07	1.38E+07	1.75E+07	2.15E+07	1.52E+07	1.98E+07
MCM4	1.89E+07	1.35E+07	1.63E+07	1.60E+07	1.23E+07	1.28E+07
HINT1	1.88E+07	4.21E+06	0.00E+00	0.00E+00	0.00E+00	0.00E+00
ABCF2	1.87E+07	1.90E+07	2.06E+07	1.70E+07	2.08E+07	1.92E+07
ELAVL1	1.87E+07	1.68E+07	1.73E+07	1.69E+07	1.47E+07	1.56E+07
ATAD3A	1.86E+07	1.78E+07	2.54E+07	2.73E+07	2.07E+07	2.64E+07
HADHA	1.85E+07	1.26E+07	1.42E+07	1.55E+07	5.34E+06	9.76E+06
SSRP1	1.85E+07	2.52E+07	1.66E+07	1.65E+07	2.91E+07	1.89E+07
CS	1.84E+07	1.27E+07	1.05E+07	1.17E+07	8.06E+06	9.61E+06
SEC22B	1.83E+07	1.62E+07	1.86E+07	1.86E+07	1.33E+07	1.51E+07
HNRNPUL2	1.81E+07	2.56E+07	1.90E+07	1.65E+07	2.41E+07	1.93E+07
ABCF1	1.81E+07	2.06E+07	1.84E+07	1.69E+07	2.08E+07	1.66E+07
GCN1L1	1.80E+07	1.30E+07	2.14E+07	2.68E+07	1.45E+07	2.72E+07
TDP43	1.80E+07	1.85E+07	2.04E+07	1.78E+07	1.70E+07	1.83E+07
VDAC1	1.80E+07	1.33E+07	1.55E+07	1.77E+07	1.55E+07	1.52E+07
CHORDC1	1.79E+07	1.41E+07	1.56E+07	1.47E+07	8.60E+06	1.18E+07
PHB	1.78E+07	1.33E+07	1.08E+07	2.09E+07	9.17E+06	1.71E+07
RBM39	1.77E+07	1.83E+07	1.93E+07	1.80E+07	1.62E+07	1.89E+07
AKR1C1	1.77E+07	1.38E+07	1.71E+07	9.80E+06	3.83E+06	9.03E+06
CAD	1.76E+07	8.12E+06	1.70E+07	1.83E+07	8.30E+06	1.96E+07
HSP90B1	1.75E+07	1.25E+07	1.26E+07	1.59E+07	1.14E+07	1.34E+07
HMGB2	1.75E+07	3.78E+07	1.80E+07	0.00E+00	2.47E+07	0.00E+00
ARF4	1.74E+07	1.63E+07	1.65E+07	1.14E+07	1.50E+07	2.02E+07
BANF1	1.73E+07	6.51E+07	3.84E+07	8.85E+06	7.95E+07	1.73E+07
KARS	1.73E+07	1.34E+07	1.13E+07	1.69E+07	1.15E+07	1.03E+07
EIF4B	1.73E+07	1.26E+07	1.32E+07	1.65E+07	1.05E+07	1.19E+07
CLIC1	1.72E+07	1.08E+07	1.10E+07	9.43E+06	4.89E+06	7.96E+06
AKR1B1	1.71E+07	8.72E+06	9.37E+06	4.98E+06	2.77E+06	2.92E+06
GLRX3	1.71E+07	1.01E+07	1.53E+07	1.18E+07	1.04E+07	5.90E+06
DNAJC7	1.70E+07	1.49E+07	1.93E+07	2.08E+07	1.30E+07	1.74E+07
SEPT7	1.70E+07	1.38E+07	1.95E+07	2.08E+07	1.45E+07	1.82E+07
DNAJA2	1.69E+07	1.63E+07	2.12E+07	1.97E+07	1.40E+07	1.53E+07
MSH2	1.69E+07	1.53E+07	1.96E+07	2.05E+07	1.64E+07	1.89E+07
LASP1	1.68E+07	1.31E+07	1.72E+07	1.54E+07	9.17E+06	1.30E+07
HSD17B4	1.67E+07	1.04E+07	1.31E+07	8.57E+06	4.27E+06	9.67E+06
EIF3A	1.64E+07	1.21E+07	1.36E+07	1.50E+07	1.06E+07	1.33E+07
CNN2	1.64E+07	7.18E+06	1.36E+07	1.17E+07	0.00E+00	6.05E+06
U2AF1	1.62E+07	1.97E+07	1.98E+07	1.68E+07	2.06E+07	1.80E+07
MYL12A	1.62E+07	1.92E+07	1.68E+07	1.44E+07	2.31E+07	8.34E+06

OTUB1	1.61E+07	1.14E+07	1.35E+07	6.32E+06	3.17E+06	4.93E+06
OXCT1	1.61E+07	1.46E+07	1.40E+07	1.04E+07	4.64E+06	0.00E+00
YWHAG	1.61E+07	7.63E+06	1.32E+07	8.81E+06	3.96E+06	9.31E+06
FTSJ3	1.60E+07	5.23E+07	1.72E+07	1.07E+07	6.03E+07	1.79E+07
RPA1	1.60E+07	1.35E+07	1.63E+07	1.57E+07	1.25E+07	1.48E+07
HSPA4	1.56E+07	8.16E+06	9.83E+06	1.27E+07	7.98E+06	1.00E+07
PDIA3	1.56E+07	9.52E+06	9.98E+06	9.97E+06	6.88E+06	3.19E+06
DDX46	1.55E+07	1.44E+07	1.86E+07	1.95E+07	1.46E+07	1.57E+07
RAB7A	1.54E+07	1.29E+07	1.50E+07	1.61E+07	1.37E+07	1.89E+07
PDCD11	1.52E+07	2.52E+07	2.00E+07	1.89E+07	3.07E+07	2.13E+07
MCM2	1.52E+07	7.24E+06	1.39E+07	4.60E+06	7.53E+06	1.36E+07
SF3B1	1.52E+07	1.10E+07	1.46E+07	1.43E+07	1.02E+07	1.10E+07
DDX54	1.51E+07	5.45E+07	2.00E+07	1.54E+07	6.48E+07	1.70E+07
SNRPB	1.51E+07	1.35E+07	1.53E+07	1.22E+07	1.69E+07	2.15E+07
VCP	1.50E+07	5.17E+06	1.11E+07	1.02E+07	0.00E+00	7.15E+06
SUGT1	1.50E+07	3.64E+06	1.53E+07	1.29E+07	0.00E+00	7.23E+06
COPB2	1.49E+07	1.27E+07	1.66E+07	1.57E+07	1.23E+07	1.55E+07
USP5	1.49E+07	5.93E+06	1.03E+07	7.27E+06	1.74E+06	9.04E+06
DEK	1.48E+07	2.61E+07	1.56E+07	1.36E+07	2.59E+07	9.26E+06
GTF2I	1.48E+07	1.19E+07	1.58E+07	1.52E+07	1.17E+07	1.37E+07
ATIC	1.47E+07	3.61E+06	1.61E+06	3.78E+06	9.43E+05	1.10E+06
SPTAN1	1.47E+07	1.63E+06	1.57E+07	2.18E+07	1.73E+06	1.53E+07
EFTUD2	1.47E+07	9.59E+06	1.40E+07	1.50E+07	1.01E+07	1.43E+07
EIF4H	1.47E+07	7.42E+06	1.05E+07	7.11E+06	0.00E+00	3.24E+06
PRPS1	1.45E+07	2.62E+06	1.02E+07	9.65E+06	0.00E+00	6.01E+06
SMC4	1.44E+07	9.89E+06	1.69E+07	2.25E+07	1.33E+07	1.66E+07
ALYREF	1.44E+07	4.14E+07	1.81E+07	9.41E+06	5.77E+07	1.57E+07
ANXA1	1.43E+07	9.10E+06	9.57E+06	1.23E+07	9.46E+06	1.23E+07
RBM28	1.43E+07	3.96E+07	1.73E+07	9.69E+06	3.79E+07	1.21E+07
PRDX5	1.42E+07	9.35E+06	8.51E+06	4.87E+06	3.35E+06	3.64E+06
YWHAZ	1.41E+07	1.03E+07	1.25E+07	1.30E+07	8.64E+06	7.62E+06
OASL	1.41E+07	1.62E+07	1.38E+07	1.74E+07	3.21E+07	1.95E+07
DYNLL1	1.41E+07	8.76E+06	1.48E+07	9.08E+06	3.58E+06	1.40E+07
MBNL1	1.41E+07	1.06E+07	1.49E+07	8.90E+06	8.46E+06	1.36E+07
IPO7	1.41E+07	7.95E+06	1.29E+07	1.44E+07	9.35E+06	1.57E+07
GSPT1	1.40E+07	1.07E+07	1.41E+07	1.59E+07	9.03E+06	1.20E+07
H2AFV	1.39E+07	1.12E+08	1.50E+07	2.14E+07	1.05E+08	2.31E+07
PPM1G	1.39E+07	1.26E+07	1.35E+07	1.21E+07	8.61E+06	9.00E+06
BOP1	1.39E+07	2.22E+07	1.66E+07	1.48E+07	2.63E+07	1.51E+07
SARNP	1.39E+07	1.40E+07	1.24E+07	1.13E+07	1.29E+07	8.93E+06
HDAC1	1.38E+07	1.32E+07	1.40E+07	1.01E+07	1.29E+07	1.36E+07
IFI16	1.38E+07	1.60E+07	1.74E+07	1.62E+07	1.86E+07	1.48E+07
PRDX4	1.38E+07	1.18E+07	1.39E+07	1.29E+07	1.25E+07	1.57E+07
TPI1	1.37E+07	1.24E+07	1.16E+07	1.75E+07	1.24E+07	1.10E+07
PABPC4	1.36E+07	6.46E+06	1.22E+07	1.29E+07	0.00E+00	1.20E+07
EIF3L	1.35E+07	3.03E+06	1.40E+07	1.27E+07	5.61E+06	1.16E+07
CACYBP	1.35E+07	6.23E+06	7.98E+06	8.99E+06	5.39E+06	1.14E+07
EIF3G	1.34E+07	9.60E+06	1.21E+07	7.97E+06	9.02E+06	8.63E+06
ACSL4	1.34E+07	6.17E+06	1.45E+07	1.48E+07	5.81E+06	1.25E+07
NIFK	1.34E+07	3.62E+07	1.73E+07	1.56E+07	4.39E+07	1.78E+07
RECQL	1.33E+07	1.47E+07	1.67E+07	1.76E+07	1.61E+07	2.34E+07
AHNAK	1.33E+07	4.21E+06	1.07E+07	8.93E+06	0.00E+00	5.65E+06
SET	1.32E+07	1.83E+07	1.14E+07	1.32E+07	1.39E+07	1.20E+07
NUP93	1.31E+07	9.30E+06	1.38E+07	1.55E+07	9.94E+06	1.33E+07
EIF3E	1.29E+07	8.12E+06	1.15E+07	9.62E+06	7.88E+06	1.00E+07
CASP8	1.28E+07	0.00E+00	0.00E+00	0.00E+00	0.00E+00	0.00E+00
KIF5B	1.28E+07	4.63E+06	1.25E+07	1.37E+07	3.05E+06	1.21E+07
RALY	1.27E+07	1.74E+07	1.45E+07	1.37E+07	1.83E+07	1.33E+07
PAPSS2	1.27E+07	1.11E+07	1.44E+07	1.54E+07	6.86E+06	1.47E+07
CDC37	1.25E+07	0.00E+00	7.47E+06	1.12E+07	1.87E+06	1.05E+07
ARF1	1.25E+07	1.17E+07	8.11E+06	1.20E+07	8.78E+06	1.27E+07
PEBP1	1.25E+07	5.91E+06	4.00E+06	4.62E+06	2.24E+06	1.82E+06
OGT	1.25E+07	9.46E+06	1.30E+07	1.34E+07	8.99E+06	1.42E+07
YWHAQ	1.24E+07	7.25E+06	1.01E+07	5.46E+06	1.44E+06	3.41E+06
NUP210	1.24E+07	7.57E+06	1.42E+07	1.59E+07	1.10E+07	1.63E+07
LMNB2	1.23E+07	1.60E+07	1.65E+07	1.67E+07	1.63E+07	1.54E+07
ST13	1.23E+07	6.93E+06	9.11E+06	9.21E+06	5.37E+06	5.41E+06
CAND1	1.21E+07	4.26E+06	1.09E+07	1.13E+07	0.00E+00	8.06E+06
RPS17	1.21E+07	2.11E+07	1.18E+07	7.28E+06	1.60E+07	1.21E+07
SMC2	1.19E+07	8.10E+06	1.00E+07	1.34E+07	7.74E+06	1.65E+07
FDPS	1.18E+07	6.73E+06	7.10E+06	6.32E+06	3.28E+06	2.20E+06
SRSF9	1.17E+07	1.79E+07	1.50E+07	1.32E+07	2.02E+07	1.38E+07
LTA4H	1.17E+07	0.00E+00	3.32E+06	0.00E+00	0.00E+00	0.00E+00
IMMT	1.15E+07	6.93E+06	1.33E+07	1.45E+07	7.51E+06	8.64E+06
SHMT2	1.14E+07	8.13E+06	8.06E+06	8.15E+06	1.81E+06	3.60E+06
AIMP2	1.12E+07	8.69E+06	1.27E+07	1.30E+07	4.74E+06	1.33E+07
TUBB6	1.11E+07	8.33E+06	1.14E+07	1.18E+07	9.54E+06	1.11E+07
NUDC	1.11E+07	6.80E+06	9.66E+06	1.11E+07	5.32E+06	5.44E+06
KTN1	1.10E+07	7.65E+06	1.65E+07	1.86E+07	7.63E+06	1.28E+07
SPTBN1	1.10E+07	0.00E+00	1.24E+07	1.48E+07	1.86E+06	1.24E+07
PSMA5	1.10E+07	5.97E+06	6.34E+06	3.18E+06	0.00E+00	0.00E+00
BZW2	1.10E+07	5.01E+06	1.17E+07	9.70E+06	0.00E+00	7.89E+06
DDX27	1.10E+07	2.76E+07	1.14E+07	9.32E+06	2.43E+07	1.08E+07
SAR1A	1.08E+07	5.51E+06	8.69E+06	4.91E+06	6.40E+06	6.67E+06
VPS35	1.08E+07	4.67E+06	5.66E+06	7.80E+06	0.00E+00	5.31E+06
EZR	1.08E+07	2.40E+06	6.29E+06	9.58E+06	1.65E+06	8.85E+06
GART	1.07E+07	5.80E+06	4.97E+06	9.00E+06	3.56E+06	8.53E+06
AIMP1	1.07E+07	7.26E+06	9.46E+06	1.07E+07	7.43E+06	1.04E+07
SRRM2	1.07E+07	1.80E+07	1.69E+07	1.48E+07	2.04E+07	1.64E+07
MSH6	1.07E+07	9.48E+06	1.33E+07	1.53E+07	1.16E+07	1.88E+07
UHRF1	1.07E+07	1.68E+07	1.65E+07	1.48E+07	2.30E+07	1.50E+07
EDF1	1.06E+07	1.12E+07	3.16E+06	6.05E+06	7.97E+06	0.00E+00
KHDRBS1	1.05E+07	1.37E+07	1.39E+07	1.26E+07	1.36E+07	8.27E+06
MYBBP1A	1.04E+07	4.29E+07	1.53E+07	1.13E+07	4.21E+07	1.09E+07
SERPINH1	1.04E+07	4.56E+06	8.26E+06	7.95E+06	3.84E+06	4.87E+06
SRP14	1.04E+07	1.13E+07	1.03E+07	8.67E+06	7.22E+06	9.62E+06
RBBP4	1.04E+07	9.94E+06	1.24E+07	7.58E+06	5.60E+06	2.86E+06
SEC61B	1.04E+07	1.50E+07	1.07E+07	7.21E+06	1.63E+07	9.41E+06
MDH2	1.04E+07	6.40E+06	3.59E+06	4.94E+06	1.26E+06	0.00E+00
CAPZA1	1.04E+07	8.89E+06	1.27E+07	1.32E+07	9.22E+06	1.12E+07
ATP5C1	1.03E+07	1.10E+07	9.63E+06	1.05E+07	1.22E+07	6.64E+06
DHX30	1.03E+07	9.45E+06	1.01E+07	1.01E+07	9.65E+06	9.88E+06

NACA	1.03E+07	7.40E+06	9.91E+06	7.70E+06	8.60E+06	0.00E+00
HMGB3	1.02E+07	1.34E+07	7.68E+06	5.52E+06	1.25E+07	9.82E+06
SEC24C	1.02E+07	2.09E+06	1.08E+07	7.01E+06	3.79E+06	1.02E+07
TBL1XR1	1.02E+07	7.19E+06	1.25E+07	1.33E+07	8.23E+06	1.18E+07
TUBA4A	1.01E+07	6.45E+06	9.41E+06	1.02E+07	8.00E+06	1.18E+07
MISP	1.01E+07	5.13E+06	1.13E+07	1.08E+07	5.87E+06	1.05E+07
PSMD10	1.01E+07	7.65E+06	1.05E+07	8.95E+06	7.01E+06	8.23E+06
TIAL1	1.00E+07	9.49E+06	9.73E+06	6.46E+06	5.18E+06	4.90E+06
LGALS3	1.00E+07	0.00E+00	0.00E+00	0.00E+00	0.00E+00	0.00E+00
SRRT	1.00E+07	9.00E+06	1.21E+07	1.15E+07	8.32E+06	7.94E+06
STAT3	1.00E+07	5.22E+06	1.08E+07	9.54E+06	7.72E+06	8.09E+06
DDX19A	9.92E+06	6.51E+06	9.79E+06	9.92E+06	6.38E+06	9.06E+06
G3BP1	9.80E+06	3.79E+06	7.19E+06	7.87E+06	7.48E+06	7.71E+06
ATP5B	9.76E+06	8.17E+06	8.38E+06	9.65E+06	7.33E+06	7.73E+06
VDAC3	9.75E+06	7.86E+06	9.38E+06	1.04E+07	9.14E+06	9.99E+06
NSF	9.71E+06	1.21E+07	9.30E+06	9.67E+06	0.00E+00	8.70E+06
EFHD2	9.71E+06	8.16E+06	9.80E+06	1.05E+07	6.54E+06	7.09E+06
RPL38	9.69E+06	6.17E+06	9.65E+06	0.00E+00	1.47E+07	1.13E+07
OLA1	9.68E+06	5.20E+06	7.92E+06	5.75E+06	1.56E+06	6.74E+06
MAP4	9.65E+06	5.41E+06	6.44E+06	1.13E+07	7.83E+06	8.12E+06
WDR74	9.64E+06	1.82E+07	1.75E+07	1.12E+07	1.90E+07	1.58E+07
CLUH	9.57E+06	4.44E+06	9.53E+06	6.44E+06	4.27E+06	2.52E+06
ARCN1	9.56E+06	8.12E+06	1.11E+07	1.01E+07	7.06E+06	9.52E+06
JUP	9.55E+06	4.33E+06	1.28E+07	1.29E+07	1.12E+07	3.14E+07
COPG1	9.52E+06	7.48E+06	1.08E+07	1.10E+07	4.78E+06	1.27E+07
IFIT1	9.48E+06	1.84E+06	6.24E+06	1.11E+07	4.53E+06	9.30E+06
EIF3F	9.45E+06	7.06E+06	7.40E+06	5.05E+06	1.62E+06	4.10E+06
CALD1	9.35E+06	4.60E+06	5.90E+06	9.15E+06	1.72E+06	4.35E+06
PRDX3	9.32E+06	4.53E+06	5.41E+06	6.34E+06	2.56E+06	2.42E+06
YWHAB	9.28E+06	6.25E+06	6.20E+06	4.91E+06	0.00E+00	2.60E+06
TLN1	9.25E+06	3.07E+06	1.14E+07	9.43E+06	4.98E+06	8.65E+06
PFKP	9.24E+06	0.00E+00	7.62E+06	8.42E+06	1.51E+06	5.76E+06
SBDS	9.21E+06	2.45E+06	8.63E+06	5.43E+06	7.07E+06	7.34E+06
CSTF1	9.12E+06	4.74E+06	9.13E+06	1.07E+07	4.74E+06	1.26E+07
THRAP3	9.04E+06	8.29E+06	8.17E+06	7.13E+06	6.12E+06	4.27E+06
BOLA2	9.02E+06	3.11E+06	5.88E+06	2.88E+06	4.73E+06	5.39E+06
NSA2	9.00E+06	3.64E+07	1.51E+07	9.13E+06	4.13E+07	9.95E+06
SRSF10	8.97E+06	1.37E+07	9.03E+06	9.30E+06	1.43E+07	1.23E+07
SMARCA4	8.84E+06	8.60E+06	1.01E+07	1.11E+07	1.01E+07	1.03E+07
SRPRB	8.83E+06	8.79E+06	9.99E+06	1.13E+07	8.06E+06	6.42E+06
RDH11	8.82E+06	7.79E+06	1.11E+07	7.37E+06	7.87E+06	6.77E+06
BAG2	8.79E+06	6.32E+06	7.74E+06	9.06E+06	5.76E+06	5.45E+06
VAPA	8.76E+06	7.91E+06	8.56E+06	9.70E+06	6.49E+06	8.49E+06
YARS	8.75E+06	5.87E+06	7.39E+06	7.34E+06	0.00E+00	3.59E+06
ARIH1	8.74E+06	8.63E+06	1.14E+07	1.15E+07	1.06E+07	1.46E+07
MYOF	8.73E+06	8.30E+06	1.05E+07	1.12E+07	8.89E+06	1.03E+07
DNAJB1	8.70E+06	7.21E+06	8.80E+06	2.95E+06	3.38E+06	7.27E+06
RPN2	8.66E+06	8.21E+06	3.32E+06	0.00E+00	6.25E+06	2.69E+06
EXOSC10	8.66E+06	7.79E+06	9.21E+06	8.09E+06	5.11E+06	9.70E+06
PARK7	8.60E+06	1.77E+06	0.00E+00	5.06E+06	0.00E+00	0.00E+00
GNAI3	8.57E+06	2.21E+06	2.51E+06	2.61E+06	0.00E+00	2.68E+06
PPP1CB	8.50E+06	7.90E+06	3.44E+06	2.28E+06	2.55E+06	5.44E+06
CENPV	8.47E+06	3.87E+07	1.06E+07	6.33E+06	4.05E+07	1.26E+07
TBL3	8.47E+06	6.25E+06	1.12E+07	1.18E+07	6.13E+06	1.09E+07
HSPE1	8.43E+06	5.95E+06	3.70E+06	6.64E+06	2.12E+06	1.67E+06
TPM4	8.43E+06	3.73E+06	5.74E+06	1.48E+07	0.00E+00	1.06E+07
PPIB	8.41E+06	6.43E+06	5.52E+06	4.53E+06	4.49E+06	2.11E+06
SRI	8.40E+06	2.38E+06	4.80E+06	4.20E+06	0.00E+00	0.00E+00
HNRNPH2	8.39E+06	3.07E+06	6.52E+06	1.01E+07	1.00E+07	1.39E+07
SNRPD1	8.39E+06	2.40E+07	0.00E+00	0.00E+00	3.45E+07	4.91E+06
EIF1AX	8.37E+06	8.02E+06	4.83E+06	0.00E+00	7.09E+06	0.00E+00
TBL2	8.36E+06	6.60E+06	9.70E+06	8.25E+06	6.76E+06	1.08E+07
TSFM	8.35E+06	6.87E+06	5.98E+06	3.58E+06	0.00E+00	0.00E+00
PMPCB	8.31E+06	5.12E+06	5.48E+06	3.50E+06	1.55E+06	1.09E+06
NNT	8.31E+06	6.12E+06	4.84E+06	5.06E+06	1.72E+06	0.00E+00
PSMC2	8.30E+06	6.14E+06	8.80E+06	8.24E+06	4.52E+06	5.39E+06
NAP1L1	8.30E+06	7.35E+06	4.43E+06	0.00E+00	4.62E+06	2.36E+06
DDX23	8.28E+06	8.75E+06	9.38E+06	8.88E+06	7.98E+06	3.25E+06
HAT1	8.22E+06	4.49E+06	7.96E+06	7.48E+06	2.08E+06	2.41E+06
DSTN	8.20E+06	5.56E+06	6.48E+06	7.42E+06	3.17E+06	7.09E+06
EWSR1	8.13E+06	8.32E+06	8.82E+06	8.94E+06	8.32E+06	8.28E+06
EIF3H	8.11E+06	4.39E+06	7.77E+06	7.10E+06	4.18E+06	4.74E+06
ALDH3A2	8.10E+06	8.23E+06	5.90E+06	1.02E+07	8.46E+06	8.94E+06
PFKM	8.10E+06	4.80E+06	4.37E+06	4.54E+06	3.10E+06	5.88E+06
SSBP1	8.08E+06	5.33E+06	6.99E+06	6.66E+06	4.25E+06	5.29E+06
ETF1	8.07E+06	3.54E+06	5.68E+06	0.00E+00	3.16E+06	3.61E+06
ETFA	8.06E+06	3.90E+06	0.00E+00	1.88E+06	1.11E+06	0.00E+00
PPAN	7.95E+06	2.28E+07	1.16E+07	5.88E+06	2.61E+07	9.21E+06
FAM98B	7.91E+06	6.53E+06	5.37E+06	5.16E+06	2.19E+06	6.58E+06
DCD	7.76E+06	4.56E+06	9.72E+06	9.78E+06	8.45E+06	5.07E+06
HNRNPUL1	7.75E+06	6.75E+06	6.97E+06	7.62E+06	3.91E+06	2.09E+06
UBTF	7.73E+06	2.16E+07	1.13E+07	3.93E+06	1.77E+07	7.27E+06
PSMA4	7.69E+06	1.26E+07	1.36E+07	4.16E+06	2.04E+06	1.07E+07
TOMM70A	7.65E+06	1.88E+06	6.22E+06	6.32E+06	0.00E+00	3.12E+06
RRP12	7.62E+06	1.35E+07	9.49E+06	7.38E+06	1.20E+07	1.02E+07
PDHB	7.62E+06	3.72E+06	2.16E+06	0.00E+00	0.00E+00	4.76E+06
EIF6	7.61E+06	9.52E+06	6.95E+06	5.99E+06	1.26E+07	4.29E+06
YWHAH	7.57E+06	5.48E+06	0.00E+00	6.87E+06	0.00E+00	0.00E+00
MYO1E	7.53E+06	5.72E+06	7.71E+06	8.25E+06	4.24E+06	9.56E+06
PRPF4	7.50E+06	6.69E+06	9.08E+06	9.33E+06	8.34E+06	8.79E+06
SNW1	7.49E+06	6.77E+06	8.28E+06	7.88E+06	3.96E+06	7.59E+06
PRPF6	7.49E+06	6.39E+06	9.45E+06	1.13E+07	7.18E+06	1.04E+07
DIS3	7.49E+06	6.79E+06	8.20E+06	9.53E+06	8.70E+06	1.09E+07
CPSF7	7.49E+06	6.64E+06	7.88E+06	8.07E+06	4.41E+06	8.28E+06
KYNU	7.45E+06	1.72E+06	2.29E+06	2.88E+06	3.24E+06	2.02E+06
RPS21	7.44E+06	9.65E+06	5.57E+06	1.73E+06	3.30E+06	3.25E+06
HK2	7.43E+06	0.00E+00	5.00E+06	7.09E+06	0.00E+00	3.80E+06
ADSS	7.43E+06	3.50E+06	4.65E+06	5.67E+06	1.70E+06	5.67E+06
RHOA	7.43E+06	5.25E+06	7.29E+06	8.60E+06	2.07E+06	0.00E+00
SRSF5	7.34E+06	1.15E+07	9.96E+06	5.57E+06	1.47E+07	5.58E+06
TECR	7.33E+06	9.46E+06	9.35E+06	5.76E+06	8.11E+06	9.15E+06
SMU1	7.31E+06	5.31E+06	7.47E+06	7.77E+06	6.02E+06	9.23E+06

TES	7.30E+06	5.90E+06	9.28E+06	8.28E+06	5.70E+06	4.36E+06
ATXN10	7.26E+06	5.72E+06	9.32E+06	8.17E+06	5.11E+06	7.08E+06
RFC2	7.26E+06	2.55E+06	8.08E+06	6.02E+06	4.08E+06	6.98E+06
ADK	7.26E+06	0.00E+00	0.00E+00	0.00E+00	0.00E+00	0.00E+00
EIF2AK2	7.22E+06	6.38E+06	6.54E+06	7.59E+06	6.67E+06	8.44E+06
RBM8A	7.19E+06	1.26E+07	6.78E+06	0.00E+00	1.48E+07	6.66E+06
ACSL3	7.18E+06	4.48E+06	7.52E+06	8.94E+06	4.18E+06	7.69E+06
PSMC1	7.18E+06	0.00E+00	3.89E+06	0.00E+00	0.00E+00	0.00E+00
COTL1	7.17E+06	2.04E+06	3.88E+06	4.48E+06	0.00E+00	0.00E+00
PABPN1	7.15E+06	7.13E+06	6.43E+06	5.60E+06	3.39E+06	4.79E+06
SNRPA1	7.15E+06	6.09E+06	5.92E+06	6.09E+06	3.63E+06	4.56E+06
RAB1A	7.09E+06	4.69E+06	8.05E+06	9.41E+06	8.13E+06	6.27E+06
PSMD2	6.99E+06	3.61E+06	6.20E+06	4.94E+06	1.69E+06	0.00E+00
GFM1	6.98E+06	5.44E+06	4.21E+06	4.31E+06	7.86E+05	7.76E+05
MAGOHB	6.98E+06	8.73E+06	7.07E+06	4.96E+06	9.40E+06	7.66E+06
TGM2	6.97E+06	4.75E+06	5.83E+06	5.89E+06	2.61E+06	3.72E+06
DDOST	6.93E+06	5.88E+06	6.49E+06	3.44E+06	6.82E+06	3.48E+06
RPLP0	6.86E+06	7.46E+06	7.13E+06	5.07E+06	6.55E+06	5.97E+06
PLAA	6.86E+06	0.00E+00	8.22E+06	8.77E+06	2.55E+06	7.99E+06
PUF60	6.85E+06	3.21E+06	0.00E+00	2.48E+06	1.37E+06	2.00E+06
LBR	6.84E+06	9.93E+06	6.56E+06	7.79E+06	9.95E+06	9.20E+06
HSPH1	6.79E+06	1.10E+06	1.38E+06	2.94E+06	9.17E+05	3.49E+06
HMGA1	6.79E+06	5.57E+07	9.59E+06	5.71E+06	4.58E+07	1.96E+06
LUC7L3	6.79E+06	4.59E+06	6.00E+06	7.71E+06	7.41E+06	5.39E+06
SF1	6.76E+06	4.94E+06	5.81E+06	6.05E+06	1.52E+06	6.01E+06
STT3A	6.73E+06	7.98E+06	8.08E+06	8.58E+06	1.06E+07	9.92E+06
SURF6	6.69E+06	3.82E+07	1.51E+07	0.00E+00	3.38E+07	7.88E+06
PAFAH1B1	6.59E+06	1.79E+06	6.37E+06	6.73E+06	3.38E+06	1.73E+06
GPATCH4	6.59E+06	1.29E+07	8.19E+06	4.40E+06	1.42E+07	6.19E+06
NMD3	6.57E+06	7.79E+06	6.82E+06	5.65E+06	5.10E+06	8.30E+06
POR	6.55E+06	5.07E+06	5.53E+06	6.23E+06	2.67E+06	5.91E+06
NOC2L	6.50E+06	1.14E+07	7.74E+06	8.32E+06	1.41E+07	8.37E+06
PSMD11	6.49E+06	1.39E+06	3.30E+06	4.16E+06	0.00E+00	0.00E+00
RPF2	6.47E+06	2.91E+07	1.19E+07	9.91E+06	3.71E+07	1.19E+07
CAT	6.43E+06	4.98E+06	7.07E+06	7.04E+06	3.59E+06	4.53E+06
RAB5C	6.41E+06	5.87E+06	7.33E+06	7.65E+06	4.36E+06	6.87E+06
RPS19	6.40E+06	7.02E+06	5.76E+06	3.82E+06	6.55E+06	6.35E+06
ACADM	6.40E+06	3.33E+06	2.74E+06	1.38E+06	0.00E+00	0.00E+00
HMGN3	6.36E+06	4.44E+07	1.54E+07	3.36E+06	4.25E+07	0.00E+00
PSMD3	6.33E+06	0.00E+00	6.95E+06	3.62E+06	0.00E+00	2.71E+06
TXNDC17	6.32E+06	3.61E+06	6.00E+06	2.03E+06	0.00E+00	1.70E+06
CPNE3	6.26E+06	1.50E+06	1.83E+06	3.46E+06	2.57E+06	4.64E+06
UBR4	6.25E+06	0.00E+00	6.48E+06	7.89E+06	0.00E+00	2.26E+06
CAP1	6.24E+06	0.00E+00	1.61E+06	3.14E+06	0.00E+00	3.04E+06
SEC13	6.22E+06	1.41E+06	4.71E+06	0.00E+00	3.52E+06	2.13E+06
PRPF3	6.22E+06	2.53E+06	2.50E+06	6.31E+06	3.41E+06	5.05E+06
SRP72	6.21E+06	6.46E+06	6.28E+06	5.32E+06	5.54E+06	5.30E+06
SEC31A	6.20E+06	3.09E+06	6.37E+06	5.73E+06	0.00E+00	3.51E+06
CPT1A	6.19E+06	0.00E+00	6.82E+06	7.55E+06	3.25E+06	7.80E+06
MAPK1	6.14E+06	1.79E+06	3.30E+06	2.80E+06	9.15E+05	0.00E+00
PAK1IP1	6.14E+06	7.83E+06	6.59E+06	5.03E+06	9.35E+06	5.54E+06
UPF1	6.14E+06	0.00E+00	3.28E+06	1.29E+06	0.00E+00	2.83E+06
SSB	6.10E+06	3.42E+06	3.21E+06	0.00E+00	0.00E+00	0.00E+00
CDC5L	6.08E+06	3.14E+06	5.89E+06	2.13E+06	2.78E+06	4.18E+06
ANP32A	6.07E+06	4.20E+06	1.42E+06	0.00E+00	1.44E+06	0.00E+00
CECR5	6.01E+06	3.05E+06	4.10E+06	0.00E+00	0.00E+00	1.23E+06
FUBP3	6.00E+06	2.73E+06	2.62E+06	8.80E+06	5.35E+06	4.41E+06
KIF4A	5.97E+06	5.23E+06	7.73E+06	8.80E+06	4.37E+06	8.56E+06
CAPZB	5.95E+06	0.00E+00	5.83E+06	1.04E+07	7.67E+06	1.02E+07
BAZ1B	5.95E+06	2.74E+07	1.05E+07	9.35E+06	4.66E+07	1.17E+07
PDLIM1	5.89E+06	1.48E+06	4.73E+06	2.97E+06	0.00E+00	1.03E+06
NUP155	5.88E+06	3.24E+06	7.99E+06	7.15E+06	1.87E+06	6.80E+06
COX5B	5.86E+06	1.55E+06	1.42E+06	0.00E+00	0.00E+00	0.00E+00
GDI2	5.84E+06	1.94E+06	0.00E+00	2.62E+06	0.00E+00	0.00E+00
NKRF	5.83E+06	8.59E+06	8.44E+06	8.30E+06	1.08E+07	7.59E+06
CHTOP	5.81E+06	1.26E+07	6.88E+06	0.00E+00	1.23E+07	4.31E+06
ZNF326	5.76E+06	6.96E+06	7.67E+06	6.31E+06	7.38E+06	6.42E+06
MTHFD1L	5.69E+06	4.12E+06	4.93E+06	3.11E+06	1.34E+06	0.00E+00
SNRNP40	5.69E+06	0.00E+00	0.00E+00	3.54E+06	3.59E+06	0.00E+00
PDCD6IP	5.66E+06	9.84E+05	3.05E+06	3.23E+06	2.49E+06	1.89E+06
ISG15	5.64E+06	4.41E+06	2.26E+06	4.49E+06	4.14E+06	3.44E+06
GSTP1	5.63E+06	1.26E+06	0.00E+00	2.41E+06	0.00E+00	0.00E+00
BCLAF1	5.62E+06	5.29E+06	6.66E+06	3.32E+06	4.10E+06	3.02E+06
CHD4	5.55E+06	1.89E+06	4.32E+06	2.66E+06	3.59E+06	3.71E+06
ACTN1	5.48E+06	2.08E+06	3.89E+06	1.64E+06	2.35E+06	5.40E+06
EIF5B	5.45E+06	5.11E+06	3.01E+06	7.46E+06	7.22E+06	3.09E+06
COPE	5.43E+06	1.52E+06	4.85E+06	4.61E+06	0.00E+00	4.05E+06
EIF4G2	5.42E+06	1.69E+06	5.32E+06	5.14E+06	0.00E+00	3.51E+06
PDLIM5	5.42E+06	4.77E+06	7.61E+06	7.38E+06	2.95E+06	6.52E+06
STOM	5.38E+06	9.43E+06	1.65E+07	1.81E+07	1.79E+07	1.37E+07
CKAP4	5.36E+06	0.00E+00	2.20E+06	4.12E+06	1.94E+06	2.15E+06
CUL4A	5.27E+06	0.00E+00	6.52E+06	4.47E+06	3.68E+06	3.44E+06
STEAP4	5.24E+06	0.00E+00	1.14E+06	3.01E+06	0.00E+00	1.44E+06
AK1	5.22E+06	1.52E+06	2.16E+06	0.00E+00	0.00E+00	0.00E+00
COPZ1	5.18E+06	1.32E+06	0.00E+00	4.75E+06	0.00E+00	9.95E+05
ATP1A1	5.18E+06	1.43E+06	1.30E+06	5.35E+06	0.00E+00	4.62E+06
TRIP13	5.14E+06	2.64E+06	4.52E+06	3.75E+06	0.00E+00	1.47E+06
KRT6B	5.10E+06	0.00E+00	0.00E+00	0.00E+00	0.00E+00	0.00E+00
GLS	5.06E+06	1.64E+06	1.40E+06	1.22E+06	0.00E+00	0.00E+00
LARP4	5.03E+06	3.01E+06	4.89E+06	5.37E+06	2.55E+06	4.05E+06
BLVRB	5.02E+06	0.00E+00	1.33E+06	0.00E+00	0.00E+00	0.00E+00
PRMT5	5.01E+06	0.00E+00	3.81E+06	5.86E+06	1.31E+06	2.66E+06
SAFB	4.99E+06	1.12E+07	9.17E+06	8.59E+06	1.29E+07	8.36E+06
DAZAP1	4.96E+06	1.95E+06	3.65E+06	2.73E+06	3.14E+06	4.96E+06
SKIV2L2	4.95E+06	4.03E+06	4.32E+06	4.42E+06	3.46E+06	5.18E+06
AIP	4.91E+06	2.85E+06	3.18E+06	3.05E+06	0.00E+00	1.30E+06
SEPT9	4.85E+06	4.45E+06	9.26E+06	9.23E+06	5.87E+06	7.75E+06
IFIT3	4.84E+06	0.00E+00	1.98E+06	7.76E+06	3.89E+06	4.09E+06
MAT2A	4.81E+06	1.16E+06	2.45E+06	1.45E+06	1.33E+06	0.00E+00
CHCHD3	4.80E+06	0.00E+00	8.13E+06	8.71E+06	0.00E+00	4.15E+06
RAB11A	4.72E+06	0.00E+00	0.00E+00	4.59E+06	0.00E+00	0.00E+00
TXLNA	4.70E+06	1.76E+06	6.66E+06	2.15E+06	0.00E+00	0.00E+00

SEPT2	4.68E+06	0.00E+00	4.65E+06	2.58E+06	0.00E+00	0.00E+00
FXR2	4.68E+06	0.00E+00	2.15E+06	1.60E+06	0.00E+00	0.00E+00
UBE2T	4.66E+06	1.46E+06	0.00E+00	0.00E+00	0.00E+00	1.23E+06
HLA-A	4.65E+06	5.93E+06	4.52E+06	7.85E+06	2.60E+06	7.02E+06
ACO2	4.64E+06	0.00E+00	0.00E+00	0.00E+00	0.00E+00	0.00E+00
NFKB2	4.64E+06	2.27E+06	1.00E+07	7.16E+06	1.57E+06	5.03E+06
EMG1	4.64E+06	7.86E+06	3.97E+06	3.73E+06	7.07E+06	7.54E+06
ILF2	4.63E+06	1.92E+06	0.00E+00	0.00E+00	1.96E+06	1.12E+06
TTLL12	4.63E+06	0.00E+00	3.18E+06	0.00E+00	0.00E+00	0.00E+00
ERLIN2	4.61E+06	4.34E+06	5.79E+06	7.08E+06	4.42E+06	5.79E+06
CANX	4.60E+06	6.04E+06	3.62E+06	1.89E+06	3.63E+06	4.55E+06
PNPT1	4.59E+06	2.55E+06	1.45E+06	0.00E+00	0.00E+00	0.00E+00
LSM12	4.53E+06	4.20E+06	3.52E+06	3.90E+06	8.44E+05	1.21E+06
DDX24	4.46E+06	2.31E+07	8.56E+06	4.70E+06	2.31E+07	1.33E+06
PSMA7	4.46E+06	2.29E+06	4.85E+06	8.55E+06	1.94E+06	2.71E+06
CDC73	4.45E+06	4.16E+06	5.58E+06	0.00E+00	1.31E+06	1.91E+06
COX4I1	4.39E+06	0.00E+00	0.00E+00	0.00E+00	0.00E+00	0.00E+00
HDGF	4.39E+06	1.50E+07	3.68E+06	0.00E+00	1.33E+07	6.17E+06
DDB1	4.39E+06	0.00E+00	0.00E+00	0.00E+00	0.00E+00	4.70E+06
RBM12	4.38E+06	2.09E+06	3.42E+06	1.28E+06	0.00E+00	0.00E+00
ANXA11	4.36E+06	0.00E+00	0.00E+00	0.00E+00	0.00E+00	0.00E+00
KIAA0020	4.32E+06	1.64E+07	3.50E+06	0.00E+00	2.11E+07	1.48E+06
UTP11L	4.31E+06	1.22E+07	4.74E+06	0.00E+00	2.23E+07	3.90E+06
AGPS	4.31E+06	1.03E+06	3.36E+06	2.15E+06	0.00E+00	1.18E+06
CTPS1	4.28E+06	4.79E+06	5.58E+06	3.58E+06	1.20E+06	5.79E+06
IGF2BP3	4.27E+06	1.38E+06	4.71E+06	0.00E+00	1.24E+06	1.43E+06
CARS	4.25E+06	0.00E+00	1.56E+06	2.85E+06	0.00E+00	1.19E+06
UBA2	4.22E+06	0.00E+00	1.47E+06	2.38E+06	0.00E+00	0.00E+00
IARS2	4.16E+06	1.99E+06	0.00E+00	0.00E+00	0.00E+00	0.00E+00
NAA15	4.16E+06	0.00E+00	0.00E+00	0.00E+00	0.00E+00	0.00E+00
DDX50	4.14E+06	2.13E+07	8.46E+06	6.25E+06	1.55E+07	4.19E+06
GLUD1	4.10E+06	1.17E+06	0.00E+00	2.24E+06	0.00E+00	0.00E+00
SRP68	4.10E+06	0.00E+00	0.00E+00	9.29E+05	0.00E+00	8.90E+05
XIAP	4.09E+06	3.28E+06	5.05E+06	5.29E+06	2.16E+06	3.50E+06
VPS26A	4.06E+06	1.95E+06	3.74E+06	2.77E+06	8.33E+05	0.00E+00
PGAM5	4.06E+06	0.00E+00	1.93E+06	5.12E+06	0.00E+00	6.05E+06
LIMA1	4.06E+06	2.61E+06	7.32E+06	1.74E+06	9.55E+05	5.34E+06
NPM3	4.05E+06	6.49E+06	2.49E+06	2.39E+06	5.43E+06	0.00E+00
MYH11	4.02E+06	0.00E+00	0.00E+00	0.00E+00	0.00E+00	0.00E+00
GCLM	4.02E+06	1.51E+06	4.29E+06	0.00E+00	0.00E+00	0.00E+00
USP14	3.95E+06	0.00E+00	0.00E+00	1.14E+06	0.00E+00	0.00E+00
RRP1B	3.94E+06	2.91E+07	1.01E+07	6.36E+06	2.29E+07	4.07E+06
VAPB	3.93E+06	0.00E+00	1.52E+06	1.38E+06	9.16E+05	1.12E+06
WDR12	3.88E+06	5.24E+06	1.86E+06	0.00E+00	5.75E+06	0.00E+00
RELA	3.87E+06	0.00E+00	5.48E+06	0.00E+00	0.00E+00	3.65E+06
STK26	3.86E+06	1.92E+06	0.00E+00	0.00E+00	8.61E+05	1.04E+06
RPS27L	3.86E+06	1.87E+07	8.80E+06	1.05E+07	2.38E+07	8.01E+06
DCAF13	3.84E+06	1.09E+07	6.92E+06	3.17E+06	1.27E+07	4.78E+06
UBE2V1	3.83E+06	0.00E+00	0.00E+00	0.00E+00	0.00E+00	0.00E+00
LYAR	3.82E+06	2.07E+07	3.13E+06	3.44E+06	2.55E+07	3.80E+06
ZC3H11A	3.75E+06	1.70E+06	4.55E+06	1.72E+06	2.00E+06	1.25E+06
RRS1	3.74E+06	3.40E+07	4.68E+06	1.37E+06	4.45E+07	7.25E+06
HDAC2	3.73E+06	1.41E+06	3.84E+06	2.82E+06	1.56E+06	4.11E+06
CYB5R3	3.71E+06	3.36E+06	3.66E+06	3.60E+06	2.90E+06	2.18E+06
SMS	3.67E+06	0.00E+00	0.00E+00	0.00E+00	0.00E+00	0.00E+00
SF3B2	3.62E+06	0.00E+00	0.00E+00	3.06E+06	0.00E+00	1.59E+06
YTHDF2	3.57E+06	1.45E+06	4.40E+06	0.00E+00	1.36E+06	0.00E+00
WDHD1	3.55E+06	0.00E+00	6.12E+06	6.46E+06	2.77E+06	7.26E+06
PCCB	3.54E+06	3.93E+06	1.22E+06	2.99E+06	1.93E+06	0.00E+00
MACROD1	3.53E+06	2.61E+06	2.89E+06	0.00E+00	0.00E+00	0.00E+00
SYNCRIP	3.51E+06	3.86E+06	3.63E+06	1.67E+06	0.00E+00	1.18E+06
NOP16	3.49E+06	1.76E+07	4.01E+06	6.39E+05	8.18E+06	0.00E+00
ACTL8	3.48E+06	1.34E+06	0.00E+00	0.00E+00	0.00E+00	0.00E+00
HACD3	3.47E+06	1.02E+07	1.18E+07	5.43E+06	1.60E+07	1.62E+07
TBCB	3.44E+06	9.95E+05	1.14E+06	0.00E+00	0.00E+00	0.00E+00
PFN2	3.39E+06	0.00E+00	0.00E+00	0.00E+00	2.07E+06	0.00E+00
RBM3	3.35E+06	4.55E+06	0.00E+00	2.36E+06	3.02E+06	2.14E+06
KPNA6	3.31E+06	1.07E+06	2.89E+06	1.03E+06	0.00E+00	0.00E+00
HSPA4L	3.29E+06	0.00E+00	0.00E+00	1.15E+06	0.00E+00	0.00E+00
FKBP3	3.25E+06	1.76E+06	0.00E+00	1.44E+06	1.37E+06	0.00E+00
PMPCA	3.24E+06	2.08E+07	4.29E+06	0.00E+00	0.00E+00	0.00E+00
NHP2L1	3.23E+06	5.51E+06	3.66E+06	3.45E+06	6.48E+06	0.00E+00
PFDN2	3.22E+06	0.00E+00	0.00E+00	0.00E+00	0.00E+00	0.00E+00
MCCC2	3.20E+06	1.91E+06	0.00E+00	8.95E+05	9.12E+05	0.00E+00
PPP2R1A	3.17E+06	0.00E+00	1.50E+06	0.00E+00	0.00E+00	0.00E+00
UBAP2L	3.16E+06	3.80E+06	4.60E+06	4.40E+06	1.29E+06	1.63E+06
DDX20	3.16E+06	0.00E+00	3.65E+06	3.66E+06	0.00E+00	5.58E+06
PCMT1	3.15E+06	0.00E+00	0.00E+00	0.00E+00	0.00E+00	0.00E+00
PSMC5	3.11E+06	2.03E+06	3.42E+06	3.00E+06	0.00E+00	6.45E+05
C1QBP	3.09E+06	0.00E+00	1.09E+06	1.09E+06	0.00E+00	1.09E+06
TLE3	3.09E+06	3.21E+06	5.47E+06	6.85E+06	3.36E+06	7.12E+06
RRP15	3.06E+06	5.02E+06	1.00E+06	0.00E+00	1.63E+06	0.00E+00
DYNC1I2	3.06E+06	1.30E+06	5.24E+06	4.17E+06	3.67E+06	4.00E+06
SF3A3	3.03E+06	0.00E+00	0.00E+00	0.00E+00	0.00E+00	0.00E+00
ZFR	3.01E+06	2.87E+06	5.58E+06	4.85E+06	2.83E+06	3.28E+06
HSDL2	3.01E+06	1.15E+06	0.00E+00	0.00E+00	0.00E+00	0.00E+00
WDR61	3.01E+06	1.81E+06	2.82E+06	3.04E+06	1.48E+06	3.67E+06
SDHB	2.98E+06	8.07E+05	0.00E+00	0.00E+00	0.00E+00	0.00E+00
DNM1L	2.97E+06	0.00E+00	0.00E+00	0.00E+00	0.00E+00	0.00E+00
STMN1	2.87E+06	0.00E+00	0.00E+00	0.00E+00	0.00E+00	4.88E+06
PRRC2C	2.86E+06	0.00E+00	2.38E+06	1.09E+06	9.23E+05	1.22E+06
CORO1C	2.85E+06	0.00E+00	1.84E+06	0.00E+00	0.00E+00	0.00E+00
CTNND1	2.82E+06	0.00E+00	3.19E+06	5.71E+06	1.73E+06	1.56E+06
AP1M1	2.81E+06	0.00E+00	0.00E+00	0.00E+00	0.00E+00	0.00E+00
CPNE1	2.78E+06	0.00E+00	0.00E+00	0.00E+00	0.00E+00	0.00E+00
PKP2	2.78E+06	4.55E+06	9.59E+06	9.53E+06	8.20E+06	9.38E+06
STAT1	2.75E+06	0.00E+00	1.12E+06	0.00E+00	0.00E+00	0.00E+00
CTNNA1	2.75E+06	9.84E+05	1.13E+06	2.51E+06	0.00E+00	1.02E+06
BLVRA	2.74E+06	7.42E+05	0.00E+00	0.00E+00	0.00E+00	8.22E+05
ATXN2L	2.73E+06	0.00E+00	3.43E+06	0.00E+00	0.00E+00	1.24E+06
WDR36	2.71E+06	2.54E+06	1.60E+06	3.15E+06	4.97E+06	5.25E+06
MRPL47	2.69E+06	4.05E+06	0.00E+00	0.00E+00	5.93E+06	2.63E+06

NCAPD2	2.62E+06	7.91E+05	3.11E+06	3.88E+06	0.00E+00	9.54E+05
WDR5	2.61E+06	3.07E+06	2.61E+06	2.60E+06	3.36E+06	4.80E+06
CAPRIN1	2.59E+06	1.91E+06	0.00E+00	2.48E+06	0.00E+00	0.00E+00
GATAD2B	2.59E+06	0.00E+00	4.45E+06	4.78E+06	1.64E+06	0.00E+00
TMEM33	2.58E+06	2.67E+06	1.28E+06	0.00E+00	0.00E+00	1.56E+06
KIF23	2.56E+06	1.72E+06	7.02E+06	4.06E+06	7.21E+06	7.56E+06
GLTSCR2	2.56E+06	1.86E+07	2.50E+06	0.00E+00	1.68E+07	6.16E+06
DNTTIP2	2.54E+06	1.02E+07	0.00E+00	0.00E+00	1.31E+07	0.00E+00
CPSF2	2.53E+06	0.00E+00	2.84E+06	1.71E+06	0.00E+00	0.00E+00
TRMT1	2.52E+06	1.42E+06	1.51E+06	1.88E+06	1.45E+06	2.65E+06
CARM1	2.50E+06	0.00E+00	0.00E+00	0.00E+00	0.00E+00	0.00E+00
NEDD8	2.49E+06	0.00E+00	0.00E+00	0.00E+00	0.00E+00	0.00E+00
EIF5	2.47E+06	0.00E+00	2.50E+06	0.00E+00	0.00E+00	0.00E+00
TARS	2.47E+06	0.00E+00	0.00E+00	2.41E+06	0.00E+00	3.24E+06
PSMA6	2.46E+06	0.00E+00	0.00E+00	0.00E+00	0.00E+00	0.00E+00
EIF3J	2.43E+06	0.00E+00	0.00E+00	0.00E+00	0.00E+00	0.00E+00
TYMS	2.39E+06	8.81E+05	7.27E+05	0.00E+00	0.00E+00	0.00E+00
PCID2	2.38E+06	1.96E+06	4.40E+06	3.35E+06	2.19E+06	4.21E+06
SOAT1	2.38E+06	3.32E+06	3.21E+06	1.69E+06	5.52E+06	2.71E+06
PRPS2	2.37E+06	0.00E+00	1.11E+06	0.00E+00	0.00E+00	0.00E+00
MGST1	2.32E+06	0.00E+00	1.90E+06	0.00E+00	0.00E+00	3.57E+06
PSMB4	2.31E+06	0.00E+00	0.00E+00	0.00E+00	0.00E+00	0.00E+00
API5	2.30E+06	0.00E+00	0.00E+00	0.00E+00	0.00E+00	0.00E+00
NUDT21	2.30E+06	0.00E+00	0.00E+00	0.00E+00	0.00E+00	0.00E+00
RABGGTB	2.23E+06	0.00E+00	0.00E+00	0.00E+00	0.00E+00	0.00E+00
UQCRC1	2.22E+06	0.00E+00	0.00E+00	0.00E+00	0.00E+00	0.00E+00
RBM26	2.21E+06	3.73E+06	2.88E+06	2.65E+06	0.00E+00	1.33E+06
DDX6	2.13E+06	0.00E+00	0.00E+00	9.55E+05	0.00E+00	0.00E+00
DNAJC8	2.11E+06	1.06E+06	1.32E+06	0.00E+00	0.00E+00	1.00E+06
PPIF	2.09E+06	0.00E+00	0.00E+00	0.00E+00	0.00E+00	0.00E+00
RAB3GAP2	2.09E+06	0.00E+00	0.00E+00	1.09E+06	0.00E+00	0.00E+00
KDM2A	2.07E+06	1.19E+06	0.00E+00	3.21E+06	3.66E+06	3.47E+06
PSMB6	2.07E+06	0.00E+00	3.77E+06	0.00E+00	0.00E+00	0.00E+00
SNRPF	2.05E+06	0.00E+00	5.04E+06	5.70E+06	1.64E+06	4.22E+06
PSMC6	2.05E+06	0.00E+00	0.00E+00	0.00E+00	0.00E+00	0.00E+00
OGDH	2.05E+06	0.00E+00	1.55E+06	1.95E+06	0.00E+00	0.00E+00
MAOB	2.03E+06	9.59E+05	2.37E+06	3.85E+06	1.02E+06	9.13E+05
ACTR2	1.99E+06	0.00E+00	3.25E+06	1.63E+06	0.00E+00	0.00E+00
DUT	1.98E+06	0.00E+00	0.00E+00	5.76E+05	0.00E+00	0.00E+00
LIG3	1.92E+06	1.98E+06	2.62E+06	2.82E+06	9.27E+05	3.39E+06
NUP98	1.91E+06	0.00E+00	0.00E+00	1.53E+06	0.00E+00	0.00E+00
SARS	1.87E+06	2.20E+06	0.00E+00	0.00E+00	0.00E+00	0.00E+00
VPS29	1.87E+06	0.00E+00	0.00E+00	0.00E+00	0.00E+00	0.00E+00
PCNA	1.86E+06	7.97E+05	0.00E+00	1.14E+06	2.11E+06	7.85E+05
HCFC1	1.84E+06	5.56E+05	8.16E+05	7.34E+05	0.00E+00	7.77E+05
CDK2	1.83E+06	0.00E+00	0.00E+00	0.00E+00	0.00E+00	0.00E+00
CPSF6	1.80E+06	0.00E+00	1.88E+06	3.00E+06	0.00E+00	2.02E+06
CSTA	1.79E+06	0.00E+00	0.00E+00	0.00E+00	0.00E+00	0.00E+00
CIAO1	1.78E+06	0.00E+00	2.26E+06	2.14E+06	0.00E+00	2.66E+06
PSMB2	1.78E+06	0.00E+00	1.71E+06	1.23E+06	0.00E+00	1.21E+06
PDS5A	1.76E+06	1.76E+06	4.23E+06	0.00E+00	0.00E+00	2.36E+06
ATL3	1.72E+06	7.29E+05	1.19E+06	0.00E+00	0.00E+00	0.00E+00
CCDC86	1.72E+06	2.78E+07	3.12E+06	4.04E+06	2.94E+07	4.06E+06
CLNS1A	1.70E+06	0.00E+00	0.00E+00	0.00E+00	0.00E+00	0.00E+00
UQCRC2	1.69E+06	0.00E+00	0.00E+00	0.00E+00	0.00E+00	0.00E+00
RNPEP	1.66E+06	0.00E+00	0.00E+00	0.00E+00	0.00E+00	0.00E+00
S100A4	1.64E+06	0.00E+00	0.00E+00	0.00E+00	0.00E+00	0.00E+00
DFNA5	1.64E+06	0.00E+00	0.00E+00	0.00E+00	0.00E+00	0.00E+00
WDR3	1.62E+06	1.82E+06	1.84E+06	0.00E+00	2.38E+06	0.00E+00
RPA2	1.59E+06	0.00E+00	0.00E+00	0.00E+00	0.00E+00	0.00E+00
CSTB	1.57E+06	0.00E+00	0.00E+00	0.00E+00	0.00E+00	0.00E+00
RAVER1	1.56E+06	0.00E+00	1.05E+06	2.00E+06	0.00E+00	9.59E+05
SLC25A13	1.55E+06	0.00E+00	1.81E+06	1.90E+06	0.00E+00	3.68E+06
POLA1	1.55E+06	0.00E+00	5.69E+06	5.11E+06	0.00E+00	3.25E+06
COL1A2	1.53E+06	0.00E+00	0.00E+00	0.00E+00	0.00E+00	0.00E+00
NUP153	1.53E+06	0.00E+00	3.39E+06	2.18E+06	0.00E+00	4.99E+06
DAD1	1.52E+06	1.21E+06	0.00E+00	9.05E+05	3.20E+06	0.00E+00
FHL1	1.51E+06	0.00E+00	0.00E+00	0.00E+00	0.00E+00	0.00E+00
RBM34	1.50E+06	2.11E+07	1.70E+06	0.00E+00	3.16E+07	0.00E+00
CELF1	1.50E+06	1.12E+06	0.00E+00	0.00E+00	0.00E+00	0.00E+00
PDHA1	1.48E+06	0.00E+00	0.00E+00	0.00E+00	0.00E+00	0.00E+00
TBCD	1.47E+06	0.00E+00	0.00E+00	1.53E+06	0.00E+00	0.00E+00
CBR1	1.47E+06	0.00E+00	0.00E+00	0.00E+00	0.00E+00	0.00E+00
MTDH	1.47E+06	4.42E+06	3.77E+06	0.00E+00	6.11E+06	1.49E+06
CYFIP1	1.46E+06	0.00E+00	1.93E+06	3.63E+06	0.00E+00	1.69E+06
PLS3	1.44E+06	0.00E+00	1.23E+06	0.00E+00	0.00E+00	0.00E+00
SRRM1	1.42E+06	1.45E+06	1.41E+06	0.00E+00	1.37E+06	0.00E+00
DHCR24	1.40E+06	2.75E+06	1.54E+06	3.41E+06	3.87E+06	5.19E+06
PPP2CA	1.40E+06	0.00E+00	1.01E+06	1.03E+06	0.00E+00	0.00E+00
LGALS1	1.40E+06	1.11E+06	0.00E+00	0.00E+00	0.00E+00	0.00E+00
DDX56	1.38E+06	5.19E+06	2.45E+06	0.00E+00	5.53E+06	1.05E+06
IKBKAP	1.38E+06	0.00E+00	0.00E+00	0.00E+00	0.00E+00	0.00E+00
RPS6KA3	1.37E+06	0.00E+00	0.00E+00	0.00E+00	0.00E+00	0.00E+00
RAC1	1.37E+06	1.98E+06	0.00E+00	1.02E+06	1.97E+06	0.00E+00
PSMD4	1.36E+06	0.00E+00	0.00E+00	0.00E+00	0.00E+00	0.00E+00
RFC3	1.34E+06	0.00E+00	0.00E+00	0.00E+00	0.00E+00	0.00E+00
EXOSC2	1.33E+06	0.00E+00	0.00E+00	0.00E+00	0.00E+00	0.00E+00
DRG1	1.33E+06	1.15E+06	0.00E+00	0.00E+00	2.41E+06	0.00E+00
MYO1C	1.33E+06	1.35E+06	3.02E+06	2.91E+06	1.40E+06	4.46E+06
ANKHD1	1.32E+06	0.00E+00	2.01E+06	0.00E+00	0.00E+00	0.00E+00
RRP8	1.32E+06	1.96E+06	0.00E+00	0.00E+00	1.98E+06	0.00E+00
METAP1	1.31E+06	1.01E+06	3.25E+06	0.00E+00	0.00E+00	0.00E+00
ABCD3	1.29E+06	0.00E+00	0.00E+00	0.00E+00	0.00E+00	1.50E+06
REXO4	1.28E+06	1.90E+07	1.84E+06	0.00E+00	1.74E+07	0.00E+00
EEF1E1	1.28E+06	0.00E+00	0.00E+00	0.00E+00	0.00E+00	0.00E+00
NCBP1	1.28E+06	0.00E+00	0.00E+00	0.00E+00	0.00E+00	0.00E+00
PGAM1	1.26E+06	0.00E+00	0.00E+00	0.00E+00	0.00E+00	0.00E+00
MORF4L2	1.26E+06	6.75E+06	3.29E+06	1.56E+06	7.77E+06	1.59E+06
ARHGDIA	1.26E+06	0.00E+00	0.00E+00	0.00E+00	0.00E+00	0.00E+00
HEATR1	1.26E+06	0.00E+00	3.21E+06	3.99E+06	3.68E+06	2.69E+06
CCDC6	1.25E+06	0.00E+00	0.00E+00	0.00E+00	0.00E+00	9.93E+05
DDX42	1.25E+06	0.00E+00	5.25E+05	0.00E+00	0.00E+00	5.01E+05

MRPL22	1.24E+06	5.78E+06	2.47E+06	0.00E+00	3.51E+06	0.00E+00
RFC4	1.22E+06	1.18E+06	4.17E+06	2.87E+06	0.00E+00	0.00E+00
NANS	1.22E+06	0.00E+00	0.00E+00	0.00E+00	0.00E+00	0.00E+00
ACTL6A	1.21E+06	9.05E+05	1.38E+06	2.28E+06	8.10E+05	9.42E+05
SART1	1.21E+06	1.35E+06	4.93E+06	1.35E+06	0.00E+00	1.38E+06
RAD50	1.20E+06	0.00E+00	4.68E+06	4.89E+06	1.88E+06	2.12E+06
GNE	1.20E+06	0.00E+00	3.78E+06	2.62E+06	1.24E+06	4.36E+06
ATP6V1A	1.19E+06	0.00E+00	0.00E+00	0.00E+00	0.00E+00	0.00E+00
MAP2K2	1.19E+06	0.00E+00	7.17E+05	0.00E+00	0.00E+00	0.00E+00
ANP32B	1.19E+06	0.00E+00	0.00E+00	0.00E+00	1.04E+06	0.00E+00
ADSL	1.16E+06	0.00E+00	0.00E+00	0.00E+00	0.00E+00	0.00E+00
HTATIP2	1.16E+06	0.00E+00	0.00E+00	0.00E+00	0.00E+00	0.00E+00
DHX16	1.16E+06	2.00E+06	2.53E+06	9.53E+05	1.96E+06	0.00E+00
ABHD14B	1.16E+06	0.00E+00	0.00E+00	0.00E+00	0.00E+00	0.00E+00
TRA2A	1.16E+06	0.00E+00	0.00E+00	0.00E+00	0.00E+00	0.00E+00
WDR70	1.14E+06	1.06E+06	1.19E+06	1.35E+06	1.40E+06	0.00E+00
KPNA2	1.14E+06	0.00E+00	1.06E+06	0.00E+00	0.00E+00	0.00E+00
CCAR2	1.14E+06	0.00E+00	0.00E+00	0.00E+00	0.00E+00	0.00E+00
ANXA5	1.11E+06	0.00E+00	0.00E+00	0.00E+00	0.00E+00	0.00E+00
BPNT1	1.11E+06	0.00E+00	0.00E+00	0.00E+00	0.00E+00	0.00E+00
RBX1	1.11E+06	0.00E+00	3.29E+06	4.16E+06	0.00E+00	0.00E+00
RAB34	1.10E+06	8.95E+05	0.00E+00	0.00E+00	0.00E+00	0.00E+00
PSMD8	1.08E+06	0.00E+00	0.00E+00	0.00E+00	0.00E+00	0.00E+00
LARP1	1.07E+06	1.21E+06	0.00E+00	0.00E+00	8.99E+05	0.00E+00
XPOT	1.07E+06	0.00E+00	1.90E+06	3.31E+06	1.83E+06	2.47E+06
NOC3L	1.05E+06	9.64E+06	5.44E+06	3.31E+06	1.30E+07	3.05E+06
ATAD1	1.05E+06	0.00E+00	0.00E+00	0.00E+00	0.00E+00	3.05E+06
SAMM50	1.03E+06	0.00E+00	0.00E+00	0.00E+00	0.00E+00	0.00E+00
ANXA3	1.03E+06	6.49E+05	0.00E+00	0.00E+00	0.00E+00	0.00E+00
TCERG1	1.03E+06	1.02E+06	1.06E+06	0.00E+00	0.00E+00	0.00E+00
TRMT10C	1.03E+06	0.00E+00	0.00E+00	0.00E+00	0.00E+00	0.00E+00
TBRG4	1.02E+06	0.00E+00	0.00E+00	0.00E+00	0.00E+00	0.00E+00
NCAPH	1.02E+06	0.00E+00	0.00E+00	0.00E+00	0.00E+00	0.00E+00
AP3B1	1.01E+06	0.00E+00	0.00E+00	0.00E+00	0.00E+00	0.00E+00
MAP2K1	1.01E+06	0.00E+00	0.00E+00	0.00E+00	0.00E+00	0.00E+00
NAPA	1.00E+06	0.00E+00	0.00E+00	0.00E+00	0.00E+00	0.00E+00
pk;ZAK	1.00E+06	7.46E+05	0.00E+00	0.00E+00	1.05E+06	1.20E+06
TMCO1	1.00E+06	2.26E+06	2.10E+06	0.00E+00	1.18E+06	8.62E+05
DLD	9.93E+05	0.00E+00	0.00E+00	0.00E+00	0.00E+00	0.00E+00
CYC1	9.85E+05	0.00E+00	0.00E+00	0.00E+00	0.00E+00	0.00E+00
UGDH	9.84E+05	0.00E+00	0.00E+00	0.00E+00	0.00E+00	0.00E+00
STT3B	9.82E+05	1.06E+06	1.34E+06	1.55E+06	3.04E+06	1.13E+06
ESYT1	9.80E+05	0.00E+00	0.00E+00	0.00E+00	0.00E+00	0.00E+00
AIFM1	9.79E+05	0.00E+00	0.00E+00	1.27E+06	1.84E+06	0.00E+00
PSMG1	9.75E+05	0.00E+00	0.00E+00	0.00E+00	0.00E+00	0.00E+00
TXNDC5	9.74E+05	0.00E+00	0.00E+00	0.00E+00	0.00E+00	0.00E+00
TRIP6	9.67E+05	0.00E+00	2.50E+06	2.76E+06	0.00E+00	4.14E+06
UCHL5	9.62E+05	0.00E+00	0.00E+00	0.00E+00	0.00E+00	0.00E+00
C19orf43	9.60E+05	8.88E+05	0.00E+00	0.00E+00	0.00E+00	0.00E+00
BMS1	9.49E+05	1.43E+07	2.95E+06	0.00E+00	1.43E+07	0.00E+00
RNF114	9.47E+05	0.00E+00	3.88E+06	0.00E+00	0.00E+00	0.00E+00
PYCR2	9.40E+05	2.27E+06	9.75E+05	0.00E+00	0.00E+00	0.00E+00
ELAC2	9.36E+05	0.00E+00	0.00E+00	0.00E+00	0.00E+00	0.00E+00
CSTF3	9.29E+05	0.00E+00	0.00E+00	0.00E+00	0.00E+00	0.00E+00
RTFDC1	9.28E+05	0.00E+00	2.88E+06	1.23E+06	0.00E+00	0.00E+00
GANAB	9.27E+05	0.00E+00	0.00E+00	0.00E+00	0.00E+00	0.00E+00
ANXA7	9.25E+05	0.00E+00	0.00E+00	0.00E+00	0.00E+00	0.00E+00
GTF3C5	9.25E+05	0.00E+00	0.00E+00	0.00E+00	0.00E+00	0.00E+00
TRIM25	9.25E+05	0.00E+00	0.00E+00	0.00E+00	0.00E+00	0.00E+00
BYSL	9.22E+05	2.02E+06	2.04E+06	1.72E+06	2.85E+06	6.47E+05
IPO4	9.06E+05	0.00E+00	0.00E+00	8.26E+05	0.00E+00	0.00E+00
SLC3A2	9.04E+05	0.00E+00	0.00E+00	2.48E+06	0.00E+00	0.00E+00
CIRBP	9.02E+05	1.68E+06	0.00E+00	0.00E+00	1.95E+06	6.18E+05
PPID	8.82E+05	0.00E+00	0.00E+00	0.00E+00	0.00E+00	0.00E+00
HSD17B12	8.76E+05	0.00E+00	0.00E+00	1.13E+06	0.00E+00	0.00E+00
MARC1	8.74E+05	0.00E+00	0.00E+00	0.00E+00	6.69E+05	1.22E+06
PDIA4	8.73E+05	0.00E+00	0.00E+00	0.00E+00	0.00E+00	0.00E+00
AHCYL2	8.71E+05	0.00E+00	0.00E+00	0.00E+00	0.00E+00	0.00E+00
KDM1A	8.71E+05	0.00E+00	0.00E+00	0.00E+00	0.00E+00	0.00E+00
USP7	8.69E+05	0.00E+00	1.03E+06	9.40E+05	0.00E+00	0.00E+00
MRPL43	8.67E+05	1.03E+06	0.00E+00	0.00E+00	9.45E+05	0.00E+00
CHERP	8.45E+05	0.00E+00	0.00E+00	0.00E+00	0.00E+00	0.00E+00
PPA1	8.44E+05	7.75E+05	0.00E+00	0.00E+00	0.00E+00	0.00E+00
KIAA1598	8.38E+05	0.00E+00	0.00E+00	0.00E+00	0.00E+00	0.00E+00
SMARCE1	8.36E+05	0.00E+00	8.74E+05	0.00E+00	0.00E+00	0.00E+00
GTF3C4	8.32E+05	0.00E+00	1.14E+06	0.00E+00	0.00E+00	0.00E+00
CBFB	8.23E+05	0.00E+00	0.00E+00	0.00E+00	0.00E+00	0.00E+00
HADH	8.14E+05	0.00E+00	0.00E+00	0.00E+00	0.00E+00	0.00E+00
GRWD1	8.08E+05	0.00E+00	0.00E+00	0.00E+00	0.00E+00	0.00E+00
WRNIP1	7.92E+05	0.00E+00	0.00E+00	0.00E+00	0.00E+00	0.00E+00
USP10	7.85E+05	5.02E+05	6.73E+05	7.19E+05	1.40E+06	7.73E+05
DNAJC9	7.85E+05	0.00E+00	0.00E+00	0.00E+00	0.00E+00	0.00E+00
C12orf10	7.84E+05	0.00E+00	0.00E+00	0.00E+00	0.00E+00	0.00E+00
TNPO3	7.71E+05	0.00E+00	0.00E+00	0.00E+00	0.00E+00	0.00E+00
RDH10	7.66E+05	0.00E+00	8.18E+05	9.76E+05	7.69E+05	1.64E+06
DFFA	7.31E+05	0.00E+00	0.00E+00	0.00E+00	0.00E+00	0.00E+00
GYS1	7.28E+05	0.00E+00	7.86E+05	0.00E+00	0.00E+00	8.31E+05
CLIP1	7.28E+05	0.00E+00	8.41E+05	0.00E+00	0.00E+00	8.08E+05
CCAR1	7.24E+05	0.00E+00	0.00E+00	0.00E+00	0.00E+00	0.00E+00
ESYT2	7.23E+05	0.00E+00	0.00E+00	0.00E+00	0.00E+00	0.00E+00
AIFM2	7.14E+05	0.00E+00	0.00E+00	0.00E+00	0.00E+00	0.00E+00
EML2	7.12E+05	0.00E+00	0.00E+00	0.00E+00	0.00E+00	0.00E+00
SEC23A	7.08E+05	0.00E+00	0.00E+00	0.00E+00	0.00E+00	0.00E+00
TPX2	6.95E+05	0.00E+00	0.00E+00	0.00E+00	8.62E+05	0.00E+00
SON	6.90E+05	5.47E+05	0.00E+00	0.00E+00	1.30E+06	0.00E+00
MCMBP	6.82E+05	0.00E+00	0.00E+00	0.00E+00	0.00E+00	0.00E+00
SPTLC1	6.70E+05	0.00E+00	0.00E+00	0.00E+00	0.00E+00	0.00E+00
XAB2	6.60E+05	0.00E+00	0.00E+00	0.00E+00	0.00E+00	0.00E+00
ACOT7	6.59E+05	0.00E+00	0.00E+00	0.00E+00	0.00E+00	0.00E+00
TAP1	6.55E+05	0.00E+00	1.24E+06	1.12E+06	0.00E+00	0.00E+00
GFPT1	6.53E+05	0.00E+00	9.17E+05	0.00E+00	0.00E+00	0.00E+00
AHSA1	6.53E+05	0.00E+00	0.00E+00	0.00E+00	0.00E+00	0.00E+00

FARSB	6.46E+05	0.00E+00	0.00E+00	0.00E+00	0.00E+00	0.00E+00
MOGS	6.31E+05	1.36E+06	0.00E+00	0.00E+00	1.43E+06	0.00E+00
P4HB	6.24E+05	0.00E+00	0.00E+00	0.00E+00	0.00E+00	0.00E+00
GPS1	6.22E+05	0.00E+00	0.00E+00	0.00E+00	0.00E+00	0.00E+00
UTP14A	6.22E+05	8.13E+05	0.00E+00	0.00E+00	1.84E+06	0.00E+00
PSME1	6.15E+05	0.00E+00	0.00E+00	0.00E+00	0.00E+00	0.00E+00
EIF4A2	6.10E+05	0.00E+00	0.00E+00	0.00E+00	0.00E+00	0.00E+00
BRD4;BRD3;BRDT	6.08E+05	0.00E+00	0.00E+00	0.00E+00	0.00E+00	0.00E+00
MOB1A;MOB1B	6.02E+05	6.21E+05	5.45E+05	0.00E+00	0.00E+00	0.00E+00
MOV10	5.91E+05	0.00E+00	0.00E+00	0.00E+00	0.00E+00	0.00E+00
SRM	5.82E+05	0.00E+00	0.00E+00	0.00E+00	0.00E+00	0.00E+00
U2SURP	5.78E+05	0.00E+00	5.71E+05	0.00E+00	0.00E+00	0.00E+00
SRSF4	5.76E+05	2.00E+06	6.77E+05	0.00E+00	9.05E+05	0.00E+00
PGP	5.69E+05	0.00E+00	0.00E+00	0.00E+00	0.00E+00	0.00E+00
DYNC1LI1	5.48E+05	0.00E+00	0.00E+00	0.00E+00	0.00E+00	0.00E+00
PDCD5	5.43E+05	0.00E+00	0.00E+00	4.40E+05	0.00E+00	0.00E+00
MAD2L1	5.27E+05	0.00E+00	0.00E+00	1.99E+06	0.00E+00	3.42E+06
WBP11	5.14E+05	0.00E+00	0.00E+00	0.00E+00	0.00E+00	0.00E+00
RBM10	4.92E+05	0.00E+00	0.00E+00	0.00E+00	0.00E+00	0.00E+00
SUCLA2	4.62E+05	0.00E+00	0.00E+00	0.00E+00	0.00E+00	0.00E+00
SNRPB2	4.61E+05	0.00E+00	0.00E+00	0.00E+00	0.00E+00	0.00E+00
DUSP3	4.60E+05	0.00E+00	0.00E+00	0.00E+00	0.00E+00	0.00E+00
MTHFD2	4.28E+05	0.00E+00	0.00E+00	0.00E+00	0.00E+00	0.00E+00
CALR	4.17E+05	0.00E+00	0.00E+00	0.00E+00	0.00E+00	0.00E+00
MLKL	4.08E+05	0.00E+00	0.00E+00	0.00E+00	0.00E+00	0.00E+00
NUP35	4.00E+05	0.00E+00	0.00E+00	0.00E+00	0.00E+00	0.00E+00
ZNF598	3.99E+05	0.00E+00	0.00E+00	0.00E+00	0.00E+00	0.00E+00
ACADVL	3.93E+05	0.00E+00	0.00E+00	0.00E+00	0.00E+00	0.00E+00
HTATSF1	3.83E+05	0.00E+00	0.00E+00	0.00E+00	0.00E+00	0.00E+00
RHOG	3.77E+05	0.00E+00	0.00E+00	0.00E+00	0.00E+00	0.00E+00
TST	3.55E+05	0.00E+00	0.00E+00	0.00E+00	0.00E+00	0.00E+00
LAMC1	3.51E+05	0.00E+00	0.00E+00	0.00E+00	0.00E+00	0.00E+00
THOC2	3.49E+05	0.00E+00	0.00E+00	0.00E+00	0.00E+00	0.00E+00
GNL2	3.14E+05	1.02E+07	1.35E+06	0.00E+00	1.45E+07	1.02E+06
IDH1	3.10E+05	0.00E+00	0.00E+00	0.00E+00	0.00E+00	0.00E+00
ACOT9	3.07E+05	0.00E+00	0.00E+00	0.00E+00	0.00E+00	0.00E+00
NCKAP1	2.87E+05	0.00E+00	0.00E+00	0.00E+00	0.00E+00	0.00E+00
ECHS1	2.72E+05	0.00E+00	0.00E+00	0.00E+00	0.00E+00	0.00E+00
PACSIN3	2.67E+05	0.00E+00	0.00E+00	0.00E+00	0.00E+00	0.00E+00
PRIM2	2.63E+05	0.00E+00	0.00E+00	0.00E+00	0.00E+00	0.00E+00
PFKL	2.60E+05	0.00E+00	0.00E+00	0.00E+00	0.00E+00	0.00E+00
UFM1	2.35E+05	0.00E+00	0.00E+00	0.00E+00	0.00E+00	0.00E+00
KIFC1	2.21E+05	0.00E+00	0.00E+00	0.00E+00	0.00E+00	0.00E+00
SMARCC2	2.08E+05	0.00E+00	0.00E+00	0.00E+00	0.00E+00	0.00E+00
FAIM	1.71E+05	0.00E+00	0.00E+00	0.00E+00	0.00E+00	0.00E+00
PPHLN1	1.54E+05	0.00E+00	0.00E+00	0.00E+00	0.00E+00	0.00E+00
TBC1D15	1.48E+05	0.00E+00	0.00E+00	0.00E+00	0.00E+00	0.00E+00
DAB2	8.51E+04	0.00E+00	0.00E+00	0.00E+00	0.00E+00	0.00E+00
SEPT10	0.00E+00	0.00E+00	0.00E+00	1.43E+06	0.00E+00	0.00E+00
SEPT11	0.00E+00	0.00E+00	2.13E+06	2.76E+06	0.00E+00	0.00E+00
ABCA2	0.00E+00	9.30E+05	0.00E+00	0.00E+00	0.00E+00	0.00E+00
ABCD1	0.00E+00	0.00E+00	1.08E+06	0.00E+00	0.00E+00	0.00E+00
ABCF3	0.00E+00	0.00E+00	8.04E+05	0.00E+00	0.00E+00	0.00E+00
ABT1	0.00E+00	5.16E+05	0.00E+00	0.00E+00	0.00E+00	0.00E+00
ACIN1	0.00E+00	0.00E+00	2.87E+06	1.24E+06	2.69E+06	1.55E+06
ACTR1A	0.00E+00	0.00E+00	0.00E+00	0.00E+00	2.23E+05	0.00E+00
ACTR3	0.00E+00	0.00E+00	0.00E+00	0.00E+00	0.00E+00	9.13E+05
ADNP	0.00E+00	0.00E+00	5.64E+05	0.00E+00	0.00E+00	0.00E+00
AHCTF1	0.00E+00	1.16E+07	5.09E+06	6.15E+06	2.37E+07	2.50E+06
ANKFY1	0.00E+00	0.00E+00	3.74E+05	0.00E+00	0.00E+00	0.00E+00
ANLN	0.00E+00	0.00E+00	0.00E+00	2.14E+05	0.00E+00	0.00E+00
ANP32E	0.00E+00	1.87E+06	0.00E+00	0.00E+00	2.10E+06	0.00E+00
AP1B1	0.00E+00	1.27E+06	1.32E+06	1.82E+06	0.00E+00	0.00E+00
AP2A1	0.00E+00	0.00E+00	0.00E+00	0.00E+00	0.00E+00	1.42E+05
AP2M1	0.00E+00	0.00E+00	0.00E+00	0.00E+00	5.32E+06	0.00E+00
AP3D1	0.00E+00	3.40E+05	0.00E+00	0.00E+00	0.00E+00	0.00E+00
APOL2	0.00E+00	7.90E+05	9.23E+05	0.00E+00	0.00E+00	0.00E+00
ARAF	0.00E+00	0.00E+00	0.00E+00	0.00E+00	0.00E+00	8.32E+05
ARL2	0.00E+00	0.00E+00	3.94E+05	0.00E+00	0.00E+00	0.00E+00
ARL6IP4	0.00E+00	1.45E+06	0.00E+00	0.00E+00	1.04E+06	0.00E+00
ASNS	0.00E+00	0.00E+00	9.10E+05	0.00E+00	0.00E+00	0.00E+00
ASUN	0.00E+00	0.00E+00	1.75E+05	0.00E+00	0.00E+00	0.00E+00
ATAD2	0.00E+00	2.16E+06	0.00E+00	0.00E+00	5.86E+06	0.00E+00
ATG3	0.00E+00	0.00E+00	1.80E+05	0.00E+00	0.00E+00	0.00E+00
ATP5F1	0.00E+00	0.00E+00	0.00E+00	0.00E+00	8.45E+05	0.00E+00
ATP5J2	0.00E+00	1.52E+06	7.67E+05	0.00E+00	1.98E+06	1.09E+06
ATP5O	0.00E+00	0.00E+00	0.00E+00	0.00E+00	1.18E+06	0.00E+00
ATRX	0.00E+00	0.00E+00	0.00E+00	1.39E+06	0.00E+00	0.00E+00
BAG3	0.00E+00	0.00E+00	0.00E+00	4.96E+05	0.00E+00	0.00E+00
BAIAP2L1	0.00E+00	0.00E+00	4.39E+05	0.00E+00	0.00E+00	0.00E+00
BAZ1A	0.00E+00	6.02E+07	1.09E+08	5.95E+06	1.70E+07	1.67E+08
BAZ2A	0.00E+00	0.00E+00	0.00E+00	0.00E+00	7.83E+05	0.00E+00
BCAS2	0.00E+00	0.00E+00	1.10E+06	0.00E+00	0.00E+00	0.00E+00
BCCIP	0.00E+00	3.34E+05	0.00E+00	0.00E+00	0.00E+00	0.00E+00
BLM	0.00E+00	0.00E+00	4.16E+06	0.00E+00	0.00E+00	0.00E+00
BRD2	0.00E+00	1.24E+06	0.00E+00	0.00E+00	2.23E+06	0.00E+00
C11orf98	0.00E+00	6.20E+06	0.00E+00	0.00E+00	4.84E+06	0.00E+00
C14orf166	0.00E+00	0.00E+00	0.00E+00	0.00E+00	0.00E+00	1.40E+06
C19orf53	0.00E+00	1.78E+07	0.00E+00	0.00E+00	1.19E+07	0.00E+00
C7orf50	0.00E+00	1.28E+06	0.00E+00	0.00E+00	0.00E+00	0.00E+00
CASC5	0.00E+00	0.00E+00	0.00E+00	0.00E+00	4.94E+05	0.00E+00
CCDC124	0.00E+00	2.25E+06	0.00E+00	0.00E+00	0.00E+00	0.00E+00
CCDC137	0.00E+00	4.64E+06	0.00E+00	0.00E+00	8.15E+06	0.00E+00
CCDC47	0.00E+00	0.00E+00	0.00E+00	0.00E+00	3.13E+05	0.00E+00
CCDC59	0.00E+00	1.44E+06	0.00E+00	0.00E+00	1.18E+06	0.00E+00
CCDC71	0.00E+00	1.18E+06	0.00E+00	0.00E+00	0.00E+00	0.00E+00
CCDC71L	0.00E+00	9.85E+05	0.00E+00	0.00E+00	2.17E+06	0.00E+00
CDCA8	0.00E+00	0.00E+00	0.00E+00	0.00E+00	5.98E+05	0.00E+00
CDK9	0.00E+00	0.00E+00	6.68E+05	0.00E+00	0.00E+00	0.00E+00
CDKN2AIP	0.00E+00	0.00E+00	0.00E+00	7.70E+05	0.00E+00	0.00E+00
CDYL	0.00E+00	6.17E+05	0.00E+00	0.00E+00	0.00E+00	0.00E+00
CEBPZ	0.00E+00	2.34E+06	0.00E+00	0.00E+00	3.23E+06	0.00E+00

CENPC	0.00E+00	1.27E+06	0.00E+00	0.00E+00	0.00E+00	0.00E+00
CEP250	0.00E+00	1.93E+06	0.00E+00	0.00E+00	0.00E+00	0.00E+00
CIRH1A	0.00E+00	4.85E+05	0.00E+00	0.00E+00	0.00E+00	0.00E+00
CKAP5	0.00E+00	0.00E+00	0.00E+00	6.61E+05	0.00E+00	0.00E+00
CLINT1	0.00E+00	0.00E+00	0.00E+00	0.00E+00	0.00E+00	7.15E+05
CLPX	0.00E+00	1.51E+06	0.00E+00	0.00E+00	0.00E+00	0.00E+00
CLTA	0.00E+00	0.00E+00	0.00E+00	4.90E+05	0.00E+00	0.00E+00
CMAS	0.00E+00	4.45E+06	0.00E+00	1.17E+06	4.48E+06	0.00E+00
CMPK1	0.00E+00	0.00E+00	0.00E+00	0.00E+00	0.00E+00	8.44E+05
CMSS1	0.00E+00	3.06E+06	0.00E+00	0.00E+00	1.68E+06	0.00E+00
CNBP	0.00E+00	2.87E+06	0.00E+00	0.00E+00	0.00E+00	1.70E+06
CNOT1	0.00E+00	0.00E+00	1.87E+05	0.00E+00	0.00E+00	0.00E+00
COASY	0.00E+00	0.00E+00	1.15E+06	0.00E+00	0.00E+00	0.00E+00
COMT	0.00E+00	0.00E+00	0.00E+00	0.00E+00	0.00E+00	1.10E+06
COPB1	0.00E+00	1.29E+06	4.51E+06	1.61E+06	1.08E+06	0.00E+00
CORO1B	0.00E+00	0.00E+00	2.29E+05	0.00E+00	0.00E+00	0.00E+00
CPSF1	0.00E+00	0.00E+00	0.00E+00	0.00E+00	0.00E+00	3.68E+05
CPSF3	0.00E+00	0.00E+00	0.00E+00	0.00E+00	0.00E+00	9.48E+05
CROCC	0.00E+00	3.72E+06	2.33E+06	0.00E+00	1.06E+07	2.27E+06
CSK	0.00E+00	0.00E+00	1.81E+06	0.00E+00	0.00E+00	1.41E+06
CSNK2A1	0.00E+00	7.42E+05	0.00E+00	0.00E+00	0.00E+00	0.00E+00
CSNK2B	0.00E+00	3.16E+06	0.00E+00	0.00E+00	3.04E+06	0.00E+00
CTBP2	0.00E+00	1.24E+06	3.35E+06	1.55E+06	1.34E+06	5.05E+06
CTDSPL2	0.00E+00	0.00E+00	0.00E+00	0.00E+00	2.51E+06	0.00E+00
CUL1	0.00E+00	0.00E+00	0.00E+00	0.00E+00	0.00E+00	3.72E+05
CWF19L1	0.00E+00	0.00E+00	0.00E+00	0.00E+00	0.00E+00	6.36E+05
CYR61	0.00E+00	1.67E+06	0.00E+00	0.00E+00	5.30E+06	1.79E+06
DBN1	0.00E+00	0.00E+00	0.00E+00	3.67E+06	0.00E+00	1.83E+06
DDRGK1	0.00E+00	0.00E+00	0.00E+00	0.00E+00	0.00E+00	3.42E+05
DDX10	0.00E+00	0.00E+00	0.00E+00	0.00E+00	3.23E+06	0.00E+00
DDX31	0.00E+00	4.31E+06	0.00E+00	0.00E+00	5.28E+06	0.00E+00
DDX39B	0.00E+00	1.46E+06	0.00E+00	0.00E+00	9.50E+05	0.00E+00
DDX49	0.00E+00	1.04E+06	0.00E+00	0.00E+00	0.00E+00	0.00E+00
DDX55	0.00E+00	0.00E+00	0.00E+00	0.00E+00	4.52E+05	0.00E+00
DHCR7	0.00E+00	3.57E+06	1.01E+07	0.00E+00	4.34E+06	3.19E+06
DHX37	0.00E+00	0.00E+00	0.00E+00	0.00E+00	7.95E+05	0.00E+00
DHX38	0.00E+00	0.00E+00	5.25E+05	0.00E+00	0.00E+00	0.00E+00
DIAPH1	0.00E+00	0.00E+00	0.00E+00	0.00E+00	0.00E+00	6.33E+05
DIMT1	0.00E+00	0.00E+00	0.00E+00	0.00E+00	7.51E+05	0.00E+00
DCTN1	0.00E+00	0.00E+00	6.40E+05	0.00E+00	0.00E+00	0.00E+00
DLST	0.00E+00	1.12E+06	0.00E+00	0.00E+00	0.00E+00	0.00E+00
DMD	0.00E+00	0.00E+00	5.12E+05	0.00E+00	0.00E+00	0.00E+00
DNAAF5	0.00E+00	0.00E+00	0.00E+00	0.00E+00	0.00E+00	6.50E+05
DNAJB12	0.00E+00	0.00E+00	4.18E+05	0.00E+00	0.00E+00	0.00E+00
DNAJB4	0.00E+00	1.20E+06	1.49E+06	0.00E+00	0.00E+00	0.00E+00
DNAJB6	0.00E+00	2.51E+05	0.00E+00	0.00E+00	0.00E+00	0.00E+00
DNM2	0.00E+00	0.00E+00	0.00E+00	0.00E+00	0.00E+00	1.85E+06
DOCK7	0.00E+00	1.84E+06	0.00E+00	0.00E+00	0.00E+00	0.00E+00
DSC1	0.00E+00	0.00E+00	0.00E+00	0.00E+00	0.00E+00	2.09E+06
DSG1	0.00E+00	7.66E+05	0.00E+00	0.00E+00	0.00E+00	7.89E+06
DSG2	0.00E+00	0.00E+00	0.00E+00	0.00E+00	1.31E+06	2.49E+06
DUS3L	0.00E+00	0.00E+00	0.00E+00	1.16E+06	0.00E+00	2.27E+06
ECT2	0.00E+00	0.00E+00	0.00E+00	5.33E+05	0.00E+00	0.00E+00
EED	0.00E+00	0.00E+00	0.00E+00	0.00E+00	6.54E+05	0.00E+00
EEF1A2	0.00E+00	0.00E+00	0.00E+00	1.67E+06	1.25E+06	0.00E+00
EHD1	0.00E+00	0.00E+00	0.00E+00	2.88E+05	0.00E+00	0.00E+00
EMD	0.00E+00	4.49E+06	7.12E+06	5.75E+06	4.41E+06	4.67E+06
EML4	0.00E+00	0.00E+00	2.84E+05	0.00E+00	0.00E+00	0.00E+00
ETFB	0.00E+00	0.00E+00	9.09E+05	0.00E+00	0.00E+00	0.00E+00
EXOSC3	0.00E+00	9.32E+05	0.00E+00	1.16E+06	0.00E+00	0.00E+00
EXOSC9	0.00E+00	0.00E+00	0.00E+00	0.00E+00	6.24E+05	0.00E+00
FAF2	0.00E+00	0.00E+00	7.02E+05	0.00E+00	0.00E+00	0.00E+00
FAM120A	0.00E+00	7.71E+05	0.00E+00	0.00E+00	0.00E+00	0.00E+00
FAM50A	0.00E+00	7.83E+05	0.00E+00	0.00E+00	0.00E+00	0.00E+00
FARSA	0.00E+00	4.82E+05	0.00E+00	0.00E+00	0.00E+00	0.00E+00
FAU	0.00E+00	4.97E+06	0.00E+00	0.00E+00	7.84E+06	0.00E+00
FCF1	0.00E+00	3.69E+06	0.00E+00	0.00E+00	5.81E+06	0.00E+00
FERMT1	0.00E+00	0.00E+00	4.51E+05	0.00E+00	0.00E+00	0.00E+00
FGD3	0.00E+00	0.00E+00	0.00E+00	1.60E+07	0.00E+00	0.00E+00
FGF2	0.00E+00	2.63E+06	0.00E+00	0.00E+00	0.00E+00	0.00E+00
FKBP8	0.00E+00	9.97E+05	2.17E+06	0.00E+00	0.00E+00	2.44E+06
FLII	0.00E+00	0.00E+00	0.00E+00	0.00E+00	0.00E+00	3.78E+05
FLOT1	0.00E+00	0.00E+00	2.37E+06	2.59E+06	1.45E+06	0.00E+00
FLOT2	0.00E+00	0.00E+00	0.00E+00	9.67E+05	0.00E+00	0.00E+00
FLYWCH2	0.00E+00	0.00E+00	9.25E+05	0.00E+00	0.00E+00	0.00E+00
FRG1	0.00E+00	0.00E+00	0.00E+00	0.00E+00	7.50E+05	0.00E+00
FYTTD1	0.00E+00	1.65E+06	0.00E+00	0.00E+00	3.40E+06	0.00E+00
G3BP2	0.00E+00	0.00E+00	0.00E+00	2.28E+06	0.00E+00	0.00E+00
G6PD	0.00E+00	0.00E+00	4.18E+05	0.00E+00	0.00E+00	0.00E+00
GALK1	0.00E+00	0.00E+00	0.00E+00	1.15E+06	0.00E+00	0.00E+00
GAR1	0.00E+00	3.87E+06	0.00E+00	0.00E+00	2.27E+06	0.00E+00
GATAD2A	0.00E+00	0.00E+00	5.08E+05	0.00E+00	0.00E+00	0.00E+00
GBE1	0.00E+00	0.00E+00	0.00E+00	1.73E+06	0.00E+00	0.00E+00
GEMIN4	0.00E+00	0.00E+00	1.42E+06	3.13E+06	0.00E+00	3.49E+06
GLYR1	0.00E+00	1.41E+06	0.00E+00	0.00E+00	1.67E+06	0.00E+00
GNG12	0.00E+00	0.00E+00	3.56E+05	0.00E+00	0.00E+00	0.00E+00
GNL1	0.00E+00	5.68E+05	0.00E+00	0.00E+00	0.00E+00	0.00E+00
GNL3L	0.00E+00	7.39E+06	0.00E+00	3.80E+06	1.19E+07	7.96E+06
GOT2	0.00E+00	0.00E+00	4.01E+05	0.00E+00	0.00E+00	0.00E+00
GPD2	0.00E+00	0.00E+00	5.79E+05	0.00E+00	0.00E+00	0.00E+00
GRPEL1	0.00E+00	1.13E+05	0.00E+00	0.00E+00	0.00E+00	0.00E+00
GRSF1	0.00E+00	0.00E+00	1.51E+05	0.00E+00	0.00E+00	0.00E+00
GTF3C1	0.00E+00	0.00E+00	0.00E+00	1.24E+05	0.00E+00	0.00E+00
GTF3C2	0.00E+00	2.29E+05	0.00E+00	0.00E+00	0.00E+00	0.00E+00
MRPS17	0.00E+00	7.33E+05	0.00E+00	0.00E+00	0.00E+00	0.00E+00
HECTD1	0.00E+00	0.00E+00	0.00E+00	0.00E+00	0.00E+00	6.68E+05
HELLS	0.00E+00	0.00E+00	0.00E+00	0.00E+00	3.73E+05	0.00E+00
HIST1H1E	0.00E+00	4.68E+07	0.00E+00	0.00E+00	5.12E+07	0.00E+00
HLTF	0.00E+00	1.60E+06	3.50E+06	1.99E+06	2.01E+06	3.35E+06
HMCES	0.00E+00	0.00E+00	6.77E+05	0.00E+00	0.00E+00	0.00E+00
HMGN1	0.00E+00	9.31E+06	0.00E+00	0.00E+00	9.57E+06	0.00E+00
HNRNPLL	0.00E+00	0.00E+00	0.00E+00	0.00E+00	2.21E+05	0.00E+00

HSP90AB4P	0.00E+00	0.00E+00	3.44E+05	0.00E+00	0.00E+00	0.00E+00
IFIT2	0.00E+00	0.00E+00	8.07E+05	0.00E+00	0.00E+00	0.00E+00
IMP3	0.00E+00	6.24E+05	0.00E+00	0.00E+00	0.00E+00	0.00E+00
IMP4	0.00E+00	1.34E+06	0.00E+00	0.00E+00	1.74E+06	1.53E+06
INF2	0.00E+00	0.00E+00	2.46E+06	1.50E+06	0.00E+00	3.03E+06
IPO8	0.00E+00	0.00E+00	0.00E+00	0.00E+00	0.00E+00	8.57E+05
ISG20L2	0.00E+00	6.53E+05	0.00E+00	0.00E+00	0.00E+00	0.00E+00
ITGA6	0.00E+00	0.00E+00	3.15E+08	0.00E+00	0.00E+00	0.00E+00
ITPA	0.00E+00	0.00E+00	2.59E+05	0.00E+00	0.00E+00	0.00E+00
KAT7	0.00E+00	0.00E+00	0.00E+00	0.00E+00	6.58E+05	0.00E+00
KDM3B	0.00E+00	0.00E+00	4.03E+05	0.00E+00	0.00E+00	0.00E+00
KIAA0368	0.00E+00	0.00E+00	0.00E+00	6.40E+05	0.00E+00	0.00E+00
KIF22	0.00E+00	3.98E+05	0.00E+00	0.00E+00	0.00E+00	0.00E+00
KIF2A	0.00E+00	0.00E+00	3.62E+05	0.00E+00	0.00E+00	0.00E+00
KIF2C	0.00E+00	7.22E+05	0.00E+00	1.23E+06	0.00E+00	0.00E+00
KLC2	0.00E+00	0.00E+00	0.00E+00	7.45E+05	0.00E+00	0.00E+00
KNOP1	0.00E+00	1.04E+07	0.00E+00	0.00E+00	7.00E+06	0.00E+00
KPRP	0.00E+00	0.00E+00	0.00E+00	0.00E+00	0.00E+00	1.98E+07
KRI1	0.00E+00	1.84E+06	0.00E+00	0.00E+00	1.77E+06	0.00E+00
KRR1	0.00E+00	2.83E+06	0.00E+00	0.00E+00	5.66E+06	0.00E+00
LAMA5	0.00E+00	0.00E+00	3.79E+05	0.00E+00	0.00E+00	0.00E+00
LARP7	0.00E+00	3.56E+05	0.00E+00	0.00E+00	0.00E+00	0.00E+00
LAS1L	0.00E+00	0.00E+00	8.39E+05	0.00E+00	0.00E+00	2.45E+06
LIMS1	0.00E+00	0.00E+00	9.28E+05	0.00E+00	0.00E+00	0.00E+00
LLPH	0.00E+00	2.96E+06	0.00E+00	0.00E+00	5.44E+06	0.00E+00
LMO7	0.00E+00	0.00E+00	1.22E+06	0.00E+00	0.00E+00	0.00E+00
LPCAT1	0.00E+00	1.37E+06	0.00E+00	0.00E+00	0.00E+00	0.00E+00
LRRC41	0.00E+00	0.00E+00	0.00E+00	0.00E+00	8.05E+05	0.00E+00
LSG1	0.00E+00	0.00E+00	0.00E+00	0.00E+00	1.07E+06	0.00E+00
MAGED2	0.00E+00	3.66E+05	0.00E+00	0.00E+00	0.00E+00	0.00E+00
MAGT1	0.00E+00	0.00E+00	0.00E+00	1.65E+06	0.00E+00	3.29E+06
MAK16	0.00E+00	6.32E+06	0.00E+00	0.00E+00	1.44E+07	0.00E+00
MAP2K3	0.00E+00	0.00E+00	3.41E+05	0.00E+00	0.00E+00	0.00E+00
MAP7	0.00E+00	0.00E+00	3.49E+05	0.00E+00	0.00E+00	0.00E+00
MAPRE1	0.00E+00	0.00E+00	3.24E+05	0.00E+00	0.00E+00	0.00E+00
MB21D1	0.00E+00	5.16E+06	0.00E+00	0.00E+00	1.16E+07	0.00E+00
MBOAT7	0.00E+00	0.00E+00	3.31E+05	0.00E+00	0.00E+00	0.00E+00
MDC1	0.00E+00	6.59E+05	0.00E+00	0.00E+00	0.00E+00	0.00E+00
MDH1	0.00E+00	0.00E+00	3.40E+05	0.00E+00	0.00E+00	0.00E+00
MECP2	0.00E+00	1.47E+06	0.00E+00	0.00E+00	0.00E+00	0.00E+00
MEMO1	0.00E+00	0.00E+00	4.29E+05	0.00E+00	0.00E+00	0.00E+00
METAP2	0.00E+00	0.00E+00	5.82E+05	0.00E+00	0.00E+00	0.00E+00
MLH1	0.00E+00	0.00E+00	0.00E+00	1.04E+06	7.81E+05	1.01E+06
MMS19	0.00E+00	0.00E+00	0.00E+00	2.94E+05	0.00E+00	0.00E+00
MMTAG2	0.00E+00	8.50E+05	0.00E+00	0.00E+00	0.00E+00	0.00E+00
MPG	0.00E+00	1.12E+06	0.00E+00	0.00E+00	0.00E+00	0.00E+00
MRE11A	0.00E+00	0.00E+00	5.33E+05	0.00E+00	0.00E+00	0.00E+00
MRPL2	0.00E+00	1.78E+06	0.00E+00	0.00E+00	1.66E+06	0.00E+00
MRPL24	0.00E+00	3.01E+06	0.00E+00	1.09E+06	1.57E+06	1.61E+06
MRPL35	0.00E+00	9.24E+05	0.00E+00	0.00E+00	0.00E+00	0.00E+00
MRPS15	0.00E+00	1.20E+06	0.00E+00	0.00E+00	0.00E+00	0.00E+00
MRPS22	0.00E+00	1.05E+06	0.00E+00	0.00E+00	0.00E+00	0.00E+00
MRPS5	0.00E+00	4.07E+06	0.00E+00	0.00E+00	4.86E+06	0.00E+00
MRTO4	0.00E+00	9.87E+06	0.00E+00	0.00E+00	1.11E+07	0.00E+00
MTCH2	0.00E+00	0.00E+00	1.42E+06	1.37E+06	1.07E+06	0.00E+00
MT-CO2	0.00E+00	0.00E+00	2.48E+06	0.00E+00	0.00E+00	0.00E+00
MYH10	0.00E+00	0.00E+00	0.00E+00	0.00E+00	0.00E+00	3.10E+05
MYPN	0.00E+00	0.00E+00	1.03E+06	0.00E+00	0.00E+00	0.00E+00
NARS	0.00E+00	0.00E+00	3.97E+05	0.00E+00	0.00E+00	0.00E+00
NCAPG	0.00E+00	3.91E+05	1.69E+06	1.90E+06	1.71E+06	2.62E+07
NCAPG2	0.00E+00	0.00E+00	0.00E+00	1.70E+06	0.00E+00	8.98E+05
NCLN	0.00E+00	0.00E+00	0.00E+00	0.00E+00	1.15E+06	0.00E+00
NCOA5	0.00E+00	0.00E+00	3.72E+05	0.00E+00	0.00E+00	0.00E+00
NDC1	0.00E+00	0.00E+00	4.17E+05	0.00E+00	0.00E+00	0.00E+00
NDUFA9	0.00E+00	3.98E+05	0.00E+00	0.00E+00	0.00E+00	0.00E+00
NFXL1	0.00E+00	0.00E+00	0.00E+00	0.00E+00	1.27E+06	0.00E+00
NGDN	0.00E+00	0.00E+00	5.57E+06	0.00E+00	5.34E+06	0.00E+00
NHP2	0.00E+00	0.00E+00	0.00E+00	0.00E+00	1.35E+06	0.00E+00
NLE1	0.00E+00	0.00E+00	0.00E+00	0.00E+00	1.13E+06	0.00E+00
NMT1	0.00E+00	5.06E+05	0.00E+00	0.00E+00	0.00E+00	0.00E+00
NOL10	0.00E+00	2.48E+06	0.00E+00	0.00E+00	1.98E+06	0.00E+00
NOL12	0.00E+00	0.00E+00	0.00E+00	0.00E+00	4.41E+06	0.00E+00
NOL6	0.00E+00	2.54E+05	0.00E+00	0.00E+00	0.00E+00	0.00E+00
NOL7	0.00E+00	6.73E+06	0.00E+00	0.00E+00	6.81E+06	0.00E+00
NOL9	0.00E+00	0.00E+00	0.00E+00	0.00E+00	1.08E+06	0.00E+00
NOP10	0.00E+00	2.33E+05	0.00E+00	0.00E+00	0.00E+00	0.00E+00
NOP14	0.00E+00	1.09E+06	0.00E+00	0.00E+00	0.00E+00	0.00E+00
NPLOC4	0.00E+00	5.54E+05	0.00E+00	0.00E+00	0.00E+00	0.00E+00
NSUN5	0.00E+00	0.00E+00	0.00E+00	0.00E+00	2.60E+05	0.00E+00
NTHL1	0.00E+00	0.00E+00	0.00E+00	0.00E+00	1.94E+05	0.00E+00
NTMT1	0.00E+00	0.00E+00	4.13E+05	0.00E+00	0.00E+00	0.00E+00
NUFIP2	0.00E+00	0.00E+00	6.05E+05	0.00E+00	0.00E+00	0.00E+00
NUP107	0.00E+00	0.00E+00	0.00E+00	0.00E+00	0.00E+00	1.42E+06
NUP133	0.00E+00	0.00E+00	0.00E+00	0.00E+00	0.00E+00	1.64E+06
NUP160	0.00E+00	0.00E+00	0.00E+00	0.00E+00	0.00E+00	1.41E+06
NUP188	0.00E+00	0.00E+00	0.00E+00	0.00E+00	0.00E+00	1.16E+06
NUP205	0.00E+00	0.00E+00	0.00E+00	0.00E+00	0.00E+00	1.03E+06
NUP50	0.00E+00	0.00E+00	1.37E+06	0.00E+00	0.00E+00	0.00E+00
NUP88	0.00E+00	0.00E+00	9.91E+05	0.00E+00	0.00E+00	0.00E+00
NUSAP1	0.00E+00	7.68E+06	0.00E+00	0.00E+00	5.13E+06	1.98E+06
NVL	0.00E+00	0.00E+00	0.00E+00	0.00E+00	0.00E+00	4.53E+05
NXF1	0.00E+00	0.00E+00	8.45E+05	0.00E+00	0.00E+00	1.13E+06
OPA1	0.00E+00	0.00E+00	0.00E+00	7.56E+05	0.00E+00	0.00E+00
OXSR1	0.00E+00	0.00E+00	3.68E+05	0.00E+00	0.00E+00	0.00E+00
PAF1	0.00E+00	0.00E+00	0.00E+00	0.00E+00	8.87E+05	0.00E+00
PALLD	0.00E+00	0.00E+00	1.49E+06	1.48E+06	0.00E+00	0.00E+00
PAPSS1	0.00E+00	3.56E+05	0.00E+00	0.00E+00	0.00E+00	0.00E+00
PARN	0.00E+00	0.00E+00	0.00E+00	0.00E+00	0.00E+00	8.35E+05
PAWR	0.00E+00	4.92E+05	0.00E+00	0.00E+00	0.00E+00	0.00E+00
PCYT1A	0.00E+00	0.00E+00	6.15E+05	0.00E+00	0.00E+00	0.00E+00
PDAP1	0.00E+00	1.01E+06	0.00E+00	0.00E+00	0.00E+00	0.00E+00
PDCD4	0.00E+00	2.61E+06	0.00E+00	0.00E+00	2.86E+06	1.38E+06

PDCD6	0.00E+00	0.00E+00	0.00E+00	0.00E+00	0.00E+00	1.09E+06
PDE12	0.00E+00	0.00E+00	6.44E+05	0.00E+00	0.00E+00	0.00E+00
PDE3A	0.00E+00	0.00E+00	0.00E+00	0.00E+00	6.69E+05	0.00E+00
PDIA6	0.00E+00	0.00E+00	1.64E+05	0.00E+00	0.00E+00	0.00E+00
PELO	0.00E+00	4.76E+05	0.00E+00	0.00E+00	0.00E+00	0.00E+00
PHF5A	0.00E+00	0.00E+00	3.56E+05	0.00E+00	0.00E+00	0.00E+00
PHF6	0.00E+00	1.84E+06	3.09E+06	0.00E+00	1.78E+06	1.51E+06
PHIP	0.00E+00	1.37E+07	1.60E+06	0.00E+00	1.73E+07	0.00E+00
PKP1	0.00E+00	0.00E+00	0.00E+00	0.00E+00	0.00E+00	2.60E+06
PKP3	0.00E+00	0.00E+00	0.00E+00	0.00E+00	0.00E+00	4.27E+05
PLK1	0.00E+00	0.00E+00	5.04E+05	0.00E+00	0.00E+00	0.00E+00
PLRG1	0.00E+00	0.00E+00	0.00E+00	0.00E+00	1.43E+06	0.00E+00
PMM2	0.00E+00	0.00E+00	1.61E+06	0.00E+00	0.00E+00	1.94E+06
PNN	0.00E+00	1.54E+06	0.00E+00	0.00E+00	0.00E+00	1.13E+06
PNO1	0.00E+00	0.00E+00	0.00E+00	0.00E+00	1.67E+06	0.00E+00
POLD1	0.00E+00	0.00E+00	0.00E+00	0.00E+00	0.00E+00	1.19E+06
POLDIP3	0.00E+00	1.22E+06	0.00E+00	0.00E+00	1.59E+06	0.00E+00
POLR1C	0.00E+00	1.38E+05	0.00E+00	0.00E+00	0.00E+00	0.00E+00
POLR1E	0.00E+00	5.48E+05	0.00E+00	0.00E+00	0.00E+00	0.00E+00
POLR2A	0.00E+00	1.67E+06	2.35E+06	1.25E+06	0.00E+00	2.25E+06
POLR2B	0.00E+00	0.00E+00	0.00E+00	1.45E+06	0.00E+00	3.73E+06
POP1	0.00E+00	0.00E+00	0.00E+00	0.00E+00	6.90E+05	0.00E+00
PPIG	0.00E+00	0.00E+00	1.23E+06	0.00E+00	0.00E+00	0.00E+00
PPIL4	0.00E+00	0.00E+00	0.00E+00	0.00E+00	4.98E+05	0.00E+00
PPL	0.00E+00	0.00E+00	0.00E+00	1.41E+06	0.00E+00	0.00E+00
PPP1CC	0.00E+00	3.22E+06	0.00E+00	0.00E+00	3.97E+06	0.00E+00
PPP1R12A	0.00E+00	0.00E+00	3.54E+05	0.00E+00	0.00E+00	0.00E+00
PRMT3	0.00E+00	0.00E+00	0.00E+00	0.00E+00	6.93E+05	0.00E+00
PRPF31	0.00E+00	2.88E+05	0.00E+00	0.00E+00	0.00E+00	0.00E+00
PRPF38A	0.00E+00	5.73E+05	0.00E+00	0.00E+00	0.00E+00	0.00E+00
PRPF38B	0.00E+00	4.08E+05	0.00E+00	0.00E+00	0.00E+00	0.00E+00
PRPF40A	0.00E+00	0.00E+00	9.87E+05	0.00E+00	0.00E+00	0.00E+00
PSIP1	0.00E+00	1.32E+07	3.10E+06	2.01E+06	1.51E+07	2.67E+06
PSMB5	0.00E+00	0.00E+00	0.00E+00	0.00E+00	8.72E+05	0.00E+00
PSMC3	0.00E+00	0.00E+00	0.00E+00	1.31E+06	0.00E+00	1.15E+06
PSMD5	0.00E+00	0.00E+00	4.78E+05	0.00E+00	0.00E+00	0.00E+00
AARSD1	0.00E+00	0.00E+00	2.41E+05	0.00E+00	0.00E+00	0.00E+00
PTPN1	0.00E+00	0.00E+00	2.10E+05	0.00E+00	0.00E+00	0.00E+00
PUS7	0.00E+00	0.00E+00	1.94E+05	0.00E+00	0.00E+00	0.00E+00
PWP1	0.00E+00	1.43E+06	0.00E+00	0.00E+00	2.58E+06	0.00E+00
PWP2	0.00E+00	3.14E+05	0.00E+00	0.00E+00	0.00E+00	0.00E+00
PYCR1	0.00E+00	0.00E+00	8.75E+05	0.00E+00	0.00E+00	0.00E+00
RAB10	0.00E+00	0.00E+00	0.00E+00	0.00E+00	0.00E+00	1.06E+06
RAB14	0.00E+00	0.00E+00	2.72E+05	0.00E+00	0.00E+00	0.00E+00
RAB2A	0.00E+00	0.00E+00	0.00E+00	0.00E+00	0.00E+00	5.92E+05
RAB6B	0.00E+00	0.00E+00	0.00E+00	0.00E+00	0.00E+00	5.54E+06
RAB8A	0.00E+00	0.00E+00	0.00E+00	0.00E+00	5.07E+05	0.00E+00
RACGAP1	0.00E+00	0.00E+00	1.83E+06	0.00E+00	0.00E+00	1.79E+06
RAI14	0.00E+00	0.00E+00	2.47E+05	0.00E+00	0.00E+00	0.00E+00
RANBP1	0.00E+00	1.04E+07	7.46E+06	6.35E+06	1.18E+07	1.58E+07
RAP1B	0.00E+00	0.00E+00	0.00E+00	0.00E+00	1.22E+06	0.00E+00
RBM15	0.00E+00	0.00E+00	0.00E+00	0.00E+00	7.05E+05	0.00E+00
RBM17	0.00E+00	0.00E+00	7.28E+05	0.00E+00	0.00E+00	0.00E+00
RBM22	0.00E+00	0.00E+00	1.61E+06	0.00E+00	0.00E+00	0.00E+00
RBM25	0.00E+00	0.00E+00	2.70E+06	5.29E+06	0.00E+00	0.00E+00
RBMX2	0.00E+00	8.91E+05	0.00E+00	0.00E+00	0.00E+00	0.00E+00
RCL1	0.00E+00	7.82E+05	0.00E+00	0.00E+00	0.00E+00	0.00E+00
RCOR1	0.00E+00	0.00E+00	2.26E+05	0.00E+00	0.00E+00	0.00E+00
RFC1	0.00E+00	1.14E+06	0.00E+00	0.00E+00	1.04E+06	0.00E+00
RHEB	0.00E+00	0.00E+00	4.27E+05	0.00E+00	0.00E+00	0.00E+00
RIF1	0.00E+00	0.00E+00	0.00E+00	0.00E+00	4.27E+06	0.00E+00
RIOK1	0.00E+00	1.06E+06	0.00E+00	0.00E+00	0.00E+00	0.00E+00
RNF20	0.00E+00	0.00E+00	8.22E+05	8.81E+05	0.00E+00	0.00E+00
RNF213	0.00E+00	0.00E+00	0.00E+00	1.37E+05	0.00E+00	0.00E+00
RNF40	0.00E+00	0.00E+00	2.80E+06	1.08E+06	0.00E+00	0.00E+00
RNPS1	0.00E+00	0.00E+00	2.31E+06	0.00E+00	4.34E+06	2.18E+06
ROCK2	0.00E+00	0.00E+00	0.00E+00	0.00E+00	0.00E+00	1.83E+06
RPF1	0.00E+00	3.23E+06	0.00E+00	0.00E+00	6.35E+06	0.00E+00
RPL26L1	0.00E+00	1.15E+06	0.00E+00	0.00E+00	1.77E+06	0.00E+00
RPL7L1	0.00E+00	4.19E+06	0.00E+00	0.00E+00	6.66E+06	0.00E+00
RPP30	0.00E+00	0.00E+00	0.00E+00	0.00E+00	0.00E+00	3.20E+05
RPS15	0.00E+00	1.37E+07	0.00E+00	0.00E+00	1.83E+07	0.00E+00
RPS28	0.00E+00	1.16E+07	3.85E+06	1.96E+06	1.19E+07	4.26E+06
RRBP1	0.00E+00	0.00E+00	0.00E+00	1.82E+06	3.65E+06	0.00E+00
RRP1	0.00E+00	1.63E+07	3.21E+06	0.00E+00	1.42E+07	7.22E+06
RRP36	0.00E+00	1.56E+06	0.00E+00	0.00E+00	2.61E+06	0.00E+00
RRP7A	0.00E+00	8.85E+05	0.00E+00	0.00E+00	2.07E+06	0.00E+00
RRP9	0.00E+00	8.12E+06	0.00E+00	0.00E+00	3.56E+06	2.04E+06
RSL24D1	0.00E+00	4.00E+06	0.00E+00	0.00E+00	8.22E+06	0.00E+00
S100P	0.00E+00	0.00E+00	1.61E+06	0.00E+00	0.00E+00	0.00E+00
SACM1L	0.00E+00	4.44E+05	0.00E+00	0.00E+00	0.00E+00	0.00E+00
SAFB2	0.00E+00	8.82E+05	0.00E+00	0.00E+00	0.00E+00	0.00E+00
SAP18	0.00E+00	8.01E+05	0.00E+00	0.00E+00	0.00E+00	0.00E+00
SCML2	0.00E+00	6.94E+05	0.00E+00	1.07E+06	0.00E+00	0.00E+00
SCYL1	0.00E+00	9.62E+05	2.43E+06	2.33E+06	0.00E+00	1.28E+06
SDAD1	0.00E+00	1.59E+06	1.13E+06	0.00E+00	3.52E+06	0.00E+00
SEC11A	0.00E+00	0.00E+00	6.19E+05	0.00E+00	0.00E+00	0.00E+00
SENP3	0.00E+00	1.43E+06	1.40E+06	1.11E+06	3.85E+06	3.36E+06
SF3A1	0.00E+00	0.00E+00	0.00E+00	0.00E+00	0.00E+00	1.16E+06
SF3A2	0.00E+00	0.00E+00	1.08E+06	0.00E+00	0.00E+00	0.00E+00
SF3B6	0.00E+00	0.00E+00	2.17E+05	0.00E+00	0.00E+00	0.00E+00
SIN3A	0.00E+00	4.63E+05	0.00E+00	0.00E+00	0.00E+00	0.00E+00
SLC25A1	0.00E+00	5.37E+05	0.00E+00	0.00E+00	0.00E+00	0.00E+00
SLC35B2	0.00E+00	0.00E+00	3.59E+05	0.00E+00	0.00E+00	0.00E+00
SLK	0.00E+00	0.00E+00	0.00E+00	0.00E+00	0.00E+00	1.77E+05
SLTM	0.00E+00	0.00E+00	0.00E+00	1.55E+06	4.38E+06	3.70E+06
SMCHD1	0.00E+00	6.31E+05	0.00E+00	0.00E+00	7.19E+05	0.00E+00
SNIP1	0.00E+00	0.00E+00	0.00E+00	0.00E+00	5.97E+05	0.00E+00
SNRPE	0.00E+00	1.77E+06	0.00E+00	0.00E+00	2.02E+06	0.00E+00
SNRPG	0.00E+00	2.62E+06	0.00E+00	0.00E+00	0.00E+00	0.00E+00
SNX1	0.00E+00	0.00E+00	5.49E+05	0.00E+00	0.00E+00	0.00E+00
SPTY2D1	0.00E+00	1.02E+06	0.00E+00	0.00E+00	0.00E+00	0.00E+00

SQSTM1	0.00E+00	0.00E+00	3.14E+05	0.00E+00	0.00E+00	0.00E+00
SRP9	0.00E+00	0.00E+00	3.10E+05	0.00E+00	0.00E+00	0.00E+00
SRPK1	0.00E+00	6.18E+05	0.00E+00	0.00E+00	0.00E+00	0.00E+00
SRPR	0.00E+00	0.00E+00	1.02E+06	0.00E+00	0.00E+00	1.03E+06
SSR1	0.00E+00	0.00E+00	1.38E+06	0.00E+00	0.00E+00	0.00E+00
SSR4	0.00E+00	1.59E+06	0.00E+00	0.00E+00	0.00E+00	0.00E+00
STUB1	0.00E+00	0.00E+00	7.76E+05	0.00E+00	0.00E+00	0.00E+00
SUGP2	0.00E+00	0.00E+00	0.00E+00	0.00E+00	0.00E+00	6.78E+05
SUMO1	0.00E+00	0.00E+00	1.23E+06	0.00E+00	0.00E+00	0.00E+00
SUMO2	0.00E+00	0.00E+00	0.00E+00	0.00E+00	0.00E+00	2.74E+06
SUPT5H	0.00E+00	0.00E+00	0.00E+00	0.00E+00	4.83E+06	0.00E+00
SURF4	0.00E+00	0.00E+00	0.00E+00	0.00E+00	9.57E+05	0.00E+00
SUV39H1	0.00E+00	2.37E+06	0.00E+00	0.00E+00	6.12E+06	0.00E+00
SUZ12	0.00E+00	9.95E+05	0.00E+00	0.00E+00	1.34E+06	0.00E+00
TARS2	0.00E+00	0.00E+00	1.08E+06	0.00E+00	0.00E+00	0.00E+00
TCEA1	0.00E+00	0.00E+00	5.08E+05	0.00E+00	0.00E+00	0.00E+00
TCOF1	0.00E+00	3.92E+06	1.67E+06	3.32E+06	6.14E+06	1.48E+06
TMA16	0.00E+00	2.28E+06	0.00E+00	0.00E+00	2.38E+06	0.00E+00
TMEM214	0.00E+00	2.92E+06	3.70E+06	4.39E+06	3.64E+06	6.41E+06
TMPO	0.00E+00	3.18E+06	0.00E+00	0.00E+00	2.80E+06	1.19E+06
TNS3	0.00E+00	0.00E+00	8.26E+05	0.00E+00	0.00E+00	0.00E+00
TOE1	0.00E+00	0.00E+00	2.63E+06	0.00E+00	0.00E+00	0.00E+00
TOMM34	0.00E+00	0.00E+00	5.84E+05	0.00E+00	0.00E+00	0.00E+00
TOP2B	0.00E+00	1.79E+06	0.00E+00	0.00E+00	1.63E+06	0.00E+00
TOR1AIP1	0.00E+00	8.99E+05	0.00E+00	0.00E+00	0.00E+00	8.18E+05
TP53BP1	0.00E+00	0.00E+00	7.09E+05	0.00E+00	0.00E+00	0.00E+00
TPM1	0.00E+00	0.00E+00	1.23E+06	0.00E+00	0.00E+00	0.00E+00
TRIM16	0.00E+00	0.00E+00	5.31E+05	0.00E+00	0.00E+00	0.00E+00
TRIM33	0.00E+00	0.00E+00	0.00E+00	0.00E+00	0.00E+00	8.36E+05
TRIP12	0.00E+00	2.62E+05	0.00E+00	0.00E+00	0.00E+00	0.00E+00
TRMT112	0.00E+00	7.64E+05	0.00E+00	0.00E+00	0.00E+00	0.00E+00
TRMT1L	0.00E+00	0.00E+00	7.47E+05	0.00E+00	0.00E+00	0.00E+00
TSR1	0.00E+00	4.47E+06	1.33E+06	1.75E+06	6.72E+06	3.66E+06
TTC37	0.00E+00	0.00E+00	2.34E+06	2.34E+06	0.00E+00	0.00E+00
TTN	0.00E+00	0.00E+00	0.00E+00	0.00E+00	0.00E+00	2.85E+06
TWF1	0.00E+00	1.22E+06	4.37E+06	1.67E+06	0.00E+00	0.00E+00
UBE2L3	0.00E+00	0.00E+00	0.00E+00	0.00E+00	1.47E+05	0.00E+00
UNC45A	0.00E+00	0.00E+00	7.84E+05	0.00E+00	0.00E+00	0.00E+00
USP3	0.00E+00	0.00E+00	0.00E+00	0.00E+00	9.41E+05	0.00E+00
USP39	0.00E+00	1.90E+06	0.00E+00	0.00E+00	8.03E+05	0.00E+00
USP48	0.00E+00	0.00E+00	8.91E+05	0.00E+00	0.00E+00	0.00E+00
USP9X	0.00E+00	0.00E+00	3.32E+06	3.84E+06	0.00E+00	2.52E+06
UTP15	0.00E+00	1.18E+06	0.00E+00	0.00E+00	1.95E+06	9.92E+05
UTP18	0.00E+00	5.04E+06	0.00E+00	0.00E+00	4.40E+06	0.00E+00
UTP20	0.00E+00	0.00E+00	0.00E+00	0.00E+00	9.77E+05	0.00E+00
UTP23	0.00E+00	1.29E+06	0.00E+00	0.00E+00	0.00E+00	0.00E+00
UTP3	0.00E+00	2.04E+06	0.00E+00	0.00E+00	0.00E+00	0.00E+00
UTP6	0.00E+00	0.00E+00	0.00E+00	0.00E+00	1.29E+06	0.00E+00
VASP	0.00E+00	0.00E+00	1.46E+06	1.29E+06	0.00E+00	0.00E+00
VRK1	0.00E+00	2.41E+06	0.00E+00	0.00E+00	7.22E+06	0.00E+00
WAPAL	0.00E+00	0.00E+00	3.48E+05	0.00E+00	0.00E+00	0.00E+00
WDR18	0.00E+00	0.00E+00	1.74E+06	0.00E+00	0.00E+00	0.00E+00
WDR33	0.00E+00	0.00E+00	4.15E+05	0.00E+00	0.00E+00	0.00E+00
WDR43	0.00E+00	0.00E+00	0.00E+00	0.00E+00	0.00E+00	1.63E+06
WDR46	0.00E+00	5.61E+06	0.00E+00	0.00E+00	8.26E+06	0.00E+00
WDR75	0.00E+00	0.00E+00	0.00E+00	0.00E+00	1.67E+06	0.00E+00
WHSC1	0.00E+00	1.64E+06	0.00E+00	0.00E+00	1.76E+06	0.00E+00
XPO5	0.00E+00	9.52E+05	0.00E+00	1.89E+06	0.00E+00	4.01E+06
XRN1	0.00E+00	0.00E+00	3.11E+05	0.00E+00	0.00E+00	0.00E+00
YBX3	0.00E+00	0.00E+00	0.00E+00	0.00E+00	1.62E+06	0.00E+00
YES1	0.00E+00	0.00E+00	1.20E+06	0.00E+00	0.00E+00	0.00E+00
YTHDC1	0.00E+00	1.90E+06	0.00E+00	0.00E+00	1.88E+06	0.00E+00
YY1	0.00E+00	0.00E+00	5.59E+05	0.00E+00	0.00E+00	0.00E+00
ZC3H14	0.00E+00	0.00E+00	3.87E+06	0.00E+00	0.00E+00	0.00E+00
ZC3H15	0.00E+00	0.00E+00	0.00E+00	0.00E+00	0.00E+00	3.76E+05
ZMPSTE24	0.00E+00	0.00E+00	0.00E+00	3.68E+05	0.00E+00	0.00E+00
ZMYM4	0.00E+00	0.00E+00	2.56E+05	0.00E+00	0.00E+00	0.00E+00
ZNF207	0.00E+00	0.00E+00	0.00E+00	0.00E+00	1.10E+06	1.50E+06
ZNF280C	0.00E+00	7.78E+05	0.00E+00	0.00E+00	6.75E+05	0.00E+00
ZNF512	0.00E+00	1.69E+07	0.00E+00	0.00E+00	1.96E+07	0.00E+00
ZNF622	0.00E+00	1.11E+06	0.00E+00	0.00E+00	1.44E+06	0.00E+00
ZRANB2	0.00E+00	0.00E+00	1.49E+06	0.00E+00	0.00E+00	0.00E+00
ZYX	0.00E+00	0.00E+00	2.82E+06	0.00E+00	0.00E+00	0.00E+00

Table S7 Significantly enriched proteins from HeLa cells in TCO nonHS compared to EV nonHS (p<0.05).

Gene names	−Log(P-value)	Difference	mean (LFQ int.) TCO nonHS	mean (LFQ int.) EV nonHS
TALE	4.6950	6.4071	27.9032	21.4961
COTL1	3.1532	1.1975	22.0918	20.8944
RHOA	2.1864	1.6099	23.0068	21.3969
OXCT1	2.7377	1.9793	23.3031	21.3238
CALM2	1.0591	2.0070	24.3234	22.3164
YWHAH	2.2745	2.2780	22.7089	20.4309
NAP1L4	3.3256	2.2935	23.7246	21.4311
MIF	3.2628	2.7101	23.9896	21.2796

Table S8 Significantly enriched proteins from HeLa cells in TCO HS compared to EV HS (p<0.05).

Gene names	−Log(P-value)	Difference	mean (LFQ int.) TCO HS	mean (LFQ int.) EV HS
TALE	4.6005	6.1878	27.3121	21.1244
HINT1	2.5601	2.6019	24.1647	21.5628
ETFA	1.9104	2.4360	22.9424	20.5064
ATIC	2.3577	2.3089	23.7908	21.4819
PARK7	5.0908	2.2913	23.0355	20.7442
LGALS3	3.3725	2.0289	23.2534	21.2245
ADK	2.0305	1.9064	22.7883	20.8818
YWHAH	3.3827	1.7896	22.8418	21.0522
CPS1	1.3180	1.7491	24.5660	22.8169
PEBP1	1.2329	1.7008	23.5705	21.8697
GNAI3	1.0432	1.6446	23.0288	21.3842
BLVRB	1.1314	1.5448	22.2569	20.7121
HSPH1	1.4810	1.4819	22.6721	21.1903
MDH2	1.5280	1.3505	23.3055	21.9550
UBA1	2.2197	1.0850	26.1969	25.1119
RBM3	2.2649	1.0283	21.6695	20.6413

Table S9 Significantly enriched proteins from HeLa cells in TCO HS compared to TCO nonHS ($p<0.05$).

Gene names	−Log(P-value)	Difference	mean (LFQ int.) TCO HS	mean (LFQ int.) TCO non HS
PTGES3	2.9582	-3.2430	24.5398	21.2968
HMGB2	4.4031	-2.9499	24.0492	21.0992
HINT1	1.7892	-2.9431	24.1647	21.2216
AKR1B1	0.9240	-2.3302	23.9924	21.6622
RPL38	3.8682	-2.3184	23.2040	20.8856
ATIC	1.2741	-2.1231	23.7908	21.6677
LTA4H	2.5476	-2.0508	23.4684	21.4176
RPN2	2.9029	-2.0411	23.0450	21.0039
ADK	3.3698	-2.0242	22.7883	20.7641
UBA1	3.5027	-2.0080	26.1969	24.1888
BLVRB	2.2097	-1.7699	22.2569	20.4871
SEC13	3.3697	-1.7696	22.5590	20.7894
LGALS3	3.4343	-1.7235	23.2534	21.5299

Table S10 Identified proteins from HEK293T cells for different genomic loci.

Gene names	mean (LFQ int.) Line1	mean (LFQ int.) Alu	mean (LFQ int.) SatII	mean (LFQ int.) SatIII	mean (LFQ int.) Telomere
Protease 1	3.64E+10	3.13E+10	3.57E+10	3.46E+10	4.23E+10
TALE	1.03E+10	1.57E+10	1.77E+10	1.13E+10	1.78E+10
KRT1	5.50E+09	6.19E+09	4.71E+09	8.94E+09	4.85E+09
KRT13	0.00E+00	3.60E+07	1.43E+09	3.49E+07	0.00E+00
KRT6C	6.17E+08	5.35E+08	1.17E+09	6.73E+08	4.40E+08
KRT9	1.14E+09	2.06E+09	1.12E+09	2.99E+09	1.11E+09
KRT2	5.29E+08	6.17E+08	7.37E+08	6.70E+08	5.91E+08
NPM1	2.46E+08	3.14E+08	4.59E+08	2.71E+08	2.89E+08
HSPA1B	1.77E+08	3.33E+08	3.93E+08	1.40E+08	1.69E+07
KRT4	0.00E+00	0.00E+00	3.50E+08	0.00E+00	0.00E+00
HSPA8	1.37E+08	2.01E+08	2.96E+08	1.23E+08	2.43E+07
HIST2H2BE	0.00E+00	2.16E+08	2.74E+08	1.09E+08	1.61E+08
HSP90AA1	1.10E+08	1.31E+08	2.66E+08	9.49E+07	4.24E+07
HIST1H4A	0.00E+00	4.35E+08	2.58E+08	2.22E+08	2.63E+08
HIST1H2AJ	0.00E+00	2.76E+08	2.08E+08	8.64E+07	9.48E+07
EEF1A1P5	2.05E+08	1.83E+08	1.94E+08	1.04E+08	4.32E+07
OGT	1.48E+08	1.77E+08	1.64E+08	6.42E+07	0.00E+00
PPIA	0.00E+00	8.16E+07	1.32E+08	0.00E+00	0.00E+00
CKB	0.00E+00	1.27E+08	1.17E+08	0.00E+00	4.97E+07
NCL	3.14E+07	7.63E+07	1.16E+08	6.54E+07	6.37E+07
TUBA1B	3.58E+07	3.41E+07	1.01E+08	0.00E+00	0.00E+00
HSP90AB1	7.75E+07	7.92E+07	1.01E+08	5.55E+07	0.00E+00
HNRNPD	1.31E+07	8.01E+07	9.13E+07	4.23E+07	4.57E+07
HNRNPK	1.65E+07	8.88E+07	8.49E+07	5.21E+07	2.16E+07
HNRNPA1	0.00E+00	0.00E+00	8.22E+07	0.00E+00	2.86E+07
TUBB	3.18E+07	6.71E+07	7.92E+07	1.79E+07	0.00E+00
PARP1	0.00E+00	9.54E+07	7.91E+07	1.65E+07	1.16E+07
DDX5	0.00E+00	5.29E+07	7.65E+07	0.00E+00	0.00E+00
EEF2	3.10E+07	6.53E+07	6.80E+07	4.02E+07	1.31E+07
ENO1	0.00E+00	7.27E+07	6.62E+07	9.22E+06	1.09E+07
TRIM28	0.00E+00	0.00E+00	5.92E+07	0.00E+00	1.96E+07
KRT16	1.81E+08	4.67E+07	5.88E+07	0.00E+00	7.04E+07
HNRNPC	2.65E+07	9.05E+07	5.84E+07	0.00E+00	3.00E+07
ANXA1	0.00E+00	0.00E+00	5.47E+07	0.00E+00	0.00E+00
KRT14	3.00E+07	7.72E+07	4.76E+07	6.49E+07	2.89E+07
PRDX1	0.00E+00	4.37E+07	4.70E+07	0.00E+00	0.00E+00
HNRNPH1	0.00E+00	4.29E+07	4.17E+07	2.18E+07	0.00E+00
HNRNPM	0.00E+00	5.72E+07	3.64E+07	0.00E+00	0.00E+00
DHX9	0.00E+00	3.47E+07	3.55E+07	0.00E+00	0.00E+00
ALDOA	0.00E+00	0.00E+00	3.55E+07	0.00E+00	0.00E+00
EIF5A	0.00E+00	0.00E+00	3.48E+07	0.00E+00	0.00E+00
PFN1	0.00E+00	3.04E+07	3.28E+07	2.04E+07	0.00E+00
SFPQ	0.00E+00	0.00E+00	2.80E+07	0.00E+00	0.00E+00
KRT6A	0.00E+00	0.00E+00	2.72E+07	0.00E+00	0.00E+00
HNRNPU	0.00E+00	3.81E+07	2.67E+07	0.00E+00	0.00E+00
HNRNPL	0.00E+00	0.00E+00	2.63E+07	0.00E+00	0.00E+00
KRT5	0.00E+00	1.47E+07	2.23E+07	2.25E+07	0.00E+00
PGK1	0.00E+00	2.51E+07	2.21E+07	0.00E+00	0.00E+00
HNRNPDL	0.00E+00	9.59E+06	2.19E+07	0.00E+00	0.00E+00
ACTG1	0.00E+00	0.00E+00	2.17E+07	0.00E+00	0.00E+00
NAP1L1	2.80E+07	1.07E+07	2.16E+07	6.77E+06	0.00E+00
PTBP1	0.00E+00	2.29E+07	2.14E+07	0.00E+00	8.69E+06
XRCC6	0.00E+00	4.21E+07	1.92E+07	8.02E+06	0.00E+00
PCBP2	2.13E+07	2.11E+07	1.85E+07	0.00E+00	0.00E+00
TUBB4B	0.00E+00	1.20E+07	1.68E+07	0.00E+00	0.00E+00
RPS8	0.00E+00	1.05E+07	1.29E+07	0.00E+00	0.00E+00
U2AF1	0.00E+00	0.00E+00	1.29E+07	0.00E+00	0.00E+00
NONO	0.00E+00	0.00E+00	1.25E+07	0.00E+00	0.00E+00
SUPT16H	0.00E+00	1.16E+07	1.21E+07	0.00E+00	0.00E+00
EEF1G	0.00E+00	0.00E+00	1.14E+07	0.00E+00	0.00E+00
RPL23	0.00E+00	0.00E+00	1.12E+07	0.00E+00	0.00E+00
PRDX2	0.00E+00	0.00E+00	1.08E+07	0.00E+00	0.00E+00
DDX3X	1.10E+07	9.31E+06	1.07E+07	0.00E+00	0.00E+00
FASN	0.00E+00	0.00E+00	1.04E+07	0.00E+00	0.00E+00
DNAJA1	0.00E+00	0.00E+00	9.97E+06	0.00E+00	0.00E+00
GNB2L1	0.00E+00	0.00E+00	9.06E+06	0.00E+00	0.00E+00
U2AF2	0.00E+00	0.00E+00	8.74E+06	0.00E+00	0.00E+00
RPS3	0.00E+00	0.00E+00	8.70E+06	0.00E+00	0.00E+00
CACYBP	0.00E+00	0.00E+00	8.56E+06	0.00E+00	0.00E+00
RPL14	0.00E+00	1.38E+07	8.54E+06	0.00E+00	0.00E+00
RSL1D1	0.00E+00	0.00E+00	7.56E+06	0.00E+00	0.00E+00
RPL13	0.00E+00	0.00E+00	7.00E+06	0.00E+00	0.00E+00
PAICS	0.00E+00	6.23E+06	6.98E+06	0.00E+00	0.00E+00
MCM3	0.00E+00	5.04E+06	4.38E+06	0.00E+00	0.00E+00
RAN	2.32E+07	0.00E+00	0.00E+00	0.00E+00	2.04E+07
ORM1	1.97E+07	0.00E+00	0.00E+00	0.00E+00	0.00E+00
AHCY	0.00E+00	1.24E+07	0.00E+00	0.00E+00	0.00E+00
CCT8	0.00E+00	4.58E+06	0.00E+00	0.00E+00	0.00E+00
DIS3	0.00E+00	6.82E+06	0.00E+00	0.00E+00	0.00E+00
DOCK7	0.00E+00	0.00E+00	0.00E+00	2.72E+08	0.00E+00
HIST1H1C	0.00E+00	0.00E+00	0.00E+00	0.00E+00	6.90E+07
HNRNPA2B1	0.00E+00	8.16E+07	0.00E+00	0.00E+00	2.37E+07
KRT78	0.00E+00	0.00E+00	0.00E+00	5.06E+06	0.00E+00
RPL11	0.00E+00	4.30E+06	0.00E+00	0.00E+00	0.00E+00
RPL30	0.00E+00	1.10E+07	0.00E+00	0.00E+00	0.00E+00
SSRP1	0.00E+00	2.26E+07	0.00E+00	0.00E+00	0.00E+00

12.6 Microscopy Images

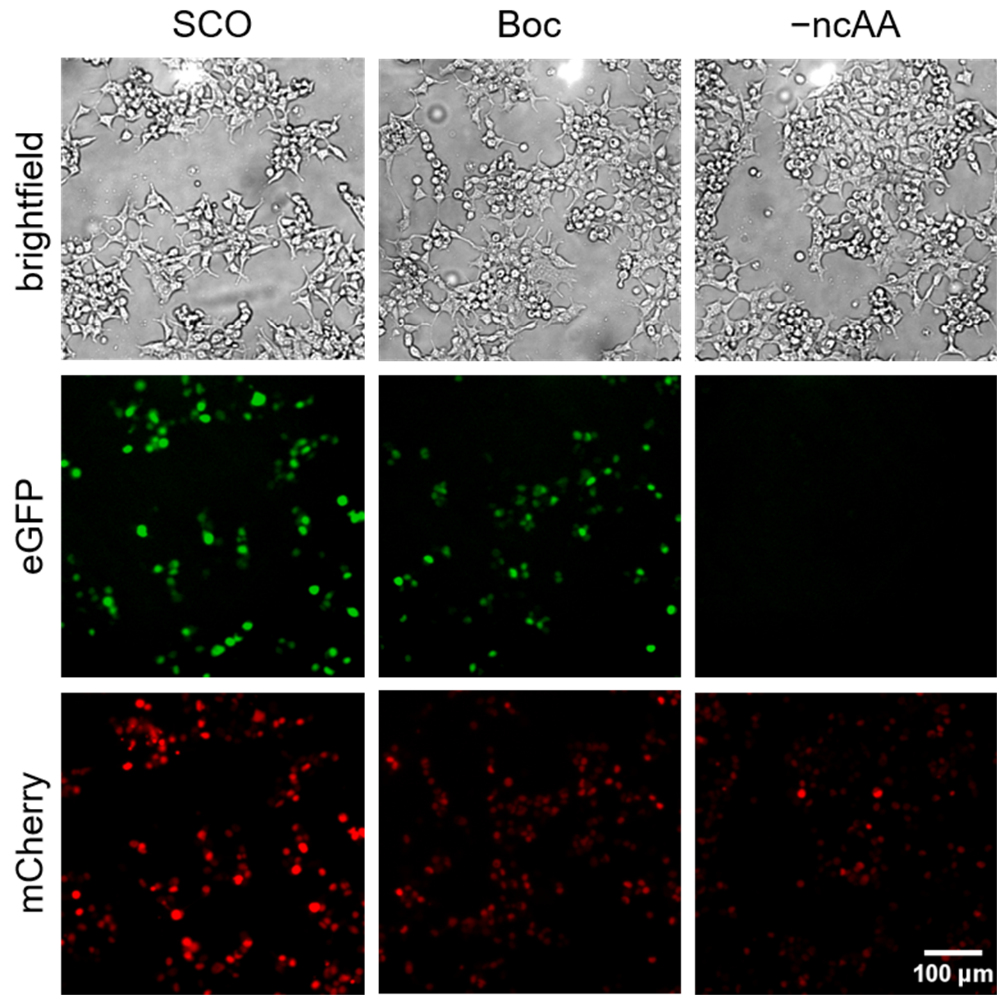

Figure S25 Additional brightfield images of fidelity of Amber Suppression using PylRS-AF/tRNA^{Pyl} pair: Fluorescent images (10x) of HEK293T cells, expressing mCherry-GFP^{Y39TAG} transfection control fusion contruct and tRNA^{Pyl}/PylRS-AF.

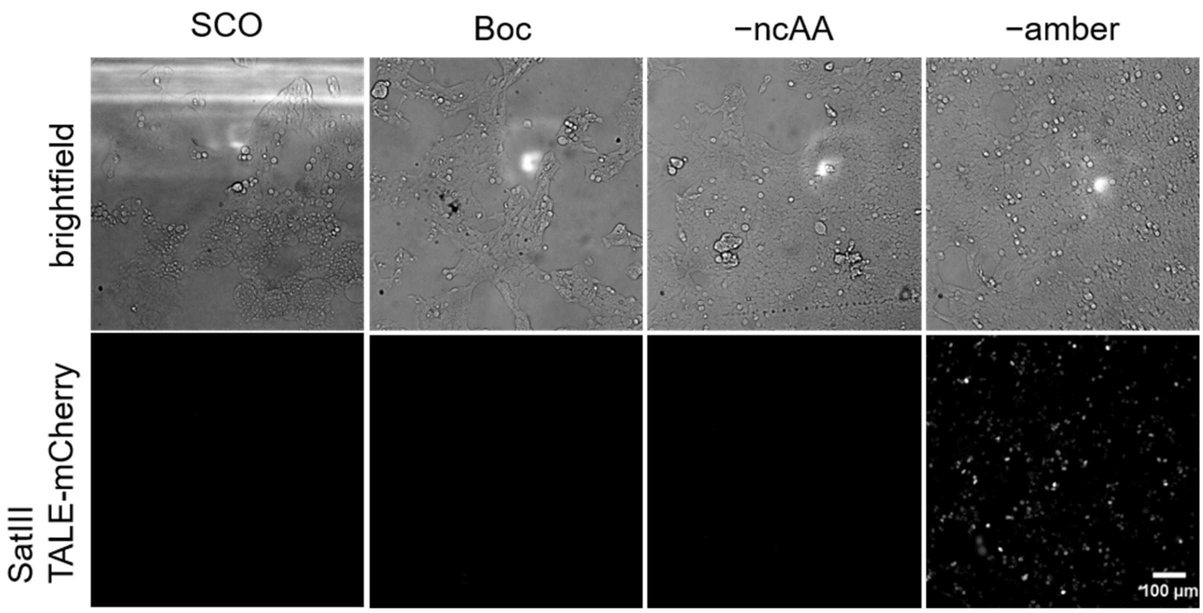

Figure S26 Additional brightfield images of incorporation efficiency at position V92 and expression efficiency of the SatIII-TALE: Fluorescent images of HEK293T cells, expressing ^{V92TAG}SatIII-TALE mCherry fusion construct and tRNA^{Pyl}/PylRS-AF. Images were taken in the brightfield channel and RFP channel showing incorporation of ncAA Boc or SCO and expression of SatIII-TALE-mCherry fusion construct. –amber: SatIII-TALE-mCherry without amber codon.

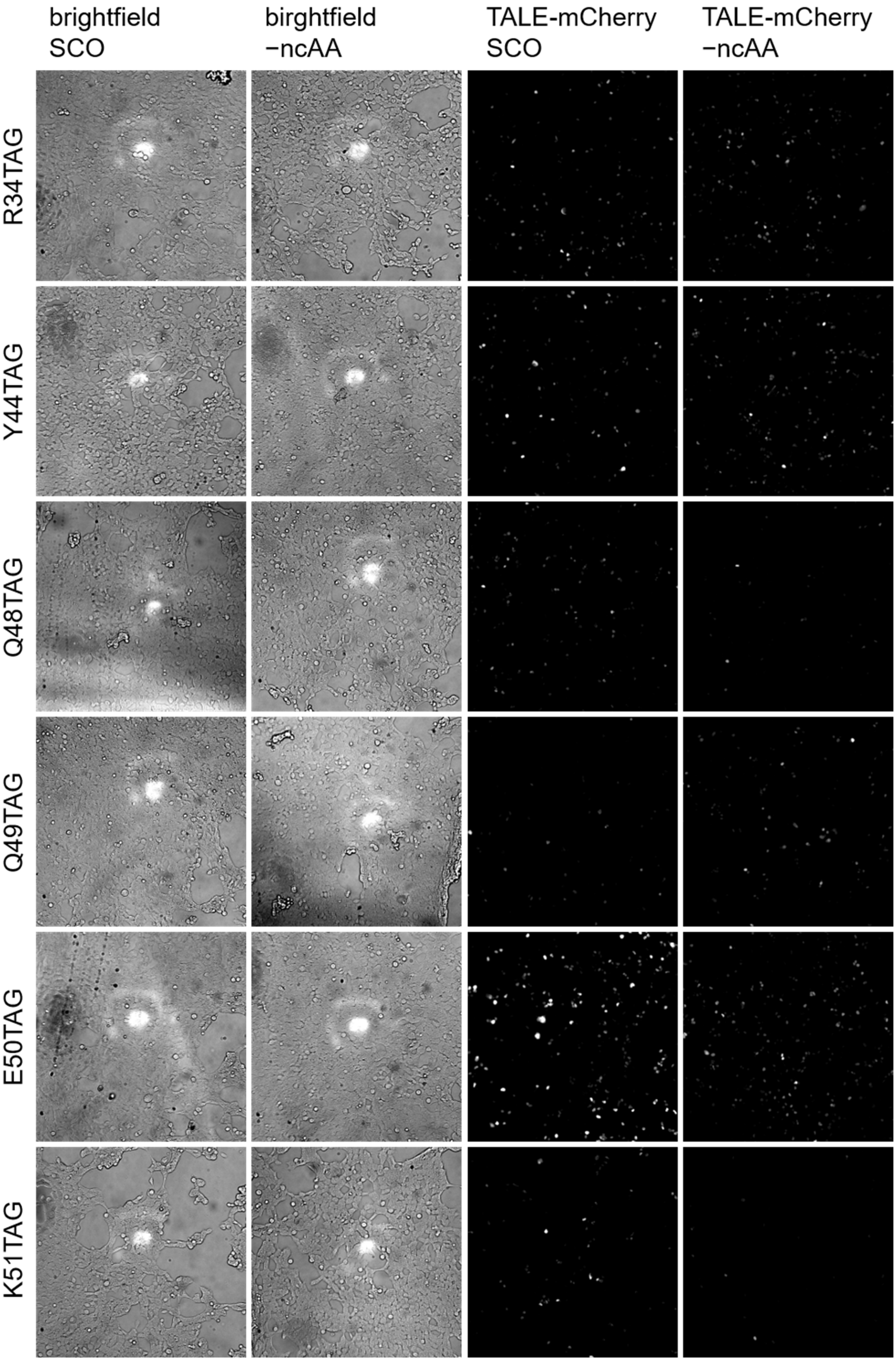
brightfield
SCO
birghtfield
−ncAA
TALE-mCherry
SCO
TALE-mCherry
−ncAA
R34TAG
Y44TAG
Q48TAG
Q49TAG
E50TAG
K51TAG

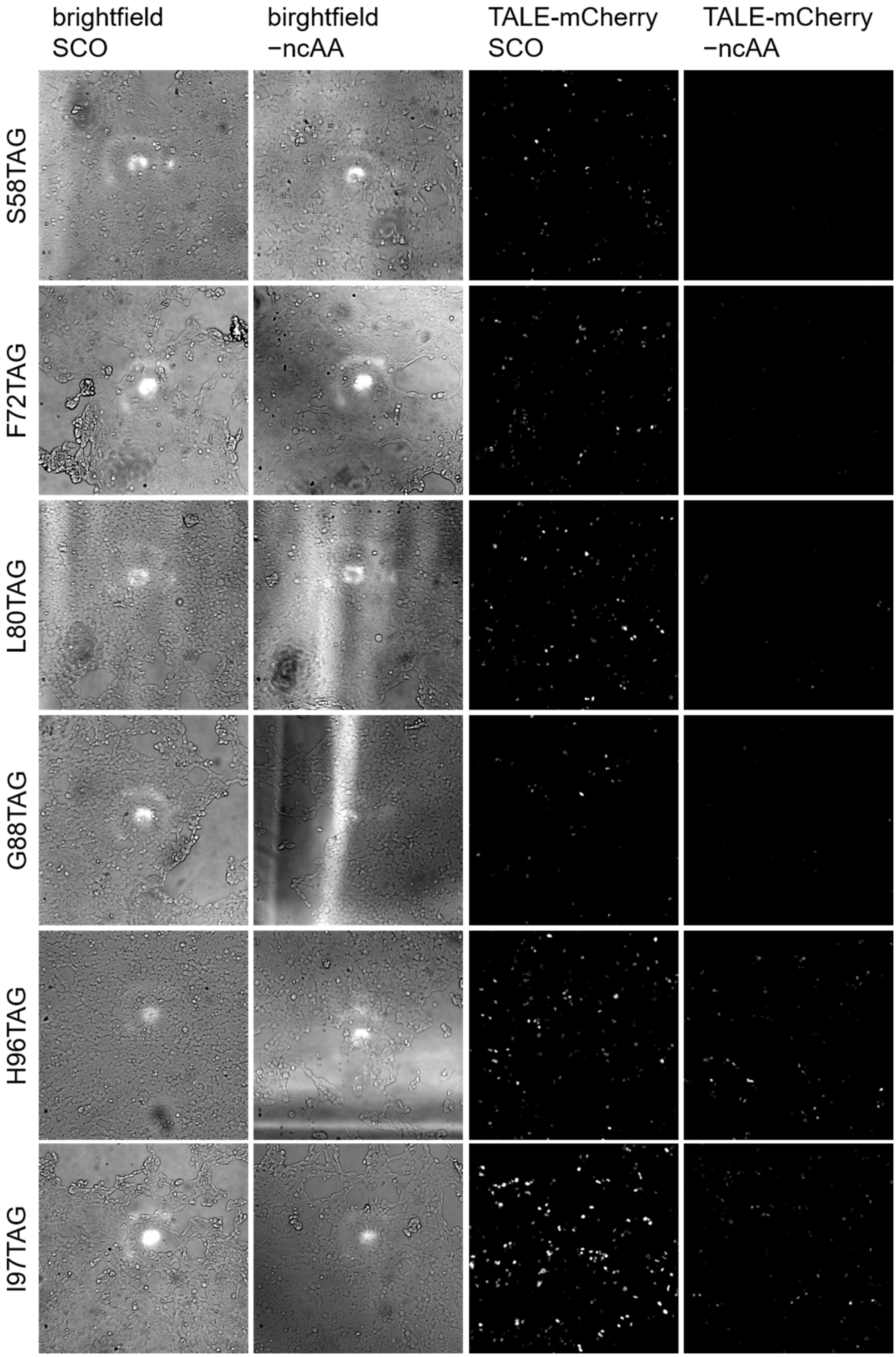
brightfield
SCO
birghtfield
−ncAA
TALE-mCherry
SCO
TALE-mCherry
−ncAA
S58TAG
F72TAG
L80TAG
G88TAG
H96TAG
I97TAG

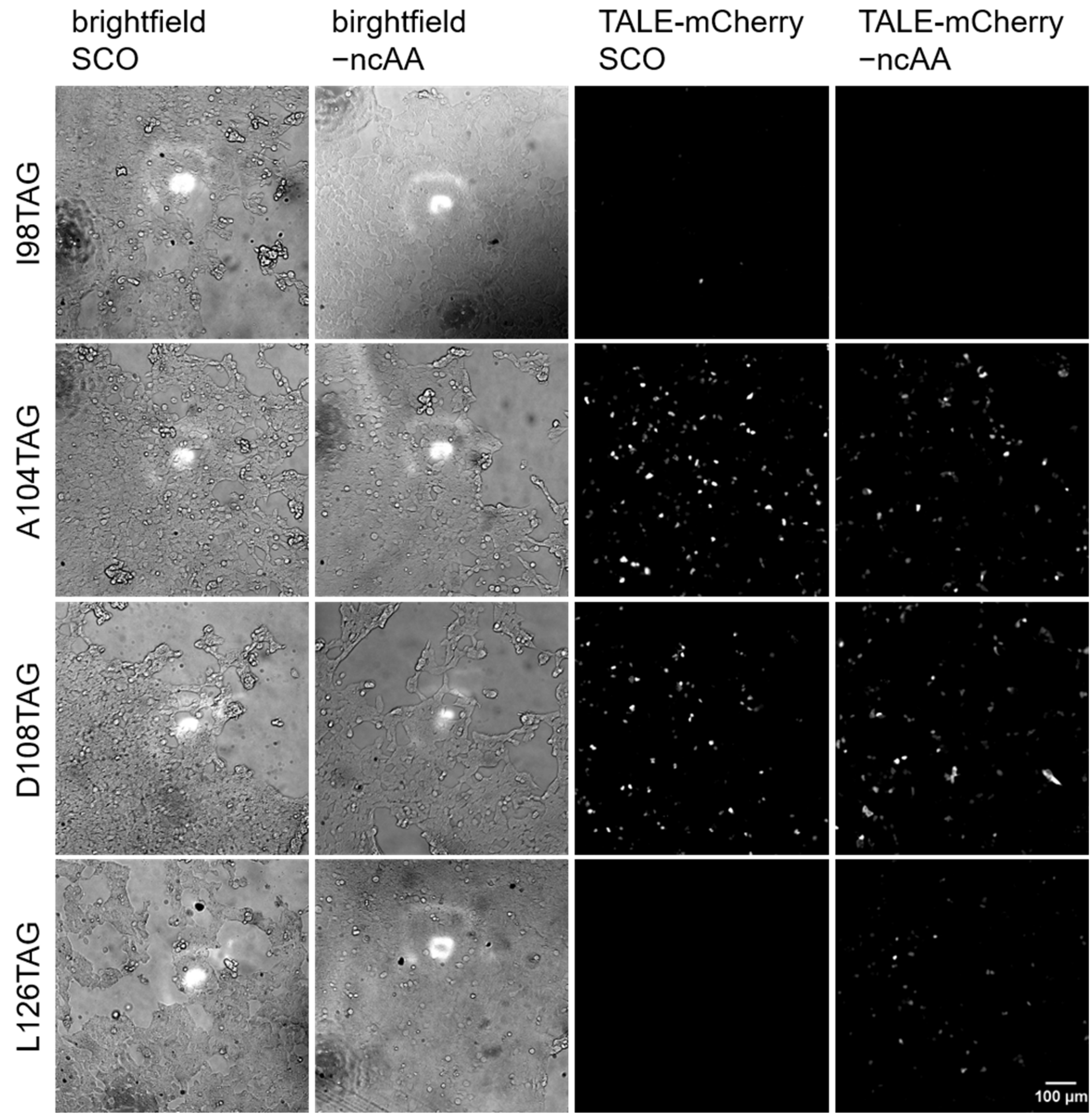

Figure S27 Whole fluorescent microscopy screen and additional brightfield images of for studying non-canonical amino acid (ncAA) incorporation efficiency into SatIII-TALE: Fluorescent images of HEK293T cells, expressing ^{TAG}SatIII-TALE mCherry fusion constructs and tRNA^{Pyl}/PylRS-AF^{NES}. Images were taken in the brightfield channel and in the RFP channel showing incorporation of SCO at different positions and expression of the SatIII-TALE-mCherry fusion construct.

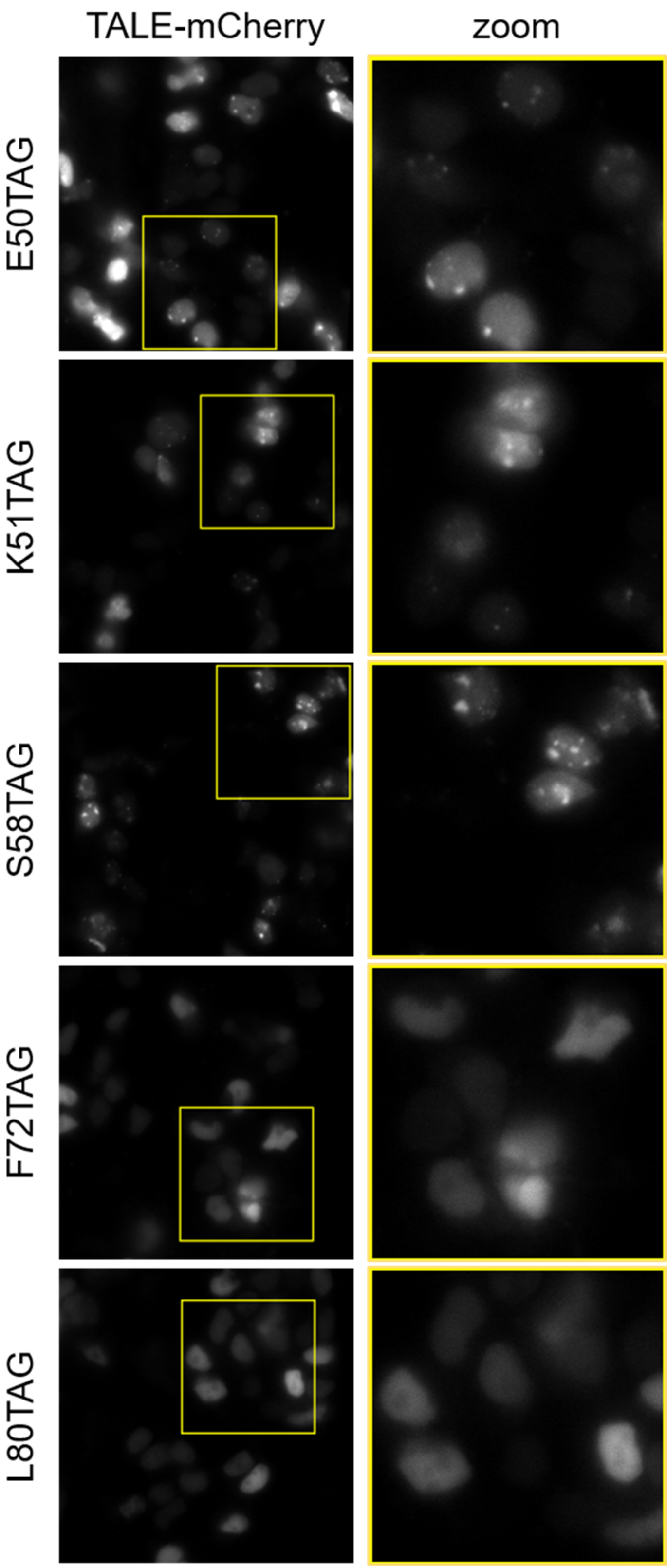
TALE-mCherry
zoom
E50TAG
K51TAG
S58TAG
F72TAG
L80TAG

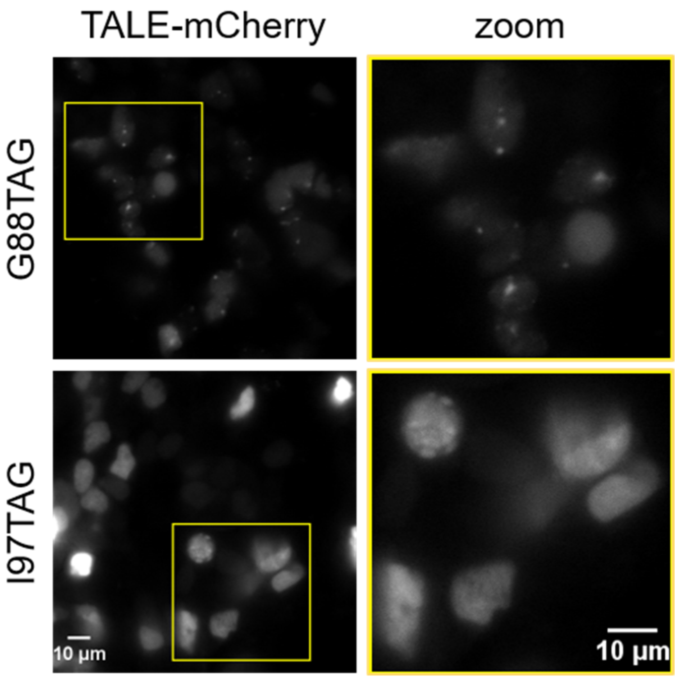

Figure S28 Whole fluorescent microscopy screen for studying non-canonical amino acid (ncAA) incorporation efficiency into SatIII-TALE and its localization: Fluorescent images (60x) of HEK293T cells, expressing ^{TAG}SatIII-TALE mCherry fusion construct and tRNA^{Pyl}/PylRS-AF^{NES}. Images were taken in the RFP channel showing incorporation of SCO at different positions and expression of SatIII-TALE-mCherry fusion construct. Furthermore, foci in the nucleus showing specific localization of the SatIII-TALE-mCherry fusion construct indicating specific DNA binding.

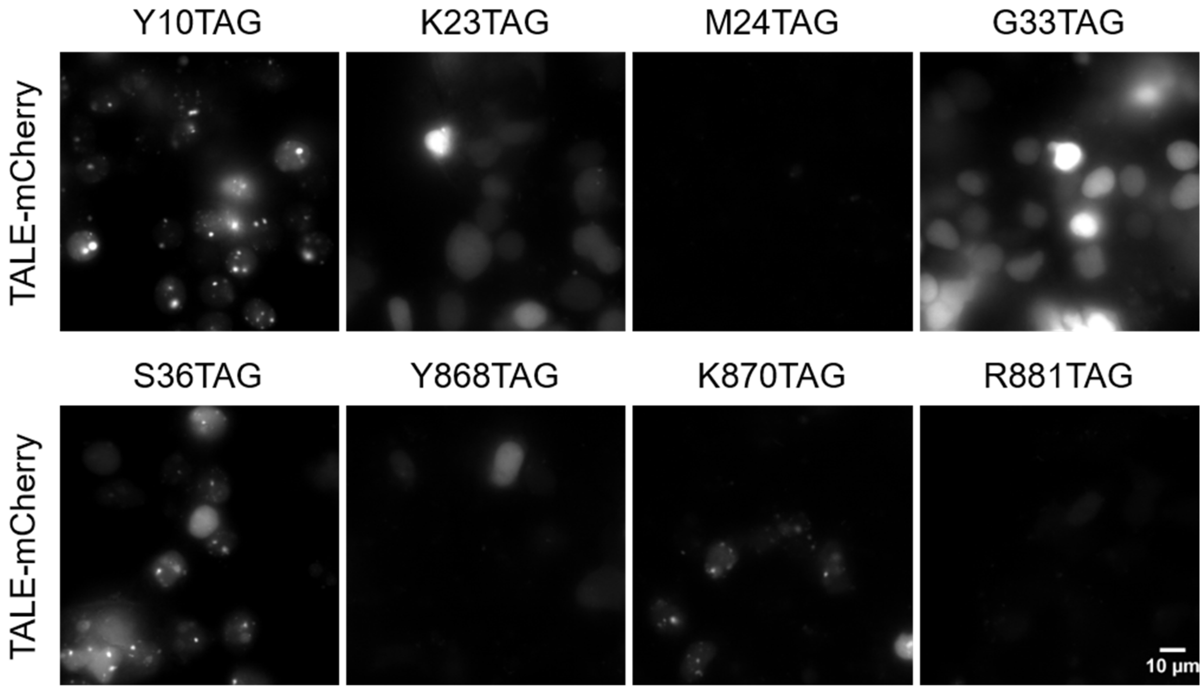

Figure S29 Whole fluorescent microscopy screen for studying non-canonical amino acid (ncAA) incorporation efficiency into SatIII-TALE: Fluorescent images (60x) of HEK293T cells, expressing ^{TAG}SatIII-TALE mCherry fusion construct and tRNA^{Pyl}/PylRS-AF^{NES}. Images were taken in the RFP channel showing incorporation of SCO at different positions and expression of the SatIII-TALE-mCherry fusion construct. Furthermore, foci in the nucleus showing specific localization of the SatIII-TALE-mCherry fusion construct indicating specific DNA binding.

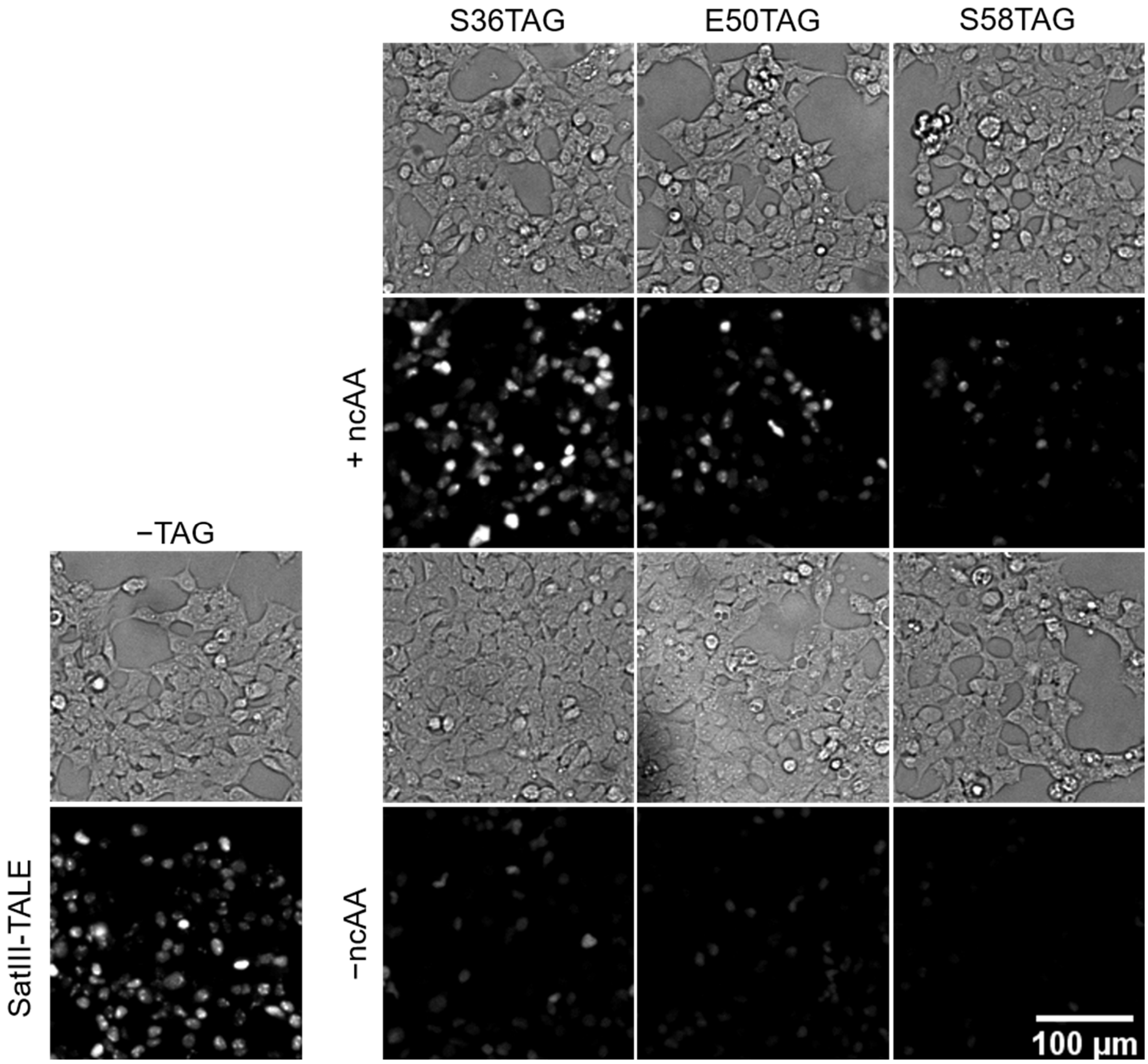

Figure S30 Additional brightfield images of studying non-canonical amino acid (ncAA) incorporation efficiency into SatIII-TALE: Fluorescent images of HEK293T cells, expressing SatIII-TALE mCherry fusion constructs and $tRNA^{Pyl}/PylRS\text{-}AF^{NES}$. Images were taken in the brightfield channel and in the RFP channel showing incorporation of TCO at the different amber codon positions, S36, E50 and S58 and expression of the ^{TAG}SatIII-TALE-mCherry fusion construct in comparison to the wild type SatIII-TALE mCherry fusion construct, not carrying an amber codon.

12.7 Agarosegels

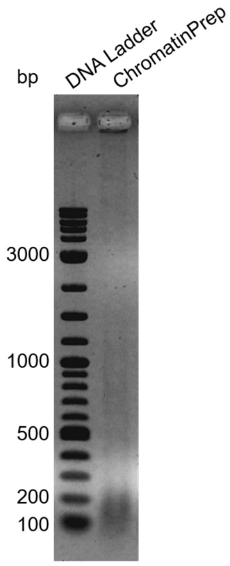

Figure S31 Agarosegel of sheared genomic DNA from HEK293T cells after reverse crosslinking: 10 Cycle 30 s on and 30 s off.

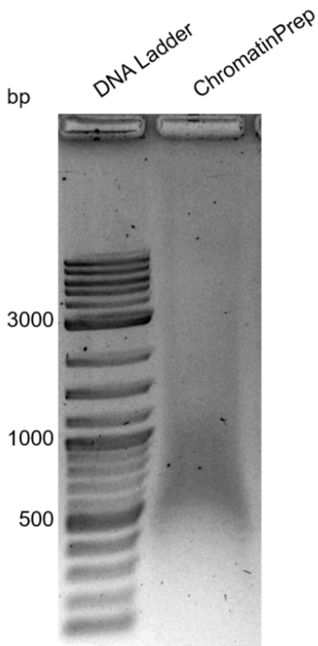

Figure S32 Agarosegel of sheared genomic DNA from HEK293T cells after reverse crosslinking: 1. 7 cycle 5 s on and 90 s off, 2. 7 cycle 10 s on and 90 s off, 3. 6 cycle 20 s on and 90 s off.

12.8 qPCR analysis of chromatin preparation

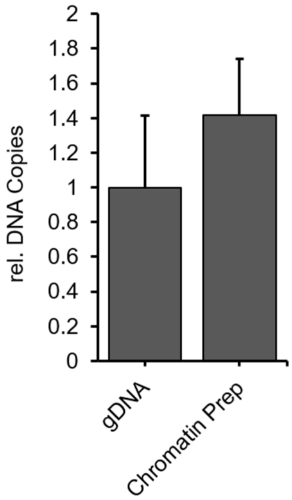

Figure S33 qPCR analysis of genomic DNA amounts using different DNA isolation methods: Diagram shows relative DNA copies of SatIII DNA from technical duplicates, depending on used DNA isolation method. Either genome isolation using QIAmp Mini Kit or chromatin purification.

13 References

[1] S. D. Byrum, S. D. Taverna, A. J. Tackett, *Nucleic Acids Res* **2013**, *41*, e195.

[2] M. Gauchier, S. Kan, A. Barral, S. Sauzet, E. Agirre, E. Bonnell, N. Saksouk, T. K. Barth, S. Ide, S. Urbach et al.J. Déjardin, *Sci Adv* **2019**, *5*, eaav3673.

[3] R. D. Kornberg, Y. Lorch, *Nat Struct Mol Biol* **2007**, *14*, 986.

[4] J. Déjardin, R. E. Kingston, *Cell* **2009**, *136*, 175.

[5] C. C. Liu, P. G. Schultz, *Annu Rev Biochem* **2010**, *79*, 413.

[6] K. Lang, L. Davis, J. Torres-Kolbus, C. Chou, A. Deiters, J. W. Chin, *Nat Chem* **2012**, *4*, 298.

[7] M. L. Blackman, M. Royzen, J. M. Fox, *J Am Chem Soc* **2008**, *130*, 13518.

[8] N. K. Devaraj, R. Weissleder, S. A. Hilderbrand, *Bioconjug Chem* **2008**, *19*, 2297.

[9] K. Lang, L. Davis, S. Wallace, M. Mahesh, D. J. Cox, M. L. Blackman, J. M. Fox, J. W. Chin, *J Am Chem Soc* **2012**, *134*, 10317.

[10] M. Tahiliani, K. P. Koh, Y. Shen, W. A. Pastor, H. Bandukwala, Y. Brudno, S. Agarwal, L. M. Iyer, D. R. Liu, L. Aravind et al.A. Rao, *Science* **2009**, *324*, 930.

[11] S. Kriaucionis, N. Heintz, *Science* **2009**, *324*, 929.

[12] S. Ito, L. Shen, Q. Dai, S. C. Wu, L. B. Collins, J. A. Swenberg, C. He, Y. Zhang, *Science* **2011**, *333*, 1300.

[13] Y.-F. He, B.-Z. Li, Z. Li, P. Liu, Y. Wang, Q. Tang, J. Ding, Y. Jia, Z. Chen, L. Li et al.G.-L. Xu, *Science* **2011**, *333*, 1303.

[14] T. Pfaffeneder, B. Hackner, M. Truss, M. Münzel, M. Müller, C. A. Deiml, C. Hagemeier, T. Carell, *Angew Chem Int Ed Engl* **2011**, *50*, 7008.

[15] O. T. Avery, C. M. Macleod, M. McCarty, *J Exp Med* **1944**, *79*, 137.

[16] E. CHARGAFF, *Experientia* **1950**, *6*, 201.

[17] X. Liu, Y. Zhang, Y. Chen, M. Li, F. Zhou, K. Li, H. Cao, M. Ni, Y. Liu, Z. Gu et al.J. Xu, *Cell* **2017**, *170*, 1028-1043.e19.

[18] J. Griesenbeck, H. Boeger, J. S. Strattan, R. D. Kornberg, *Mol Cell Biol* **2003**, *23*, 9275.

[19] E. Schmidtmann, T. Anton, P. Rombaut, F. Herzog, H. Leonhardt, *Nucleus* **2016**, *7*, 476.

[20] X. D. Gao, L.-C. Tu, A. Mir, T. Rodriguez, Y. Ding, J. Leszyk, J. Dekker, S. A. Shaffer, L. J. Zhu, S. A. Wolfe et al.E. J. Sontheimer, *Nat Methods* **2018**, *15*, 433.

[21] W. Qiu, Z. Xu, M. Zhang, D. Zhang, H. Fan, T. Li, Q. Wang, P. Liu, Z. Zhu, D. Du et al.Y. Liu, *Nucleic Acids Res* **2019**, *47*, e52.

[22] S. A. Myers, J. Wright, R. Peckner, B. T. Kalish, F. Zhang, S. A. Carr, *Nat Methods* **2018**, *15*, 437.

[23] E. Schrödinger, *What is life? The physical aspect of the living cell : and Mind and matter*, Cambridge University Press, Cambridge, **1967**.

[24] J. D. WATSON, F. H. CRICK, *Nature* **1953**, *171*, 737.

[25] M. H. F. WILKINS, A. R. STOKES, H. R. WILSON, *Nature* **1953**, *171*, 738.

[26] M. Bansal, *Current Science* **2003**, 1556.

[27] P. Yakovchuk, E. Protozanova, M. D. Frank-Kamenetskii, *Nucleic Acids Res* **2006**, *34*, 564.

[28] L. Stryer, J. Berg, J. Tymoczko, G. Gatto, *Biochemistry,* 9. Aufl., Macmillan Learning, New York, **2019**.

[29] B. Alberts, A. Johnson, J. Lewis, D. Morgan, M. Raff, K. Roberts, P. Walter, J. Wilson, T. Hunt, *Molecular biology of the cell*, Garland Science Taylor and Francis Group, New York, NY, **2015**.

[30] R. E. FRANKLIN, R. G. GOSLING, *Nature* **1953**, *172*, 156.

[31] R. LANGRIDGE, W. E. SEEDS, H. R. WILSON, C. W. HOOPER, H. F. WILKINS, L. D. HAMILTON, *J Biophys Biochem Cytol* **1957**, *3*, 767.

[32] H. R. Drew, R. M. Wing, T. Takano, C. Broka, S. Tanaka, K. Itakura, R. E. Dickerson, *Proc Natl Acad Sci U S A* **1981**, *78*, 2179.

[33] C. A. Bingman, G. Zon, M. Sundaralingam, *J Mol Biol* **1992**, *227*, 738.

[34] A. H. Wang, G. J. Quigley, F. J. Kolpak, J. L. Crawford, J. H. van Boom, G. van der Marel, A. Rich, *Nature* **1979**, *282*, 680.

[35] A. Rich, S. Zhang, *Nat Rev Genet* **2003**, *4*, 566.

[36] H. Robinson, Y. G. Gao, R. Sanishvili, A. Joachimiak, A. H. Wang, *Nucleic Acids Res* **2000**, *28*, 1760.

[37] D. Bancroft, L. D. Williams, A. Rich, M. Egli, *Biochemistry* **1994**, *33*, 1073.

[38] F. H. CRICK, *Symp Soc Exp Biol* **1958**, *12*, 138.

[39] F. Crick, *Nature* **1970**, *227*, 561.

[40] J. D. Watson, *Molecular biology of the gene*, Benjamin, New York, **1965**.

[41] H. Zheng, W. Xie, *Nat Rev Mol Cell Biol* **2019**, *20*, 535.

[42] K. Luger, A. W. Mäder, R. K. Richmond, D. F. Sargent, T. J. Richmond, *Nature* **1997**, *389*, 251.

[43] R. D. Kornberg, *Annu Rev Biochem* **1977**, *46*, 931.

[44] A. L. Olins, D. E. Olins, *Science* **1974**, *183*, 330.

[45] D. E. Olins, A. L. Olins, *Nat Rev Mol Cell Biol* **2003**, *4*, 809.

[46] G. Arents, R. W. Burlingame, B. C. Wang, W. E. Love, E. N. Moudrianakis, *Proc Natl Acad Sci U S A* **1991**, *88*, 10148.

[47] C. D. Allis, M.-L. Caparros, T. Jenuwein, D. Reinberg (Hrsg.) *Epigenetics*, CSH Press Cold Spring Harbor Laboratory Press, Cold Spring Harbor, New York, **2015**.

[48] A. Li, Y. Yu, S.-C. Lee, T. Ishibashi, S. P. Lees-Miller, J. Ausió, *J Biol Chem* **2010**, *285*, 17778.

[49] P. J. J. Robinson, L. Fairall, A. T. van Huynh, D. Rhodes, *Proc Natl Acad Sci U S A* **2006**, *103*, 6506.

[50] D. Canzio, E. Y. Chang, S. Shankar, K. M. Kuchenbecker, M. D. Simon, H. D. Madhani, G. J. Narlikar, B. Al-Sady, *Mol Cell* **2011**, *41*, 67.

[51] N. J. Francis, R. E. Kingston, C. L. Woodcock, *Science* **2004**, *306*, 1574.

[52] J. T. Finch, A. Klug, *Proc Natl Acad Sci U S A* **1976**, *73*, 1897.

[53] J. D. McGhee, J. M. Nickol, G. Felsenfeld, D. C. Rau, *Cell* **1983**, *33*, 831.

[54] B. Dorigo, T. Schalch, A. Kulangara, S. Duda, R. R. Schroeder, T. J. Richmond, *Science* **2004**, *306*, 1571.

[55] G. Li, D. Reinberg, *Curr Opin Genet Dev* **2011**, *21*, 175.

[56] T. Schalch, S. Duda, D. F. Sargent, T. J. Richmond, *Nature* **2005**, *436*, 138.

[57] F. Song, P. Chen, D. Sun, M. Wang, L. Dong, D. Liang, R.-M. Xu, P. Zhu, G. Li, *Science* **2014**, *344*, 376.

[58] M. Amendola, B. van Steensel, *Curr Opin Cell Biol* **2014**, *28*, 61.

[59] A. L. Turner, M. Watson, O. G. Wilkins, L. Cato, A. Travers, J. O. Thomas, K. Stott, *Proc Natl Acad Sci U S A* **2018**, *115*, 11964.

[60] T. Hirano, *Genes Dev* **2012**, *26*, 1659.

[61] K. Nasmyth, C. H. Haering, *Annu Rev Genet* **2009**, *43*, 525.

[62] H. Cedar, Y. Bergman, *Nat Rev Genet* **2009**, *10*, 295.

[63] C. H. Waddington, *Endeavour* **1942**, 18.

[64] V. E. A. Russo (Hrsg.) *Cold Spring Harbor monograph series*, *Vol. 32*, Cold Spring Harbor Laboratory Press, Plainview, NY, **1996**.

[65] V. G. ALLFREY, R. FAULKNER, A. E. MIRSKY, *Proc Natl Acad Sci U S A* **1964**, *51*, 786.

[66] W. K. Paik, S. Kim, *Science* **1971**, *174*, 114.
[67] S. Sidoli, L. Cheng, O. N. Jensen, *J Proteomics* **2012**, *75*, 3419.
[68] Y. Zhao, B. A. Garcia, *Cold Spring Harb Perspect Biol* **2015**, *7*, a025064.
[69] R. Marmorstein, M.-M. Zhou, *Cold Spring Harb Perspect Biol* **2014**, *6*, a018762.
[70] E. Seto, M. Yoshida, *Cold Spring Harb Perspect Biol* **2014**, *6*, a018713.
[71] X. Cheng, *Cold Spring Harb Perspect Biol* **2014**, *6*.
[72] Y. G. Shi, Y. Tsukada, *Cold Spring Harb Perspect Biol* **2013**, *5*.
[73] J. C. Black, C. van Rechem, J. R. Whetstine, *Mol Cell* **2012**, *48*, 491.
[74] S. Wang, Y. Wang, *Biochim Biophys Acta* **2013**, *1829*, 1126.
[75] Y. Dou, M. A. Gorovsky, *Mol Cell* **2000**, *6*, 225.
[76] Y. Wei, L. Yu, J. Bowen, M. A. Gorovsky, C.D. Allis, *Cell* **1999**, *97*, 99.
[77] D. Rossetto, N. Avvakumov, J. Côté, *Epigenetics* **2012**, *7*, 1098.
[78] D. E. Wright, C.-Y. Wang, C.-F. Kao, *Front Biosci (Landmark Ed)* **2012**, *17*, 1051.
[79] S. Messner, M. O. Hottiger, *Trends Cell Biol* **2011**, *21*, 534.
[80] J. A. Hanover, M. W. Krause, D. C. Love, *Nat Rev Mol Cell Biol* **2012**, *13*, 312.
[81] C. Dhalluin, J. E. Carlson, L. Zeng, C. He, A. K. Aggarwal, M. M. Zhou, *Nature* **1999**, *399*, 491.
[82] R. H. Jacobson, A. G. Ladurner, D. S. King, R. Tjian, *Science* **2000**, *288*, 1422.
[83] D. J. Patel, *Cold Spring Harb Perspect Biol* **2016**, *8*, a018754.
[84] K. S. Zaret, J. S. Carroll, *Genes Dev* **2011**, *25*, 2227.
[85] P. B. Becker, J. L. Workman, *Cold Spring Harb Perspect Biol* **2013**, *5*.
[86] G. J. Narlikar, R. Sundaramoorthy, T. Owen-Hughes, *Cell* **2013**, *154*, 490.
[87] G. Orphanides, G. LeRoy, C.-H. Chang, D. S. Luse, D. Reinberg, *Cell* **1998**, *92*, 105.
[88] D. Reinberg, R. J. Sims, *J Biol Chem* **2006**, *281*, 23297.
[89] R. J. Sims, R. Belotserkovskaya, D. Reinberg, *Genes Dev* **2004**, *18*, 2437.
[90] S. J. Petesch, J. T. Lis, *Trends Genet* **2012**, *28*, 285.
[91] R. C. Allshire, K. Ekwall, *Cold Spring Harb Perspect Biol* **2015**, *7*, a018770.
[92] R. Holliday, J. E. Pugh, *Science* **1975**, *187*, 226.
[93] S. Augui, E. P. Nora, E. Heard, *Nat Rev Genet* **2011**, *12*, 429.
[94] G. Kubik, M. J. Schmidt, J. E. Penner, D. Summerer, *Angew Chem Int Ed Engl* **2014**, *53*, 6002.
[95] J. A. Law, S. E. Jacobsen, *Nat Rev Genet* **2010**, *11*, 204.
[96] Z. D. Smith, A. Meissner, *Nat Rev Genet* **2013**, *14*, 204.

[97] P. A. Jones, *Nat Rev Genet* **2012**, *13*, 484.

[98] C. G. Spruijt, M. Vermeulen, *Nat Struct Mol Biol* **2014**, *21*, 949.

[99] A. Bird, *Genes Dev* **2002**, *16*, 6.

[100] W. Ren, L. Gao, J. Song, *Genes (Basel)* **2018**, *9*.

[101] F. Lyko, *Nat Rev Genet* **2018**, *19*, 81.

[102] E. Li, Y. Zhang, *Cold Spring Harb Perspect Biol* **2014**, *6*, a019133.

[103] E. Ghedin, S. Wang, D. Spiro, E. Caler, Q. Zhao, J. Crabtree, J. E. Allen, A. L. Delcher, D. B. Guiliano, D. Miranda-Saavedra et al.A. L. Scott, *Science* **2007**, *317*, 1756.

[104] M. Okano, S. Xie, E. Li, *Nat Genet* **1998**, *19*, 219.

[105] M. Okano, D. W. Bell, D. A. Haber, E. Li, *Cell* **1999**, *99*, 247.

[106] R. Z. Jurkowska, T. P. Jurkowski, A. Jeltsch, *Chembiochem* **2011**, *12*, 206.

[107] H. Zhu, G. Wang, J. Qian, *Nat Rev Genet* **2016**, *17*, 551.

[108] G. Kubik, D. Summerer, *Chembiochem* **2016**, *17*, 975.

[109] M. R. Branco, G. Ficz, W. Reik, *Nat Rev Genet* **2011**, *13*, 7.

[110] X. Wu, Y. Zhang, *Nat Rev Genet* **2017**, *18*, 517.

[111] C. Loenarz, C. J. Schofield, *Trends Biochem Sci* **2011**, *36*, 7.

[112] H. Wu, Y. Zhang, *Genes Dev* **2011**, *25*, 2436.

[113] L. Hu, J. Lu, J. Cheng, Q. Rao, Z. Li, H. Hou, Z. Lou, L. Zhang, W. Li, W. Gong et al.Y. Xu, *Nature* **2015**, *527*, 118.

[114] J. Lu, L. Hu, J. Cheng, D. Fang, C. Wang, K. Yu, H. Jiang, Q. Cui, Y. Xu, C. Luo, *Phys Chem Chem Phys* **2016**, *18*, 4728.

[115] S. Liu, J. Wang, Y. Su, C. Guerrero, Y. Zeng, D. Mitra, P. J. Brooks, D. E. Fisher, H. Song, Y. Wang, *Nucleic Acids Res* **2013**, *41*, 6421.

[116] D. Globisch, M. Münzel, M. Müller, S. Michalakis, M. Wagner, S. Koch, T. Brückl, M. Biel, T. Carell, *PLoS ONE* **2010**, *5*, e15367.

[117] M. Bachman, S. Uribe-Lewis, X. Yang, H. E. Burgess, M. Iurlaro, W. Reik, A. Murrell, S. Balasubramanian, *Nat Chem Biol* **2015**, *11*, 555.

[118] M. Mellén, P. Ayata, S. Dewell, S. Kriaucionis, N. Heintz, *Cell* **2012**, *151*, 1417.

[119] C. G. Spruijt, F. Gnerlich, A. H. Smits, T. Pfaffeneder, Jansen, Pascal W T C, C. Bauer, M. Münzel, M. Wagner, M. Müller, F. Khan et al.M. Vermeulen, *Cell* **2013**, *152*, 1146.

[120] L. Wang, Y. Zhou, L. Xu, R. Xiao, X. Lu, L. Chen, J. Chong, H. Li, C. He, X.-D. Fu et al.D. Wang, *Nature* **2015**, *523*, 621.

[121] C. G. Lian, Y. Xu, C. Ceol, F. Wu, A. Larson, K. Dresser, W. Xu, L. Tan, Y. Hu, Q. Zhan et al.Y. G. Shi, *Cell* **2012**, *150*, 1135.

[122] J. F. Costello, M. C. Frühwald, D. J. Smiraglia, L. J. Rush, G. P. Robertson, X. Gao, F. A. Wright, J. D. Feramisco, P. Peltomäki, J. C. Lang et al.C. Plass, *Nat Genet* **2000**, *24*, 132.

[123] J. P. Ross, K. N. Rand, P. L. Molloy, *Epigenomics* **2010**, *2*, 245.

[124] The ENCODE Project Consortium, *Nature* **2012**, *489*, 57.

[125] E. S. Lander, L. M. Linton, B. Birren, C. Nusbaum, M. C. Zody, J. Baldwin, K. Devon, K. Dewar, M. Doyle, W. FitzHugh et al.Y. J. Chen, *Nature* **2001**, *409*, 860.

[126] T. R. Gregory, *Nat Rev Genet* **2005**, *6*, 699.

[127] J. Padeken, P. Zeller, S. M. Gasser, *Curr Opin Genet Dev* **2015**, *31*, 12.

[128] A. Bird, *Nature* **2007**, *447*, 396.

[129] I. S.-R. Vaisertrager, O. I. Podgornaya, N. I. Enukashvily, *Cell Tiss. Biol.* **2007**, *1*, 50.

[130] B. D. Fodor, N. Shukeir, G. Reuter, T. Jenuwein, *Annu Rev Cell Dev Biol* **2010**, *26*, 471.

[131] H. S. Malik, S. Henikoff, *Cell* **2009**, *138*, 1067.

[132] J. C. Peng, G. H. Karpen, *Curr Opin Genet Dev* **2008**, *18*, 204.

[133] R. Valgardsdottir, I. Chiodi, M. Giordano, A. Rossi, S. Bazzini, C. Ghigna, S. Riva, G. Biamonti, *Nucleic Acids Res* **2007**, *36*, 423.

[134] A. Goenka, S. Sengupta, R. Pandey, R. Parihar, G. C. Mohanta, M. Mukerji, S. Ganesh, *J Cell Sci* **2016**, *129*, 3541.

[135] M. Hussong, C. Kaehler, M. Kerick, C. Grimm, A. Franz, B. Timmermann, F. Welzel, J. Isensee, T. Hucho, S. Krobitsch et al.M. R. Schweiger, *Nucleic Acids Res* **2017**, *45*, 382.

[136] R. Valgardsdottir, I. Chiodi, M. Giordano, F. Cobianchi, S. Riva, G. Biamonti, *Mol Biol Cell* **2005**, *16*, 2597.

[137] Y. Saito, Y. Kanai, M. Sakamoto, H. Saito, H. Ishii, S. Hirohashi, *Hepatology* **2001**, *33*, 561.

[138] M. Gauchier, G. van Mierlo, M. Vermeulen, J. Déjardin, *Nat Methods* **2020**.

[139] L. C. Boffa, E. M. Carpaneto, V. G. ALLFREY, *Proc Natl Acad Sci U S A* **1995**, *92*, 1901.

[140] T. Higashinakagawa, H. Wahn, R. H. Reeder, *Developmental Biology* **1977**, *55*, 375.

[141] J. L. Workman, J. P. Langmore, *Biochemistry* **1985**, *24*, 7486.

[142] X. Y. Zhang, W. Hörz, *Nucleic Acids Res* **1982**, *10*, 1481.

[143] S. D. Byrum, A. Raman, S. D. Taverna, A. J. Tackett, *Cell Rep* **2012**, *2*, 198.

[144] F. Pourfarzad, A. Aghajanirefah, E. de Boer, S. ten Have, T. van Bryn Dijk, S. Kheradmandkia, R. Stadhouders, S. Thongjuea, E. Soler, N. Gillemans et al.F. Grosveld, *Cell Rep* **2013**, *4*, 589.

[145] S. Hamperl, C. R. Brown, A. V. Garea, J. Perez-Fernandez, A. Bruckmann, K. Huber, M. Wittner, V. Babl, U. Stoeckl, R. Deutzmann et al.J. Griesenbeck, *Nucleic Acids Res* **2013**, *42*, e2.

[146] Z. J. Waldrip, S. D. Byrum, A. J. Storey, J. Gao, A. K. Byrd, S. G. Mackintosh, W. P. Wahls, S. D. Taverna, K. D. Raney, A. J. Tackett, *Epigenetics* **2014**, *9*, 1207.

[147] H. Guillen-Ahlers, P. K. Rao, M. E. Levenstein, J. Kennedy-Darling, D. S. Perumalla, A. Y. L. Jadhav, J. P. Glenn, A. Ludwig-Kubinski, E. Drigalenko, M. J. Montoya et al.M. Olivier, *Genomics* **2016**, *107*, 267.

[148] K. E. van Holde, A. Rich, *Chromatin*, Springer New York, New York, **1989**.

[149] E. A. Hoffman, B. L. Frey, L. M. Smith, D. T. Auble, *J Biol Chem* **2015**, *290*, 26404.

[150] M. Vermeulen, J. Déjardin, *Nat Rev Mol Cell Biol* **2020**.

[151] K. Müller-Ott, F. Erdel, A. Matveeva, J.-P. Mallm, A. Rademacher, M. Hahn, C. Bauer, Q. Zhang, S. Kaltofen, G. Schotta et al.K. Rippe, *Mol Syst Biol* **2014**, *10*, 746.

[152] P. Marzec, C. Armenise, G. Pérot, F.-M. Roumelioti, E. Basyuk, S. Gagos, F. Chibon, J. Déjardin, *Cell* **2015**, *160*, 913.

[153] N. Saksouk, T. K. Barth, C. Ziegler-Birling, N. Olova, A. Nowak, E. Rey, J. Mateos-Langerak, S. Urbach, W. Reik, M.-E. Torres-Padilla et al.E. Simboeck, *Mol Cell* **2014**, *56*, 580.

[154] S. Ide, J. Dejardin, *Nat Commun* **2015**, *6*, 6674.

[155] K. E. Buxton, J. Kennedy-Darling, M. R. Shortreed, N. Z. Zaidan, M. Olivier, M. Scalf, R. Sridharan, L. M. Smith, *J Proteome Res* **2017**, *16*, 3433.

[156] J. Kennedy-Darling, H. Guillen-Ahlers, M. R. Shortreed, M. Scalf, B. L. Frey, C. Kendziorski, M. Olivier, A. P. Gasch, L. M. Smith, *J Proteome Res* **2014**, *13*, 3810.

[157] H. Fujii, T. Fujita, *Int J Mol Sci* **2015**, *16*, 21802.

[158] C. Kuscu, S. Arslan, R. Singh, J. Thorpe, M. Adli, *Nat Biotechnol* **2014**, *32*, 677.

[159] C. Tsui, C. Inouye, M. Levy, A. Lu, L. Florens, M. P. Washburn, R. Tjian, *Proc Natl Acad Sci U S A* **2018**, *115*, E2734-E2741.

[160] J. K. Joung, J. D. Sander, *Nat Rev Mol Cell Biol* **2013**, *14*, 49.

[161] T. Fujita, Y. Asano, J. Ohtsuka, Y. Takada, K. Saito, R. Ohki, H. Fujii, *Sci Rep* **2013**, *3*, 3171.

[162] L. Grolimund, E. Aeby, R. Hamelin, F. Armand, D. Chiappe, M. Moniatte, J. Lingner, *Nat Commun* **2013**, *4*, 2848.

[163] J. Majerská, S. Redon, J. Lingner, *Methods* **2017**, *114*, 28.

[164] T. Fujita, H. Fujii, *PLoS ONE* **2011**, *6*, e26109.

[165] H.-W. Rhee, P. Zou, N. D. Udeshi, J. D. Martell, V. K. Mootha, S. A. Carr, A. Y. Ting, *Science* **2013**, *339*, 1328.

[166] S. Kay, U. Bonas, *Curr Opin Microbiol* **2009**, *12*, 37.

[167] S. Schornack, A. Meyer, P. Römer, T. Jordan, T. Lahaye, *J Plant Physiol* **2006**, *163*, 256.

[168] F. F. White, B. Yang, *Plant Physiol* **2009**, *150*, 1677.

[169] E. Weber, T. Ojanen-Reuhs, E. Huguet, G. Hause, M. Romantschuk, T. K. Korhonen, U. Bonas, R. Koebnik, *J Bacteriol* **2005**, *187*, 2458.

[170] J. Boch, U. Bonas, *Annu Rev Phytopathol* **2010**, *48*, 419.

[171] D. Büttner, D. Gürlebeck, L. D. Noël, U. Bonas, *Mol Microbiol* **2004**, *54*, 755.

[172] B. Szurek, E. Marois, U. Bonas, G. van den Ackerveken, *Plant J* **2001**, *26*, 523.

[173] S. Kay, U. Bonas, *Curr Opin Microbiol* **2009**, *12*, 37.

[174] A. N.-S. Mak, P. Bradley, A. J. Bogdanove, B. L. Stoddard, *Curr Opin Struct Biol* **2013**, *23*, 93.

[175] D. Deng, C. Yan, X. Pan, M. Mahfouz, J. Wang, J.-K. Zhu, Y. Shi, N. Yan, *Science* **2012**, *335*, 720.

[176] M. J. Moscou, A. J. Bogdanove, *Science* **2009**, *326*, 1501.

[177] J. Boch, H. Scholze, S. Schornack, A. Landgraf, S. Hahn, S. Kay, T. Lahaye, A. Nickstadt, U. Bonas, *Science* **2009**, *326*, 1509.

[178] S. Maurer, M. Giess, O. Koch, D. Summerer, *ACS Chem Biol* **2016**, *11*, 3294.

[179] A. N.-S. Mak, P. Bradley, R. A. Cernadas, A. J. Bogdanove, B. L. Stoddard, *Science* **2012**, *335*, 716.

[180] H. Gao, X. Wu, J. Chai, Z. Han, *Cell Res* **2012**, *22*, 1716.

[181] J. F. Meckler, M. S. Bhakta, M.-S. Kim, R. Ovadia, C. H. Habrian, A. Zykovich, A. Yu, S. H. Lockwood, R. Morbitzer, J. Elsäesser et al.E. P. Baldwin, *Nucleic Acids Res* **2013**, *41*, 4118.

[182] J. C. Miller, S. Tan, G. Qiao, K. A. Barlow, J. Wang, D. F. Xia, X. Meng, D. E. Paschon, E. Leung, S. J. Hinkley et al.E. J. Rebar, *Nat Biotechnol* **2011**, *29*, 143.
[183] T. Cermak, E. L. Doyle, M. Christian, L. Wang, Y. Zhang, C. Schmidt, J. A. Baller, N. V. Somia, A. J. Bogdanove, D. F. Voytas, *Nucleic Acids Res* **2011**, *39*, e82.
[184] M. T. Murakami, M. L. Sforça, J. L. Neves, J. H. Paiva, M. N. Domingues, A. L. A. Pereira, A. C. d. M. Zeri, C. E. Benedetti, *Proteins* **2010**, *78*, 3386.
[185] D. Voet, J. G. Voet, *Biochemistry,* 4. Aufl., Wiley, Hoboken, NJ, **2011**.
[186] Clancy, S. and Brown, W., *Nature Education* **2008**, 101.
[187] R. Boyer, *Biochem. Mol. Biol. Educ.* **2006**, *34*, 461.
[188] G. A. Khoury, R. C. Baliban, C. A. Floudas, *Sci Rep* **2011**, *1*.
[189] D. P. Clark, N. J. Pazdernik, A. Held, B. Jarosch, *Molekulare Biotechnologie. Grundlagen und Anwendungen*, Spektrum Akademischer Verlag, Heidelberg, **2009**.
[190] B. G. Barrell, A. T. Bankier, J. Drouin, *Nature* **1979**, *282*, 189.
[191] S. Osawa, T. H. Jukes, *J Mol Evol* **1989**, *28*, 271.
[192] P. O'Donoghue, J. Ling, Y.-S. Wang, D. Söll, *Nat Chem Biol* **2013**, *9*, 594.
[193] R. Uy, F. Wold, *Science* **1977**, *198*, 890.
[194] J. Donovan, P. R. Copeland, *J Mol Biol* **2010**, *400*, 659.
[195] G. Srinivasan, C. M. James, J. A. Krzycki, *Science* **2002**, *296*, 1459.
[196] E. A. Lemke, D. Summerer, B. H. Geierstanger, S. M. Brittain, P. G. Schultz, *Nat Chem Biol* **2007**, *3*, 769.
[197] R. B. Merrifield, *Adv Enzymol Relat Areas Mol Biol* **1969**, *32*, 221.
[198] T. W. Muir, *Annu Rev Biochem* **2003**, *72*, 249.
[199] M. Ghosh, I. Ichetovkin, X. Song, J. S. Condeelis, D. S. Lawrence, *J Am Chem Soc* **2002**, *124*, 2440.
[200] M. E. Hahn, T. W. Muir, *Angew Chem Int Ed Engl* **2004**, *43*, 5800.
[201] D. R. Liu, P. G. Schultz, *Proc Natl Acad Sci U S A* **1999**, *96*, 4780.
[202] C. J. Noren, S. J. Anthony-Cahill, M. C. Griffith, P. G. Schultz, *Science* **1989**, *244*, 182.
[203] D. R. Liu, T. J. Magliery, M. Pastrnak, P. G. Schultz, *Proc Natl Acad Sci U S A* **1997**, *94*, 10092.
[204] L. Wang, A. Brock, B. Herberich, P. G. Schultz, *Science* **2001**, *292*, 498.
[205] J. C. Anderson, N. Wu, S. W. Santoro, V. Lakshman, D. S. King, P. G. Schultz, *Proc Natl Acad Sci U S A* **2004**, *101*, 7566.

[206] J. Xie, P. G. Schultz, *Methods* **2005**, *36*, 227.

[207] L. Wang, P. G. Schultz, *Chemistry & Biology* **2001**, *8*, 883.

[208] N. Wu, A. Deiters, T. A. Cropp, D. King, P. G. Schultz, *J Am Chem Soc* **2004**, *126*, 14306.

[209] C. Polycarpo, A. Ambrogelly, A. Bérubé, S. M. Winbush, J. A. McCloskey, P. F. Crain, J. L. Wood, D. Söll, *Proc Natl Acad Sci U S A* **2004**, *101*, 12450.

[210] S. K. Blight, R. C. Larue, A. Mahapatra, D. G. Longstaff, E. Chang, G. Zhao, P. T. Kang, K. B. Green-Church, M. K. Chan, J. A. Krzycki, *Nature* **2004**, *431*, 333.

[211] B. Hao, W. Gong, T. K. Ferguson, C. M. James, J. A. Krzycki, M. K. Chan, *Science* **2002**, *296*, 1462.

[212] T. Yanagisawa, M. Kuratani, E. Seki, N. Hino, K. Sakamoto, S. Yokoyama, *Cell Chem Biol* **2019**, *26*, 936-949.e13.

[213] J. M. Kavran, S. Gundllapalli, P. O'Donoghue, M. Englert, D. Söll, T. A. Steitz, *Proc Natl Acad Sci U S A* **2007**, *104*, 11268.

[214] W. Wan, J. M. Tharp, W. R. Liu, *Biochim Biophys Acta* **2014**, *1844*, 1059.

[215] K. Lang, J. W. Chin, *Chem Rev* **2014**, *114*, 4764.

[216] K. Lang, J. W. Chin, *ACS Chem Biol* **2014**, *9*, 16.

[217] X. Shi, Y. Jung, L.-J. Lin, C. Liu, C. Wu, I. K. O. Cann, T. Ha, *Nat Methods* **2012**, *9*, 499.

[218] D. Rideout, *Science* **1986**, *233*, 561.

[219] E. G. Sander, W. P. Jencks, *J Am Chem Soc* **1968**, *90*, 6154.

[220] D. A. Nauman, C. R. Bertozzi, *Biochimica et Biophysica Acta (BBA) - General Subjects* **2001**, *1568*, 147.

[221] W. P. Jencks, *J Am Chem Soc* **1959**, *81*, 475.

[222] L. K. Mahal, K. J. Yarema, C. R. Bertozzi, *Science* **1997**, *276*, 1125.

[223] R. J. Griffin in *Progress in Medicinal Chemistry* (Hrsg.: G. P. Ellis, D. K. Luscombe), Elsevier, Amsterdam, London, **1994**, S. 121–232.

[224] H. Ovaa, P. F. van Swieten, B. M. Kessler, M. A. Leeuwenburgh, E. Fiebiger, A. M. C. H. van den Nieuwendijk, P. J. Galardy, G. A. van der Marel, H. L. Ploegh, H. S. Overkleeft, *Angew Chem Int Ed Engl* **2003**, *42*, 3626.

[225] D. J. Vocadlo, H. C. Hang, E.-J. Kim, J. A. Hanover, C. R. Bertozzi, *Proc Natl Acad Sci U S A* **2003**, *100*, 9116.

[226] M. J. Hangauer, C. R. Bertozzi, *Angew Chem Int Ed Engl* **2008**, *47*, 2394.

[227] E. Saxon, C. R. Bertozzi, *Science* **2000**, *287*, 2007.

[228] J. A. Prescher, D. H. Dube, C. R. Bertozzi, *Nature* **2004**, *430*, 873.
[229] M.-L. Tsao, F. Tian, P. G. Schultz, *Chembiochem* **2005**, *6*, 2147.
[230] T. Yanagisawa, R. Ishii, R. Fukunaga, T. Kobayashi, K. Sakamoto, S. Yokoyama, *Chemistry & Biology* **2008**, *15*, 1187.
[231] F. L. Lin, H. M. Hoyt, H. van Halbeek, R. G. Bergman, C. R. Bertozzi, *J Am Chem Soc* **2005**, *127*, 2686.
[232] V. V. Rostovtsev, L. G. Green, V. V. Fokin, K. B. Sharpless, *Angew. Chem. Int. Ed.* **2002**, *41*, 2596.
[233] C. W. Tornøe, C. Christensen, M. Meldal, *J Org Chem* **2002**, *67*, 3057.
[234] A. E. Speers, B. F. Cravatt, *Chemistry & Biology* **2004**, *11*, 535.
[235] N. J. Agard, J. M. Baskin, J. A. Prescher, A. Lo, C. R. Bertozzi, *ACS Chem Biol* **2006**, *1*, 644.
[236] F. Wolbers, P. ter Braak, S. Le Gac, R. Luttge, H. Andersson, I. Vermes, A. van den Berg, *Electrophoresis* **2006**, *27*, 5073.
[237] V. Hong, N. F. Steinmetz, M. Manchester, M. G. Finn, *Bioconjug Chem* **2010**, *21*, 1912.
[238] N. J. Agard, J. A. Prescher, C. R. Bertozzi, *J Am Chem Soc* **2004**, *126*, 15046.
[239] J. M. Baskin, J. A. Prescher, S. T. Laughlin, N. J. Agard, P. V. Chang, I. A. Miller, A. Lo, J. A. Codelli, C. R. Bertozzi, *Proc Natl Acad Sci U S A* **2007**, *104*, 16793.
[240] X. Ning, R. P. Temming, J. Dommerholt, J. Guo, D. B. Ania, M. F. Debets, M. A. Wolfert, G.-J. Boons, F. L. van Delft, *Angew Chem Int Ed Engl* **2010**, *49*, 3065.
[241] C. S. McKay, J. Moran, J. P. Pezacki, *Chem Commun (Camb)* **2010**, *46*, 931.
[242] M. F. Debets, S. S. van Berkel, J. Dommerholt, A. T. J. Dirks, F. P. J. T. Rutjes, F. L. van Delft, *Acc Chem Res* **2011**, *44*, 805.
[243] S. Flade, J. Jasper, M. Gieß, M. Juhasz, A. Dankers, G. Kubik, O. Koch, E. Weinhold, D. Summerer, *ACS Chem Biol* **2017**, *12*, 1719.
[244] G. Kubik, S. Batke, D. Summerer, *J Am Chem Soc* **2015**, *137*, 2.
[245] G. Kubik, D. Summerer, *Chembiochem* **2015**, *16*, 228.
[246] P. Rathi, S. Maurer, G. Kubik, D. Summerer, *J Am Chem Soc* **2016**, *138*, 9910.
[247] P. Rathi, A. Witte, D. Summerer, *Sci Rep* **2017**, *7*, 15067.
[248] J. Yang, Y. Zhang, P. Yuan, Y. Zhou, C. Cai, Q. Ren, D. Wen, C. Chu, H. Qi, W. Wei, *Cell Res* **2014**, *24*, 628.
[249] D. J. Segal, J. F. Meckler, *Annu Rev Genomics Hum Genet* **2013**, *14*, 135.

[250] P. Perez-Pinera, D. G. Ousterout, J. M. Brunger, A. M. Farin, K. A. Glass, F. Guilak, G. E. Crawford, A. J. Hartemink, C. A. Gersbach, *Nat Methods* **2013**, *10*, 239.

[251] D. L. Bernstein, J. E. Le Lay, E. G. Ruano, K. H. Kaestner, *J Clin Invest* **2015**, *125*, 1998.

[252] T. Plass, S. Milles, C. Koehler, J. Szymański, R. Mueller, M. Wiessler, C. Schultz, E. A. Lemke, *Angew Chem Int Ed Engl* **2012**, *51*, 4166.

[253] I. Nikić, T. Plass, O. Schraidt, J. Szymański, J. A. G. Briggs, C. Schultz, E. A. Lemke, *Angew Chem Int Ed Engl* **2014**, *53*, 2245.

[254] T. Plass, S. Milles, C. Koehler, C. Schultz, E. A. Lemke, *Angew Chem Int Ed Engl* **2011**, *50*, 3878.

[255] J. D. Sander, L. Cade, C. Khayter, D. Reyon, R. T. Peterson, J. K. Joung, J.-R. J. Yeh, *Nat Biotechnol* **2011**, *29*, 697.

[256] M. Pott, M. J. Schmidt, D. Summerer, *ACS Chem Biol* **2014**, *9*, 2815.

[257] M. J. Schmidt, D. Summerer, *Angew Chem Int Ed Engl* **2013**, *52*, 4690.

[258] I. Nikić, G. Estrada Girona, J. H. Kang, G. Paci, S. Mikhaleva, C. Koehler, N. V. Shymanska, C. Ventura Santos, D. Spitz, E. A. Lemke, *Angew Chem Int Ed Engl* **2016**, *55*, 16172.

[259] Á. Muñoz-López, B. Buchmuller, J. Wolffgramm, A. Jung, M. Hussong, J. Kanne, M. R. Schweiger and D. Summerer, *Angew Chem Int Ed Engl* **2020**, accepted.

[260] A. J. Hobro, N. I. Smith, *Vibrational Spectroscopy* **2017**, *91*, 31.

[261] S. Kozubek, E. Lukásová, J. Amrichová, M. Kozubek, A. Lisková, J. Slotová, *Anal Biochem* **2000**, *282*, 29.

[262] C. Stadler, M. Skogs, H. Brismar, M. Uhlén, E. Lundberg, *J Proteomics* **2010**, *73*, 1067.

[263] A. Fraschini, C. Pellicciari, M. Biggiogera, M. G. Manfredi Romanini, *Histochem J* **1981**, *13*, 763.

[264] J. A. Wagner, D. Mercadante, I. Nikić, E. A. Lemke, F. Gräter, *Chemistry* **2015**, *21*, 12431.

[265] H. Tian, T. P. Sakmar, T. Huber, *Chem Commun (Camb)* **2016**, *52*, 5451.

[266] E. Col, N. Hoghoughi, S. Dufour, J. Penin, S. Koskas, V. Faure, M. Ouzounova, H. Hernandez-Vargash, N. Reynoird, S. Daujat et al.C. Vourc'h, *Sci Rep* **2017**, *7*, 5418.

[267] S. H. Barghout, A. D. Schimmer, *Oncotarget* **2018**, *9*, 34198.

[268] D. Ayusawa, S. Kaneda, Y. Itoh, H. Yasuda, Y. Murakami, K. Sugasawa, F. Hanaoka, T. Seno, *Cell Struct Funct* **1992**, *17*, 113.

[269] J. C. Cook, P. B. Chock, *J Biol Chem* **1992**, *267*, 24315.

[270] H.-M. Lin, R. G. Pestell, A. Raz, H.-R. C. Kim, *Oncogene* **2002**, *21*, 8001.

[271] J. S. Hardwick, D. Ptchelkine, A. H. El-Sagheer, I. Tear, D. Singleton, S. E. V. Phillips, A. N. Lane, T. Brown, *Nat Struct Mol Biol* **2017**, *24*, 544.

[272] L. Lercher, M. A. McDonough, A. H. El-Sagheer, A. Thalhammer, S. Kriaucionis, T. Brown, C. J. Schofield, *Chem Commun (Camb)* **2014**, *50*, 1794.

[273] M. W. Szulik, P. S. Pallan, B. Nocek, M. Voehler, S. Banerjee, S. Brooks, A. Joachimiak, M. Egli, B. F. Eichman, M. P. Stone, *Biochemistry* **2015**, *54*, 1294.

[274] S. Ji, H. Shao, Q. Han, C. L. Seiler, N. Y. Tretyakova, *Angew Chem Int Ed Engl* **2017**, *56*, 14130.

[275] M. W. Kellinger, C.-X. Song, J. Chong, X.-Y. Lu, C. He, D. Wang, *Nat Struct Mol Biol* **2012**, *19*, 831.

[276] T. T. M. Ngo, J. Yoo, Q. Dai, Q. Zhang, C. He, A. Aksimentiev, T. Ha, *Nat Commun* **2016**, *7*, 10813.

[277] L. Wang, Y. Zhou, L. Xu, R. Xiao, X. Lu, L. Chen, J. Chong, H. Li, C. He, X.-D. Fu et al.D. Wang, *Nature* **2015**, *523*, 621.

[278] E. A. Mahé, T. Madigou, A. A. Sérandour, M. Bizot, S. Avner, F. Chalmel, G. Palierne, R. Métivier, G. Salbert, *Genome Res* **2017**, *27*, 947.

[279] D. G. Gibson, L. Young, R.-Y. Chuang, J. C. Venter, C. A. Hutchison, H. O. Smith, *Nat Methods* **2009**, *6*, 343.

[280] Q. Chen, Y. Chen, C. Bian, R. Fujiki, X. Yu, *Nature* **2013**, *493*, 561.

[281] H. Ma, P. Reyes-Gutierrez, T. Pederson, *Proc Natl Acad Sci U S A* **2013**, *110*, 21048.

[282] B. Vissel, K. H. Choo, *Nucleic Acids Res* **1987**, *15*, 6751.

[283] J. Prosser, M. Frommer, C. Paul, P. C. Vincent, *J Mol Biol* **1986**, *187*, 145.

[284] R. K. Moyzis, J. M. Buckingham, L. S. Cram, M. Dani, L. L. Deaven, M. D. Jones, J. Meyne, R. L. Ratliff, J. R. Wu, *Proc Natl Acad Sci U S A* **1988**, *85*, 6622.

Eidesstattliche Versicherung (Affidavit)

Name, Vorname
(Surname, first name)

Matrikel-Nr.
(Enrolment number)

Belehrung:

Wer vorsätzlich gegen eine die Täuschung über Prüfungsleistungen betreffende Regelung einer Hochschulprüfungsordnung verstößt, handelt ordnungswidrig. Die Ordnungswidrigkeit kann mit einer Geldbuße von bis zu 50.000,00 € geahndet werden. Zuständige Verwaltungsbehörde für die Verfolgung und Ahndung von Ordnungswidrigkeiten ist der Kanzler/die Kanzlerin der Technischen Universität Dortmund. Im Falle eines mehrfachen oder sonstigen schwerwiegenden Täuschungsversuches kann der Prüfling zudem exmatrikuliert werden, § 63 Abs. 5 Hochschulgesetz NRW.

Die Abgabe einer falschen Versicherung an Eides statt ist strafbar.

Wer vorsätzlich eine falsche Versicherung an Eides statt abgibt, kann mit einer Freiheitsstrafe bis zu drei Jahren oder mit Geldstrafe bestraft werden, § 156 StGB. Die fahrlässige Abgabe einer falschen Versicherung an Eides statt kann mit einer Freiheitsstrafe bis zu einem Jahr oder Geldstrafe bestraft werden, § 161 StGB.

Die oben stehende Belehrung habe ich zur Kenntnis genommen:

Official notification:

Any person who intentionally breaches any regulation of university examination regulations relating to deception in examination performance is acting improperly. This offence can be punished with a fine of up to EUR 50,000.00. The competent administrative authority for the pursuit and prosecution of offences of this type is the chancellor of the TU Dortmund University. In the case of multiple or other serious attempts at deception, the candidate can also be unenrolled, Section 63, paragraph 5 of the Universities Act of North Rhine-Westphalia.

The submission of a false affidavit is punishable.

Any person who intentionally submits a false affidavit can be punished with a prison sentence of up to three years or a fine, Section 156 of the Criminal Code. The negligent submission of a false affidavit can be punished with a prison sentence of up to one year or a fine, Section 161 of the Criminal Code.

I have taken note of the above official notification.

Ort, Datum
(Place, date)

Unterschrift
(Signature)

Titel der Dissertation:
(Title of the thesis):

Ich versichere hiermit an Eides statt, dass ich die vorliegende Dissertation mit dem Titel selbstständig und ohne unzulässige fremde Hilfe angefertigt habe. Ich habe keine anderen als die angegebenen Quellen und Hilfsmittel benutzt sowie wörtliche und sinngemäße Zitate kenntlich gemacht.
Die Arbeit hat in gegenwärtiger oder in einer anderen Fassung weder der TU Dortmund noch einer anderen Hochschule im Zusammenhang mit einer staatlichen oder akademischen Prüfung vorgelegen.

I hereby swear that I have completed the present dissertation independently and without inadmissible external support. I have not used any sources or tools other than those indicated and have identified literal and analogous quotations.

The thesis in its current version or another version has not been presented to the TU Dortmund University or another university in connection with a state or academic examination.*

*Please be aware that solely the German version of the affidavit ("Eidesstattliche Versicherung") for the PhD thesis is the official and legally binding version.

Ort, Datum
(Place, date)

Unterschrift
(Signature)